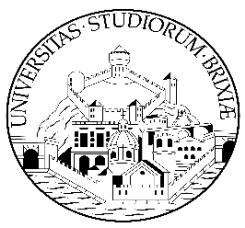

UNIVERSITÀ
DEGLI STUDI
DI BRESCIA

DOTTORATO DI RICERCA IN INGEGNERIA MECCANICA E INDUSTRIALE

SCIENZA E TECNOLOGIA DEI MATERIALI

CICLO XXXV

INJECTION MOLDING PROCESS OPTIMIZATION OF RUBBER COMPOUNDS FOCUSED ON THE SUSTAINABILITY

MATTIA RAMINI (DOTTORANDO)

PROF. SILVIA AGNELLI (SUPERVISORE)
GERMANA BERGOMI (CO-SUPERVISORE, ITALIAN GASKET S.p.A)
PROF. PIETRO POESIO (COORDINATORE)

ACKNOWLEDGEMENTS

It is a great satisfaction for me that the hard work, devotion and energy invested during last three years for the conclusion of industrial PhD thesis has been appreciated by both the scientific and the industrial communities. One of the main objectives of this industrial PhD was to build as a "bridge" between the academic community and the "application world" of the rubber processing industry. This goal has been successfully achieved thanks to the continuous exchange of knowledge and experience with my supervisor *Prof. Silvia Agnelli*.

Nevertheless, I wish to thank *Germana Bergomi*, board member of *Italian Gasket*, for having wanted and started, in the 2019, the collaboration between *Italian Gasket S.p.A*. and the *University of Brescia*. Germana gave me this opportunity with the purpose to build a fruitful collaboration by *Italian Gasket S.p.A*. and the *Department of Mechanical and Industrial Engineering of the University of Brescia*.

Obviously, I affectionately thank the *Bergomi Family* for having invested in my professional growing through this industrial PhD, and above all because they are endowed with that foresight, unfortunately still very rare in the Italian rubber industry.

In the meantime, thanks to this strictly collaboration, a young and promising mechanical engineer, *Mario Costardi*, has been part of the R&D department of *Italian Gasket S.p.A* of which I am the manager for about 6 years.

Another important thanks go to *Dr. Tommaso Viola* and *Dr. Luisa Paganin* for having contributed as an industrial partner to the study of devulcanized FKM rubber compounds.

Furthermore, I would also like to thank *Sergio Foschi*, *Fabio Tonioli* and *Vittorio Bertasi*, very experienced managers of my previous work experiences in the rubber field, for have been "life and work teachers".

Last, but not least, I thank my *LORD*, my *wife Sara*, *parents*, and *family*, for educating me with aspects focused on the science, and for absolute support and encouragement to pursue my interests, even when the interests went beyond the boundaries of language, field and geography.

CONTENT

NOMENCLATURE

ACM	Polyacrylate rubber
ACN	Acrylonitrile
AEM	Ethylene acrylate rubber
AI	Artificial intelligence
ATF	Automatic transmission fluids
ATR-FTIR	Attenuated total reflection Fourier transform infrared
BR	Butadiene rubber
BTPPC	Benzyltriphenylphosponium chloride
CAE	Computer-aided engineering
CB	Carbon black
CaO	Calcium oxide
$Ca(OH)_2$	Calcium hydroxide
CO_2	Carbon dioxide
CVJ	Constant velocity joint
DMA	Dynamic mechanical analysis
DTDM	4,4'-dithiodimorpholine
DOE	Design of experiment
DP	Degree of polymerization
DSC	Differential scanning calorimeter
E	Calorimetric sensitivity
G'	Storage modulus
G''	Loss modulus
EAF	Electric arc furnace
ENB	5-ethylidene-2-norbornene
EP(D)M	Ethylene propylene diene monomer
EPDM	Ethylene propylene diene rubber (terpolymer)
EPM	Ethylene propylene rubber (copolymer)
EU	European Union
FDA	Food and Drug Administration
Fe_2O_3	Iron oxide (III)
F_f	Friction force
FIFO	First in first out
FKM	Fluorocarbon rubber
FMEA	Failure mode and effect analysis

HF	Hydrogen fluoride
HFP	Hexafluoropropylene
HMDA	Hexamethylene diamine
HMDC	Hexamethylene diamine carbamate
HNBR	Hydrogenated acrylonitrile butadiene rubber
HP-HNBR	High Performance Zetpol®
HPE	High performance elastomers
HSN	Highly Saturated Nitrile
IMDS	International Material Data System
IR	Isoprene rubber
IRHD	International rubber hardness degree
LCM	Molten-salt bath
L/D	Screw length over diameter ratio
LIFO	Last in first out
MDR	Moving die rheometer
MgO	Magnesium oxide
M_L	Minimum torque
MPT	Monsanto Processability Tester
NBR	Acrylonitrile butadiene rubber
NMR	Nuclear magnetic resonance
NR	Natural rubber
ODR	Oscillating disc rheometer
OEM	Original equipment manufacturer
phr	Parts per hundred rubber
P_i	Injection pressure
PLS	Partial least square
PMVE	Polymethylvinylether
PVC	Polyvinyl chloride
PVT	Pressure - Volume - Temperature curves
RICM	Reactive injection compression molding
RPA	Rubber process analyzer
RT	Room temperature
SBR	Styrene butadiene rubber
T_{barrel}	Barrel temperature setup
Tc	Curing temperature

tc	Curing time
t_i	Filling or injection time
T_g	Glass transition temperature
TGA	Thermogravimetric analysis
TMDT	Trimethylene tetrathiafulvalene dithiolate
T_{SH}	Shear heating temperature
TT-FKM	Thermal treated FKM
UHF	Ultrahigh frequency
VMQ	Silicone rubber
XNBR	Carboxylated nitrile rubber
η_{SH}	Shear heating parameter
η^*	Dynamic complex viscosity
δ	Solubility parameter
$\tan\delta$ (G''/G')	Mechanical energy dissipation

1 ABSTRACT

Since automotive manufacturers of original equipment require high quality level of gaskets, it is mandatory that the gasket manufactures achieve a stability of production runs with minimized defects (zero-defect) and scraps amount. Therefore, a suitable process control for rubber injection molding able to take into account process fluctuations has to be developed.

From the point of view of sustainability, rubber waste doesn't degrade and remains for a long period of time in the environment. Therefore, to increase the sustainability of rubber products, the first strategy is to reduce the generated waste. Reducing rubber waste during production involves not only material savings, but also energy savings.

The principal aim of this thesis is to develop a method for process optimization with the purpose to reduce scraps amount, and to increase the sustainability of rubber products by recycling the waste materials as well.

The existing approaches reported in the literature are manly focused both on the technology improvement of conventional laboratory instruments such as RPA and capillary rheometer, and also on the technology improvement of the injection molding machine, used as a laboratory rheometer (*e.g.* slit die rheometry). Although specific sensors were employed directly in the injection molding machine to provide an online monitoring of pressure and temperature, however these devices were too susceptible to handling, wear and fouling especially if installed to monitor continuously these signals in daily industrial operation.

Therefore, this research activity aims to develop an integrated approach, merging laboratory data and process data, useful to improve the injection molding process control, and to reduce the defects and scraps amount during the manufacturing process of rubber parts by injection molding.

The proposed method is based on a very fast online monitoring of the surface rubber temperature (shear heating temperature, T_{SH}) by an infrared thermal camera, pointed toward the rubber leaving the extruder barrel of the injection molding machine.

This measured temperature led to the calculation of a technological parameter designated shear heating parameter, η_{SH}, which also takes into account physical material properties (density and specific heat capacity) and process conditions (screw L/D ratio).

Therefore, monitoring also η_{SH} allowed to get an added value in terms of quantitative and precise indication of the quality of molded part. Furthermore, log η_{SH} values of a production run, combined with M_L values, give indication of the "real output" of the injection molding process by comparison of this data with a well-established roadmap, obtained from stable production runs of different rubber compounds and process conditions.

Moreover, this integrated approach (operating roadmap), has the advantage of being fast and provides information about the stability of the process, while it is running, well before completing the production run, by optimizing the injection molding process for rubbers where knowledge about thermal history is lacking.

The integrated approach should be as general as possible, potentially applicable to any rubber compound processable by injection molding. It was therefore validated not only for industrial compounds, but also for two types of innovative compounds, characterized by a high level of sustainability: recycled rubbers coming from devulcanization process, such as fluorocarbon rubber (FKM) on one side, and acrylonitrile butadiene (NBR) rubber compounds containing electric arc furnace (EAF) slag (a by-product of steel industry) as reinforcing filler on the other side.

Finally, the research activity is also focused on the possibility to use the shear heating temperature, T_{SH}, in the setup of computer-aided engineering simulations (CAE) useful for mold design and injection molding process optimization.

Here below the ABSTRACT in Italian language.

1.1.Sintesi del lavoro

Poiché i produttori di autoveicoli richiedono un sempre più elevato livello di qualità delle guarnizioni, è ormai indispensabile che i produttori di guarnizioni raggiungano cicli di produzione molto stabili caratterizzati da una minima quantità di difetti e scarti. Pertanto, per lo stampaggio a iniezione della gomma è divenuto necessario sviluppare un adeguato controllo di processo tale da tener conto delle sue fluttuazioni.

Dal punto di vista della sostenibilità, gli scarti di gomma non si degradano e rimangono a lungo nell'ambiente. Pertanto, per aumentarne la sostenibilità, la prima strategia è quella di ridurre i rifiuti generati. La riduzione dei rifiuti di gomma durante la produzione comporta non solo un risparmio di materiale, ma anche di energia. L'obiettivo principale di questa tesi è quello di sviluppare un metodo per l'ottimizzazione del processo con lo scopo di ridurre la quantità di scarti e di aumentare la sostenibilità dei prodotti in gomma anche attraverso il loro riciclo.

In letteratura scientifica sono riportati approcci focalizzati sia sul miglioramento tecnologico degli strumenti di laboratorio convenzionali, come l'RPA e il reometro capillare, che sul miglioramento tecnologico della macchina per lo stampaggio a iniezione, utilizzata come reometro di laboratorio (ad esempio, slit die rheometry). Sebbene siano stati impiegati specifici sensori di pressione e temperatura direttamente sulla macchina per lo stampaggio a iniezione, tali da fornire un monitoraggio in linea; tuttavia, questi sono risultati troppo suscettibili alla manipolazione, all'usura ed alle incrostazioni.

Pertanto, questa attività di ricerca mira a sviluppare un approccio integrato, tale da combinare dati di laboratorio e di processo, utile a migliorare il controllo del processo di stampaggio a iniezione ed a ridurre la quantità di difetti e scarti.

Il metodo proposto si basa su un rapido monitoraggio in linea della temperatura superficiale della gomma (shear heating temperature, T_{SH}) mediante una termocamera a infrarossi, posizionata verso l'uscita dell'estrusore della macchina di stampaggio a iniezione.

Questa temperatura misurata ha portato al calcolo di un parametro tecnologico denominato shear heating parameter, η_{SH}, che tiene conto sia delle proprietà fisiche del materiale (densità e capacità termica) che delle condizioni di processo (rapporto lunghezza / diametro della vite, L/D).

Pertanto, il monitoraggio di η_{SH} ha consentito di ottenere un valore aggiunto per definire quantitativamente la qualità dell'articolo stampato. Inoltre, i valori log η_{SH} di un ciclo produttivo, combinati con i valori M_L, forniscono indicazioni sul "real output" del processo di stampaggio a iniezione, confrontando questi dati con una roadmap consolidata, ottenuta da cicli produttivi stabili di diverse mescole di gomma con diverse condizioni di processo. Inoltre, questo approccio integrato (operating roadmap) ha il vantaggio di essere veloce e di fornire informazioni sulla stabilità del processo, mentre è in corso, ben prima di completare il ciclo produttivo, ottimizzando così il processo di stampaggio a iniezione per le gomme in cui la conoscenza della storia termica è assente.

L'approccio integrato dovrebbe essere applicabile su qualsiasi mescola di gomma processabile mediante stampaggio ad iniezione. Pertanto è stato validato non solo su mescole industriali, ma anche su due tipi di mescole sostenibili: le gomme riciclate provenienti da processi di devulcanizzazione, come la gomma FKM, e le mescole di gomma NBR contenenti scorie di forni elettrici ad arco (EAF), un sottoprodotto dell'industria siderurgica, come riempitivo di rinforzo.

Infine, l'attività di ricerca si è concentrata sulla possibilità di utilizzare shear heating temperature, T_{SH} nell'implementazione di simulazioni computer-aided engineering (CAE), utili per la progettazione di stampi e l'ottimizzazione del processo di stampaggio a iniezione.

2 INTRODUCTION

Currently, rubber is broadly being used to produce a wide range of products for several applications such as automotive, building and construction, material handling, packaging, toys, etc [1]. Rubber is defined as "a material that is capable of recovering from large deformations quickly and forcibly and can be, or already is, modified to a state in which it is essentially insoluble (but can swell) in boiling solvents, such as benzene, methylethylketone, and ethanol-toluene azeotrope" (*ASTM D1566-21*). Their peculiar mechanical hyperelastic behaviour makes it the first choice for sealing elements. Such technical rubber products are mostly produced by the injection molding process. This process is the most important, widespread, and productive procedure of rubber compounds processing, and offers production of very complicated product geometry in one cycle, possibilities of production of several identical or different products in the same cycle, production of multicolour or multi-component products, production of hollow products, and production of macro and micro products as well. Nowadays, the rubber industry requires sealing and gaskets manufacturing process with very high-quality level. Manufacturing defects and scraps are a huge problem in many processes, especially due to the fact that their reduction depends on skilled employees. An increase of production process efficiency would bring about at least two advantages: (i) higher quality parts; (ii) higher sustainability.

From the point of view of production quality, zero-defect manufacturing and flexibility of production processes are some of the main challenges for European manufacturing, in the automotive sector especially. Due to the high competitiveness of rubber gasket suppliers, the Tier 1 and original equipment manufacturer (OEM) require high quality level of the final parts to be assembled and equipped in their factories. Therefore, it is mandatory that the gasket manufactures achieve a high level of production runs stability with minimized defects (zero-defect) and scraps amount. Instead the flexibility is based on the continuous change in automotive standards and requirements, thus the R&D, technical and production departments of rubber companies must adapt their solutions to new, constantly evolving standards. Traditionally, the decisions in manufacturing lines to reduce the defects were taken only by skilled employees (*e.g.*, chemist and engineer). Nevertheless, nowadays automated factories, computer tools and new technology can help significantly to collect data, translate them into information, detect process fluctuations and generate decisions to initiate corrective actions. However, this automation has some additional difficulties on unexpected external and internal disturbances or uncertainties in the production process (*e.g.*, a failure of temperature regulation device may not be detected by an automated control system). In order to perform a correct real-time process control, these uncertainties, which propagate from the raw material until the final product, need to be considered [2]. Therefore, a suitable process control for rubber injection molding able to take into account process fluctuations still has to be developed, and is in accordance with the technological improvement in the rubber field.

From the point of view of sustainability, rubber waste (material after the end of life and scrap materials from technical items production process) doesn't degrade and remains for a long period of time in the environment. The rubber industry produces every year about 2.97 million tonnes of rubber wastes, mostly from tires of

automobiles, trucks and motorcycles, but also of industrial waste and scrap coming from rubber compound, molding and finishing process of gasket, sealing and technical items [3]. Due to the low market value of the scraps and the lack of effective solutions for their recovery, the only option currently is disposal by incineration or landfill (for industrial scraps, this currently costs around € 240/ton for landfill and € 130/ton for incineration). Combustion and landfilling as traditional methods of polymer waste elimination have several disadvantages such as the formation of dust, fumes, and toxic gases in the air, as well as pollution of under-ground water resources. The increase of rubbers waste materials' generation in the world led to the need to develop suitable methods to reuse these waste materials and decrease their negative effects by simple disposal into the environment. The European Union (EU) waste policy provides a framework to improve waste management, which is defined in the Directive 2008/98/EC of the European Parliament and of the Council. The Directive defines a 'hierarchy' to be applied by EU Member States in waste management, which gives a priority order in waste prevention and management legislation and policy, namely: (a) prevention; (b) preparing for re-use; (c) recycling; (d) other recovery, *e.g.*, energy recovery; and (e) disposal.

Therefore, to increase the sustainability of rubber products, the first strategy is to reduce the generated waste. The main aim of this thesis is to develop a method for process optimization with the purpose to reduce scraps coming mainly from the molding phase. An estimated rubber scraps amount from industrial injection molding process is 15-20%, comprising purges from start-up phase, scraps from molding (mold flash), scraps from finishing phases, such as deburring and post-curing, and defected / not conformed parts from final control.

Reducing rubber waste during production involve not only material savings, but also energy savings. In recent years, decrease of energy consumption in the field of equipment for injection moulding is a general trend. Along with energy saving during injection molding cycle, energy efficient injection molding should be considered even in early phases of moulded part design, selection of molded part material, and mold design. Energy efficient injection moulding has not only economically, but also environmentally positive impact. It is the fact that consumption of 1 kWh of electric energy presents approximately equivalent of 0.43 kg of carbon dioxide [4].

Another strategy to increase sustainability of rubber products is recycling the waste materials. The treatments currently used for the recovery of plastic and rubber are based on different concepts: in the case of thermoplastics, the material can be recycled through a melting and regranulation procedure of suitably mixed waste, while in the case of rubber (thermoset elastomers) treatment is more complex because a devulcanization (either chemical or mechanical) process for the molecular modification of the product is needed [5]. The latter could be investigated case by case in accordance with elastomer type, fillers and curing system types. Furthermore, the chemical devulcanization process had only a limited industrial scale up. Considering new European Union directives and objectives on Circular Economy, Environment and Recycling, the automotive sector has started to review the car design and production to meet higher environmental sustainability requirements [6]. A way to achieve these objectives is to work on new rubber materials improving the reuse of polymeric materials and

finding alternative paths to produce new green polymers [7]. In this thesis, the proposed process control is investigated also for a recycled rubber, combining both waste reduction and recycling strategies.

The approach proposed in the present work is based on the measurement of rubber temperature, aware of the fact that this is the most influencing parameter affecting the injection molding process. Injection molding process of rubber is influenced by the rubber rheological behaviour, which in turn is affected by viscosity, pressure, temperature and shear rate [8-11]. The pressure introduced to the rubber during plasticizing in the injection molding machine extruder, and during the injection process as materials are forced through the injection sprue, deforms the material by shear [8]. Due to the high viscosity level of rubber, the temperature of rubber increases during flow. The heat generated by shearing the rubber during the injection process, can also significantly reduce the required cure time, especially when compared to other molding processes. Therefore, one of the most important parameters to be measured and controlled is temperature [9-11]. A traditional injection molding machine relies on both controlled heating system and internal shear heat generation (shear heating) to provide the necessary heat to bring the polymer up to the necessary temperature in a plasticizing extruder [9-10]. The last factor is a phenomenon where internal friction within the rubber, while it is flowing, generates heat and locally reduces the viscosity [9-28]. This phenomenon is often present in the industrial processing of rubbers and, although it is advantageous to increase the temperature of the rubber by saving energy, it complicates the control of the temperature and also of the viscosity. Therefore, the higher cure temperatures mean shorter cure cycles. Many rubber parts are therefore cured at higher temperature ranges to achieve a greater productivity, provided that risk of scorching, reversion, mold fouling, and thermal degradation is not a problem at these higher temperatures. An optimal rubber temperature must ensure a balance between not having excessively high viscosity, scorch safety, and thermal degradation. Therefore the measure and control of the rubber temperature is crucial to obtaining high quality rubber parts.

The actual rubber temperature in an injection molding machine, mostly generated by shear heating, is very difficult to replicate in the laboratory by typical rheological instruments such as a moving die rheometer (MDR), because the MDR doesn’t reproduce properly the physical process occurring in the injection stage of the molding machine extruder.

Therefore, there is a need to develop tests which realistically predict the processing behavior, with the purpose to improve the process control for optimal injection molding of rubber parts [29]. Establishing correlations between process parameters and the rheological behavior provides a more accurate and reliable approach to process optimization.

2.1 Aim of the work

This research activity aims to develop an *integrated approach* useful to improve the injection molding process control, and to reduce the defects and scraps amount during the manufacturing process of rubber parts by injection molding. The proposed method is based on a very fast online monitoring of the surface rubber temperature (shear heating temperature, T_{SH}) by an infrared thermal camera, pointed toward the rubber leaving the extruder barrel of the injection molding machine. Correlations between experimental laboratory data (from MDR laboratory measurements) and process data (from T_{SH}) were investigated and their advantages and potentialities explored.

The integrated approach should be as general as possible, potentially applicable to any rubber compound processable by injection molding. It was therefore validated not only for industrial compounds, but also for two types of innovative compounds, characterized by a high level of sustainability: recycled rubbers coming from devulcanization process, i.e. instance high performance elastomers (HPE) such as fluorocarbon rubber (FKM) on one side, and acrylonitrile butadiene (NBR) rubber compounds containing electric arc furnace (EAF) slag (a by-product of steel industry) as reinforcing filler on the other side.

Finally, the research activity is also focused on the possibility to use the shear heating temperature, T_{SH}, in the setup of computer-aided engineering simulations (CAE) useful for mold design and injection molding process optimization.

Figure 1 shows the simplified block diagram that summarizes the guideline to improve the process control in injection molding machine, and based on the integrated approach highlighted in this research activity.

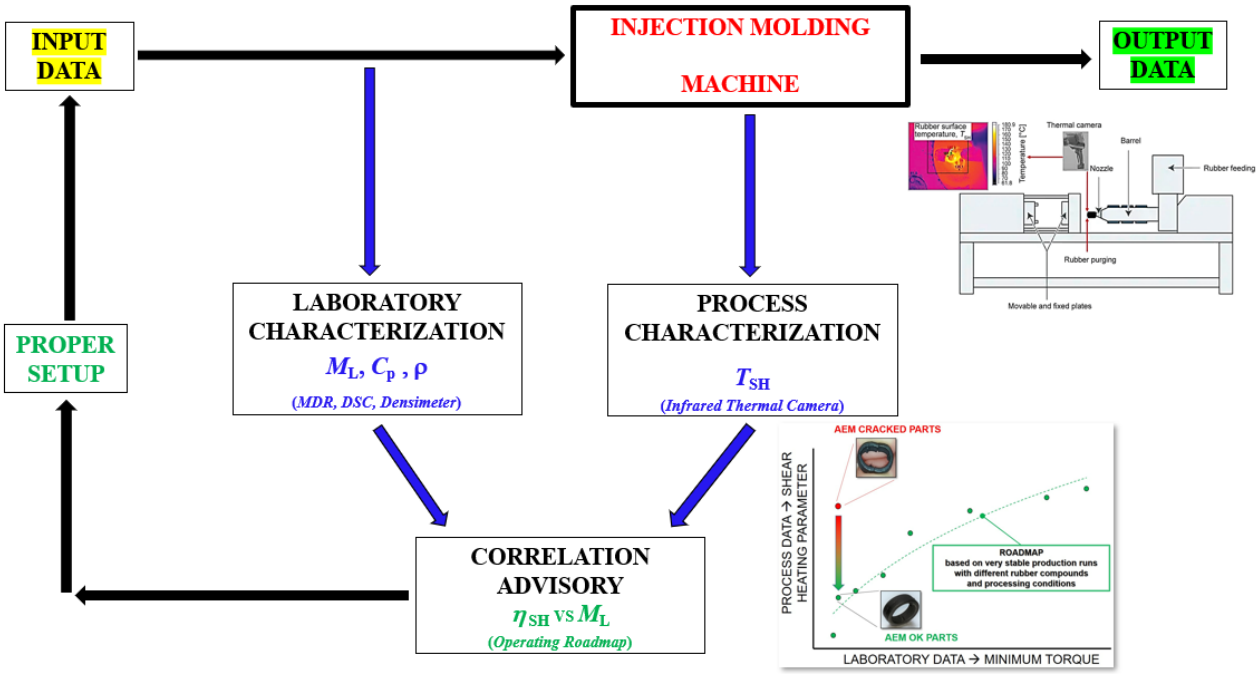

Fig.1. Integrated approach to improve the process control in injection molding machine.

2.2 Structure of the thesis

In *Chapter 3*, an appropriate literature review in the context of the thesis has been provided. A detailed overview related to the designation, types, curing systems, properties and performance, as well as applications of the rubbers is reported. Furthermore, the rubber processing by injection molding, including the machine, process parameters setup, thermal history and the main next industrial steps such as stabilization, deburring, and post-curing especially, as well are explored. This chapter especially provides the importance of process control in the injection molding based on the common approaches already used, such as design of experiment (DOE), computer-aided engineering (CAE) simulations, and the slit die rheometry of thermoplastics and elastomers by using the processing machines. Besides, the existing technologies about the rubber recycling are reported in this chapter.

In *Chapter* 4, the theoretical background in the context of the thesis has been provided. This research activity started by evaluating the studies of Nishizawa about the heat controls and rubber flow behavior in the extruder and injection machine and the problems occurring in these processes [16]. Especially, the equation reported in Nishizawa studies related the temperature rising from shear heating of rubber in injection molding machine extruder to the rubber compound viscosity during the injection phase. The equation was modified and used to calculate a technological parameter (the shear heating parameter, η_{SH}) useful for the process control, starting from the online measured shear heating temperature (T_{SH}) of the rubber. Obviously, approximations and limits of the above-mentioned equation also are explored. This chapter describes the new parameter for online control of rubber rheology behavior during the injection molding process.

Chapter 5 is concerned with the detailed description of the analytical instrumentation and experimental procedures adopted in the present research activity. The experimental section was designed to describe an overview of both the laboratory characterization on standard rubber samples and final products, and the processing trials performed directly in injection molding machines during daily production runs. The thermal controls performed by the infrared (IR) camera as well are described.

In *Chapter 6*, the results along with the discussion have been presented. Firstly, in this chapter the effects of various process parameters (*e.g.*, injection pressure, injection speed, screw speed rotation, screw length over diameter ratio) on T_{SH} were investigated for an ethylene acrylate rubber (AEM) compound. Moreover, also the effect of material properties, varied due to exceeding the shelf life, was investigated.

Secondly, the effect of the variation of T_{SH} on the final properties of the AEM rubber components was investigated via physical-mechanical characterization.

Thirdly, the integrated approach based on the correlation between two technological parameters such as shear heating parameter (η_{SH}) vs minimum torque (M_L), operating roadmap, likewise its use in industrial production runs, is reported. To show the potential of this tool, it was successfully used to optimize the injection molding of industrial production of AEM rubber compound affected by scorching and thermal degradation issues.

Fourthly, this chapter also reports the results about the implementations of T_{SH} and η_{SH} in the setup of CAE simulations.

Finally, remarks about the application of T_{SH} and η_{SH} in the processing trials of recycled FKM rubber compounds, and NBR rubber compounds containing EAF slag as reinforcing filler, have been presented.

In conclusion in *Chapter 7*, the potentialities of T_{SH} and η_{SH} application with the purpose to reduce defects and scraps amount in the industrial practice by promptly optimizing of the process parameters, has been summarized. In addition, it is emphasized the importance to develop an integrated approach based on the operating roadmap, proposed as new and very suitable tool for industrial practice. An outlook on future possible applications of this operating roadmap (η_{SH} vs M_L, correlation), in artificial intelligence (AI) as predictive algorithm; and of the shear heating parameter, η_{SH}, in CAE simulations as viscosity of the rubber compounds, is also reported.

Most of the results of the doctoral thesis have been published on refereed international journals:

Publication I: presentation of the shear heating parameter useful for process control in injection molding process [10].

Publication II: on the applications of shear heating parameter for injection molding process optimization of AEM rubber compounds [27].

Publication III: on the influence of process parameters on shear heating effects during injection molding of rubber [28].

The original papers are reported in the appendix.

3 LITERATURE REVIEW

This chapter provides a general overview about the features of rubbers, also including their processing by injection molding, Furthermore, the process control in the injection molding machine, and the existing technologies about the rubber recycling are also reported.

3.1. Rubber

The term rubber (or elastomer) in scientific literature refers almost exclusively to cross-linked (or cured) material defined as a viscoelastic solid incapable of giving rise to shearing phenomena. The principal characteristic of elastomers is their high deformability and their ability of recovering deformations after removal of stress. For uncured elastomer matrices, there does not exist the great wealth of information, models and correlations that can be found for vulcanized elastomers or for plastic materials. Moreover, industrial raw rubbers are compounds based on elastomer and other ingredients (solid powers and viscous liquids) that give it heterogeneity responsible for its unique rheological behavior, which is difficult to investigate and requires continuous effort to find suitable operating conditions [30].

3.1.1. Rubber history

The first written evidence of rubber relates to the product of a plant native to South America, *Hevea Brasiliensis*, and goes back to the middle of the Sixteenth century. However, the first European who probably discovered the existence of natural rubber was Christopher Columbus during his voyage of 1493-96. In other parts of the world, the original name cau'uchu has been retained, literally meaning the "tree that cries".
Nevertheless, natural rubber remained a mere curiosity until 1823, when Charles Macintosh patented the use of solutions of natural rubber in light oils for waterproofing textiles. In 1830, Thomas Hancock subjected natural rubber to intense mechanical stress (mastication), and discovered that, in this way, its marked elastic characteristics were progressively reduced to the point where a material adaptable to molding was obtained.
The absence of elastic properties and dimensional stability, however, limited its use until, in 1839, in the United States, Charles Goodyear discovered that superior qualities could be conferred on rubber by heating it with sulfur and lead oxide. Hancock exploited this process, introducing the term vulcanization (or curing), to produce materials with a reduced tendency to becoming sticky upon warming and which were insoluble in common solvents.
The large availability of natural rubber, however, rendered research on the subject somewhat unattractive, but this situation changed at the start of the First World War, which created a serious shortage of rubber, in Germany and Russia in particular. Research, which during the war enabled the Germans to produce about 2,350 tonnes of methyl rubber, suffered an immediate slowdown at the end of the war, but was quickly resumed with greater intensity in those countries that considered the availability of synthetic rubber to be strategically

important. It was, in fact, in Germany in the 1930s that industrial production of polybutadiene and, subsequently, of the copolymers styrene-butadiene and styrene-acrylonitrile began. Preparation technologies were devised in the United States in the period preceding the Second World War and subsequently further developed. After the war, which together with the advent of new polymerization technologies, these technologies made it possible to produce materials with enhanced end-use properties and to develop new materials that would satisfy the demands of the emerging aerospace industry [30-31].

3.1.2 Rubber structure

The basic material in elastomeric compounds is rubber which can be natural, obtained from the latex of *Hevea brasiliensis*, or synthetic, obtained following a chemical synthesis process. The rubber is added with many types of ingredients to obtain an almost infinite number of compound recipes, each with properties, features and different performances.
However, each rubber compound has various aspects in common with the others:

- consists of a base elastomer with a polymeric structure;
- needs addition with specific additives;
- undergoes mechanical processing and curing reaction;
- during exercise, is affected by aging phenomena due to atmospheric agents, temperature and contact with chemicals;
- has its typical shelf life of use.

The base elastomer is the key ingredient that determines the mechanical, thermal, physical and chemical behavior of the rubber compound, performance and cost as well. Elastomers are macromolecules made by the repetition of the same base unit called “monomer”, the number of monomers repeated in the chain rep-resents the degree of polymerization (DP) of the macromolecule [32]. It is calculated as the ratio of molecular weight of a polymer and molecular weight of the repeat unit [33].
Macromolecules, depending on their spatial arrangement, can be classified in linear, branched or reticulated. They generally have no precise order or crystalline structure, except in rare cases, but they are entangled with each other. Elasticity is the property that enables a material, after being deformed, to return to its original shape once the cause of deformation is removed. This property characterizes cured elastomers in an altogether specific way: unlike metals and glass, they can stand very high levels of deformation without breaking and then go back to their original shape. In polymers, the smallest unit involved in the rotation around a single bond is called a conformer and, unlike simple molecules, involves molecular segments.
The condition through which a polymer chain becomes flexible is represented, therefore, by a reasonable ability to rotate around a significant number of bonds in a chain; only long polymer molecules without sterically hindered side groups have the potential of easily reaching a high number of isoenergetic conformations.

To build a three-dimensional structure capable of a reversible response to large deformations, the elastomer chains must be linked by permanent bonds called cross-links. These links are made by chemical bonds introduced during the curing process.

Figure 2 shows a structural model of cross-linked elastomers (rubber), made by macromolecules which are thermally cross-linked irreversibly through covalent bonds. The number of cross-links, the distribution of the dimensions of the elastically active chains and the type of the various structural elements of the elastic network depend on the way in which the elastomer has been vulcanized, and are of great importance in determining its properties [30-32].

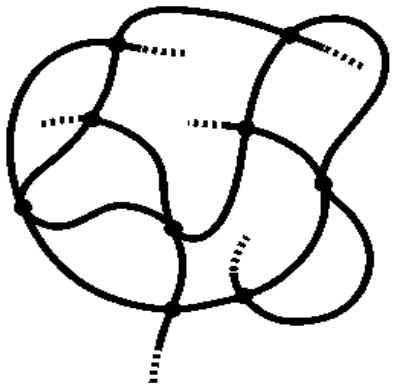

Fig.2. Structural model of cross-linked elastomers (rubber).

3.1.3 Rubber classification

Natural rubber (NR) is the precursor of all elastomers and has good mechanical characteristics even without reinforcing fillers. Its molecule is high molecular weight 1,4-cis-polyisorpene $(C_5H_8)_n$ and is obtained by polymerization of isoprene. The latter is obtained from the *Hevea Brasiliensis* lattice in which it is represent the 35% of the volume. Natural rubber is used in a wide range of applications, mainly in the tire industry, where it is required high elasticity, high resistance to abrasion, traction and tearing. Nowadays it has been replaced in many applications from synthetic rubbers, but NR can also be used in mixture with them to improve tack and mechanical properties.

Instead, the synthetic rubbers are synthetized in the laboratory starting from monomeric precursors to the polymerization reaction. The Russians, in 1910, prepared such a rubber, known chemically as polybutadiene. In the 1930s, the Germans began the commercial production of a synthetic rubber called Buna-S (styrene butadiene copolymer). With the outbreak of the Second World War, both the USA and Europe were extremely vulnerable to a shortage of supply of natural rubber, which could have had a catastrophic effect on the war effort. A massive R&D project was initiated, between government and industry in the United States. Styrene butadiene rubber (SBR) was improved, then manufactured on a large scale and called Government Rubber-Styrene (GR-S), later to be known generically as SBR, which today is a major material in the rubber industry.

In 1934 production was started in Germany, of an oil resistant rubber called Buna-N, the name later changed in 1937 to Perbunan, generically nitrile rubber (NBR). Other significant materials are Viton (FKM, fluoro-elastomer) by DuPont (now Chemours) in the 1950s and ethylene propylene rubber (EP(D)M) in the 1960s.
Nowadays, there are about thirty different types of synthetic rubbers, divided into groups according to their applications, polarity, bond saturation, and atoms bonded to their polymer chains. Therefore, the rubbers can be classified depending on the type of atoms that form the monomer of the polymer chains and which consequently influence the features and performance of final products [31-32].
As far regarding their applications/performance, the rubbers can be divided in:

- general purpose rubbers: *e.g.*, NR, isoprene rubber (IR), butadiene rubber (BR), SBR. They are used in tire production and technical articles in series;
- special rubbers and high performance rubbers: *e.g.*, EP(D)M, NBR, hydrogenated acrylonitrile butadiene rubber (HNBR), polyacrylate rubber (ACM), AEM, FKM and others. They are developed to meet thermal stability/fire resistance, heat aging resistance, chemical resistance, and swelling resistance in non-polar oils.

Depending on their polarity, the rubbers can be divided in:

- non-polar rubbers (*e.g.*, NR, IR, BR, SBR, EP(D)M): elastomers based on pure hydrocarbons without polar groups;
- polar rubbers (*e.g.*, NBR, HNBR, ACM, AEM, FKM): elastomers which in addition to having C and H atoms present in their structure also different atoms (Cl, F, etc.) or groups (-CN, -$COOC_2H_5$) which give this type of rubber better resistance to some agents such as gasoline and mineral oils [34].

In organic chemistry, a hydrocarbon chain is called to be saturated when each carbon atom (C) directs to form four simple bonds. In the opposite sense a chain is called to be unsaturated when for complete the valence of C double or triple bonds must be formed [35].
Increasing the number of double bonds decreases the resistance to oxidation reaction and atmospheric agents, however they are easier and faster to cross-link. Therefore, on the basis of the abovementioned definition, the rubbers can be divided in:

- saturated rubbers (*e.g.*, EP(D)M, AEM, FKM, HNBR): elastomers with better resistance to aging and oxidation.
- unsaturated rubbers (*e.g.*, NR, IR, BR, SBR, NBR): elastomers with lower resistance to aging and oxidation, and prone to cross-link.

According to *ASTM D1418-22* the rubbers shall be classified also from the chemical composition of the polymer chain in the following manner:

- *M* group: rubbers having a saturated chain of the polymethylene type;
- *R* group: rubbers having an unsaturated carbon chain;
- *O* group: rubbers having oxygen atoms;

- *N* group: rubbers having nitrogen, but not oxygen or phosphorus atoms;
- *Q* group: rubbers having silicon and oxygen atoms;
- *T* group: rubbers having sulfur atoms;
- *U* group: rubbers having carbon, oxygen, and nitrogen atoms;
- *Z* group: rubbers having phosphorus and nitrogen atoms [32, 34].

3.1.4 Rubber compounding

In the rubber industry, with the purpose to design and to produce a rubber product that satisfies precise technical requirements and performance, it is mandatory to:

1. select the proper raw materials;
2. blend them in the correct proportions in appropriate equipment;
3. form the resulting blend into the desired shape;
4. provide the finished product dimensionally stable.

The first stage, well-known as compounding, belongs to the formulation of a blend of rubber and various ingredients. These are first thoroughly mixed (stage 2) and then formed (stage 3). All the operations characteristic to the blending of the various ingredients and their forming constitute the processing. The physical properties of an uncured elastomer do not permit a manufactured item to retain its dimensional and mechanical characteristics over time; therefore, it is necessary to generate a stable molecular network (stage 4), making use of a chemical reaction capable of joining the polymer chains one to the other. This process is known as curing reaction, which takes a place within the mold cavity during the injection molding process [30]. Figure 3 shows a simple flow chart of rubber processing.

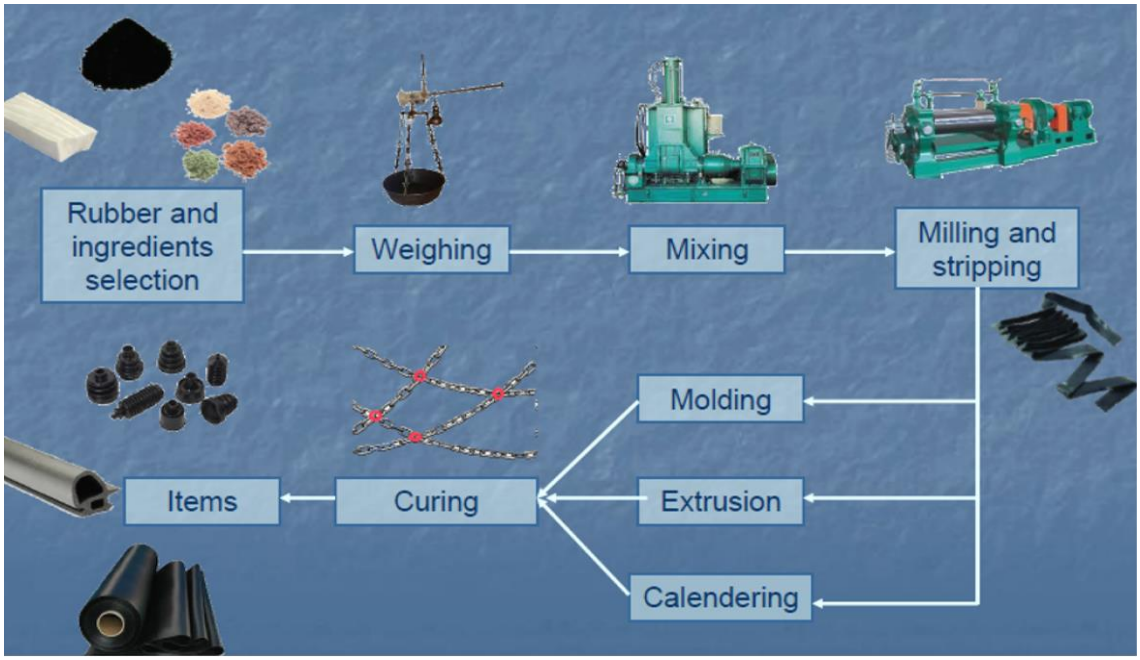

Fig.3. Rubber processing flow chart.

First of all must be established the characteristics of the final rubber product, then the base elastomer and the other ingredients required to obtain the properties required are selected. The recipe of the compound consists of a list of the many ingredients, and guidelines on how to mix them. Rubber chemists use the term parts per hundred rubber (*phr*), meaning parts of any non-rubbery material per hundred parts of base elastomer (rubbery material). They prefer this rather than expressing an ingredient as a percentage of the total compound weight. Parts can mean any unit of weight (kg, lb, etc.) if the same weight unit is used throughout the formulation. The ingredients required for the preparation of a rubber compound belong to the categories indicated here below.

- *Base elastomer*: main ingredient can consist of natural or synthetic rubber, or thermoplastic elastomers.
- *Curing system*: chemicals required to generate the three-dimensional network that gives the rubber its typical characteristics, a typical curing agent is sulfur, used in the range of 0.5-3.0 phr.
- *Accelerators*: chemicals that interact with the curing agent to reduce the cure time, typically used in the range of 0.5-1.5 phr.
- *Activators*: made up of metal oxides, of carbonates and of alkaline hydroxides, added in the range of 2.0-3.0 phr, by forming chemical compounds with the accelerators and by modifying the cure rate and the cure state (cross-linking density).
- *Retarders*: chemicals that interact with the curing-accelerator-activator system, creating a period of time during which curing reaction does not take place. They also avoid pre-curing (as a scorch-retarder) and are used in the range of 0.1-0.5 phr.
- *Organic acids*: their reaction with the activators provides the cations necessary for the formation of chemical complexes with the accelerators. Monobasic acids such as stearic, oleic, lauric, palmitic, and myristic acids, and hydrogenated palm, castor and linseed oils are used in the range of 1.0-3.0 phr.
- *Antioxidants*: they protect the rubber from oxidation, accelerated by UV light and ozone, which generally initiates a structural modification to a lesser or greater degree in the polymer chain with consequent variations to its mechanical properties. Secondary amines, phenols hindered by t-butyl groups in the ortho-position and organic phosphite's are added in the range of 1.0-2.0 phr
- *Fillers*: initially added to rubber in the form of small particles for economic reasons, and after 1904, the addition of carbon black to NR had a reinforcing effect, improving some characteristics such as resistance to abrasion and tearing, and increasing the values of the elastic modulus and of the tensile strength. Fillers are subdivided into two groups: reinforcing fillers and inert fillers. The inert fillers (*e.g.*, kaolin, barytes, carbonates of calcium and of magnesium, of iron and of lead), powdered to dimensions of 0.1 mm, are used to modify some technological characteristics of the cured elastomer such as its hardness, its density or its electrical properties. The reinforcing fillers (*e.g.*, carbon black and silicas), instead, have a most important effect on the mechanical and dynamic characteristics of

the cured elastomer in that, by interacting with the macromolecules, they take part in the elastic network. Furthermore, carbon black, added to the mixture can give excellent resistance to UV light in an otherwise non-resistant elastomer. This is an supplementary bonus for using carbon black, since it is normally added for other reasons.

- *Plasticizers*: chemicals accomplished of improving processability, of reducing the hardness of the rubber compound and increasing their elasticity and cold flexibility. Rubber compounds are generally plasticized by non-volatile solvents to reduce the viscosity of cured parts. They belong to two main classes: extender oils, from the petroleum refining industry, suitable for diene-based rubbers such as SBR, NR and BR, and esters, which are recommended for polar rubbers such as AEM, NBR and HNBR rubbers. The selection of the most suitable plasticizer is based on a criterion of compatibility [30-32, 36]. Chemical interaction between polymers and plasticizers must be considered. The solubility parameter (δ) should be as closest as possible to that of the elastomer for good compatibility [37].
- *Processing aids*: additives typically used to improve the other ingredients incorporation (peptizers and dispersing agents), to regulate the processing (lubricants), and or to facilitate the demolding (mold release agents). Processing aids are used in relative low amount (1.0-5.0 phr). The selection of processing aid depends on both the application and the elastomer involved: it has to be selected according to the desired effect in rubber compounds.
- *Other ingredients*: chemicals of many types that are added in variable amounts and proportions such as flame retardants (aluminum hydroxide), antistatics (metal powders or fibers, carbon black) and colorants (metal oxides).

The final properties of rubber compound depend on its composition and primary structure, but also on the degree of homogeneity with which the many ingredients have been dispersed within it. The mixing of solid particles with highly viscous material is a very complex operation, which is divided into incorporation, dispersion and distribution. The incorporation starts with the separate ingredients of the compound and ends with a homogeneous mass capable of flowing. When a polymer is mixed with a rigid additive, the viscosity of the compound increases with the volumetric fraction of the additive and its elastic memory diminishes. The use of plasticizers and oils, which produce greater molecular mobility, allows the polymer to quickly exit the voids of the reinforcing filler aggregates, thereby diminishing the proportion of entrapped rubber, reducing the viscosity of the mass and favoring the subsequent phase of dispersion. The latter involves the fragmentation of filler agglomerates into smaller aggregates and primary particles.

It is followed by the distribution stage, which is split into macro-scale distribution, where the homogenization is carried out on large dimensions and micro-scale distribution, which operates on small sizes and affects, above all, the separation of fragments of the filler aggregates after their disruption.

During mixing, the temperature rises especially, and the viscosity decreases along with the amount of applied power; the mixing time should therefore be increased, but not beyond certain limits in order to avoid premature

curing. The time interval, measured from the moment that the compound containing curing agents is heated to the moment at which the reaction of cross-linking starts, is called the scorch time. This time can be modified by using retardants as well as by the choice of cure system including accelerator.

For the processing of rubber, batch mixers are mainly utilized, involving typically of open mixers or open mill (two roll mills) and of internal mixers. In an open mixer (Figure 4a), there exist three zones: one is located between the high powered (internally cooled) rollers; another, the bench, acts as a reservoir to feed the region between the rollers where the process of encapsulation takes place; the third, the belt, carries the rubber from the previous two areas. The rollers rotate in opposite directions at different speeds with a ratio that varies between 1 and 1.1. This mixing technology is suitable for small-scale production, or as the second stage of a mixing process that uses an internal mixer as a first stage. Internal mixer (Figure 4b) is the mixing machine mostly used in the rubber industry due to its versatility and ability to accept base elastomers in bales. The machine contains a diagram of the two counter-rotating rotors, of the piston, which allows for the introduction of the many ingredients of the blend into the mixing chamber when lifted, but which keeps the rubber in the mixing area when lowered, and of the discharge door. Cooling water passes through the rollers, the walls of the chamber and the discharge door. In 1916 Mr. Fernley H. Banbury, improved on an 'internal mixing machine' built by Werner & Pfleiderer by designing the *Banbury* mixer. The *Banbury* mixer had modified rotors and the addition of a floating weight. Observing the mixing of rubber in a roll mill makes it possible to identify two limiting situations: a dry behavior, which shows a critical factor relating to the shearing of the elastomer (the rubber breaks up); and a cheesy behavior, typical of materials characterized by poor elastic behavior and poor tensile properties, mainly related to the absence of high molecular weight fractions [30-32, 36].

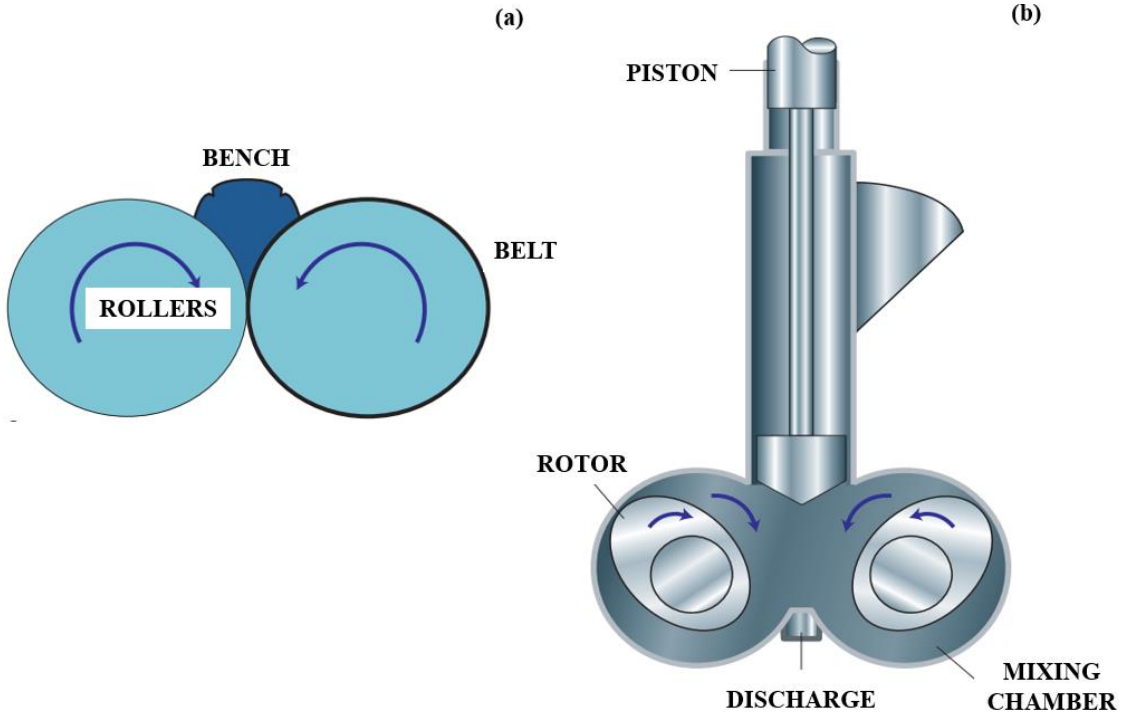

Fig.4. a Open mixer. **b** Internal mixer [30].

3.1.5 Curing reaction

The curing reaction causes the formation, between the macromolecules, of bonds that are randomly spaced along the molecular axis with a frequency of one link every 50-100 monomer units. The bonds formation between the macromolecules leads to significant physical modifications of the elastomer, which changes from a fluid soluble in solvents to an insoluble elastic solid with technologically useful mechanical properties. The rubber properties depend on the type and number of the links that connect the elastomer chains. Since the moment of network formation, the rubber becomes essentially insoluble in any solvent, and it cannot be processed by any means that requires it to flow, similar to processing in a mixer or extruder; on a mill or calendar; or during shaping, forming, or molding. Thus, it is essential that curing reaction takes place only after the rubber part is in its final geometric form. Figure 5 shows the effects of curing reaction on final properties, where it should be well-known that static modulus increases with curing. As the cure state increases, hysteresis is greatly reduced, there is an increase in hardness, while the permanent set values after compression (*compression set*) decrease. Hysteresis is the ratio of the rate dependent or viscous component to the elastic component of deformation resistance. It is also a measure of deformation energy, which is not stored but is converted into heat. Curing reaction then causes a trade-off between elastic and viscous behavior. Tear strength, fatigue life, and toughness are related to the breaking energy. Values of these properties increase with small amounts of cross-linking, but they are reduced by further crosslink formation. Properties related to the energy to break increase with increases in both the number of network chains and hysteresis. Since hysteresis decreases as more network chains are developed, the energy-to-break related properties are maximized at some intermediate crosslink density. It should be highlighted that the properties showed in Figure 5 are not functions only of crosslink density, but they are affected also by the type of curing system, base elastomer and amount/type of filler [36].

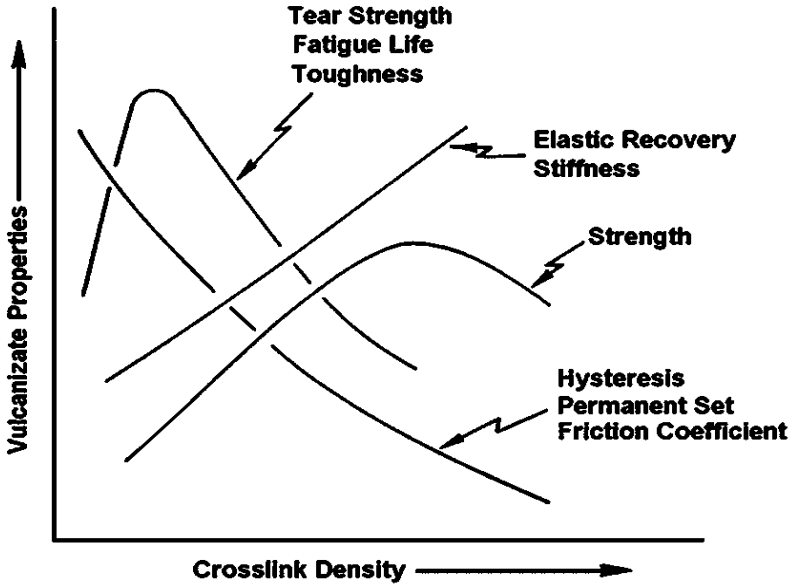

Fig.5. Effects of curing reaction on final properties [36].

The period of time needed to start the curing reaction (induction time), and both cure rate and cure state are measured in laboratory with cure meters or rheometers. There are two types of rheometers in the rubber industry, oscillating disc rheometer (ODR) and moving die rheometer (MDR), although their function are the same according to *ASTM D5289-95* [34]. However the laboratory tests performed in industrial practice with ODR and MDR, are used for the quality control of rheological parameters and of uniformity of rubber compounds. ODR and MDR record the so called curing curve, i.e. the torque needed to apply a sinusoidal oscillating shear strain to a specimen, initially uncured, at fixed temperature, recorded as a function of time. In ODR the rubber sample is enclosed in a heated cavity, and embedded in the rubber is a metal disc that oscillates sinusoidally around its axis, thus applying a rotational shear strain to the sample. In MDR one half of the die is stationary, while the other half oscillates. The sample is much smaller and heat transfer is faster. Also, because there is no rotor, the temperature of the cavity and sample can be changed more rapidly. In either case, ODR and MDR, torque is automatically plotted against time, giving the curing curve (see Figure 6). The measured minimum torque value (M_L), expressed in dN·m, is a rough indication of the rubber compound viscosity; hence variations of M_L affect the rubber processability [17].

Curing reaction is measured by the increase in the torque required to maintain a given amplitude of oscillation at a given temperature. The torque is proportional to a low-strain modulus of elasticity. Since this torque is measured at the elevated curing temperature, the viscous component is minimal. Thus, it has been assumed that the increase in torque during curing is proportional to the number of cross-links formed per unit volume of rubber. The torque is automatically plotted against time to give a so-called rheometer curve, or typically curing curve. Figure 6 shows a typical curing curve that gives a rather complete overview of the overall kinetics of cross-link formation and even cross-link break (reversion) for a given rubber compound. In a few cases, instead of reversion, a long plateau or marching cure can occur [36].

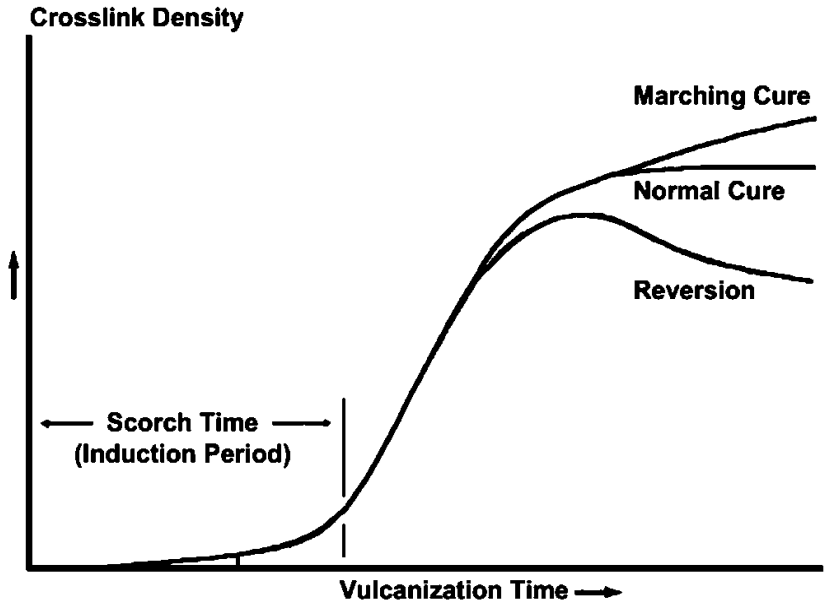

Fig.6. Curing curve from rheometers [36].

Reversion is a term usually associated to the loss of network structures by nonoxidative thermal aging. It is commonly employed with isoprene rubbers sulfur-cured.
It can be the result of excessive cure time (overcure) or of hot aging of thick sections. It is most severe at temperatures above about 155°C. It occurs in rubbers containing a large number of polysulfide bonds, C—S_x—C (x>2). Instead some rubber compounds can exhibit what is sometimes known as marching modulus, where the cure rate 'marches' on more and more slowly as the curing reactions proceeds.
Curing systems commonly employed in the rubber industry are sulfur cured (accelerated sulfur and sulfur donor), peroxide cured, diamine cured and bisphenol (ionic) cured [30-32, 36, 38-39].

3.1.5.1 Sulfur curing

The use of sulfur in the curing of rubber, discovered in 1839 by C. Goodyear and T. Hancock, is not suitable because the process is slow and inefficient. In the past, curing of natural rubber was carried out with 8 phr of sulfur for 5 hours at 140°C. In 1881, Rowley noticed that the presence of ammonia brought about an acceleration in the cross-linking reaction and, in 1906, G. Oenslager highlighted the advantages deriving from the use of aniline. In the years coinciding with the start of the First World War, the use of zinc oxide together with fatty acids was introduced and the time needed for successful curing was reduced to 3 hours. In 1907, due to its toxicity, aniline was replaced by a derivative resulting from its reaction with CS_2 (thiocarbanilide); a further development led to guanidine, to the dithiocarbamates and to the thiurams. None of these accelerators guaranteed the absence of cross-linking reactions during the blending phase of the ingredients, making the compounding operation difficult. It was only in 1925 that the first retarded accelerators were introduced, which made it possible the industrial manufacture of cord-ply pneumatic tyres. For many years, the adjustment of the scorch time was carried out by means of salicylic or benzoic acid or N-nitrosodiphenylamine until the first curing inhibitors were introduced in 1968: they represent an important class of substances that make it possible to reduce the risk of scorch (premature cure onset) without substantially altering the rate of the process. During curing reaction with sulfur, an evolution of the type and number of intermolecular bonds is observed, with consequent variations over time of the properties of the rubber: polysulfide bonds, C—S_x—C (x>2), progressively decrease as the cure time increases, the monosulfide bonds, C—S—C, increase and the disulfides, C—S—S—C, remain constant (about 20%). The introduction of an accelerator into a system consisting of polyisoprene and sulfur leads to the formation of a linear polysulfide (slow reaction), which, reacting in turn with the olefinic unsaturation, leads to the formation of a species where the accelerator is linked to the macromolecule through a polysulfide bond. The most widely used rubbers cured with sulfur, and containing a diene site for cross-linking, and are NR, IR, BR, SBR, EP(D)M and NBR.
About sulfur donor systems an increase in the accelerator/sulfur ratio leads to a continuing increase in the number of monosulfide intermolecular bonds. If the sulfur amount is less than 0.5 phr, however, acceptable elastic modulus values are not obtained. Some chemical compounds containing sulfur can be used as sulfur

donors during the curing reaction in formulations without sulfur. Some of these molecules are for example, trimethylene tetrathiafulvalene dithiolate (TMDT), play a role both as donors in formulations without sulfur and as accelerators in formulations with sulfur, while other substances, like 4,4'-dithiodimorpholine (DTDM), are not accelerators [30-32, 38-40].

3.1.5.2 Peroxide curing

Most rubbers having saturated hydrocarbon such as EP(D)M (copolymers), AEM (copolymers), HNBR, FKM and silicone rubbers (VMQ) can be cured with action of organic peroxides. Diacyl peroxides, dialkyl peroxides, and peresters have been used. Dialkyl peroxides and t-butyl perbenzoate give efficient cross-linking. Di-t-butyl peroxide and dicumyl peroxide give very good permanent set properties, but the former is too volatile for general use. Dicumyl peroxide is widely used, however its rubber parts have the odor of acetophenone, which is a byproduct of the curing process. Concerning the injection molding dicumyl peroxide allows very fast cure rate, meanwhile mold fouling phenomena increases. Ethylene propylene copolymers and ethylene propylene terpolymers are cured with peroxide and have more heat resistance compared to sulfur curing systems. This is due to the more stable C—C bonds as opposed to C—S—C sulfur bonds.
Figure 7 shows the mechanism of peroxide curing (free radical mechanism) consisting in the following steps: peroxide decomposition, where peroxide is decomposed by heat into free radicals (≥160°C for Dicumyl peroxide); hydrogen abstraction by radical that abstract hydrogen atom from elastomer to produce elastomer radical, and final cross-link by elastomer radicals in combination with each other to produce C—C bond.

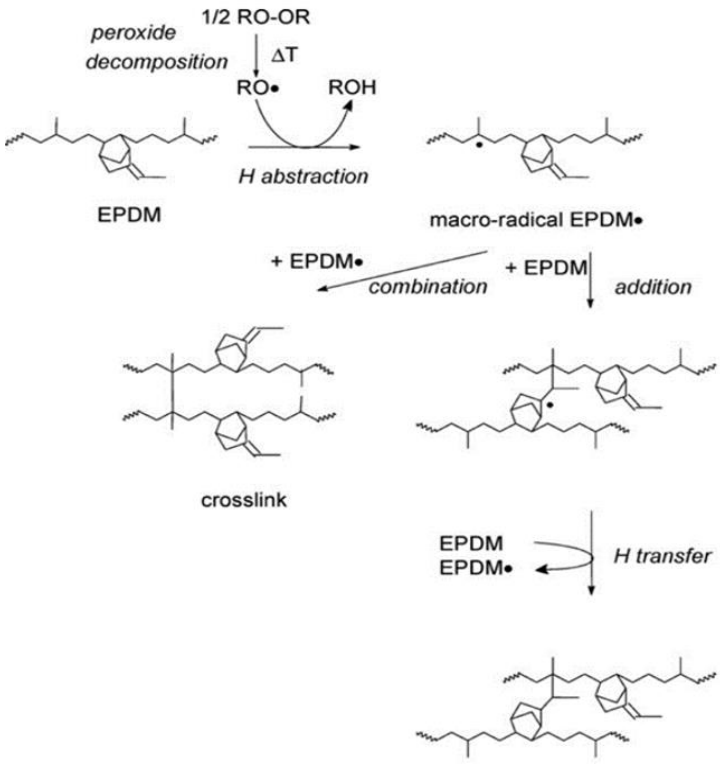

Fig.7. Peroxide curing mechanism of EP(D)M [41].

The peroxides essentially differ for the “half-life time”. The “half-life” is the time in which the peroxide loses half of its concentration at a given temperature. Therefore, the more thermally stable peroxides have a longer half-life time. The shorter the half-life time, shorter the curing time and the faster the decomposition and curing time at a given temperature. Peroxide curing leads to effective cross-link formation but also to some competing reactions, which detract from productive use of radicals. The competitive reactions include polymer scission or other degradation reactions. The utility of co-agents comes from promoting more efficient cross-link formation by establishing a higher concentration of reactive sites and reducing the chance of deleterious radical side reactions. This curing system offers some advantages such as better compression set and thermal resistance, meanwhile several disadvantages such as poor mechanical properties and the impossibility of varying the scorch time [29, 35, 39-42].

3.1.5.3 Diamine curing

Generally polar rubbers such as ACM, AEM (terpolymers), HNBR (high performance grades from *Zeon*), FKM can be cured with diamines. For instance, in AEM terpolymers made by ethylene, methyl acrylate and an acidic cure site monomer, the latter monomer is chemically functional to the primary diamines cross-link. The diamine curing system is generally composed by hexamethylene diamine carbamate (HMDC) which converts to hexamethylene diamine (HMDA) and carbon dioxide (CO_2) upon exposure to the high temperatures of the curing reaction. In an ideal curing reaction, each end of the HMDA reacts with the cure site monomer of a different elastomer chain to link the two elastomer chains together. The particularity of this curing system is that the acidic cure site monomer reacts with the diamine in two stages. In the first stage, an amide is formed and in the second stages an imide is formed (Figure 8).
The first step is the source of the scorch. Scorch issues can cause molding problems such as underfilling the mold cavity and problems at knit lines, which necessitate extra processing aids to lower viscosity. Scorch reactions are a function of time and temperature, and they become an issue for AEM terpolymer compounds at temperatures above 100°C. The imide formation is one of the keys for providing the characteristic good heat resistance and good compression set properties to final parts. About curing cycle, the amide formation is relatively fast while the imide formation is relatively slow.
For the injection molding process the assumption is that the amide formation takes place quickly in the mold cavity of the machine where a typical cycle time might be two minutes at 180°C. Another assumption is that the imide is formed in the post-curing phase, by a relatively long thermal treatment, which runs at 175°C for four hours in an air industrial oven. After the injection molding process, the part has dimensional stability, but the compression set is high (70 to 90% after one week at 150 °C), and the hardness and modulus are relatively low. The post-curing stage increases the hardness until the required specification, and the compression set drops to about 20-30%.

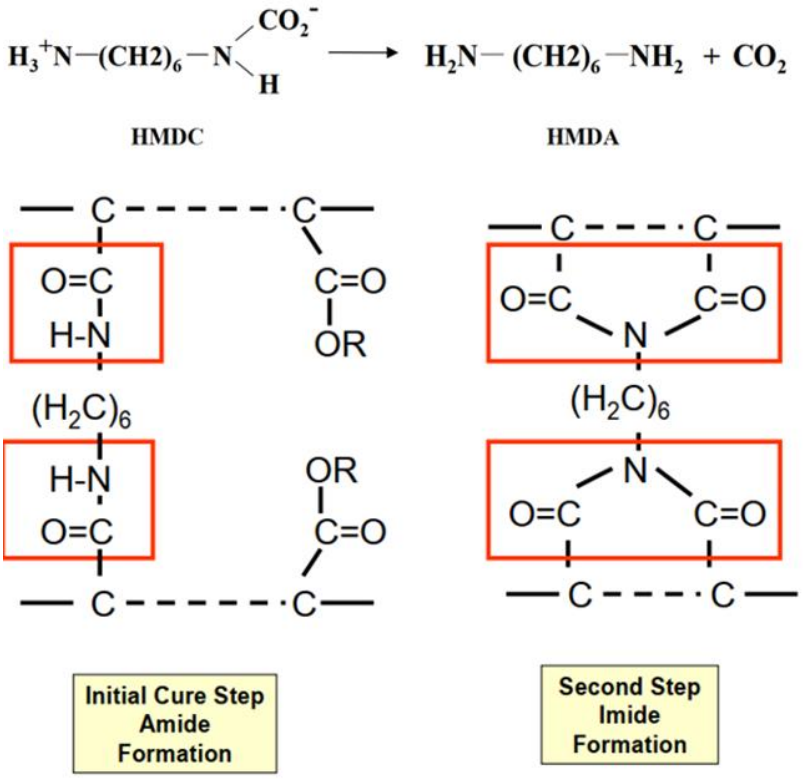

Fig.8. Mechanism for diamine curing system [43].

Thus an average increase in Shore A hardness with the post-curing stage is 5-6 points for standard specimens according to Shore A [34], and about 10-15 IRHD M (International Rubber Hardness Degree) Microhardness points for final parts as O-rings according to *ISO 48* [27].

Therefore, for rubber compounds diamine cured, the post-curing stage significantly changes the properties of compounds: the biggest effect is on compression set (lower/better) and on modulus (higher), the tensile strength and hardness increase and the percent elongation decreases. Most of the change in the properties occurs in the first 30 minutes of post-curing. Laboratory studies were conducted to eliminate the need for a post-curing stage for molded part by modifying the formulation and increasing the mold temperature. However the compression set values for the compounds that had not been post-cured were still relatively poor after these changes [27, 43-47].

About diamine curing system for FKM copolymer compounds the usual acid acceptor was magnesium oxide (MgO) added as curing auxiliaries. In this case, the mechanism proposed involves reaction of the amine base with elastomer chains to eliminate hydrogen fluoride (HF) and form double bonds, followed by reaction of the nucleophilic diamine with the double bonds to form cross-links with imine structure. The exact nature of active sites in the chains or of the resulting cross-links was not determined. Water produced from the neutralization of HF by magnesium oxide had to be removed by post-curing in an air oven. With water present in the cured parts at high temperature, hydrolysis of cross-links could occur, forming carbonyl structures on the elastomer chains with regeneration on the amine curing agent.

Even in this case the curing system has considerable processing deficiencies, giving scorch at 100°C to 140°C and relatively slow cure time at mold temperature between 160°C and 180°C, as well as sticking and fouling problems. Cured parts are characterized by good properties, but high temperature compression set resistance is mediocre, and retention of physical properties on long exposure to temperature about 200°C is relatively poor [48-49], therefore nowadays FKM is mostly cured by peroxide or bisphenol curing.

3.1.5.4 Bisphenol curing

FKM-based rubber compounds are typically cured both with peroxide and via bisphenol systems, in which the use of peroxides leads to formation of C—C bonds (352 kJ/mol), while the use of bisphenols leads to the formation of C—O—C bonds, where C—O (358 kJ/mol), hence very similar binding energies.

Starting in 1970, the bisphenol curing system displaced the diamine system for curing reaction of both copolymer and terpolymer FKM compounds. Bisphenol curing system has the advantages of excellent processing safety, fast cure time and higher cure state, and especially high temperature compression set resistance in the seals. The most preferred curing agent is Bisphenol AF, 2,2-bis-(4-hydroxyphenyl)-hexafluoropropane.

The mechanism of bisphenol curing system has been studied by Schmiegel in a series of reactions with inorganic bases, amines, and phenols in a solution, using nuclear magnetic resonance (NMR) measurements with the purpose to determine structural changes in the elastomers. From these studies Schmiegel concluded that, in practical curing situations, a bisphenol-derivate phenolate interacts with the diene structure in the FKM elastomer leading to dienic phenyl ether cross-links (Figure 9).

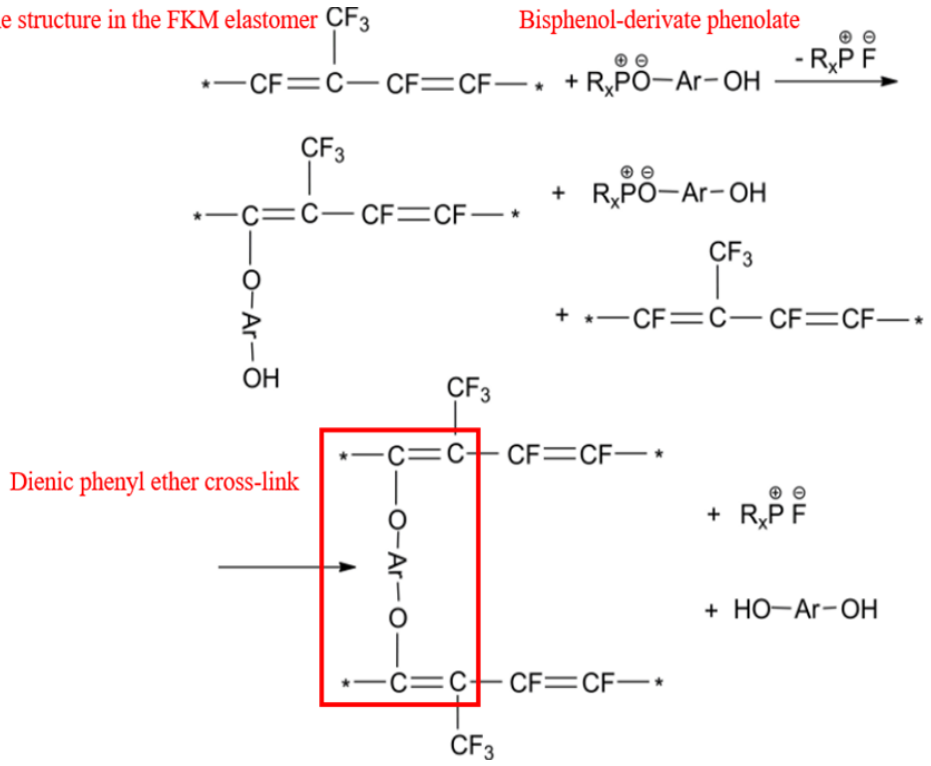

Fig.9. Mechanism for bisphenol curing system [52].

An accelerator such as benzyltriphenylphosponium chloride (BTPPC) is mandatory, along with inorganic bases, typically calcium hydroxide ($Ca(OH)_2$) and MgO. Bisphenol and accelerator concentrations can be adjusted to vary cure rates and cure states for many applications and processing technologies. The cure state is proportional to Bisphenol AF concentrations in the range 0.5 to 4.0 phr, whereas by reducing the concentration of $Ca(OH)_2$ from 6.0 to 4.0 phr the cure rate is reduced. The FKM colored compounds are colored by the additions of some phr of inorganic metal oxides of iron and chromium (Fe_2O_3 red and Cr_2O_3 green), which are inhibitors of bisphenol curing system [48, 50-52].

3.1.6 EP(D)M rubber

EPM is a copolymer consisting of ethylene and propylene units as part of the main elastomer chain and can be cured radically by means of peroxides. A small amount of built-in third non-conjugated diene monomer, usually 5-ethylidene-2-norbornene (ENB), in ethylene propylene diene rubber (EPDM) allows conventional curing with sulfur at the allylic carbon atoms relative to the pendent sites of carbon–carbon unsaturation. Secondly, EPDM rubber can be extended with fillers and plasticizers to a very high concentration, and still give good processability and properties in final articles. This leads to an attractive price/performance ratio for these rubbers. Copolymers of ethylene and propylene (EPM) and terpolymers of ethylene, propylene, and a diene (EPDM) as manufactured today are rubbers based on the early work of Natta and co-workers. The terms EP(D)M includes both copolymer EPM and terpolymers EPDM.

EP(D)M elastomer manufacturers offer the usual viscosity variations plus different ethylene/propylene ratio grades. A higher ethylene content gives more tensile strength which can help the rubber processor in the mill mixing. However, a high ethylene content gives poorer low temperature properties. EPM/EPDM compounds are cured on all of the common rubber factory equipment: press cure, transfer molding, steam cure, hot-air cure, and injection molding are all practical. Where profile extrusion is the shaping technique, hot-air tunnel curing and ultrahigh frequency (UHF) electromagnetic heating followed by a hot-air tunnel or molten-salt bath (LCM) cure are the most common curing techniques.

EP(D)M is largely unaffected by weather with very good resistance to ozone. Low temperature flexibility is very good and compares well with NR, and like NR and SBR, EP(D)M has very poor oil resistance. Also useful to the compounder is the ability of EP(D)M to accept large amounts of filler and oil-based compounding ingredients, which can be lower in cost than the rubber compounds.

Mechanical properties depend considerably on the structural characteristics of the EP(D)M and the type and amount of fillers in the compound. A wide range of hardness can be obtained with EP(D)M. The elastic properties are superior to those of many other synthetic rubbers, particularly of butyl rubber, but they do not reach the level obtained with NR of SBR rubbers. The resistance to compression set is surprisingly good, in particular for EPDM with a high ENB content or when cured with peroxide. Resistance to a number of concentrated mineral acids and bases is significantly better than that of NR or SBR.

EPM copolymer compounds are used as an ethylene based plastic impact modifier and as a viscosity index improver for lubricating oils. The use of EPDM terpolymer compounds is dominant in roof membrane linings and extruded channels for windows because of the above properties. EP(D)M has also been used as a blend with NR in tire sidewalls to improve resistance to cracking by ozone attack. The excellent electrical resistance of EP(D)M promotes its use in medium and high voltage cable covers. The main uses of EP(D)M are in automotive applications as weatherstrip profiles, automotive coolant hoses, air-conditioning and brake hoses, and seals. Considerable amounts EP(D)M are also used in blends with thermoplastics, *e.g.*, as impact modifier in quantities up to about 25 wt.% for polyamides, polystyrenes, and particularly polypropylene. The latter products are used in many exterior automotive applications such as bumpers and body panels [30-32, 40, 53].

3.1.7 AEM rubber

Ethylene acrylate rubbers (AEM) were first introduced to the market more than 40 years ago. Since its introduction by DuPont under the trade name Vamac® in 1975, AEM elastomers were introduced commercially to meet the escalating temperature and fluid resistance requirements of the automobile industry. This high-performance elastomer was designed to combine high heat and service fluid resistance with good low-temperature properties. Good physical strength of vulcanizates, excellent ozone and weather resistance, and excellent damping characteristics over a broad temperature range, are a consequence of the chemical composition of AEM. They are non-crystalline copolymers of ethylene and methyl acrylate. Vamac® terpolymers contain a small amount of a polar cure site monomer with carboxylic acid functionality. Both ethylene and methyl acrylate monomers contribute to the high-temperature stability of the AEM elastomers. Good low-temperature properties are obtained from the non-polar ethylene monomer, while the polar methyl acrylate monomer provides the oil and fluid resistance, including mineral oil-based synthetic fluids. Ethylene-methyl acrylate ratios have been optimized and produce the basis for the different grades of Vamac. The completely saturated halogen-free elastomer is non-corrosive and the saturated backbone imparts excellent resistance to ozone, oxidation, UV radiation, and weathering.

Vamac® elastomers are commercially available as copolymers of ethylene and methyl acrylate (D grades) or terpolymers of ethylene, methyl acrylate, and an acidic cure site monomer (G grades). In both the copolymer and terpolymer classes there are elastomers with increased methyl acrylate concentrations for lower volume swell in automotive service fluid environments. These grades have an ‘‘LS’’ designation, that is, DLS and GLS grades. The D grades are cured with peroxides and may not require a post-cure to optimize properties. The terpolymer G grades are cured with diamines and do require a post-curing to optimize properties, especially modulus and compression set (chapter 3.1.5.3). About heat resistance, the useful life with continuous exposure at 121°C is approximately 2 years, decreasing to 5 days at 204°C. Cured un-extended AEM elastomers have brittle points below -60°C with good low-temperature flexibility.

Although the addition of fillers causes the brittle point to increase, selected low-volatility plasticizers can be incorporated to improve low-temperature performance. Practical AEM rubber compounds can be formulated to meet low-temperature brittleness requirements to temperatures lower than -40°C.

Concerning fluid and chemical resistance AEM rubbers are serviceable in fluids such as: lubricating oils and greases, automatic transmission fluids (ATF), mineral-based engine oils, synthetic engine oils, diesel fuel, kerosene, mineral oil-based hydraulic fluids, water to 100°C, diluted acids and bases and wet and dry sour gas. The fluids to avoid with AEM rubbers are gasoline, aromatic hydrocarbons, esters and ketones, as well as concentrated acids.

AEM compounds combine high physical strength with excellent compression set. However, they are high physical strength is retained at elevated temperatures. Vamac® elastomers are halogen-free and therefore do not promote corrosion and are suitable for use in noncorrosive, flame-retardant applications. The permeability of Vamac® to gases is low, compared with that of butyl rubber. In addition, AEM compounds have good adhesion to a variety of metals, fibers, and other elastomers.

Injection and transfer molding are chosen for AEM compounds because of their low viscosity. In addition, because of their low viscosity, care must be taken to avoid trapped air and blisters. Typical injection molding set up temperatures for AEM compounds at the nozzle should be in the range of 70°C-85°C. The cold runner block systems should be set in the same range of 70°C-85°C. Scorch can be a serious problem if the temperature exceeds 100°C-110°C. Mold cavity temperatures are typically 175°C-190°C for injection molding cycle times of 1–3 minutes. External mold release agents are generally required and are secondary over-sprays. External mold release is necessary to reduce the coefficient of friction at the compound/mold interface to allow trapped air to escape, reducing the tendency for the development of sink marks and blisters. Care must be taken in the application of external mold release since excess mold release is one of the principle causes of mold fouling and weld lines.

AEM compounds are used in many automotive hose applications including turbo charger hoses, oil coolant hoses, air conditioning hoses, and power steering hoses. Furthermore, they can be used to manufacture O-rings, lathe-cut or machined gaskets with a broad range of diameters and thickness. Because of the excellent compression set of AEM rubbers, it is the material of choice for high-temperature applications in contact with automotive fluids. Depending on the location of the vehicle, AEM rubbers can be used in Constant Velocity Joint (CVJ) boots in environments where good fluid resistance is required.

The resistance to degradation at high operating temperatures in the wide variety of fluids encountered in the oil industry, coupled with the resistance of AEM to wet and dry sour gas, make these rubber compounds good candidates for elastomeric oil field applications [43-47, 54-59].

3.1.8 NBR rubber

Acrylonitrile butadiene rubber (NBR), also known as nitrile rubber, was first developed by Konrad, Tschunkur, and Kleiner at I.G. Farbenindustrie, Ludwigshafen, then with Oppau and Hoechst as a joint development in 1930 and commercialized in 1934. The original name was Buna N and later changed to Perbunan. The Second World War prevented export to Great Britain and the United States; hence Standard Oil Company and other companies, licensees of I.G. Farbenindustrie, began production in 1941 by Goodyear, Firestone, U.S. Rubber, and B.F. Goodrich as part of the war effort in the United States. In addition, Polymer Corporation in Sarnia, Ontario, Canada, began nitrile production in 1948. There has been considerable consolidation of producers and production facilities in recent years so this information may become outdated with time. The oil, fuel, and heat resistance of NBR, have made this rubber very important to the automotive non-tire and industrial rubber business.

NBR is an unsaturated synthetic copolymer of acrylonitrile (ACN) and butadiene. The ACN monomer improves the oil and fuel resistance and at the same time deteriorates the low-temperature properties. ACN content varies from 18% to 50%. A random distribution of ACN and butadiene will give a better balance of low-temperature properties and oil resistance than elastomers that are produced with connected blocks of ACN and butadiene. A most important compounding issue is the plasticizer type and content. Plasticizers will give a considerable improvement in low-temperature properties, depending on the type and concentration used. Unfortunately, good low-temperature plasticizers are often more easily extracted by oils and fuels and are more volatile, thus providing poorer high-temperature resistance.

The addition of NBR with polyvinyl chloride (PVC) resin results in a much-improved ozone and abrasion resistance as well as the processability. A minimum of 25% PVC resin provides ozone resistance, hence most simple NBR/PVC blends are 70/30 blends. The presence of PVC resin reduces both the low- & high temperature resistance. The 70/30 blend grades are often used in hose jackets or cable covers. An added benefit is flame resistance when compounded with flame-retardant fillers and plasticizers. These 70/30 NBR/PVC blends also offer improved abrasion resistance and lower coefficient of friction.

There are basically six types of cross-linking mechanisms for NBR elastomers, very high sulfur for a special ebonite, normal sulfur, semi-EV (semi-efficient vulcanization or low sulfur systems), EV (efficient vulcanization with sulfur donors alone), peroxide and zinc oxide/peroxide for carboxylated nitrile rubber (XNBR).

Molding of NBR compounds is realized by compression, transfer, or injection presses with no real difficulty. When curing at elevated temperatures it is important to use low mold-fouling types of NBR, avoid volatile plasticizers, use small or no stearic acid or replace with lauric acid, reduce the zinc oxide to 3.0 phr, and meet the cure rate and scorch safety to the process. The demand for high quality at lower cost has grown the use of injection molding at high temperatures, especially for automotive applications. This has led to the development of ‘‘low mold-fouling NBR grades’’ by many manufacturers of nitrile rubber.

With a temperature range of -40°C to +125°C, NBR rubbers resist all but the most severe automotive applications (where AEM rubbers can be preferred). On the industrial side NBR finds uses in roll covers, hydraulic hoses, conveyor belting, graphic arts, oil field packers, and seals for all kinds of plumbing and appliance applications. Finished products are found in the marketplace as injection or transfer molded products (seals and grommets), extruded hose or tubing, calendered sheet goods (floor mats and industrial belting), or various sponge articles [30-32,36, 53-55].

3.1.9 HNBR rubber

Hydrogenated nitrile rubber (HNBR), is produced by the catalytic hydrogenation of NBR, and originally, HNBR's were known as for highly saturated nitrile (HSN), although the HNBR designation was later adopted as standard. Generally, some residual unsaturation remains from the catalytic hydrogenation reaction to provide sites for sulfur or peroxide vulcanization. The catalytic hydrogenation reaction does not affect the Carbon–Nitrogen triple bond of the acrylonitrile group. However, the remaining unsaturation in the HNBR material is usually quite low compared to the starting NBR material. however, it is very important to understand that the polymerization of NBR and the subsequent formation of HNBR by catalytic hydrogenation of NBR is very expensive.

As above-mentioned NBR as some of the oldest and most used oil-resistant rubbers have an excellent balance of properties and durability, but they are subject to oxidation and sulfur attack due to the high level of unsaturation. The HNBR rubbers are much more resistant to oxidation and sulfur attack at higher temperatures compared with NBR and provide the compounding flexibility and toughness of NBR with improved temperature and chemical resistance. HNBR rubber also have tear resistance, abrasion resistance, wear resistance and overall toughness that rubbers having similar class, such as ACM and AEM cannot match. Therefore, the combination of increased high-temperature performance and improved wear resistance helps explain the niche that HNBR fills in the oil-resistant elastomer market. While ACM and AEM rubbers, are cost effective for application up to 150°C, the HNBR rubbers are much tougher, more abrasion-resistant materials. The Fluorocarbon, FKM rubbers have excellent upper temperature limits, but the euro/volume costs are heavily influenced by the relatively high density of these compounds.

Although NBR is easily reactive to active sulfur and sulfur donor curing agents due to its high level of unsaturation, HNBR rubbers are much less reactive since most of the highly reactive unsaturation sites have been saturated with hydrogen. Likewise, it takes low levels of organic peroxides to cure conventional NBR, while it takes much higher levels of organic peroxides to cure HNBR rubbers and often coagents are required to provide the preferred properties of organic peroxide cured HNBR [30-32, 53-55]. While peroxide cured HNBR provides long term sealing across a variety of demanding applications, it may not provide optimum performance when it comes to thin sectioned articles.

As a global innovator in the synthetic rubber market, *Zeon* has developed a diamine cured HNBR to maintain long term compression set on thin sectioned articles without compromising its temperature resistance or mechanical strength. Zeon has named this class of elastomer *High Performance Zetpol*® (HP-HNBR) [60].
Italian Gasket worked in technical partnership with Zeon Europe by investigating both physic-mechanical properties and above all the processability behavior by injection molding of two HP-HNBR rubber compounds, one black and one colored diamine cured, where the data are reported in chapters 5 and 6.
Unlike NBR, HNBR benefits from oven post-curing processes, which is very effective in improving compression set resistance. These improvements in compression set resistance without significant impact on original physical properties generally hold true for both sulfur and peroxide and are mandatory for diamine cured materials.
Generally, HNBR is a usable rubber because of the combination of fluid resistance, toughness and abrasion resistance, higher temperature resistance compared with NBR, and its overall value in many applications, which experience temperatures in the range of 125°C-150°C. Therefore, the typical temperature range is between -30°C and 150°C. HNBR rubbers are a good choice for O-Ring seal application having both engine oil and coolant at 125°C maximum temperature with typical operation in the range of 100°C-120°C. Conventional NBRs do not have sufficient durability at 125°C to survive in the application, EPDMs have great coolant resistance but have poor resistance to engine oils, and FKMs are quite expensive and have poor resistance to high-temperature water-based systems. About seal for automotive water pumps, such as protective bellows around the water pump seal, since the engine compartment heat has risen to 125°C, continuous, with stop-and-go traffic excursions up to 150°C, the NBR bellows does not meet the requirements. Therefore, for overall toughness, weather resistance, splash fluid resistance, and cost, HNBR is a good choice. Typical applications also include accumulator bladders, diaphragms, and gaskets. Limitations include poor electrical properties, poor flame resistance and swelling with aromatic oils [30-32, 53-55].

3.1.10 FKM rubber

Fluoroelastomers (FKM) are typically used when other elastomers fail in harsh environments. Chemical resistance and heat resistance are the two main attributes that gave FKM successful growth since their introduction in 1957 by *DuPont*. FKM rubbers are typically characterized by saturated backbone that imparts excellent resistance to ozone, oxidation, UV radiation, and weathering. Furthermore, high service temperature, low oil swelling, high resistance to chemicals and acids, as well as high flammability are the peculiar strengths. Nevertheless, their weaknesses are the high cost, poor low temperature flexibility and poor resistance to organic bases like amines. Applications range from niche applications in aerospace to large series applications with O-rings and shaft seals in the automotive industry. The latter include fuel hose liners and seals and fuel duct expansion joints, where high temperatures and acidic products from gas desulfurization are involved.

Use of FKM continues to grow due to ever more demanding applications, in automotive to more stringent regulations, and in the chemical industry to support environmental protection. FKM have excellent heat resistance with continuous service temperature of 205°C. They are referenced as FKM with 250°C heat resistance and excellent oil resistance, and less than 10% swell at 150°C as per the ASTM D2000 classification (Figure 10). Fluoroelastomers can withstand limited exposure to 300°C. However, they should not be exposed to temperatures higher than 315°C as HF emissions could occur.

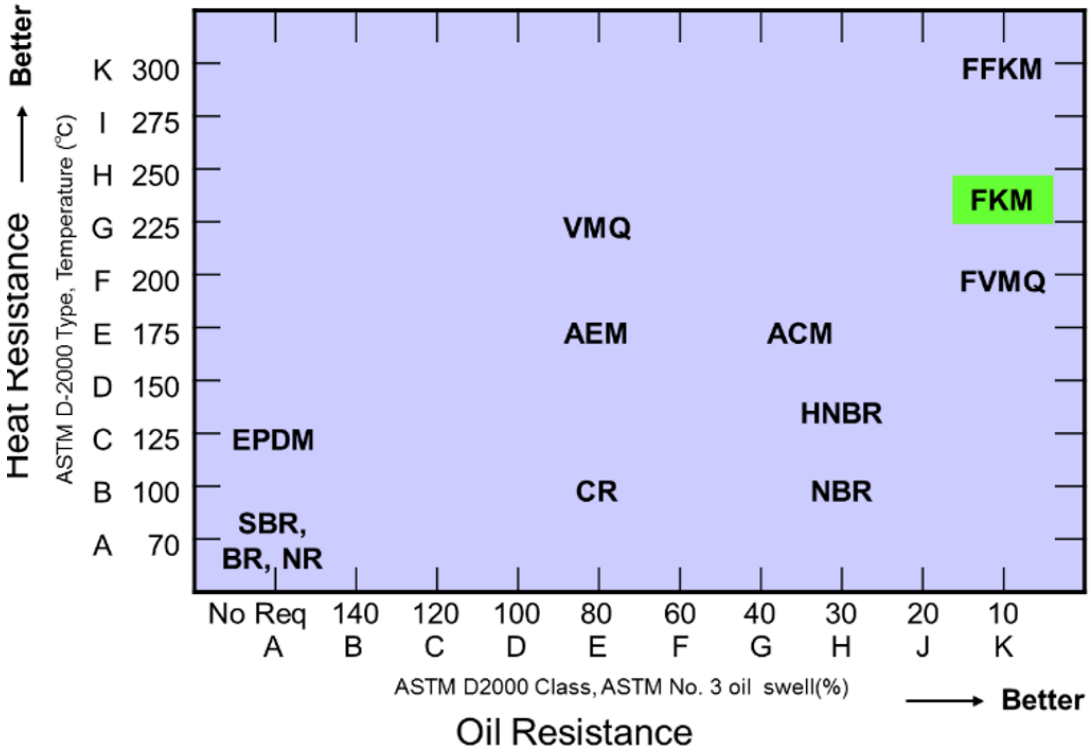

Fig.10. ASTM D2000 comparison of rubbers heat vs oil (ASTM No.3) resistance.

FKM are used widely in O-rings and gaskets because they have very good compression set resistance, and excellent resistance to fuels, solvents, and oils. Steam and acid resistance is satisfactory with bisphenol cured FKM, and very good with peroxide cured FKM. As above-mentioned, initially fluoroelastomers were cured with amines (chapter 3.1.5.3), however, the scorchy nature of those cure systems as well as a rather poor compression set resistance led to the development of bisphenol cure systems (chapter 3.1.5.4). Peroxide curing is performed thanks to the addition of a cure site monomer for compositions that cannot be cured with bisphenol, such as high fluorine content, low-temperature elastomers where the monomer hexafluoropropylene (HFP) has been substituted by polymethylvinylether (PMVE). Oven post-curing stage for both bisphenol and peroxide is mandatory with the purpose to improve the compression set and tensile strength.

The FKM market has a product class that was developed in the 1970, with pre-compounds or curing-incorporated products.

Therefore, FKM suppliers developed this offering to help the customers handle the difficulty to mix and handle bisphenol curing systems. Most products are available in pre-compounded form but peroxide curable are usually not pre-compounded because of bin stability.

Fluoroelastomers can be processed by injection and compression molding, where the major difference than most rubbers is to consider is high density of FKM elastomer, that is, approximately 1.8 g/cm^3, and most compounds have densities between 1.8 and 2.0 g/cm^3. The other major difference is the higher thermal expansion of FKM than most rubbers, leading to shrinkage of 2%–4% depending on formulation and mold temperature. Industrially, the most common injection molding defects are flow lines, tear when demolding (hot tear), knit lines when excessive process aids are present in the formulation, and blisters from undispersed ingredients, trapped water, and contaminants from other stocks or trapped air before molding. [30-32, 47, 53-55]

3.1.11 Rubber storage

Rubber compounds are cured inside the cavity mold of the injection molding process after the injection phase, and therefore are chemically active [61]. The rubber compounder needs to consider the shelf life of chemicals during storage of the raw material prior to compounding; for example, sulphenamide accelerators are sensitive to high humidity levels, the presence of which will reduce shelf life. The accelerator story can get quite interesting. In a compound, the accelerators amount and types (often different types are combined) are selected to get just the right amount of processing safety (protection scorch), cure rate (time is money) and cure state (which affects final properties). The cost of the accelerator also needs to be considered [31].

This activity represents a major challenge for the manufacturers of rubber products, as the rubber compounds change their properties with storage time and temperature. Depending on the rubber compound formulation, rubber compound storage under cooled environment can therefore be required. Two main effects related to the storage of a rubber compound can be found: the viscosity typically increases, which leads to a stiffening of the material, and the incubation time decreases. These effects alter the injection molding process and potentially lead to problems. The reduced incubation time diminishes the processing operating window, as it can cause a premature start of the curing reaction during the filling phase which almost definitely leads to defective parts. Furthermore, it reduces the time when the injection gate is fully cured, which changes the shrinkage potential of a part. This is especially important for thick-walled parts with a high material volume. The stiffening of the rubber compound can lead to dosing problems like tearing of the rubber strip and increases the dissipation energy if the dosing speed is kept constant. Furthermore, even under proper storage conditions, after some weeks the incubation time decreases, thus causing a risk of premature start of curing reaction, and a viscosity increase. This is reflected in deteriorated mechanical properties of the cured rubber [28, 61].

A prolonged storage time of some rubber compounds affects the material microstructure and they become very difficult to inject, especially with rubbers having curing systems like sulfur, diamine and bisphenol (*e.g.* EP(D)M, NBR, AEM, ACM, FKM). Instead, peroxide curable rubber compounds (*e.g.* EP(D)M, HNBR, FKM) are more stable.

Another topic is the effects of cooled storage on rubber compounds, where exposures to temperatures below 10°C causes a crystallization of the elastomers which becomes not processable (typical of elastomers containing olefins such as ethylene in their main polymer chain). However, this condition could be reversible, because if suitably heated to a temperature above 15°C, a recovery of processability is likely. Storage temperatures above 23°C accentuate problems of stickiness of the rubber strip, and also increase the scorching. Therefore, the range between 15°C and 23°C turns out to be the ideal temperature range for rubber storage [62].

Furthermore, according to the *ISO 2230:2002—Rubber products—Guidelines* for storage, it is necessary to control the storage humidity at a value <70%. Other storage environmental factors like heat, light, radiation, ozone, deformation, contact with liquid and semi-liquid materials, metals and dusting powder must be absent.

Figure 11 shows the viscosity variation by Mooney Scorch at 121°C of AEM rubber compounds during storage time, where an acceptable storage condition of 23°C and 50% humidity (red line), and unacceptable condition of 38°C and 95% humidity (blue line) are reported [62]. Typically, the AEM rubber compounds are characterized by a shelf life of about 1 month, obviously if properly stored [28].

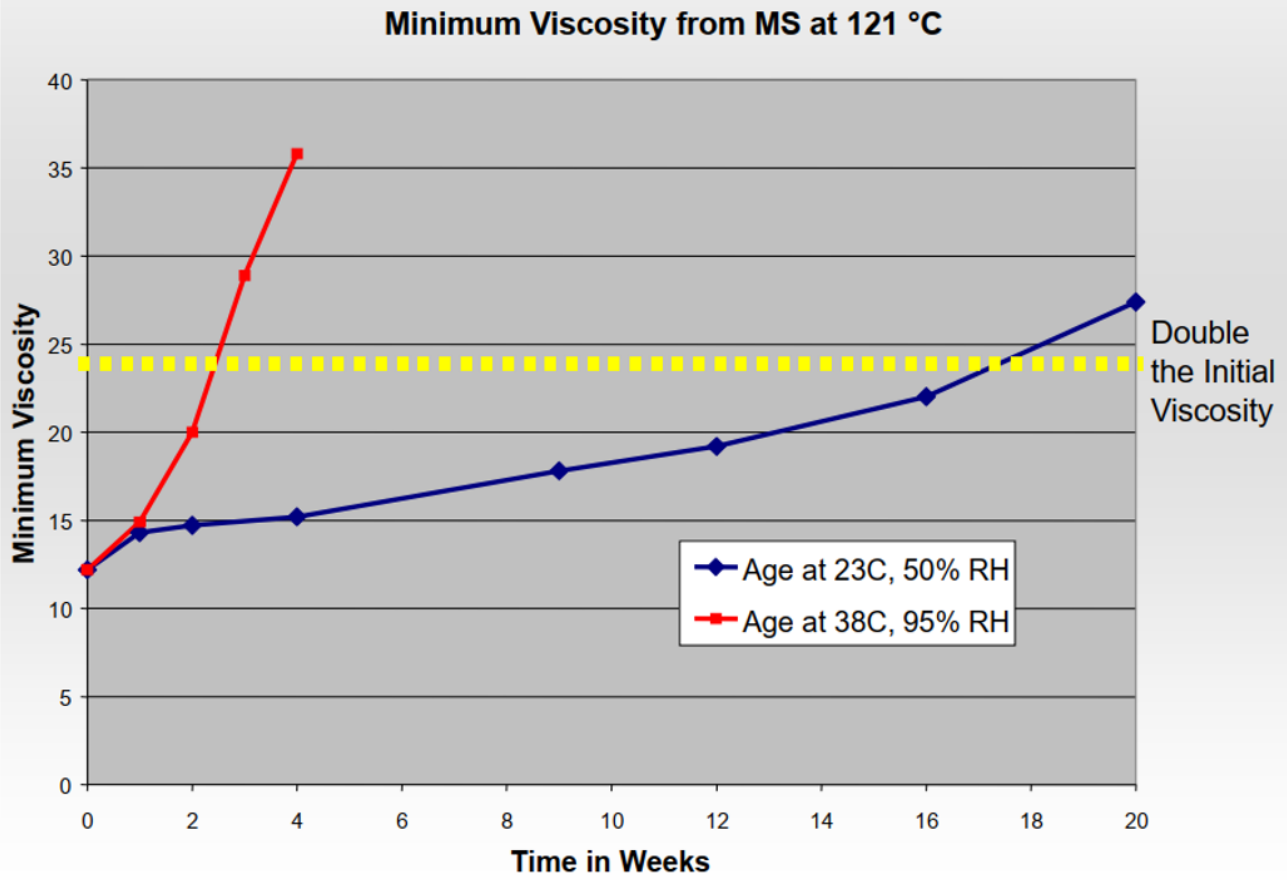

Fig.11. Minimum viscosity from Mooney scorch at 121°C vs time for AEM rubbers [62].

3.2. Rubber molding

Extrusion and molding have both similar and different features. During extrusion of rubber through a die, the die shapes the rubber in the section plane of the die. After exiting the die, the unrestricted dimensions of the extrudate are free to change. During molding, a mold cavity shapes and confines the rubber in all three dimensions. A wide range of equipment and compounds are available for molding rubber compounds. The main molding methods include compression, transfer, injection, and combinations of these, with compression molding being the earliest used method [63, 64].

There are differences and similarities between molding behavior of low and high viscosity rubbers. Low viscosity materials become rubberlike only after they react with another material in a mold (*e.g.* liquid silicon rubber). Conversely, high viscosity materials are rubberlike before they enter a mold. However, low and high viscosity rubber compounds are alike because they both cross-link within mold cavity. Materials having intermediate viscosity (*e.g.* caulking compound) are typically avoided in molding. Reasons for this are that they are difficult to handle because they show a relevant tendency to trap air during compounding and molding processes. Therefore, the retained air is often clear as porosity in the molded part. The higher viscosity rubber compounds can then be molded by high pressure methods such as compression, injection or transfer molding. High molding pressure acts on this viscosity rubber compounds and squeezes out of the air, by minimizing porosity. Many automotive rubber parts are also cured through compression molding, transfer molding, or injection molding.

Compression molding is a method of molding in which the molding material, generally preheated, is first placed in an open, heated mold cavity. The mold is closed with a top force, pressure is applied to force the rubber compounds into contact with all mold areas, while heat and pressure are kept until the molding material has cured. In the practical way compression molding involves several steps as follows:

- uncured rubber compound is formed to the proper shape and size based on the finished part configuration. This uncured rubber shape (preform) is prepared to be molded. Each mold will have a different shape and size preform that works properly;
- the preform is placed into the cavity of a heated mold. The mold is then closed. Heat and pressure are applied in a compression molding machine. Critical parameters such as temperature, pressure and time to ensure molding takes place within a prescribed tolerance window are to be properly set;
- the mold is then opened. The cured rubber part is removed along with its flash;
- the cured part is then moved through the manufacturing operation to undergo post-molding processing, such as deburring, post-curing, automated inspection and packaging.

Advantages of compression molding are lowest cost tooling, good for small production runs and for large parts, as well as no gates, sprues or runners. However its main disadvantage is the higher labor cost than

injection molding process (requires more man power), and it is not suitable for complex molds, may show environment contamination (*e.g*. handling operator) and it is difficult to control flash.
Instead, in one sense, transfer molding is a variation of compression molding, even this molding methodology uses the pre-formed material, and it begins by weighting the molding material and placing this uncured rubber in a "pot" that is a part of the mold. The mold is then closed, and a plunger compresses the material. As heat is applied, pressure forces transfer the uncured rubber through sprues into the mold's cavities, giving this molding process its name. The mold remains closed during the curing reaction and is later opened to remove rubber parts for deflashing. As with compression molding, large transfer molding are unwieldly, and for large transfer molds the plunger can be attached to the upper platen of a curing machine. The cavity plate can be taken from the machine for parts removal. Therefore, parts removal could be done by hand or automated. Transfer molding also provides tight control of dimensional tolerances. Pre-formed materials are required, but a single pre-form can fill hundreds of mold cavities. Plus, because pre-forms are cut by hand, there is a reduced risk of contaminating color parts. Although some transfer molds produce flash, rubber molders can also use flash-less tooling. Sometimes, a flash-less tool is preferred in a transfer process [15].

3.2.1 Rubber injection molding

As briefly reported in the introduction, the injection molding process of rubber compounds began in the early 1940's, and the screw injection molding was first reported by Cousino and Chrysler Corporation, being used today for the manufacturing of a wide range of industrial products.
The main difference between compression or transfer molding and injection molding is that in the last one rubber compound as strips is fed automatically through an injection unit (screw) to the mold. Another difference is that systems for injection molding are much more complex that those for compression or transfer molding; there are several controls to fine tune such as temperature, pressure and other variables. These controls are not normally part of compression and transfer molding systems.
With compression and transfer molding, the machine provides the force to close a mold. However, in injection molding a machine is referred to as a "press". A press is an integral part of an injection molding machine. Injection molds are usually attached to the press plates and thus open and close with the press. One reason for attachment between mold and press is the need for proper alignment between an injection molding machine and its mold. Injection molding must be capable of withstanding extremely high pressures without mold distortion. The pressure reached in an injection mold is averagely 200 MPa, thus ten times greater than that for compression and transfer molding.
Operatively, rubber compound is plasticized and heated in an injection unit, then it's forced to flow through a nozzle into the cavity of a heated injection mold. The cavity is composed by a sprue, channels and finally the part cavities. For multi cavity molds, industrially the most frequently used, the distribution system for the rubber compounds is every so often quite complex.

A simple distribution system having four-cavity mold is showed in Figure 12. The injected rubber compound flows through the sprue and enters in the runners and feed the gates. The gate is the final restrictive pathway into a mold cavity [15, 32, 63].

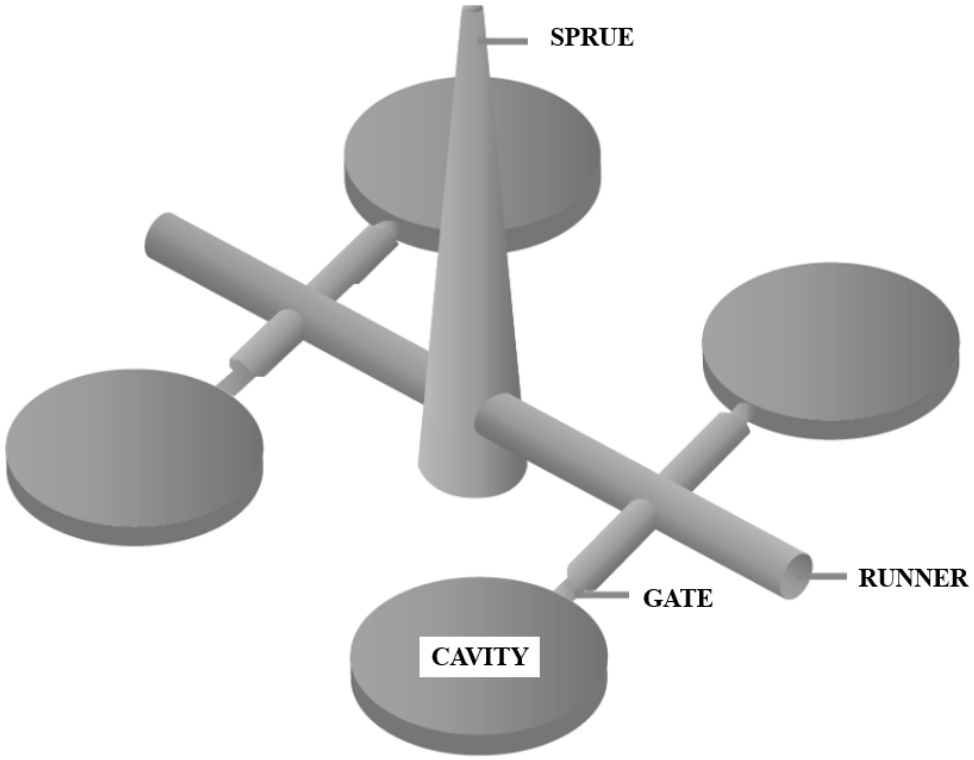

Fig.12. Distribution system for an injection mold.

Although it is possible to produce rubber molded parts on virtually any machine with sufficient knowledge of the equipment or technology, there are features of the equipment that need to be understood in terms of their function and interaction with the whole process. Therefore, it is important to understand that process analysis and failure prevention is achieved, only if referred to as Failure Mode and Effect Analysis (FMEA). This is an analysis method used in the rubber industry in the selection of the proper injection molding machine, and of it effective operation.

Early injection molding machines had a ram which was smaller in diameter and traveled farther during injection, relative to the plunger on a transfer mold. Figure 13 here below shows a ram-type injection molding machine attached to a two plate with single cavity mold. Nowadays, the injection unit is equipped with a screw to plasticize and sometimes also inject the rubber compound into the mold.

Heating fluid circulates in the barrel of the ram machine; rubber compounds is fed into its throat with the ram in the retracted (left) position. During injection molding, this ram forces rubber compound advancing (to the right) into the injection chamber, passing through the nozzle and mold sprue where it then enters the mold cavity. Before rubber compound enters the mold cavity, it has been heated by the inner barrel wall, and then it becomes hotter, preferable avoiding scorch, as it passes through the nozzle and sprue at very high shear rates.

The rubber temperature rises significantly as rubber flows from the nozzle to the gate and through the gate (see Figure 12). The gate could be small and it restricts the rubber flow, increases the shear rate and decreases viscosity [15]. The high temperature reached by rubber compound due to the shear heating while in the injection chamber of a ram type machine is very partially limited to the temperature setup of the chamber wall. This wall transfers heat relatively slowly to the rubber compound by conduction, because this process is slow and its temperature is less uniform than would be desirable [15, 32].

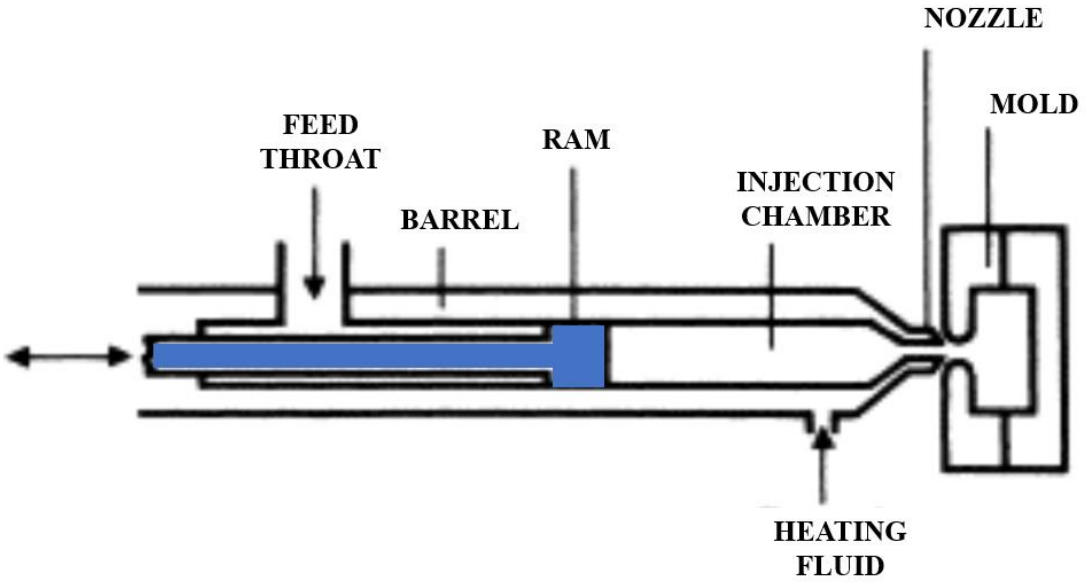

Fig.13. Ram type machine for injection molding [15].

3.2.1.1 Injection molding machine

The injection molding machines used in the rubber industry are composed by five fundamental parts:

1. *injection unit*, which contains the extruder and the chamber (plasticizing extruder). First the extruder plasticizes and heats the rubber compound, which is stored in the injection chamber before its injection into the mold cavity;
2. *clamping unit*, which opens and closes the mold, and keeps the mold closed during the injection stage and curing reaction;
3. *hydraulic power pack,* which generates the amount of power used to drive the hydraulic components;
4. *heat exchanger system,* which allows the proper heat transfer;
5. *control system,* which manly allows the proper process parameters setup [15, 63-66].

Furthermore, the modern molding machines also could be equipped with robots especially used for rubber parts demolding. There are several types of injection machines, and the difference is made by how injection and clamping units are arranged. In the rubber industry horizontal injection machines and vertical injection machines are the mostly used.

The horizontal injection molding machines (Figure 14) are most frequently used in the factory, also considering the technological automation improvement in the rubber industry, based on the application of collaborative robots to assist in demolding of rubber parts in the clamping unit. The aid of the robot allows the plant operator to focus the attention on the technical control of the production runs, by avoiding any manual operations as in the past and as in compression molding process.

Fig.14. Horizontal injection machine located in *Italian Gasket* plant.

Injection molding involves the high pressure injection of the rubber compound into a mold, which shapes the rubber into the required form. Molds can be of a single cavity or multiple cavities. In multiple cavity molds, cavities can be either identical to each other or different from each other. Molds are generally made from tool steels, but stainless steels and aluminum molds are suitable for certain applications. Many steel molds are designed to process well over a million parts during their lifetime and can cost thousands of euros.

Parts to be injection-molded must be very meticulously designed to facilitate the molding process; thus the used rubber compound for the part, the desired shape and features of the part, the material of the mold, and the properties of the molding machine must all be taken into account. The flexibility of injection molding is facilitated by this breadth of design considerations and possibilities.

3.2.1.2 Plasticizing extruder

Injection unit is the most critical part which constitutes the injection molding machine and contains the plasticizing extruder. Plasticizing is the term given to the conversion of uncured rubber to a hot, relatively soft, homogeneous rubber mass. This is achieved by the rotation of a metal screw within a heater-jacketed barrel. The relationship between the temperature of plasticized rubber compound and that of the jacketed barrel is dynamic, as the rubber may either transfer heat internally generated by shear deformation to the barrel or gain more heat.

Rubber strip is fed to the throat (Figure 13), or inlet to the screw where it is sheared between the wall of the barrel and the screw flights. The plasticized rubber compound (rubber extrudate) is then forced by the screw past its tip and into the heat-jacketed injection barrel (injection chamber), where it is head pending the injection stroke.

The plasticization is controlled by the screw type and design (length, diameter, depth or flight and screw pitch), the screw speed rotation, the gap between the screw and the containing wall, and the ease with which the rubber compound can flow form the screw into the injection barrel (pressure applied against this rubber flow is well known as back-pressure), and obviously the material constituting the screw as well. Reference may also be found in the literature to ram injection molding machines, however as above-mentioned these were initially introduced as a modification of early plastic injection molding machine, which a ram forced the rubber toward a “heated torpedo” to achieve plasticization. Furthermore, there were numerous problems of unsatisfactory mixing and “dead areas”, and thus the system has been largely replaced by the reciprocating screw machine.

It must be considered that the way the rubber feeds into the screw has a significant influence on the final product quality and performance. Designs that allow the rubber compound to be cut off in the feed throat by the screw flight can cause extra work for the plant operator, that usually increases the screw speed rotation as the “starved” screw empties itself. This results in a rapid shear heating effect (internal friction between different rubber compound layers inside the flow) and possibility to increase the risk of scorching in the injection unit, if it is not immediately detected and corrected. Three solutions are commonly adopted in the industrial practice to overcome rubber strip feed problems:

- motorized rollers able to maintain proper contact between rubber compound strip and screw;
- localized increase of the distance between screw and the barrel wall at the throat, by allowing an initial contact between the screw flight and the wide part of the strip;
- teeth-like notches cut into the screw flights in the feed throat.

Therefore, the plasticizing extruder of injection unit must allow the rubber compound to be injected uniformly without scorching. There should be a smooth pathway for the rubber compound, free from the “dead zones“ in which there is little or no rubber flow.

Rubber compound that collects in such zones will soon cure to form hard “nibs” that will grow in size until they re-enter the material flow, impede the injection, and produce molding faults. This problem arises in many existing machines, where the first rubber compound passing into the injection barrel is the last to be injected (Last In, First out, or LIFO type-screw). Therefore, it seems very appropriate to control and to monitor the rubber shear heating effect in the injection unit, as proposed in this research activity, especially for rubber compounds having curing system very prone to scorch and thermal degradation issues such as AEM, ACM, FKM. The measured rubber temperature (T_{SH}) is a process indicator giving the thermal history of the rubber compound injection and process safety [9-10,16, 22-24, 26-28].

Therefore, the design of the injection unit is crucial to molding machine operation [63]. The most commonly used injection units in the rubber industry are reciprocating type-screw, First In First Out (FIFO type-screw), and as above LIFO type-screw.

In the reciprocating type-screw machine (Figure 15) its throat, barrel, injection chamber, nozzle, heating fluid and mold are nearly identical to counter parts in the ram machine. The main difference with Ram type machine for injection molding is that reciprocating screw machine is fitted with a screw which rotates inside the barrel. This screw not only rotates, but it also moves back and forth on its axis like the ram.

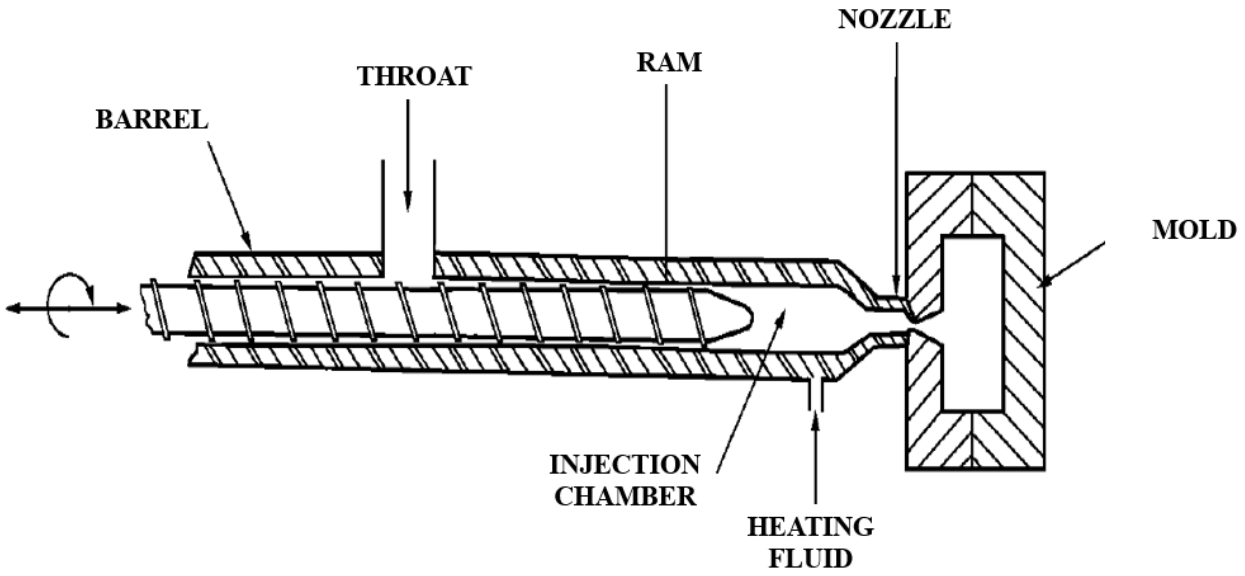

Fig.15. Reciprocating type-screw machine for injection molding [15].

Rubber compound is fed into the throat of a reciprocating screw machine, where it then contacts the rotating screw. The screw has the function to plasticize the rubber compound and move or pumps it to the front of injection chamber (nozzle outlet of the extruder barrel). Rubber compound accumulates there because the screw retracts (moves to left) to provide the needed volume in the injection chamber. Therefore, when a sufficient volume of rubber compound accumulates, the screw moves toward the sprue and the mold and fills the cavity or cavities.

In this way the reciprocating screw acts as pump and a ram, although it develops less pressure and doesn't meter rubber compound as accurately as a ram. These unfavorable features occur because the clearance between ram and barrel wall is usually less than between screw and barrel wall. The clearance between ram and wall can be as small as 0.05 mm, and with this small clearance, less leakage of rubber compound occurs during injection stage. Hence, higher injection pressure setup and more accurate shots are achievable with the ram-type machine compared with the screw-type machine [15].

The reciprocating screw along the flow direction is divided into three areas: feeding area (50% of the screw), compression zone (25% of the screw) and dosing area (25% of the screw).

The external diameter of the screw remains constant throughout its length. The pitch of the screw (distance between a thread and the other) is commonly equal to the diameter of the screw, therefore the characteristic length of the screw is defined based on screw length over diameter ratio (L/D ratio). Typically, the L/D ratio for reciprocating screw-type machine varies in the range 15-20.

Due to the screw thread the rubber compound is heated by viscous dissipation (shear heating), and moves along injection chamber to fill the mold cavity or cavities. The rubber temperature is raised above the barrel temperature setup, and the higher temperature reduces rubber compound viscosity [15]. Typically, high viscosity rubber compounds such as FKM's generate higher shear heating, conversely, a low viscosity rubber compounds like VMQ's are more susceptible to the heating fluid effect (heating by the barrel walls).

The FIFO type-screw instead, is forced backwards by movement with the rubber compound it has plasticized. Therefore, the plasticizing extruder becomes the holding unit for the plasticized rubber compound. Injection is then achieved by hydraulically forcing the screw back into the barrel (Figure 16).

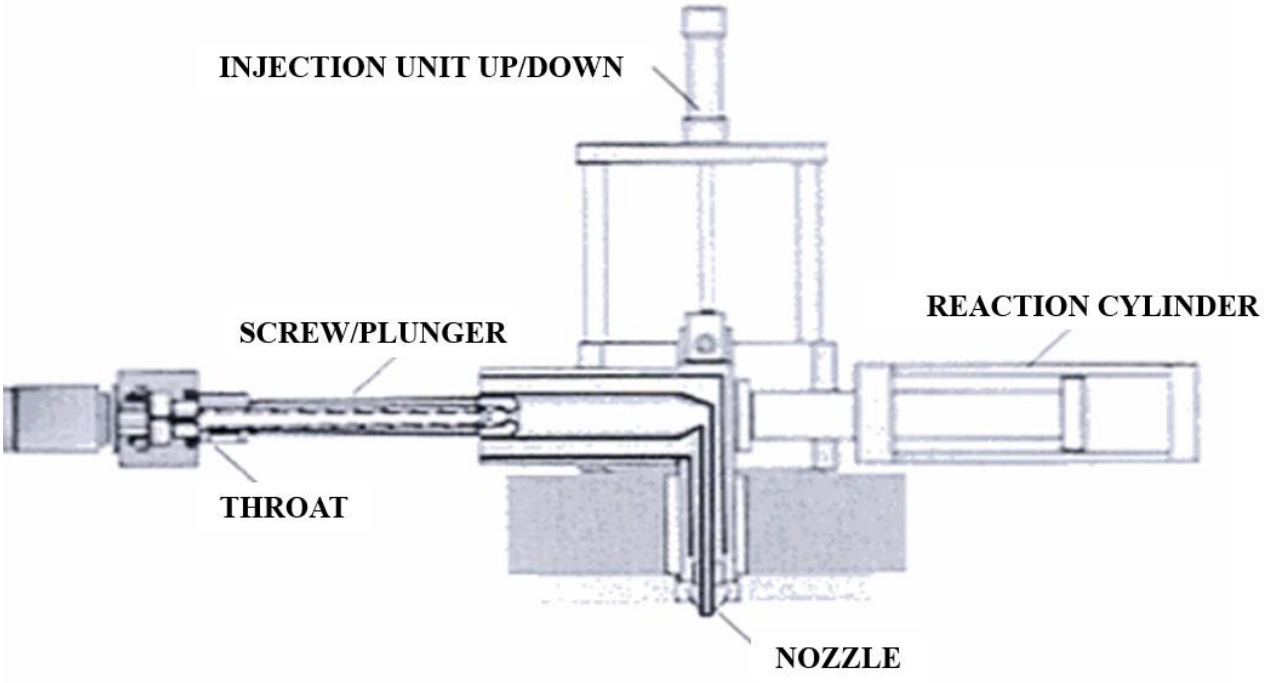

Fig.16. FIFO type-screw machine for injection molding [63].

The temperatures of the screw cylinder, plunger, injection cylinder and nozzle need to be controlled. This is best achieved with jackets of oil circulating around each zone at precisely regulated temperatures. This same system must be able to provide emergency cooling to prevent scorching of the rubber compound in the case of prolonged delay in the molding cycle. FIFO type-screw may incorporate a check valve that enables the rubber compound to be lightly compressed as it is plasticized, generating a back-pressure against the end of the screw unit. Control of this pressure generates certain benefits such as increased temperature in the rubber stock, elimination of entrapped air and improved shot weight capability. Nevertheless, the use of back-pressure requires care since the relationship to scorch is logarithmic in character and influenced by small change in rubber compound viscosity [63]. This injection unit was developed ad hoc to ensure optimal processing of a wide range of rubber compounds. The rubber compound first plasticized, is again the first to be injected into the mold. In this way the thermal history of the entire injected rubber compound volume remains constant. Furthermore, a very short injection nozzle allows to keep the injection pressure almost completely unchanged during the filling of the mold cavity or cavities.

Figure 17 shows the LIFO type-screw machine in which the screw and the ram are separated (Y-structure). In this machine, the screw doesn't move back and forth on its axis; it only rotates, heating and pumping rubber compound to a 3-way valve. The heated rubber compound flows through the valve into the injection chamber. A ram then forces rubber compound from the injection chamber to the mold cavity, passing through the 3-way valve, the nozzle and mold sprue as well. Hence the best features of a ram machine and a reciprocating screw machine are combined in a single machine [15].

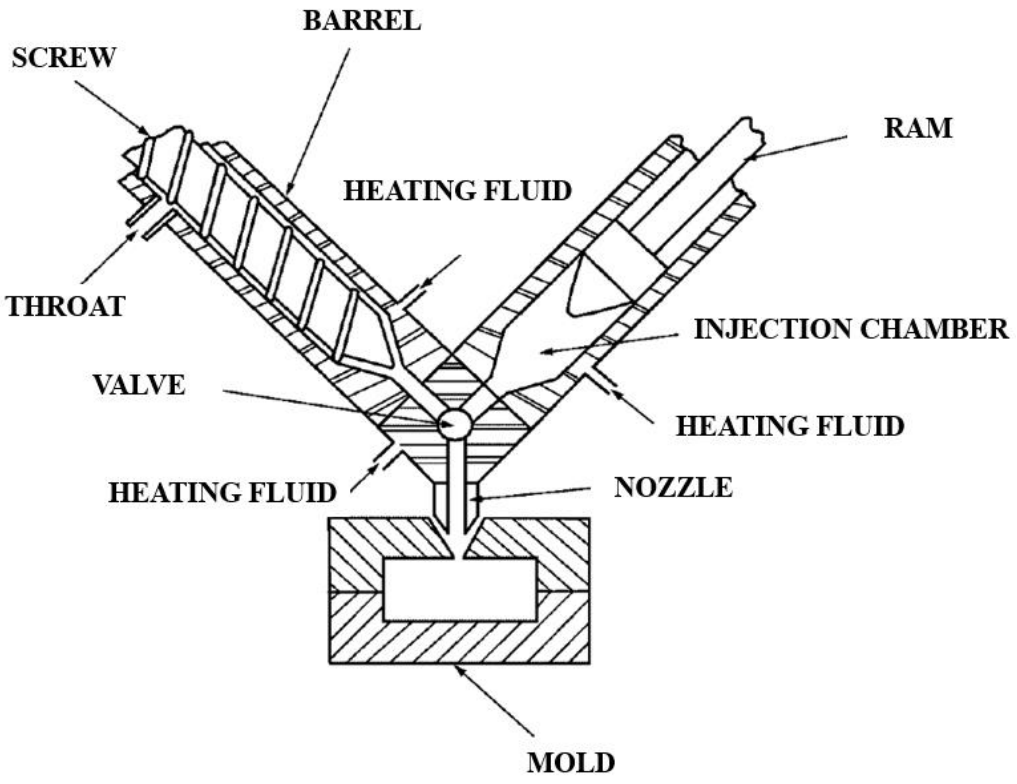

Fig.17. LIFO type-screw machine for injection molding [15].

The Y-structure is a proven principle. The separation of the plasticization and injection functions, associated with the regulation system, gives the entire injection unit unrivalled accuracy and regularity in rubber compound injection stage. For the same volume, with separation of the plasticizing and injection functions, means an injection plunger diameter 25% smaller than with the FIFO technique. Therefore, for the same injected volume, this injection unit is twice as accurate as a FIFO injection unit. Metering accuracy is further improved by scheduling the plasticizing extruder to slow down before the set point is reached.

One of the most relevant manufacturers of injection molding machines equipped with LIFO injection unit, REP from *Corbas* (France), has been improved the feed intake chamber with a helicoidal sleeve, in which a progressive start and stop of the plasticizing extruder prevents any risk of feed strip rupture. Other improvements have concerned the temperature control through-out all phases of the mixing process, a material probe at the plasticizing extruder output for control of shear heating. Furthermore, a regulator fitted on the injection unit, with two short and independent circuits, allowed with fast response times, to homogenize the temperature and to ensure proper regulation which is therefore without risk.

Arrangements of the components of an injection molding machine fall in the two main categories of machines: horizontal and vertical. The reciprocating screw is typically used for horizontal injection molding machine, instead FIFO and LIFO screws for both horizontal and vertical injection molding machines.

The nozzle is the final point of leaving for rubber compound from the injection unit. It channels the rubber compound directly into the mold through a hemispherical mating face to flat top of the sprue bush in the mold, which leads to the center of the rubber system. Most injection molding machine manufacturers design the nozzle with a parallel bore at its exit. For minimum pressure drop through the nozzle it is advantageous that the nozzle is made with a smooth conical path to its end (Figure 18).

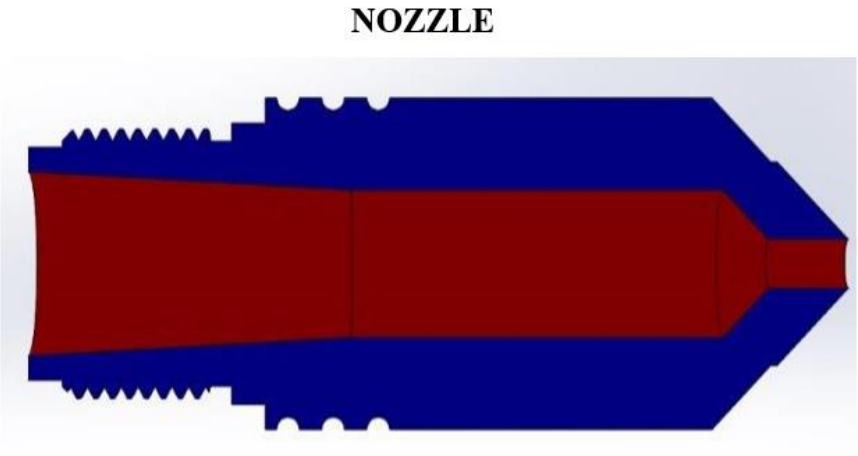

Fig.18. Nozzle for injection molding machines [63].

The type of rubber compounds to be processed may require that special metals must be selected for the construction of both screw and barrel.

Halogen containing rubbers such as FKM can generate extremely corrosive breakdown products and their proposed use must certainly be discussed with the machinery manufacturer, who may advise the use of certain non-ferrous alloys. Furthermore, some rubber compounds contain fillers such as silica and silicates that have a significant abrasive effect on the screw and barrel. Special steel may be suitable to minimize wear, and additionally, the amount of wear should be measured and recorded on a regular basis, at least annually [63].

3.2.1.3 Process parameters

When using injection molding, both processing variables and rubber compound variables have a noticeable effect on rates of scorch, cure rate, cure state, cycle time and general injection stage performance. Rubber cure temperatures can generally range from as low as 150 to more than 200°C. The higher cure temperatures lead to shorter cure cycles. Therefore, many rubber products are cured at higher temperature ranges (180°C-200°C) for greater productivity, provided that reversion or thermal degradation issue is not a problem at these higher temperatures. Most rubber products are also cured under pressure to avoid gas formation and porosity [17]. During the injection stage the rubber compound flows from the injection chamber into the mold (filling stage), the injection shoot is usually introduced under control of ram speed, but instead of filling the complete mold under ram speed control, part of the shoot can be introduced under ram speed control and the remaining part of the shoot under control of pressure, that is, a pressure holding stage is applied [65].

Injection pressure (Pi) can be considered as the fill pressure (primary pressure) and the hold pressure (secondary pressure). Generally, the filling pressure will be set higher than the holding pressure. The injection pressure expressed in bar, is one of the most important and critical process parameters to ensure the proper rubber compound filling pressure distribution on the cavity [31]. Therefore, for some rubber compounds a relevant variation of the injection pressure setup could directly affect the filling or injection time (ti).

Another relevant process parameter influencing the filling distribution and time is the injection speed (vi), typically expressed in mm/s or %. Generally in the case of thin molded parts or multi-cavity molded parts for which critical size precision is required, slower injection speed is required. In contrast, faster injection speed is better for thick molded product.

Instead, the screw speed rotation expressed in rpm or %, influences the shear rate of rubber compound flowing along the screw direction toward the nozzle and sprue. Moreover, the screw speed rotation is also used to facilitate rubber strip feed, but cannot be increased too significantly because this would increase the risk of scorching in the injection unit. The barrel temperature setup (T_{barrel}) is a further process parameter to be considered for the injection stage because should allow plasticization temperature for the rubber compound. Like many other industrial processes, temperature control is a critical consideration in injection molding. Effective temperature control prevents quality issues such as shrinkage, flow/knit lines, burn marks and in the worst case, thermal degradation issue [9-10, 22-24, 26-28].

3.2.1.4 Thermal history

In the rubber injection stage, the compound has thermal history starting from room temperature (RT) when the rubber strip enters the plasticizing extruder and reaches up to the final parts when it is cooled down to RT. In many cases, a post-cure process is performed by positioning the stabilized and deburred rubber parts in air industrial oven for a certain period of time according to the rubber compound.

Figure 19 shows the typical simplified pathway of rubber compound. At point 1, “plasticization”, the rubber compound is plasticized and heated to achieve the optimum temperature. This rubber temperature has to be measured so that it can be optimized and maintained in the next step of the process. At point 2, the rubber compound is inside the injection chamber, ready for the injection. At point 3, “injection”, the rubber compound flows into the runners where it is heated again. Heating up is mainly produced through rubber compound shearing but also contact with the hot mold walls. The point 4 concerns the “curing reaction”, where, once the cavity is filled, the rubber compound has not yet reached the mold temperature even if it has undergone a shear heating effect in the previous steps. The rubber compound continues to heat during the beginning of curing reaction until reaching the mold temperature setup. Therefore, to allow the best performance in terms of cure rate, cure state and cycle time, the proper curing time (*t*c) and curing temperature (*T*c) for both fixed and movable plates must be set depending on to the type rubber compound (base elastomer), curing system, parts thickness as well. In the point 5, “cooling”, once the rubber parts being demolded from the cavities, it needs a certain amount of time to cool down and continues tom cure. A total control over the process also includes a control over the parts cooling conditions.

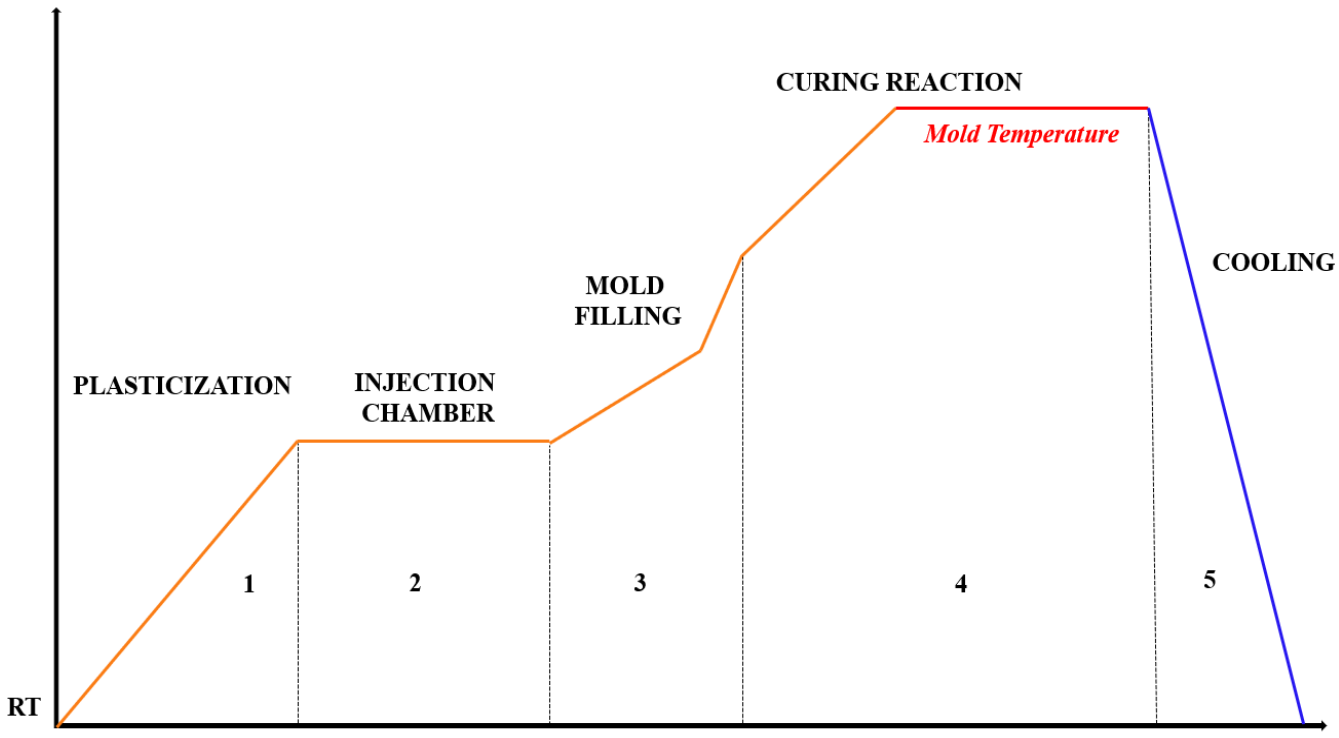

Fig.19. Simplified pathway of rubber compound thermal history.

Therefore, an accurate temperature control loop is necessary to have a consistent injection unit temperature and mold temperature. As for the mold, there is a distance between the heating platen and the cavity so there can be a big and variable difference in temperature between both. To control the process, it is important to regulate the cavity, which is where the rubber compound is. This makes the regulation loop more difficult to do, but makes the process much more consistent, and it can allow for instance to set a higher mold temperature and cure time reduction, thus by improving in the productivity.

The outside surface of the mold could cause heat loss that cools down the sides of the mold. This heat loss is typically called the "edging effect" and will induce a lower mold temperature on the sides and corners than in the center of the mold. The mold temperature is limited by the highest temperature cavities, and curing time is given by the lowest temperature cavities that produce a longer than necessary curing time. Therefore, Isothermould® has been develop by REP to compensate the edging effect and ensuring thermal homogeneity in all the mold cavities, with curing time reduction.

A traditional injection molding machine relies on both controlled heating system and internal shear heat generation to provide the necessary heat to bring the polymer up to the necessary temperature in a plasticizing extruder [15-16, 25]. Three main sources of heat can increase the rubber temperature in the injection molding process: the heating system of the machine, the exothermal curing reaction, and shear heating. The last factor is a phenomenon where internal friction between different rubber compound layers inside the flow, generates heat and locally reduces the viscosity [9-28]. This phenomenon is often present in the industrial processing of rubbers and, although it is advantageous to increase the temperature of the rubber by saving energy, it complicates the control of the temperature and of the viscosity [16, 25].

This general principle is based on the fact that the higher the pressure is, the higher the shear rate and the higher the rubber compound temperature entering into the cavity. Therefore, an injected rubber compound having higher temperature could cure faster, but if the risk of scorching must be avoided. A too higher injection pressure has a dangerous limit, which is what level of shear the rubber compound can support. As a consequence, shearing and stressing too much the rubber compound, this might shorten the lifetime of the final parts too. On top of that, if there are runners, there is a risk of scorching before the rubber compound reaches the cavity.

The examination the rubber compound flow during injection molding shows a shear heating effect very different depending on the locations in the flow. According to shear-thinning theory the rubber compound flowing in the channel is characterized by laminar flow. Therefore, in the injection unit, or in the mold, the rubber can reach relatively higher temperatures near the outer wall. This is because the flowing material experiences a higher shear rate in this region; in contrast, the flowing material in the center region of the bulk has a much lower shear rate [10, 15, 17, 67-68]. This heterogeneous warm up causes heat to concentrate in some regions, which are the first to be affected by excessive shear, rubber compound scorching and degradation. These localized regions limit the overall possible warming up. Meanwhile some portions of the rubber compound

will have slight shear and thus very slight warm up during injection molding. As these portions on the rubber compound are the coolest one, the final curing time will result from them.

Figure 20 shows the laminar flow effect the on rubber compound injected inside the runner. The rubber compound is adhering (no velocity) to the runner wall whereas the center of the flow is the faster. The shear is the difference in velocity between layers that causes friction between them. On one side, the adjacent laminates have very big difference in velocity creating high shear and warm up in the outside layers of the flow.

On the contrary, in the center of the flow, adjacent layers are all flowing close to the same velocity, creating low shear and low warm up. The result is a high temperature on the outside versus a low temperature in the center of the flow.

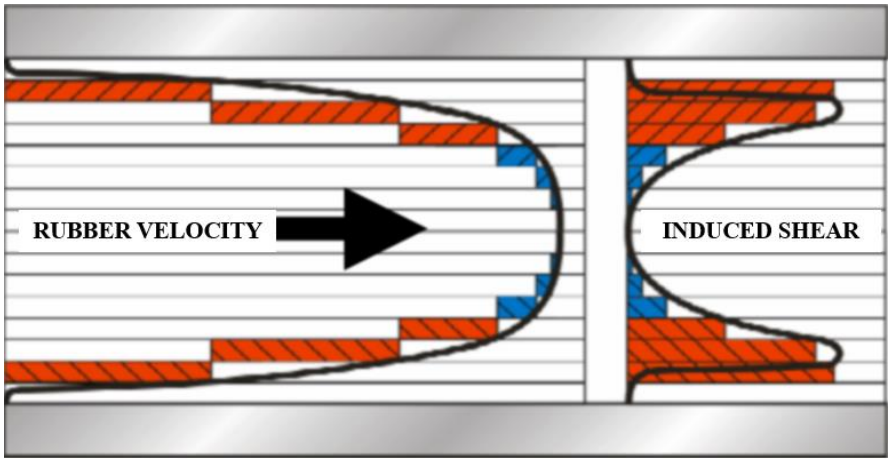

Fig.20. Effect of laminar flow on the injected rubber compound [67].

This laminar flow effect is real in every rubber flow, in the injection unit, in a cold rubber or in the mold. When examining more closely what happens inside the mold, the runners walls are also at high temperature which will add some warm up by conduction to the outside layers of the flow and not to the inside. The overall result will be a much higher temperature on the outside laminates than in the center of the flow. The laminar flow will not allow a mixing between the outside and inside layers, thus this temperature difference will increase over the flow length and lead to high temperature heterogeneity especially at the nozzle outlet. Although the temperature of the rubber compound as it leaves the plasticizing extruder is not homogeneous, thus it can be more conservative and careful to measure the rubber temperature on the surface (shear heating temperature, T_{SH}) where temperature itself is higher, as proposed and investigated in this research activity [10, 26-28], to improve the process control.

Graf and co-authors in 1989, in order to study rubber's processability, modified an injection machine by introducing pressure and temperature transducers in the injection nozzle; here a "spider mold" was used which was equipped also with these sort of transducers. Tests were performed with a black SBR rubber compound but the process control of pressure and temperature was not applied in industrial production runs [69].

About the rubber compound temperature rise during the injection stage it was stated that the rubber mass is heated up by shear of friction. Two types of flow can occur in rubber compounds, plug flow and laminar flow. If there is no wall slippage, a shear gradient develops. Consequently, there is a higher temperature in the zone with the highest shear gradient and the core stays a bit colder. In case of plug flow, outside layers moves as fast as "the core" and a shear gradient over the cross-section cannot be assumed. It means that neither shear heating nor friction happens. In plug flow during the injection, the pressure raises and that would be dependent on viscosity because there is no shear. The rubber compound flowing in the runner, gates and cavities has a length (flow path) and it need pressure and time to push the rubber mass to the end of the flow path. The Equation (1) [70] here below describes the average temperature increase (ΔT) through dissipation of heat under adiabatic conditions and no shear:

$$\Delta T = \frac{\Delta P_{plug}}{\rho\, C_p} \tag{1}$$

where ΔP_{plug} is the pressure drop along the plug flow, ρ is rubber density and C_p is the specific heat capacity. It can be confirmed with an EP(D)M injection molding compound, which is a non-polar rubber and shows plug flow. Additionally, it is known the rule of thumb: temperature rise 5°C / 100 bar pressure. Regarding the volume flow rate, it was observed a pressure rise with volume flow rate increasing, but a slight effect on the temperature. The bigger portion of the pressure is converted in volume flow rate [70].

Instead about laminar flow, there is a critical pressure at which the flow changes from plug flow to laminar flow. Above the critical pressure there is laminar flow: outside layer of the flowing rubber compound is moving slow and has much longer residence time (10-20 times longer than the core, which is moving fast) and may scorch over time in cold runner block. After some time in production, it will end as a deposit in the runner and needs to be removed [70-71]. Below critical pressure, most of work input is converted into output and much less into heat. Therefore, the temperature rise is less than expected [72]. However polar rubber compounds such as NBR, HNBR, AEM and FKM, show a significantly shear heating, is some cases almost two fold. For the polar rubber compounds the rule of thumb for the temperature rise is 8°C-9°C / 100 bar. Therefore, the Equation (1) requires a term to overcome the forces due to shear (ΔP_{shear}):

$$\Delta T = \frac{\Delta(P_{plug} + P_{shear})}{\rho\, C_p} \tag{2}$$

To achieve the same volume output, a much higher pressure is required, and the shear gradient and shear heating become larger. Regarding the laminar flow, it was observed that a pressure rise has slight effect, but with relevant effect on the temperature rise (a high portion of the energy is turned into heat) [68].

3.2.2 Rubber post-curing

As briefly reported in Figure 19, once the rubber parts have been from the cavities, it needs a certain amount of time to cool down and continues to cure. A rule of thumb considers that curing occurs up to about 90% of its optimum level into the mold cavity, while the remaining 10% of cross-linking is achieved during the cooling and stabilization (at least 1 day). In some cases, this percentage can be decreased if, after the parts deburring, it is added another stage, called post-curing or post-cure. Commonly, post-curing is a thermal treatment performed in oxygen atmosphere, and it takes a place in air industrial ovens (static or rotary) with the following aims:

- to complete cross-linking reaction (*e.g.* for diamine and bisphenol curing systems);
- to remove volatile by-products and additives to obtain enhanced, stable physic-mechanical properties;
- to increase the hardness until the required specification (*e.g.* for diamine cure system);
- to improve the compression set, tensile strength and modulus (*e.g.* for diamine, peroxide and bisphenol curing systems) [22, 24, 64];
- to obtain the required dimensions (internal/external diameters and thickness for O-ring's);
- to guarantee the achievement of the required quality standards.

During the rubber curing in the mold cavity, and especially during the post-curing stage, oily vapors and fumes containing processing aids, plasticizers and others high and low boiling point organic compounds are developed. This thermal treatment removes the gaseous residues produced during the curing reaction that could break chemical bonds in the cross-linking network, having negative effects on the final physical-mechanical properties. Typically, post-curing leads to an increase in tensile strength and modulus, improves the compression set and reduces the elongation at break. About peroxide cured rubber compounds used in applications where Food and Drug Administration (FDA) certification is necessary, the molded parts must generally be post-cured for 4 hours at 200°C, to remove any by-products having toxicity with the human health (*e.g.* VMQ rubber parts).

Process aids such as carnauba wax can be volatilized out from FKM compounds during an oven post-curing cycle. Furthermore, FKM parts should not be placed in a post-curing oven with other parts made from different elastomers, especially parts based on VMQ rubber parts, as chemical interactions between silicone rubber and small amounts of hydrogen fluoride generated during the post-cure of the bisphenol curable FKM rubber compound can damage or destroy parts. Typically, the post-curing stage may be either as short as 2 hours, or as long as 24 hours. Post-curing oven temperatures typically range from 150°C up to 250°C, although temperatures between 200-232°C are most common. Optimal post-curing operating conditions, mainly time and temperature, depend on specific FKM rubber compound formulation, curing system type (bisphenol or peroxide), and on the required specification. The majority of improvements in properties are typically obtained after the first 2-4 hours in the oven, with smaller incremental improvement after longer post-curing times.

Bisphenol curable FKM molded parts commonly require long post-curing cycles with a deep impact on production time and costs. Post-curing for a period of 16-24 hours at 200-260°C should develop maximum physical and mechanical properties, namely tensile strength and compression set resistance. Thus, the method of post-curing can strongly affect the final quality of the FKM parts. However, for some applications, a post-cure stage may not be necessary [22, 24].

About AEM rubber compound diamine cured the post-curing stage is mandatory because the imide is formed in the relatively long thermal treatment, which runs at 175°C for four hours in an air industrial oven. The post-curing stage increases the hardness until the required specification, and the compression set drops to about 20-30% [27, 43-47].

The optimal operating conditions of post-curing, as a type of oven, time and temperature, strongly depends on the type of rubber compound, on its formulation, on curing system and final application. The diffusion and evaporation of gaseous substances must arise at a temperature higher than the service temperature.

The operating conditions are typically reported in the technical data sheet of the rubber compound, even if these data are to be considered as suggested, because they are obtained after compression molding by laboratory presses. The setup of temperature and time is suggested to remove properly the by-products and gaseous residues from curing. In the case of parts with high thickness, these are gradually brought to the temperature of post-curing required. This is mainly the case of FKM parts having low gas permeability.

In applications where chemical resistance is required (oils, solvents and acids), post-curing is often mandatory to obtain a more compact cross-linking network. In applications where a low value of compression set is required, the post-curing is almost always mandatory.

However, the operating conditions must be properly tested by laboratory and industrial trials, in order to search the compromise between the physical-mechanical properties required, the industrial costs, electrical energy consumption and environmental impact by gas emissions [22, 24].

3.2.3 Process control in injection molding

Injection molding is an increasingly popular processing method in the rubber industry [66]. The earliest studies on the process control were focused to understand some macroscopic defects such as the shrinkage of the rubber parts.

Nakashima and co-authors in 1973, demonstrated how the shrinkage in the parallel direction is larger than in the perpendicular direction, and anisotropic shrinkage increases with the increase of curing temperature and flow distance. The shrinkage is independent of the ‘expanded orientation’ (i.e., macromolecular orientation due to material thermal expansion and perpendicular to rubber flow), but is strongly associated with the shear orientation, while the mechanical properties are affected by the expanded orientation [73]. Therefore, how the rubber parts are processed in terms of both injection time and temperature, and both curing time and temperature, obviously affect the shrinkage and the mechanical properties of the molded parts.

Although methods of injection molding have been available for many years, the complex flow properties of rubber compounds made it difficult to accurately predict their processability. Conventional rubber processability tests such as Mooney viscometer provide partial information about the compound at temperatures and flow rates may be significantly different from real injection molding conditions [66].

Byam, Colbert and co-authors in 1980, proposed a more effective model of injection molding process by using information from ODR, Mooney viscometer and Capillary rheometer. This model involved a computer analysis of rubber compound flow and heat transfer in both the mold and injection molding machine. These elaborate models were very useful in providing a detailed analysis of injection molding process, but the everyday use of injection molding method required a simpler, more rapid analysis [66, 74].

Sezna and DiMauro in 1984, proposed another simple model based on the use of the Monsanto Processability Tester (MPT), a capillary rheometer for rubber and the use of an ODR. This model is compared to injection molding test by using non-polar rubber compounds based on NR and SBR. This laboratory model successfully predicted the effects of adjusting injection pressure, mold temperature and barrel temperature on injection times and scorch conditions. Such a model enabled an injection molding operator to predict the effect of adjusting molding conditions, optimize his process for a given mold and rubber compound, and control processability on his compounds batch to batch [66]. Nevertheless, although it is able to provide some correlations with process parameters of the machine, it has the limit to have been applied only on the non-polar rubber compounds, and above all it was not applied to industrial production runs of rubber parts and did not considered the significant effect of thermal history during the injection stage.

Leblanc and co-authors in 1991, sensorized a center-gated disk with three pressure transducers, and made injection trials with compounds of NR, EPDM and FKM. Pressures into the injection nozzle and mold temperature signals were also recorded and injection trials were made using different combinations of flow rate and injection temperature. Although a constant value of flow rate was programmed, they concluded that the real flow rate fluctuated differing from that which was programmed, thus providing too dispersed results [75].

Karam in 1995, made injection trials on a spiral shape mold equipped with two pressure transducers for a wide range of different process conditions using two compounds based on SBR and EPDM. He also recorded pressure and temperature signals inside the injection nozzle. Experimental pressure traces were compared to simulation results using Fill software. It was concluded that to define the temperature at which the rubber was introduced into the mold, the best approach was to make a shoot into air at the same process conditions; make a compact ball with the shoot and measure its internal temperature with the aid of a temperature transducer [64, 75]. Therefore, in this thesis, the rubber temperature measured by an infrared camera during rubber purging at the nozzle outlet of the injection molding machine extruder (T_{SH}), is taken as a process indicator giving the thermal history of the rubber compound injection and process safety [9-10, 16, 22-24, 26-28].

Arrillaga and co-authors in 2008, instead recorded the signals of pressure at three points during the filling of a spiral shape part. The objective was to investigate and monitor cavity pressure profiles during rubber injection-molding of two non-polar rubber compounds, NBR and EPDM. Two injection molding machine were used having respectively FIFO and LIFO injection units. A variety of permutations of process conditions (DOE), including mold temperature, rubber temperature, ram speed and injection molding with and without pressure holding stage, were studied. In all conditions, the transducer positioned in proximity to the gate displays pressure-decaying phenomenon observed near the gate. Furthermore, initial CAE simulations have been carried out using Moldflow software to check the capability of this software to calculate pressure decay during the filling stage. Moldflow has been incapable of predicting real hydraulic pressure and pressure profiles at a given defined position, because the software doesn't have the utility to compute variations in rubber temperature during the injection phase [65].

Hoster, Jaunich and Stark in 2009, described the first results of tests with the ultrasound curing monitoring of rubber compound during the process. An injection molding machine from Krauss Maffei was used and no industrial production runs were monitored. The method was applied to three polar rubber compounds, NBR, ACM and AEM, where the ACM and AEM results were unsatisfying. The main problem was caused by a loss of the ultrasound signal when the holding pressure could not be reached or was not kept for the whole time. Here evidently the viscosity of the rubber compound plays an important role. Obviously the rubber compound is still heated up when it reaches the sensor. The shear heating in the nozzle and the flow through the injection channel and a part of the mold are not enough to reach the mold temperature [77].

Always concerning ultrasound method, Hutterer, Berger, Praher, and Friesenbichler in 2018 investigated the applicability of ultrasound based temperature measurements to quantify dissipation heating of an NBR compound stored in both cool and warm conditions. The ultrasonic temperature measurements provided two advantages compared to thermocouples: they do not require direct contact with the material and allowed to measure an average temperature across the diameter of the material [78].

Nevertheless, even if in pilot-scale, these approaches showed the first investigations based on the online monitoring of curing and filling stages respectively in an injection molding process.

Ramorino and co-authors in 2010, discussed the results of a 3D finite element simulation of the injection molding process of a rubber component, including the stages of the mold filling dynamics and material curing, using the Moldflow CAE software. A differential scanning calorimeter (DSC) and a capillary rheometer were employed to characterize the rubber material to obtain appropriate curing reaction and viscosity models, respectively. The model parameters were used to simulate the injection molding process for an engineering rubber component with a complex geometry having a thickness distribution that ranges from 1.5 mm to 20 mm. The computations were noticed in good agreement with the experimental results, indicating that reliable information on rubber viscosity and curing kinetic play a key role for well-founded predictions [79].

Javadi and coworker in 2011, confirmed the importance of CAE simulations to improve the injection molding process control, and focused their simulations on the rubber curing process in a 3D finite element model. The effects of mold temperature on curing process and quality of final product were investigated. The results were compared with the experimentally measured data, which confirmed the accuracy and applicability of the method [80].

Stanek and co-authors in 2011, worked on the influence of cavity surface roughness and technological parameters on the flow length of rubber into mold cavity. The fluidity of rubber compounds is affected by many parameters such as rubber temperature injection speed and pressures and by the flow properties of materials. A spiral shape cavity was designed and produced for injection molding, and a vertical injection molding machine REP V27/Y125 having LIFO screw, and equipped with electrical heating system of the mold has been used for testing samples preparation. The results of experiments carried out with rubber compounds, such as NBR, proved a minimal influence of surface roughness of the runners on the rubber flow [81].

Kyas, Cerny, Stanek and co-authors in 2012, compared the results from temperature-pressure sensors in real process with flow analyses in Cadmould Rubber computational software. A mold having two cavities is supplied with two temperature-pressure sensors in begin and in the end of the runner. Some non-polar rubber compounds based on EPDM, NBR, NR and SBR were investigated in a vertical injection molding machine REP V27/Y125 having LIFO screw [82]. The collected data should be helpful and advantageous for the rubber industry, where the introduction of sensors together with CAE flow analysis could be a good way for right process parameters setup [82, 83].

The online monitoring directly in the injection molding machine continued with the study of Zhang and Gilchrist in 2012. They have proposed an interesting online rheology measurement system using a slit die, but attached to a micro injection molding machine. This system allowed to process monitoring and rheological characterization with the purpose to understand the behavior of rubber flows during manufacturing of high quality parts. Two combined pressure and temperature sensors were embedded into the slit die to measure the pressure drop. The plasticization has induced a thermo-mechanical history that has also influenced the rubber compound viscosity, even though it is neglected in conventional rheology measurements [84]. Nevertheless, these sensors will be very susceptible to handling, wear and fouling especially if installed to monitor continuously the pressure and temperature in industrial production runs.

Fasching, Berger, Friesenbichler and co-authors in 2015, proposed a process control for rubber compounds injection molding with the use of systematic simulations and improved material data. Therefore, systematic CAE simulations using Varimos software has demonstrated an effective solution to understand the influences of the process parameters and their interactions. It therefore enabled automatically to optimize mold and process according to the required quality criteria. As a result, it was possible not only to save valuable machine time, but also to define the processing window and thus to improve economic efficiency of the process while at the same time ensuring the necessary process stability.

However, a significant weak point of this process control is that, the CAE simulation results were verified within the framework of a reduced experimental design in real injection molding experiments, and using a test mold with a single cavity [85]. Therefore, this process control should be applied systematically on the industrial production runs with molds having more number of cavities.

Friesenbichler, Neunhäuserer, and Duretek in 2016, showed their results concerning slit die rheometry using injection molding machine. With processing machines it is possible to perform measurements close to processing conditions in the industry (especially regarding pre-shearing). In this field several developments at Montanuniversitaet Leoben for machine rheometers were performed and measuring materials such thermoplastics and rubbers. A special slit-die system (Figure 21) was used for the examination of the pressure-dependent viscosity and the characterization of rubber compounds. As a result of the shear heating, after performing the rheological measurements for high-viscous rubbers, a temperature-correction of the apparent values was introduced [86].

As above-mentioned, although these sensors are very useful to collect pressure and temperature data by online monitoring, however they are too susceptible and also cumbersome to the daily operation of industrial processes. Furthermore, the cost-benefit ratio and durability of these slit die rheometry must be also properly investigated in industrial production runs.

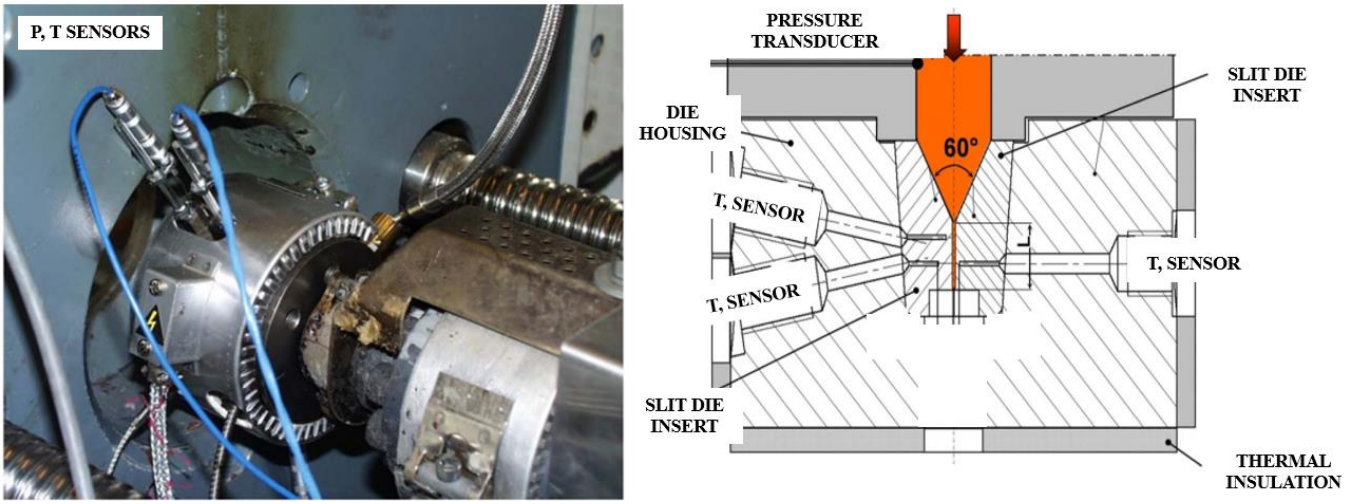

Fig.21. Slit die rheometry using injection molding machine [86].

Friesenbichler in collaboration with Mitsoulis and co-authors in 2017, also studied the flow behavior of an industrial SBR rubber compound with 70 Shore A hardness, in a capillary and injection molding dies in the temperature range of 80°C -120°C. The injection molding die designs had a tapered angle ranging from 40° up to 150°. This study compared the entrance pressures at the capillary rheometer as well as at the injection molding nozzle with viscous and viscoelastic simulations.

The rheological characterization of the rubber compound in the capillary dies showed that rubber slips at the wall. The pressure drops in the system were measured for all tapered dies. Figure 22 shows the FIFO injection

molding unit and prototype injection mold with exchangeable conical dies used during the experiments (P the position for pressure measurement) [87, 88].

This system, even though based on very interesting rheological characterization that also includes injection molding machine nozzle, was focused only on the pressure measurement, neglecting the shear heating temperature, and only on one type of rubber compound. Therefore, it can be considered as a prototype tool for research and development applications.

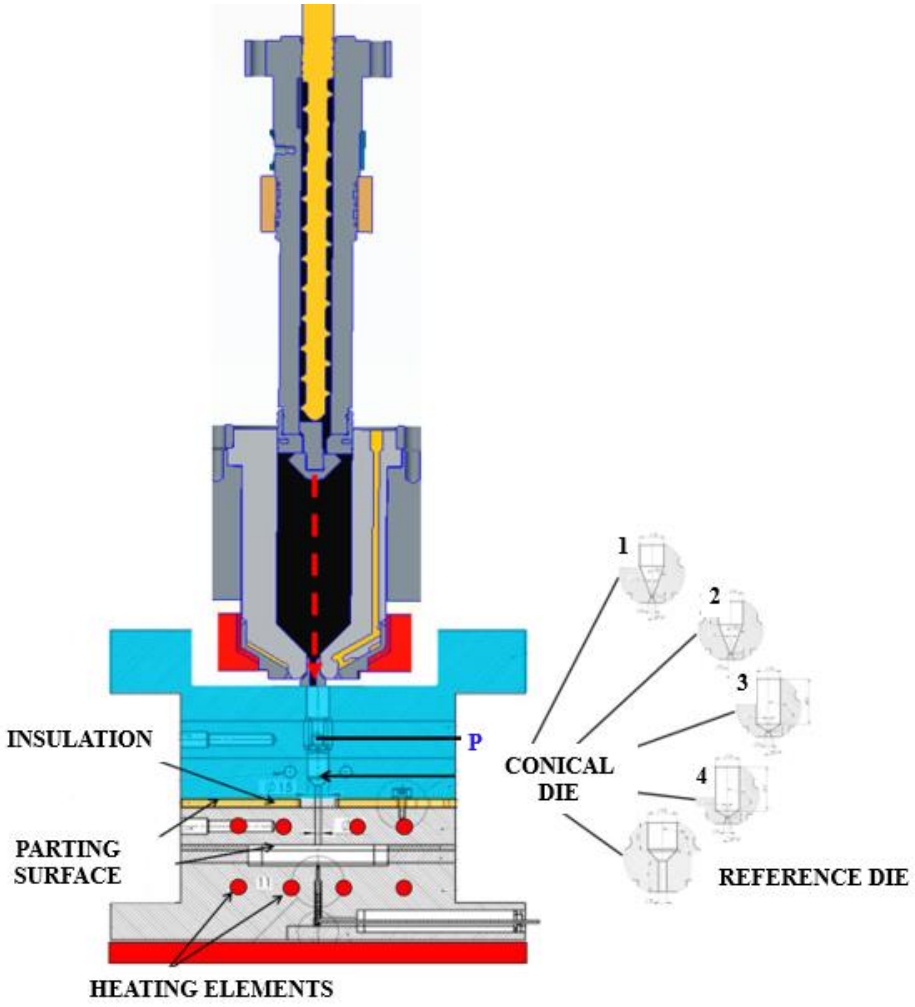

Fig.22. FIFO injection unit and prototype injection mold with conical dies [87].

About investigations focused on the die and nozzle of injection molding machine, Rochman and Zahra in 2018 applied various static mixers inside the nozzle chamber, together forming a mixing nozzle, for three rubber compounds, NBR, EPDM and FKM. The use of these mixers resulted in improved homogeneity and properties of the molded parts despite a curing time reduction of 10 s. This was due to the increase in mixing and shearing introduced a higher rate of cross-linking formation in the molded parts. Also this methodology of process control are to be verified in industrial practice, because the use of these mixer although improve the flow homogeneity, but it can increase the shear heating effect with risk of scorching [89].

Stieger, in collaboration with Friesenbichler, Mitsoulis and co-authors in 2019, proposed the flow visualization as a useful technique for the optimization and design of injection molding dies and injection units. NBR, HNBR and SBR rubber compounds were investigated, which exhibited not inlet vortices but dead zones in contraction areas. Dead zones have been suppressed using tapered dies with an inlet angle lower than 90°. An entirely developed cross-flow depends in injection units with conveying screw L/D ratio, viscosity and process parameters [90].

In industrial practice, the control of the process is exerted through: setup of machine parameters and laboratory tests on rubber compounds before production run, and/or sorting of faulty parts after production run. However, an online monitoring could potentially help the modification of machine setup parameters at the first symptoms of defect formation, thus minimizing the time between the occurrence of defects and the fast corrective measures implementation [91-92]. For this reason, with the rise of Industry 4.0-related technology, Farahani and co-authors in 2019, evaluated different online data sources in the plastic injection molding process to determine their relative degree of importance in predicting variations on final part quality indices (part weight, thickness, and diameter). These data were obtained during each injection molding cycle using a data acquisition system connected to eight in-mold sensors and four machine data sources. Using the standard coefficients from partial least square (PLS) regressions, rankings of the correlations between the extracted values and final part quality indices were generated [91]. Always in 2019, Chen and co-authors have emphasized the importance of quality control as a crucial issue to obtain a high yield rate and reducing production cost. This study proposed a quality index based on the clamping force increment during the injection cycle, as determined by four strain gauges attached to the tie bars of the plastic injection molding machine. Also, various quality indexes for online quality monitoring and prediction of pressure, viscosity, and energy features extracted from the pressure profiles obtained at the load cell, nozzle, and molding cavity, respectively, were compared [92].

Meanwhile about the CAE simulations to optimize the process control of complex parts, Ramorino, Agnelli and Guindani in 2020, reported for the first time the results of a 3D finite element simulation of reactive injection compression molding (RICM) by commercial software (Moldflow) for the production of rubber diaphragms. In particular, the filling and curing stages were analyzed and the results verified with experimental tests. DSC and a capillary rheometer were employed to characterize the rubber to achieve an appropriate curing reaction and viscosity models, respectively. Both initial melt and mold temperature used as input for the simulation were experimentally checked with a thermocouple. Melt temperature was measured on rubber purging at the outlet of the injection unit. The computations were found to be in good agreement with the experimental results using an NBR rubber compound, and for sure the measurement of the real temperature of rubber at the nozzle was essential to get this result [93].

Instead, Traintinger and co-authors in 2021, focused their process simulations with various definitions of the rubber inlet temperature, ranging from a stepwise increase, but constant temperature, to an exact axial rubber temperature profile prior to injection. The latter was obtained with a specially designed plasticizing cylinder

equipped with pressure sensors, a throttle valve for pressure adjustments, and a measurement bar with thermocouples for the determination of the actual state of the rubber temperature. Shear heating is a physical process in rubber injection molding that begins before the entry of the rubber compound into the mold at the first moment after passing the feed and continues in the transport through the injection chamber, nozzle and mold cavity. Neglecting this effect in CAE process simulations inevitably leads to significant deviations of the rubber mass temperature in the cold runner and ends in a potentially considerable difference of the curing reaction. Firstly, it was evident that the reliability of the numerically-determined results is significantly improved when the thermal history of a rubber compound related to the injection phase is considered in injection molding simulation [94, 95].

Therefore, the possibility to use the shear heating temperature, T_{SH}, in the setup of rubber temperature in CAE simulations, could provide outputs very close to the real condition [96].

3.2.4 Infrared thermal monitoring

Nowadays, the rubber industry requires rubber parts of very high quality. Therefore, it is advisable to improve control of the injection molding process, especially in the machine [12]. The quality of the final product is the result of a combination of factors, including the rubber, mold design, the process, and injection molding machine capability. Consequently, rubber processing by injection molding is very complex and influenced by several parameters, such as temperature, pressure, and shear rate. One of the most important control parameters is temperature. Even though the mold temperature is very easy to control by using thermocouples or other in-mold sensors, on the contrary, the rubber temperature is very difficult to control because it varies according to parameters such as injection pressure, injection speed and screw rotation speed. In particular, the rubber temperature is not only critical for the curing stage but also for the filling stage. If the rubber temperature increases too much, it can start to cure during cavity filling, which can generate defects in the molded parts with possible elongation decrease because the cure progressed too quickly, causing scorch [13, 27]. On the other hand, if the curing reaction occurs while rubber is flowing, viscosity increases sharply, and flow will virtually stop, so that some areas of the mold may not fill properly. Therefore, the mold cavity should be filled completely with rubber before curing commences [13, 15, 27].

Nevertheless, it will be important to guarantee a suitable rubber temperature, a compromise between scorch safety and cure commencing, to improve the cycle time and productivity.

When rubber flows too fast into one specific cavity, faster than the cavity immediately beside it, there is a shear rate difference. The higher the shear rate, the greater the shear heating and the larger the effect on viscosity. The problem is that the viscosity is not affected uniformly everywhere, but it is only affected in the material at the higher shear rate, whereas the lower viscosity rubber flows more easily under pressure and a filling imbalance is created [13, 27].

Other molding problems due to rubber temperature being too high are mold fouling and sticking phenomena, mainly due to diffusion of rubber compound ingredients [10-27].

However, as the temperature further increases, there will be a point at which the viscosity starts to increase due to the scorching of the compound. Furthermore, in the worst cases, if the rubber temperature increases too much due to higher shear rates, thermal degradation by loss of plasticizer and processing aids can start.

An optimal rubber temperature must ensure a balance between not having excessively high viscosity, scorch safety, and thermal degradation. The actual rubber temperature in an injection molding machine, mostly generated by shear heating, is very difficult to replicate in the laboratory by typical instruments such as MDR rheometer, because the MDR does not reproduce properly the physical process occurring in the injection stage of the molding machine extruder. The shear heating generated inside the injection molding machine extruder depends on the screw length to diameter ratio L/D, and mostly on the process parameter setup, such as screw rotation speed, injection pressure, speed and time, barrel temperature setup and other factors [10-27, 29].

Saito, Satoh, and Kurosaki in 2002, proposed a new concept of active temperature control for an injection molding process based on the use infrared radiation heating. By directly heating the molded polymer with radiation energy, precise and rapid temperature control and a small effect on the cooling duration were expected. This experimental technique was applied to actively control the polymer temperature and to improve the quality of molded products [97].

Vera-Sorroche and co-authors in 2015, applied an infrared temperature sensor to give real time quantification of the thermal homogeneity of plastic extrusion. The non-intrusive sensor was located in the barrel of a single screw extruder, positioned such that it provided a measurement of temperature in the channel of the metering section of the extruder screw. The rapid response of the technique enabled polymer temperature within the extruder screw channel to be monitored in real time, allowing quantification of the thermal stability of the extrusion process. Moreover, the data generated by the infrared sensor were found to be highly sensitive to thermal fluctuations relating to the performance of the extruder screw. Comparisons were made with an intrusive thermocouple grid sensor located in the extruder die, and suggested that the infrared technique was able to provide a similar level of information without disturbing the process flow. The application on infrared thermometry is highly useful for industrial rubber process monitoring and optimization [98].

Furthermore, Straka and co-authors two years later, proposed a novel ultrasound system based on reflection measurements for the online determination of high pressure, high temperature, rotational and axial screw movement. The system was compared to an infrared camera system, which measures the rubber temperature during an air shot in front of the nozzle. The recorded data of the measurement systems were used to study the influence of process parameter variations on the rubber temperature profile in the reciprocating screw of injection molding machine [99].

Eventually, Ageyeva, Horváth and Kovács in 2019, presented a comprehensive overview of in-mold process monitoring tools and methods for injection molding process control. Industry 4.0 requires a great deal of data

for manufacturing process control. The most popular pressure sensors are piezoelectric sensors and strain gauges, while the most popular temperature sensors are thermocouples. However, certain imperfections of the well-known measuring tools inspired researchers to develop new devices, based on ultrasonic, infrared, thin-film and other technologies. The future of temperature measurement is infrared measuring devices, as they provide very fast response and, unlike thermocouples, can measure the temperature of the rubber directly [100].

Therefore, this research activity aims to develop an integrated approach useful to improve the control of industrial injection molding of technical rubber parts based on the measurement of rubber temperature. The approach is based on very fast online process control, which is suggested in order to be used in industrial practice, and consists of the direct measurement of rubber surface temperature (T_{SH}) by the infrared thermal camera at the nozzle outlet of the injection molding machine extruder. Although the temperature of the rubber leaving the extruder is not homogeneous, it can be more conservative in measuring the rubber temperature on the surface where the temperature is higher (according to shear-thinning theory) [10, 15, 17, 27, 67]. It is proven that the use of an infrared thermal camera does not disturb the rubber flow and is a noncontact method characterized by a very fast response [97-101].

3.3. Rubber recycling

Recycling of rubber is of growing importance worldwide due to increasing raw material costs, diminishing resources, and growing awareness of environmental issues and sustainability. Many different recycling processes for rubber have been investigated and developed throughout the years. Several in depth reviews discussing the state of the art of rubber recycling were published in 1974, 2002 and 2012 [103-105].

The main recycling methods hierarchically classified in the order of environmental and economic preference are devulcanization, grinding, pyrolysis or other processes. The lowest level is burning vulcanized rubber for energy recovery, and the second level is based on feedstock methods, such as pyrolysis of used rubber to recover gas, oil and chemicals. The third method at the next level is material recycling by transforming used rubber into products with inferior quality compared to the original material, or using recovered rubber for the production of new rubber products. The most efficient rubber recycling route or the highest level on the recycling ladder is transforming used rubber into products with characteristics equal to those of the original materials, *e.g.*, used tire rubber back into tires [102-105].

Physical processes, such as grinding, are based on cutting, shearing, or impact fragmentation, depending on the equipment (knife, shredder, granulator, extruder, disk grinder, or impact mill) and the grinding conditions (ambient, wet, or cryogenic grinding). The choice of the process is based on the requirements for the final product, such as particle size and particle size distribution, morphology of the particles, and purity of the rubber powder. Cutting, in general, is only a pre-comminution step for rubber parts, such as tires, in which rubber products can be reduced to a particle of size a few centimeters. Specially adjusted mills, called cracker-mills, are used for rubber grinding. At least one of the rolls has a corrugated surface, and the rolls counter-rotate at a speed of 30 to 50 rpm with a very narrow gap and large friction. The final particle size is determined by the profile of the rolls, the gap and the friction between the mill rolls, as well as the cooling efficiency. Moreover, twin screw extruders can be used for grinding of rubber. A grinding extruder is equipped with two independent co-rotating screws with a set of grinding elements. Starting with a material having a granulometry of some millimeters, the final powder can have an average particle size of a few hundred micrometers.

Wet grinding can be also used: the concept of jet mills is an acceleration of the pre-ground rubber granulate by the air jet. Once the kinetic energy of the particles is high enough, collisions with other particles or different parts of the mill cause disintegration of the particles. Disintegration of the particles can also be achieved by turbulences in the mill. An ultra-high-pressure water jet allows the disintegration of a coarse granulate down to a rubber powder with a particle size of 200 μm. Disadvantages of this process are the insufficient separation of rubber and reinforcing material, as well as a high energy consumption caused by the drying step. Nevertheless, cryogenic grinding can be very suitable, where the rubber can be cooled down to a temperature in the glass transition area by liquid nitrogen. In the glassy state, rubber can be efficiently ground by impact.

Therefore, the optimal grinding temperature is just above the rubber glass transition temperature (T_g). A final particle size less than 0.6 mm can be achieved. The cryogenic grinding process, as such, is consuming less

energy than the ambient grinding process, but this comparison does not take into account the energy consumption for pre-grinding and drying of the powder [106].

The rubber compound powders obtained from grinding can also be used as fillers for a new rubber compound. This procedure enables for the obtainment of a “new raw rubber material” which can be cured again.

About the physic-chemical processes used in the rubber recycling, two types of rubber network breakdown simultaneously occur: reclamation and devulcanization (Figure 23). Reclaiming and devulcanization are frequently referred to as comparable processes. In spite they are similar in the procedure, however they are essentially different in the degree of rubber network breakdown and the molecular structure of the elastomer. Therefore, the main difference between “reclaimed” and “devulcanized” rubber lies in different ratios of cross-link versus polymer chain scission.

The devulcanization is the most ideal method of recycling rubber and aims to reverse vulcanization as far as possible without damaging the polymer. In sulfur vulcanization, formation of a rubber network by both, carbon-sulfur bonds (C—S) and sulfur-sulfur bonds (S—S), takes place; therefore, only these bonds should be broken during devulcanization. Devulcanization is the process of cleaving the monosulfide (C—S—C), and polysulfide bonds, C—Sx—C (x>2) cross-links of vulcanized rubber.

Reclamation is different from devulcanization due to the scission of the carbon-carbon bonds (C—C) of the elastomer chains. Reclaiming is a process in which vulcanized rubber is converted into a state in which it can be mixed, processed and vulcanized again by using conventional processes. Transforming the cured rubber into a reprocessable material is done by breaking the links between, and partly within, the elastomer chains.

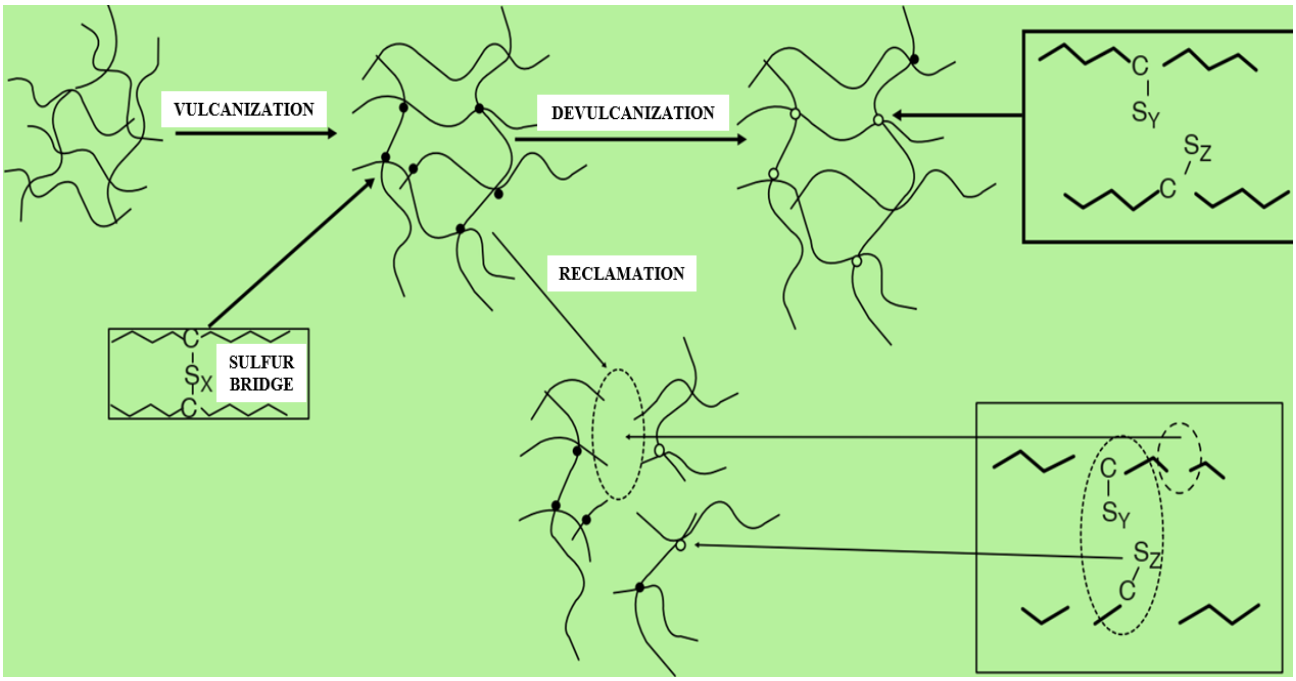

Fig.23. Devulcanization versus reclamation [102].

This technology is sometimes incorrectly referred to as devulcanization. For reclaimed rubber, relatively poor mechanical properties are frequently reported, originating from changes of the molecular structure of the elastomer that occur during the reclaiming process. Extensive elastomer scission and a partial recombination result in highly branched chain segments that differ greatly from virgin rubber.

Therefore, the conversion of used rubber into a reprocessable and reusable material by the currently used physic-chemical processes should be called reclamation rather than devulcanization. If the rubber is devulcanized, ideally only sulfur cross-links are broken (obviously for sulfur curing system), while the elastomer chains remain intact, resembling the original structure and quality.

An improvement of the properties of recycled rubber by developing a more selective breakdown process or efficient devulcanization will be an important challenge for rubber recycling technology [102-105, 107].

During the latest decades a growing interest in vulcanized elastomeric goods and scraps reuse has been observed because of an increased sensitivity to environmental problems and related Government policy [108, 109].

Tyre recycling plays obviously the most important role due to the high involved volumes; nevertheless, high performance elastomers reuse possesses interesting perspectives [108, 110-112].

Devulcanization technology is of great importance for HPE since it can combine the green approach to the maintenance of rubber compound high properties via the proper devulcanization procedure followed by tailored compounding [108].

Cervellati and Viola in 2013 have patented (Assignee: *Dott. Viola & Partners Chemical Research S.r.l*) a process for devulcanizing FKM bisphenol cured. The process including a step of heating the vulcanized FKM in the presence of a hydrolysis composition having one or more chemical selected from water, water soluble alcohols, water soluble glycols and mixtures thereof, at a temperature from 350°C to 430°C [113].

The integrated approach proposed in this thesis has been applied on green FKM rubber compound containing devulcanized scraps from black bisphenol cured fluoroelastomer used to produce technical goods [107].

The investigated FKM rubber compound was designed in collaboration with *Dott. Viola & Partners Chemical Research S.r.l.*

In conclusion, Schuster and co-authors in 2022 has proposed a review overview of recycling methods for FKM being a very expensive material with excellent properties. The deposition of fine grinded FKM powders in virgin rubber and the devulcanization of FKM and successive compounding with virgin rubber have proven to be viable recycling methods providing good thermal stability by maintaining the mechanical properties of original FKM [114].

3.4. EAF slag as reinforcing filler for NBR

Carbon black is the most widely used reinforcing filler for rubber. The studies of the reinforcement mechanism of carbon black can be dated back to 1960s. However, the knowledge of its mechanism still remains fragmentary today. While normally the addition of particle charges in polymeric matrices increases the elastic modulus but reduces elongation, in elastomeric matrices the addition of carbon black increases both modulus and elongation at break. With the presence of carbon black, the physical properties of rubber compounds, such as tear and tensile strength, can be improved. Carbon black increases the hardness and viscosity of rubber- compounds and it is considered one of the most efficient fillers [115], mostly due to its nanostructured shape. Carbon black is made up of over 90% pure form of elemental carbon, which is made up of tiny, mostly spherical carbon atoms that fuse together into groups called aggregates. Several aggregates then group together as agglomerates which break down during the mixing period of the rubber. Normally, the diameter of the carbon black particle ranges from 10 nm to 500 nm [116].

Since the carbon black production derived from the partial combustion of heavy hydrocarbons, its carbon footprint is enormous [116]. It has been estimated that the production of 1 ton of carbon black implies the emission of 2.4 tons of carbon dioxide, compared to 0.8 tons of carbon dioxide per ton of cement during production [117].

Given the increased demand for rubber quality and the rising price of elastomers and other ingredients, the rubber industry has made great efforts to limit costs and increase competitiveness. There are several concerns regarding the traditional carbon black fillers. On the one hand, the price of hydrocarbons sees a gradual increase every year. The cost of the raw material represents 30-35% of the total selling price of carbon black. On the other side, due to the non-degradability of the carbon black fillers, it can cause serious environmental problems. The conservation of the environment is a permanent issue, much research is undertaken with the aim of reducing the dependence of carbon black on fossil fuels and transforming it into a sustainable material base. For these reasons, sustainable alternatives to carbon black are being studied such as rice husk ash, peanut shell powder etc.

Gobetti, Cornacchia, and Ramorino in the last years proposed as substitute, or partial substitute to carbon black. A standard NBR (carbon black filled) has been compared with an NBR filled with EAF slag 100% and an NBR filled with EAF slag 50% and carbon black 50%. First of all, for a safe reuse of the slag it is necessary to maintain under control the leaching behavior, so that the leaching of slag incorporated into the rubber matrix has been measured confirming that NBR shields the slag particles preventing them from leaching. Then the comparison between the tree compounds has been carried out in terms of processability (rheometric curves and complex viscosity), mechanical properties (hardness, tensile test, compression test, stress relaxation and permanent set), swelling behavior, thermal conductivity and tribological behavior. The filler-rubber interaction has investigated as bound rubber, immobilized rubber fraction, and non-linear dynamic effect confirming the existence of slag-NBR interaction.

From a mechanical point of view, it was found that the EAF slag filled NBR has the same mechanical properties of standard NBR with the same hardness. These preliminary results are promising to continue the research for the best compound formulation according to the final application [118, 119].

The rubber compounds based on NBR filled with EAF slag 100% and an NBR filled with EAF slag 50% and carbon black 50% were investigated with processing trials by injection molding and using the integrated approach proposed in this thesis. These injection molding trials aimed to understand the processing behavior by using the shear heating temperature, (T_{SH}) by an infrared thermal camera, and the shear heating parameter (η_{SH}).

4 THEORY FRAMEWORK

This research activity started by evaluating the studies of Nishizawa about the heat controls and the rubber flow behaviour in extruders and in the injection unit of injection machines, and the problems occurring in these processes as well [16]. The equation to calculate the temperature rising from shear heating of rubber in an extruder reported in Nishizawa studies, was used to calculate the proposed shear heating parameter.

According to Nishizawa [16], temperature rise (ΔT, K) due to shear heating of rubber in an extruder may be related to rubber viscosity (η, Pa·s) by the following Equation (3):

$$\Delta T = \eta \frac{4\,\dot{\gamma}\,\mathrm{L}}{\rho\, C_p\, \mathrm{D}} \tag{3}$$

where η is the viscosity of the rubber (Pa·s), C_p is the specific heat (J/kg/K), $\dot{\gamma}$ is the shear rate (s^{-1}), L is the screw length (m), D is the screw diameter (m), and ρ is the density of the rubber (kg/m^3).

No reference was provided for this equation, therefore it was derived by the author in this thesis work. The hypotheses and the demonstration are here reported. Let's assume that the screw barrel is modelled as a simple cylindrical channel (Figure 24), a tube with dimensions L (length) and D (diameter). This hypothesis is very unrealistic, but it will allow to deal with the complex geometry of the screw and obtain Equation 3. A Newtonian fluid is flowing in the channel with a stationary laminar flow with $\dot{\gamma}$ as wall shear rate. Let's assume that there is no wall slip, and that the flow is adiabatic (no heat transfer to the surroundings).

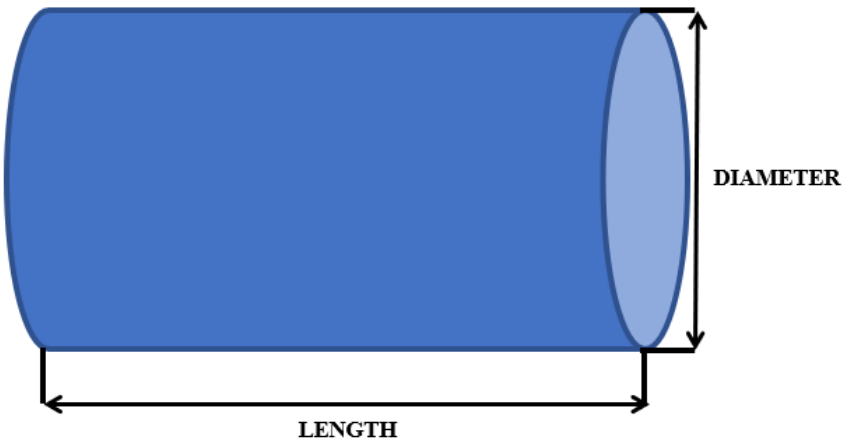

Fig.24. Tube with dimensions L (length) and D (diameter).

In this system the wall shear stress τ can be defined as follows [120]:

$$\tau = \frac{\Delta P \cdot \mathrm{R}}{2\mathrm{L}} \tag{4}$$

where ΔP is the pressure drop along the tube and R the tube radius (R = D/2).

The constitutive law for a Newtonian fluid defines the viscosity η as the ratio of shear stress over shear rate [120], therefore Equation 5 can be obtained from this definition and from Equation 4:

$$\eta = \frac{\tau}{\dot{\gamma}} = \frac{\Delta P \cdot \mathrm{R}}{2\mathrm{L}\dot{\gamma}} \tag{5}$$

The average temperature rise ΔT along the tube can be calculated from the total mechanical energy input under the hypotheses of an adiabatic flow, no fluid slip at the wall, and incompressible material, as follows [19]:

$$\Delta T = \frac{\Delta P}{\rho\, C_\mathrm{p}} \tag{6}$$

where ρ is rubber density and C_p is the specific heat capacity.

This gives an estimation for the maximum bulk temperature rise [19, 120]. Therefore, from Equation (6) it comes that:

$$\Delta P = \rho\, C_\mathrm{p}\, \Delta T \tag{7}$$

By introducing ΔP from Equation (7) into (5):

$$\eta = \frac{\Delta P\, \mathrm{R}}{2\mathrm{L}\dot{\gamma}} = \frac{\rho\, C_\mathrm{p} \Delta T\, \mathrm{R}}{2\mathrm{L}\dot{\gamma}} = \Delta T\, \frac{\rho\, C_\mathrm{p}\, \mathrm{D}}{4\mathrm{L}\dot{\gamma}} \tag{8}$$

By reversing Equation (8), Equation (3), here reported also as Equation (9) is obtained [16]:

$$\Delta T = \eta\, \frac{4\,\dot{\gamma}\,\mathrm{L}}{\rho\, C_\mathrm{p}\, \mathrm{D}} \tag{9}$$

The author is aware that many of the assumptions used to derive Equation (3) do not apply to rubber. Firstly, the barrel/screw geometry is totally different from a simple tubular channel. Secondly, rubber is a non-Newtonian pseudoplastic fluid: filled rubbers don't show any Newtonian plateau, rather their viscosity is related to shear rate by a power law Equation [16]. Very often rubber slips on the screw surface.

Nevertheless, the author was inspired by Equation (3) to derive a technological parameter (η_{SH}) with the purpose of providing a suitable process parameter setup during the injection phase [10, 26-28]. Such technological parameters combine material properties and process parameters in a similar way as Equation (3). Material properties (rubber density and specific heat capacity) are the same as in Equation (3), whereas $\dot{\gamma}$ and L/D ratio have been substituted by other more technological parameters having the same dimensions. Therefore, η_{SH} is a technological parameter having dimensions of viscosity (Pa·s), and is defined as follows:

$$\eta_{\mathrm{SH}} = \Delta T_{\mathrm{SH}}\, \frac{\rho\, C_\mathrm{p}}{4\,\nu}\, \alpha \tag{10}$$

where ΔT_{SH} (°C) is the difference between online measured shear heating temperature (T_{SH}) of the rubber compound and the initial room temperature (considering 20°C as initial temperature), v (s^{-1}) is a flow rate parameter, and α is a function of process parameters such as D/L, screw rotation speed, injection pressure, speed and time, barrel temperature setup and other factors.

Due to the complexity of the injection molding process, a thorough investigation needs to be performed to define α and its dependence on the process parameters. However, in this work, α is approximated as equal to screw D/L because, according to experimental data, it is one of the most relevant factors contributing to shear heating during the injection stage. In the present work, $\alpha = 1/(L/D)$.

Moreover, the flow rate parameter v in Equation (10) replaces the shear rate. In the present work, v is conventionally set at a value of 10 s^{-1}, chosen based on the commonly achievable order of magnitude of shear rate in the plasticizing extruder of the injection molding machine.

The results of η_{SH} were compared with minimum torque, M_L, from MDR routine rheometric laboratory measurements for several different industrial rubber compounds, based on AEM, HNBR, FKM and EP(D)M. The measured M_L value is a rough indication of the rubber compound viscosity; hence variations of M_L affect the rubber processability. Instead, the calculated η_{SH} value combines both rubber composition and operating condition effects, giving more information about the thermal history of the rubber injection stage and process safety [10, 26-28]. Therefore, the integrated approach proposed in this thesis is based on the correlation between two technological parameters, M_L from laboratory measurements and η_{SH} from the process, with the purpose to provide an operating roadmap to support the process engineer in the improvement of process control by thermal online measurements [10, 24, 26-28, 84, 91-92].

Besides the work of Nishizawa [16], other literature works provided the basis for this thesis work.

1. The studies of Friesenbichler about the rheometry of thermoplastics and elastomers by using processing machines, were also taken into consideration [86]. About Friesenbichler studies, the same philosophy to investigate rubber rheometry by using injection molding machines is applied. However, Friesenbichler applied a slit die rheometry in injection molding machine equipped with servo-hydraulically controlled back pressure units for measuring the pressure-dependent viscosity. Although, the developed injection molding machine rheometers have characterized in laboratory scale both thermoplastics and rubber compounds, near to the processing conditions, however they are too susceptible and also cumbersome to the daily operation of industrial processes. Furthermore, the cost-benefit ratio and durability of these slit die rheometry must be also properly investigated in industrial production runs. Whereas this thesis is based on measurements taken directly from industrial injection molding machines and industrial production runs, with a space-saving and especially fast temperature measurement system.

2. The approach proposed by Chen on the online monitoring of polymer injection molding has been of absolute relevancy [92]. About Chen studies, various quality indexes for online quality monitoring were compared, for instance based on the clamping force increment during the injection cycle, prediction of pressure, viscosity, and energy features obtained at the load cell, nozzle, and molding cavity, respectively. Although, a similar approach to this thesis about the online monitoring has been applied, however only the plastic injection molding was investigated, and laboratory scale tests were performed.
3. Finally, in this work T_{SH} was measured by an infrared camera. The studies of Vera-Sorroche confirmed that the use of thermal camera is a useful tool for monitoring the extrusion process of polymers [98].

Nevertheless, the content of this thesis will represent an interesting alternative to the works reported in the literature, since unlike them it focuses more on solving the real operating problems occurred during daily industrial production runs.

5 METHODS CHAPTER

This chapter collects all the experimental details about materials investigated, testing methodologies and instruments used to carry out the work of this thesis. Before showing the details, the following paragraphs provide a short overview of the investigations carried out in the thesis.

With the aim of providing useful tools for process control, a parameter for online monitoring of shear heating phenomenon is proposed. This parameter is based on direct measurement of rubber surface temperature by infrared thermal of the rubber as it leaves the extruder barrel of the injection molding machine. Therefore, a very fast online process control of industrial injection molding is proposed. The online monitoring is based on the shear heating temperature (T_{SH}) measurement, which is a process indicator giving the thermal history of the rubber compound injection and process safety.

This fast process control is applied to industrial cases to investigate the processing behavior of different rubber compounds. In particular, the relationships between T_{SH} vs injection pressure, vs injection speed, vs screw speed rotation and vs screw length over diameter ratio (L/D ratio) and vs AEM rubber compound properties variation due to exceeding the shelf life are investigated.

The measured T_{SH} is then converted into a parameter having dimensions of viscosity, the shear heating parameter, η_{SH}. The calculated η_{SH} values increase with increasing M_L values. The M_L value is a rough indication of the rubber compound viscosity, where its relevant variations are sensitive only to large variations of rubber processability. Meanwhile η_{SH} is more sensitive to small processability variations and more accurate because it considers the thermal history during the injection stage. A robust correlation between η_{SH} and viscosity from rheometric laboratory measurements was achieved for different rubber compounds. This represents an operating roadmap to support the process engineer in the improvement of process control [10, 24, 26-28].

Furthermore, laboratory characterization on AEM molded parts, focused on swell ratio testing, tribology testing (friction tests) sensitive to surface roughness and / or accumulation of lubricants on the surface of the rubber parts, as well as the Payne effect by using dynamic mechanical analysis (DMA), are reported.

Besides relating to CAE, implementations of T_{SH} and η_{SH} in the setup of simulations is also examined [96].

Finally, T_{SH} measurements and η_{SH} calculation in the processing trials of recycled FKM rubber compounds, and NBR rubber compounds containing EAF slag as reinforcing filler, are also explored [108, 118-119].

5.1 Experimental

5.1.1. Materials

Nine different rubber compounds based on different elastomers were investigated. These industrial grade rubber compounds were developed in accordance with automotive industry standard specifications, and their formulations cannot be disclosed for confidentiality reasons. The materials were compounded and purchased by industrial compounders. Table 1 reports their code, color, Shore A hardness and filler type and content in accordance with available *International Material Data System* (IMDS) data. The codes used to label the compounds indicate both the cure system (DIA = diamine, PO = peroxide, S = Sulphur, BP = bisphenol), the elastomer (EPDM, AEM, FKM, HNBR) and the hardness (60 or 70 Shore A). The black filler was usually carbon black type N 990. Black and colored filled rubber compounds were characterized by both laboratory tests and processing trials in the molding machine during industrial daily production runs [10, 26-28].

Table 1. Rubber compounds investigated with their filler type and content according to IMDS data.

Rubber compound	Color	Hardness, Shore A*	Filler Content wt.%	Filler Type
DIA-AEM60-1	Black	60±5	40.0-46.0	Carbon black
DIA-AEM60-2	Black	60±5	35.0-45.0	Carbon black
DIA-AEM70-1	Black	70±5	30.0-40.0	Carbon black
DIA-AEM60-3	Brown	60±5	38.0-46.0	Silicon dioxide
PO-EPDM60	Black	60±5	28.0-33.0	Carbon black
S-EPDM60	Black	60±5	26.3-33.5	Carbon black
DIA-HNBR60-1	Black	60±5	44.5-48.5	Carbon black
DIA-HNBR60-2	Red	60±5	40.0-48.0	Calcined kaolin
PO-FKM60	Green	60±5	18.0-23.0	Barium sulphate

* according to *ASTM D2240-15*.

Table 2 instead reports the data of sustainable compounds based on FKM and NBR.

Bisphenol cured FKM rubbers, black colored with 75 Shore-A hardness, were investigated. One is the virgin reference (FKM-REF) compound, whereas FKM-A and FKM-B are compounds containing 10 and 20 wt.%, respectively, of recycled FKM-REF.

Recycled FKM, also called “thermal treated FKM” (TT-FKM), is obtained from scraps of FKM-REF, which were selectively collected from an industrial production of gaskets which have been obtained via injection molding. Scrap collection is carefully done avoiding both environmental pollution and contamination by different elastomers. The scraps were coarsely mechanically grinded to obtain 5-7 mm granules which are fed to a 22 mm extruder working at high temperature. Choosing the proper working parameters, in terms of screw design, temperature profile along extruder length, screw rotation speed and fed quantity, a continuous stripe

devulcanized fluoroelastomer (TT-FKM) is obtained. The thermo-mechanical treatment determines a partial cross-link break together with partial polymer chain scission leading to a product whose appearance is quite close to an uncured compound.

The TT-FKM is constituted by two different fractions: soluble and insoluble in common FKM solvents like methylethylketone or tetrahydrofuran. These fractions are separated via solvent extraction and characterized. Soluble fraction consists in medium to low molecular weight FKM while insoluble fraction is a network of FKM strictly bonded to the fillers which can be compared to "carbon gel" or "bound rubber" [108, 113, 121].

Finally, also three compounds based on NBR elastomer were investigated. The reference compound is a sulfur cured, black colored, NBR rubber with 60 Shore A hardness. NBR-EAF100 is obtained by substituting the carbon black (CB) filler with a powder from electric arc furnace (EAF) slag and keeping the same total volume of filler in the compound. NBR-EAF50 is obtained from NBR-REF by substituting half of CB content with the same volume amount of EAF slag [108, 118-119].

Also, the rubber compounds reported in Table 2 were characterized by both laboratory tests and processing trials in the molding machine.

Table 2. "Green" rubber compounds investigated with their filler type and content.

Rubber compound	Color	Hardness, Shore A*	Filler Content wt.%	Filler Type
FKM-REF	Black	75±5	21.0-23.5	Carbon black
FKM-A (TT-FKM 10 wt.%)	Black	75±5	21.0-23.0	Carbon black
FKM-B (TT-FKM 20 wt.%)	Black	75±5	21.0-22.5	Carbon black
NBR-REF	Black	60±5	32.0-33.0	Carbon black
NBR-EAF100 (EAF slag 100%)	Black	45±5	51.0-54.0	EAF slag
NBR- EAF50 (EAF slag 50%)	Black	50±5	30.0-32.0	EAF slag/CB

* according to *ASTM D2240-15.*

5.1.2. Laboratory characterization

The above-mentioned rubber compounds were analyzed by using both in the uncured and cured state (both on standard specimens and final molded parts). The analytical instrumentation is located in the R&D laboratory of *Italian Gasket* plant, and in the laboratory of *Department of Mechanical and Industrial Engineering*, *University of Brescia*.

5.1.2.1 Uncured samples

The uncured samples were used to measure the minimum torque M_L data by an MDR 2000 from *Alpha Technologies* (Figure 25a) according to *ASTM D5289-95* at a frequency of 1.7 Hz and 3° oscillation amplitude. An uncured rubber test piece is contained in a die cavity which may be closed or almost closed and maintained at an elevated temperature. The cavity is formed by two dies, one of which is oscillated through a small rotary amplitude, corresponding to a sinusoidal alternating or torsional strain in the test piece. This action produces a sinusoidal torque which depends on the stiffness (shear modulus) of the rubber compound.

The envelope curve, which is defined as the amplitude of the torque, is continuously recorded as a function of time. The stiffness of the rubber test piece increases as curing proceeds. The test is completed when the recorded torque rises to either an equilibrium or maximum value, or when a predetermined time has elapsed. The time required to obtain a vulcanization curve is a function of the test temperature and the characteristics of the rubber compound [34].

Typically, the trend of the curing is described, at a given temperature, by the torque, in dN·m, as a function of time (curing curve). As already mentioned, M_L, is the minimum torque value that rubber compound can achieve, just before the curing reaction start. Therefore, in this graphical representation, M_L (Figure 25b) is taken at the lowest point in the curing curve [29, 34]. In the present work, the curing curve of each rubber compound was measured for 12 minutes at 177 °C because this is a historical and well-established internal methodology in *Italian Gasket*. The Monsanto MDR usually has 350°F as the test temperature, corresponding to 177°C. Moreover, this temperature can be easily reached in an injection molding machine to achieve the curing of a rubber compound [10, 26-28].

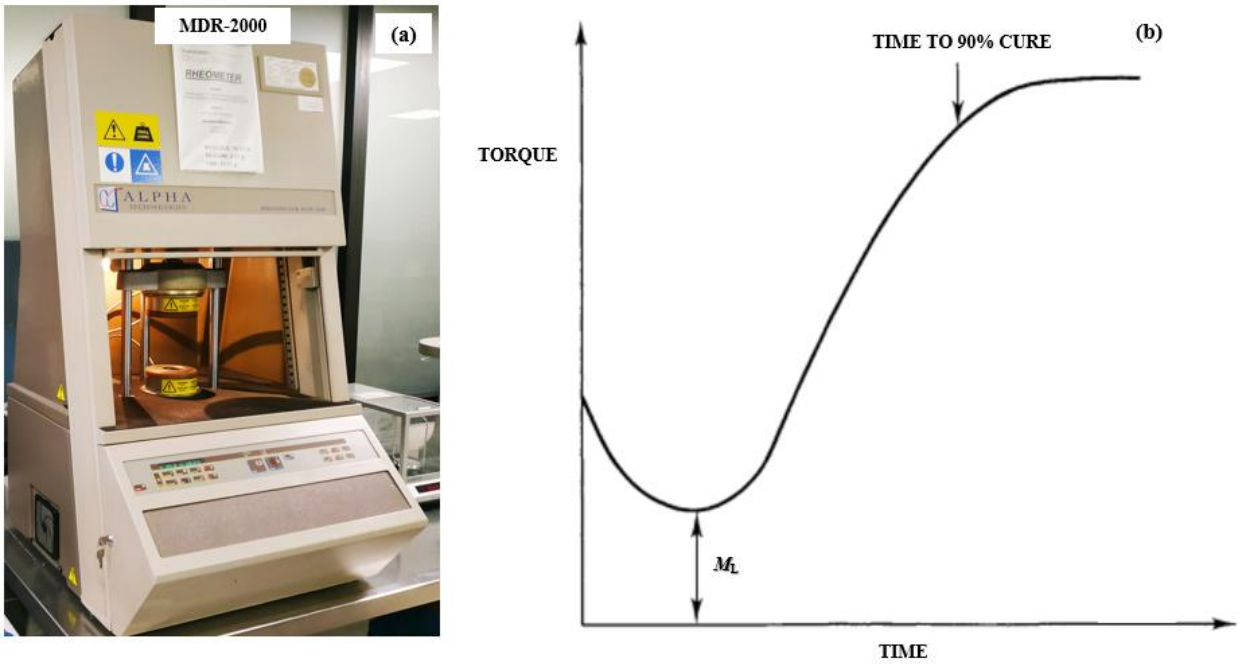

Fig.25. a MDR 2000 from *Alpha Technologies*. **b** Graphical representation of M_L [29, 34].

A laboratory compression molding press from *Gibitre Instruments Srl* (Figure 26) was used to cure and to mold standard samples such as buttons (cylinders) with thickness of 6 mm, and 200×200×2 mm slabs. Furthermore, also buttons and slabs were cured for 12 minutes at 177 °C.

Fig.26. Laboratory compression molding press from *Gibitre Instruments Srl*.

5.1.2.2 Cured samples

After 24 hours of stabilization, the cured standard samples were used for hardness and density (ρ) measurements, performed at room temperature, by a digital Shore-A durometer from *Gibitre Instruments Srl* (resolution: 0.01 Shore), and digital densimeter from *Doss* (accuracy: 0.001 g), in accordance with *ASTM D 2240-15* and *ASTM D297-15* respectively.

A hardness measurement is a simple way of obtaining a measure proportional to the elastic modulus of a rubber by determining its resistance to a rigid indenter under an applied force. The hardness of rubber compounds was measured according to the Shore-A scale. The Shore-A hardness measurement is based on indentation after a specified period of time, applied on cured standard samples with thickness of 6 mm. The standard time of application of the load is 3 s [29, 34].

Density is defined as mass per unit volume, whereas relative density is the mass of the substance compared to the mass of an equal volume of a reference substance (usually water) and is, hence, dimensionless. Relative density used to be commonly known as specific gravity but this term is now deprecated and should not be used. In practice, the method of measurement often involves the determination of the relative density to water but the density of water is assumed to be 1 g/cm^3. Furthermore, the determination is often made by observation of gravitational forces but for convenience the forces are expressed in mass units [29].

There are two basic test procedures: method A and method B. The more common being method A, in which the specimen is weighed in air then weighed when immersed in distilled water at 23°C using a sinker and wire to hold the specimen completely submerged as required [34].

The density value to be used for Equation (10) should be measured at the temperature and pressure in the injection molding machine extruder. However, to use an applicable industrial method, the density at room temperature and pressure was considered to be a reasonable approximation of density at higher temperature and pressure. This approximation is supported by the rubber material data reported in the CAE simulation software database, where a typical density variation is 5% with temperature increase from RT to 100°C and pressure increase from 0 to 200 MPa [10, 26-28].

Moreover, the cured samples were used for specific heat capacity (C_p) measurements by DSC in a 214 Polyma from *Netzsch Geraetebau GmbH* (Figure 27a). The C_p were recorded from 45 to 245°C with a heating rate of 20°C/min and referring to *ASTM E1269-11(2018)*.

This test method consists of heating 10-15 mg of cured samples at a controlled rate (20°C/min) in a controlled atmosphere (N_2, nitrogen) through the region of interest (from 45°C to 245°C). The difference in heat flow between the test material and a reference material or blank due to energy changes in the material is continually monitored and recorded. For the C_p determination, first of all the E value (calorimetric sensitivity) is calculated, which is a parameter specific to each DSC instrument. Then, the difference, D_{st}, between the empty specimen holder and sapphire standard at the same temperature, and the difference, D_s, between the empty specimen holder and test specimen at the same temperature are measured (Figure 27b).

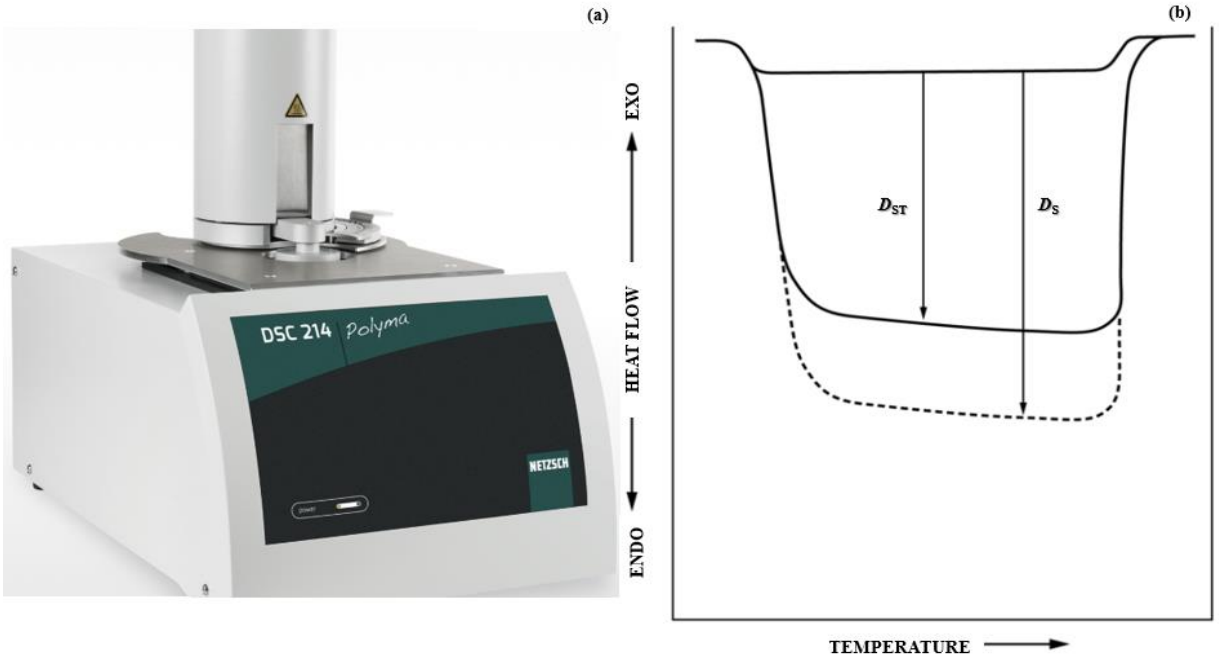

Fig.27. a DSC from *NETZSCH*. **b** C_p, thermal curves of standard sapphire and specimen [122].

Therefore, by using the calorimetric sensitivity, E, the C_p (J/kg/°C) of cured rubber sample at a given temperature is calculated by the following Equation (11):

$$C_p = \frac{60\,E\,D_s}{Ws\,b} - \frac{\Delta W\;C_p(c)}{Ws} \tag{11}$$

where D_s is vertical difference between the specimen holder and the specimen DSC thermal curves at the given temperature, (mW); Ws is the mass of rubber sample (mg); b is the heating rate (°C/min); ΔW the difference in mass between the empty specimen holder and the test specimen holder if the same holder is not used for both runs [122].

DSC instrument was also used to measure the calorimetric glass transition T_g of some molded parts both OK and KO (*i.e.* hardened and cracked) from the industrial production runs of DIA-AEM60-2. Measurements were carried out by using 5-10 mg of sample in the temperature range -80°C to 40°C, in nitrogen atmosphere (purge) and recording the first and the second heating with a heating rate of 10°C/min and referring to *ASTM D3418-21*. Moreover, injection molded O-rings (80 x 4 mm: internal diameter 80 mm, section diameter 4 mm) based on DIA-AEM70-1, and characterized by different shear heating temperatures, were analyzed in the temperature range -90°C to 20°C, in nitrogen atmosphere with a heating rate of 10°C/min [123].

Therefore, cured samples are also rubber parts obtained from industrial production runs. For instance, DIA-AEM60-2 parts, both OK and KO were used to qualitatively analyze their specific IR absorption frequencies (bending, stretching, etc.) by attenuated total reflection-Fourier Transform Infrared (ATR-FTIR) spectroscopy, using an ALPHA II FT-IR spectrometer from *Bruker Italia Srl* equipped with a Ge ATR crystal (Figure 28).

ATR- FTIR technique provides information related to the presence or absence of specific functional groups, as well as the chemical structure of polymer materials. Attenuated Total Reflectance (ATR) is a sampling method that introduces IR light onto a sample in order to acquire structural and compositional information. ATR is one of the most used sampling technologies for FTIR Spectroscopy. Using the ATR method the IR light passes through a crystal (diamond, ZnSe or Germanium) and interacts with the sample, which is pressed onto the crystal [35, 124-126].

The sample measurements were run at a resolution of 4 cm^{-1} and applied 24 scans from 400 to 4000 cm^{-1}. The rubber sample was measured using the Ge crystal, and after baseline correction the spectrum (absorbance as a function of wavenumber in cm^{-1}) is obtained for qualitative identification of the main functional groups present in the rubber parts. Elastomers, plasticizers, processing aids, antioxidants and white fillers can be easily detected by ATR-FTIR. Especially, for some DIA-AEM70-1 based O-rings (80 x 4 mm) from the injection molding and post-curing stages, and characterized by different shear heating temperatures, ATR-FTIR was used with the purpose to detect the absorption frequencies of imide groups (a weak band of C=O stretching vibration near 1700 cm^{-1}) [127].

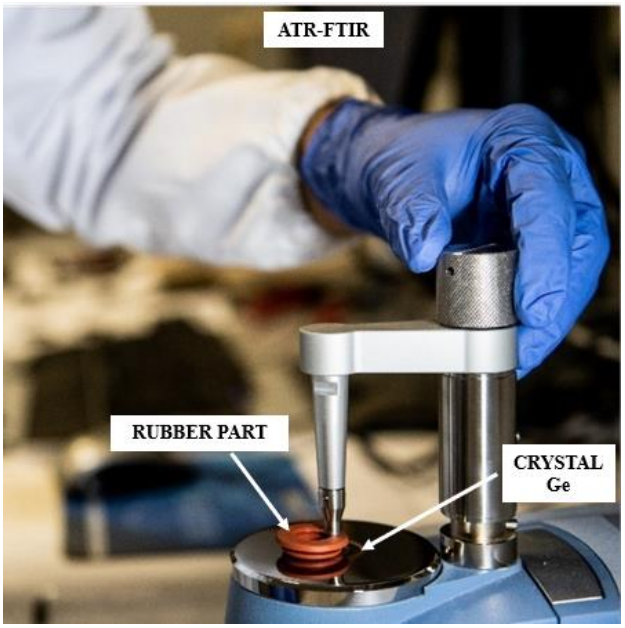

Fig.28. ATR-FTIR from.

Furthermore, DIA-AEM60-2 parts, both OK and KO, were used to quantitatively analyze their composition (*e.g.*, elastomers, volatile organic compounds such as plasticizers, and fillers as well) by thermogravimetric analysis (TGA), by using a TG 209 F3 Tarsus® from *Netzsch Geraetebau GmbH* (Figure 29a).

TGA is a system of thermal measurement where fluctuations in physical and chemical characteristics of ingredients are quantified as a function of temperature or time. Typically, variation in mass is attributed to a number of thermal events such as absorption, oxidation, desorption, vaporization, sublimation, reduction, and disintegration. These processes are investigated as the sample is exposed to a predetermined schedule of temperature change. Consequently, TGA is used in the analysis of volatile materials and gases liberated during reactions involving elastomers, plasticizers, processing aids, fillers such as carbonates and carbon black, antidegradants as well [128].

Practically, the cured samples of AEM parts (about 10 mg) were placed in a Al_2O_3 (alumina) crucible and heated in a thermobalance; the measurements were run in an N_2 atmosphere heating from RT to 600°C at 20°C/min, cooling from 600°C to 400°C at 40°C/min, holding for 2 minutes at 400°C, then heating from 400°C to 850°C at 20°C/min in an oxygen atmosphere and holding for 5 minutes at 850°C, the latter to facilitate the carbon black and ashes content measurement.

Figure 29b shows an indicative example of the results of TGA, also called thermogram, which is a simple 2D plot reporting the changes in the mass as a function of temperature. The thermograms can be either integral (TG) or differential (DTG).

TGA instrument was also used for the quantitative analysis of molded technical articles based on FKM-REF, FKM-A (TT-FKM 10 wt.%) and FKM-B (TT-FKM 20 wt.%). In this case FKM parts (about 10 mg) were placed in a platinum crucible and heated in a thermo-balance; the measurements were run in an N_2 atmosphere heating from RT to 150°C at 20°C/min, and from 150°C to 850°C at 10°C/min, then heating from 850°C to

950°C at 20°C/min in an oxygen atmosphere. This schedule of temperature was used to investigate potential compositional differences in the area of elastomers and fillers between FKM-REF and two compounds with recycled FKM.

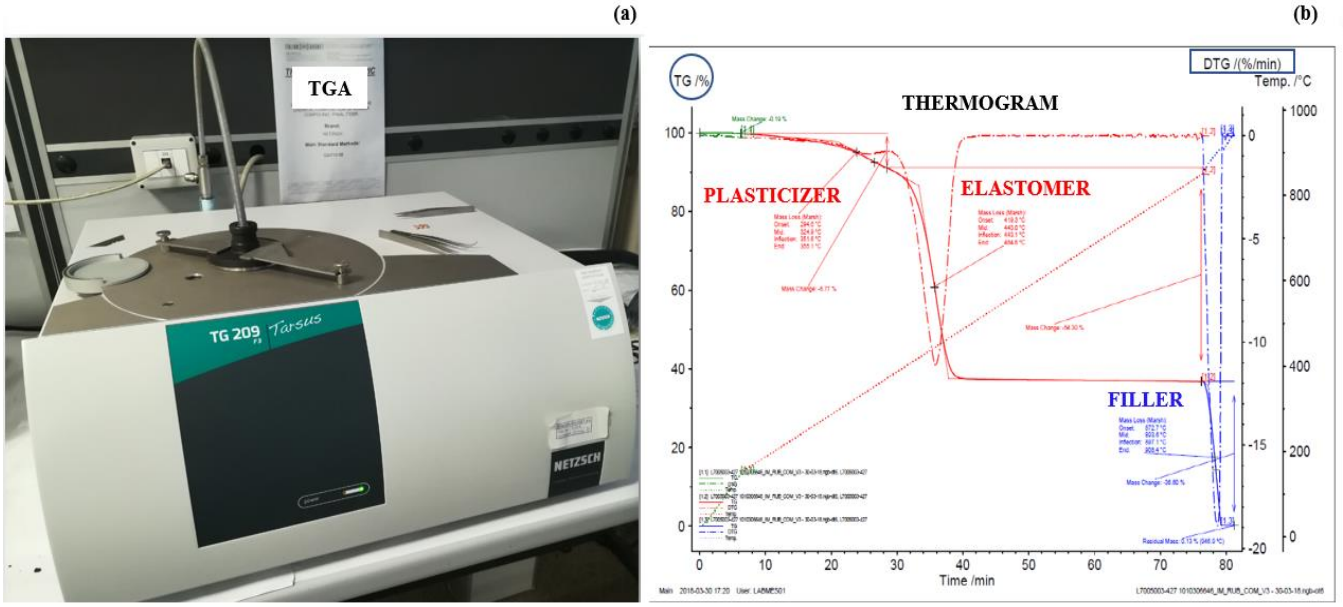

Fig.29. a TGA from *NETZSCH*. **b** Thermogram with TG and DTG.

Finally, the DIA-AEM70-1 based O-rings (80 x 4 mm) with different shear heating temperatures, were characterized also by other laboratory tests:

1. swelling ratio test (SR) [29];
2. tribology testing (friction test);
3. dynamic mechanical analysis (DMA) [29].

In the swelling ratio test, O-rings were cut in order to obtain samples of about 50 mg each, both from the bulk and from surface regions. Since the surface is thin, additional samples were used to reach the weight of 50 mg required for the test. Bulk and surface samples were immersed in ethyl acetate (CAS 141-78-6) in sealed glass tubes for 48 hours at room temperature. Weight measurements were carried out after swelling (M_r), and after 24 hours of drying at 80°C (M_f).

Therefore, the swelling ratio (SR) is calculated by the following Equation (12):

$$SR = \frac{M_r}{M_f} \tag{12}$$

In the friction test, the friction force of O-rings sliding on a metal plate was measured by an Instron 3366 test machine from *Instron*, equipped with a load cell of 50 N, and a sled (Figure 30), specifically designed to hold the O-ring, and made with a PLA polymer, by a fused deposition modelling printer (3D Raise3D Pro2). The measurements were carried out with a maximum displacement of 150 mm, at a displacement rate of 50 mm/min and a normal load (vertical load on the sled) of 1.35 N. From the friction test, the force at 10 mm, the

force at 100 mm, and the mean force were obtained. This test was sensitive to surface roughness and / or accumulation of volatile organic compounds, such as plasticizer and processing aids, which may migrate in the surface of the AEM rubber parts due to higher shear heating temperature effect [129, 130].

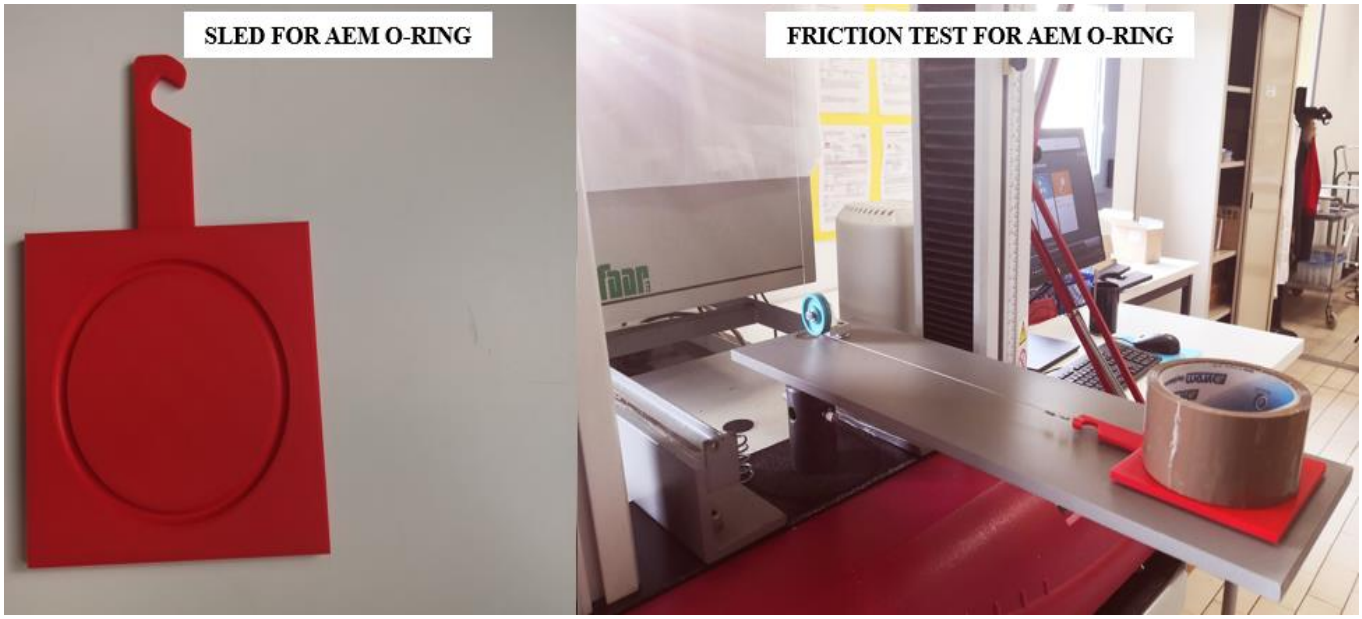

Fig.30. Friction test on AEM O-ring.

DMA test were carried out by a Dynamic Mechanical Thermal Analyser Q800 from *TA instruments*, in shear sandwich configuration, and in strain sweep mode, to measure the Payne effect. Cylindrical specimens were obtained by cutting sections from the O-rings with shear heating temperature of 130°C and 226°C. The measurements were run at room temperature, frequency of 1 Hz, and strain amplitude range between 0.1 µm and 800 µm. Two scans were performed on each sample, the first one to mechanically condition the specimen, the second scan data is reported. The Payne effect is a particular feature of the stress–strain behavior of rubber, especially of rubber compounds containing fillers such as carbon black [131-132]. The effect is sometimes also known as the Fletcher-Gent effect, after the authors of the first study of the phenomenon (Fletcher & Gent 1953) [133]. Physically, the Payne effect can be attributed to reversible deformation-induced changes in the material's microstructure, that is cross-linking, and interactions between filler and elastomer, or to breakage and recovery of weak physical bonds linking adjacent filler clusters [134].

Microhardness IRHD M and compression set tests were carried out on AEM parts, both OK and KO (*i.e.* cracked), from industrial production runs of DIA-AEM60-2.

The IRHD M hardness was measured on the AEM cured parts by using a digital IRHD M durometer from *Bareiss* (resolution: 0.1 IRHD) in accordance with *ISO 48-2-2018* [135]. The IRHD M hardness measurement is based on indentation after a specified period of time, applied on cured standard samples with minimum thickness of 1 mm. The standard time of application of the load is 30 sec.

Compression set is defined as the decrease in thickness of a rubber specimen after it has been deformed under specific conditions of load, time and temperature. The compression set was measured on the AEM cured parts in accordance with the Volkswagen standard *PV3330* by using stainless steel compression set device from *Gibitre Instruments Srl*. The device is designed for the testing of the permanent deformation of technical parts and O-rings. The distance of the platens is set using with 4 spacers. Compression was applied for 94 hours at 150°C and 40% of deformation. The required specification to be achieved for DIA-AEM60-2 parts under these conditions is ≤50.0%, according to automotive requirements from Volkswagen [136]. The compression set (Set), expressed as a percentage of the initial compression, is given by the following Equation (13)

$$\text{Set} = \frac{h_0 - h_1}{h_0 - h_s}\ 100 \tag{13}$$

where h_0 is the original specimen thickness, h_1 is the specimen thickness after testing, and h_s is the spacer thickness or the specimen thickness during the test. The lower the percentage, the better the material resists permanent deformation under a given deflection and temperature range [29, 137].

5.1.3. Processing characterization

The processing characterization started by following the industrial production run of O-rings based on DIA-AEM60-2, and especially investigating the process parameters setup effects on the rubber shear heating temperature (T_{SH}).

Later, the processing injection tests of the rubber compounds reported in Table 1 and Table 2 were performed using horizontal injection molding machines located in the Italian plant of *Italian Gasket*.

Regarding the rubber compounds reported in Table 1, six horizontal injection molding machines were selected for the daily production runs processing characterization. The processing trials have concerned daily production runs of each rubber compound, and after the start-up stage, the thermal controls by the infrared (IR) camera were performed.

Instead concerning the "green" rubber compounds reported in Table 2, two horizontal injection molding machines were selected. The processing trials were mainly focused on the injection stage of molding process.

The shear heating temperature, T_{SH}, collected for each rubber compound in each daily production run, was used to calculate the corresponding shear heating parameter, η_{SH}, by Equation (10), then correlated with minimum torque M_L results from MDR measurements [10, 26-28].

Figure 31 shows the online monitoring scheme of rubber surface temperature control as it leaves the extruder barrel of the injection molding machine by IR thermal camera during daily production runs.

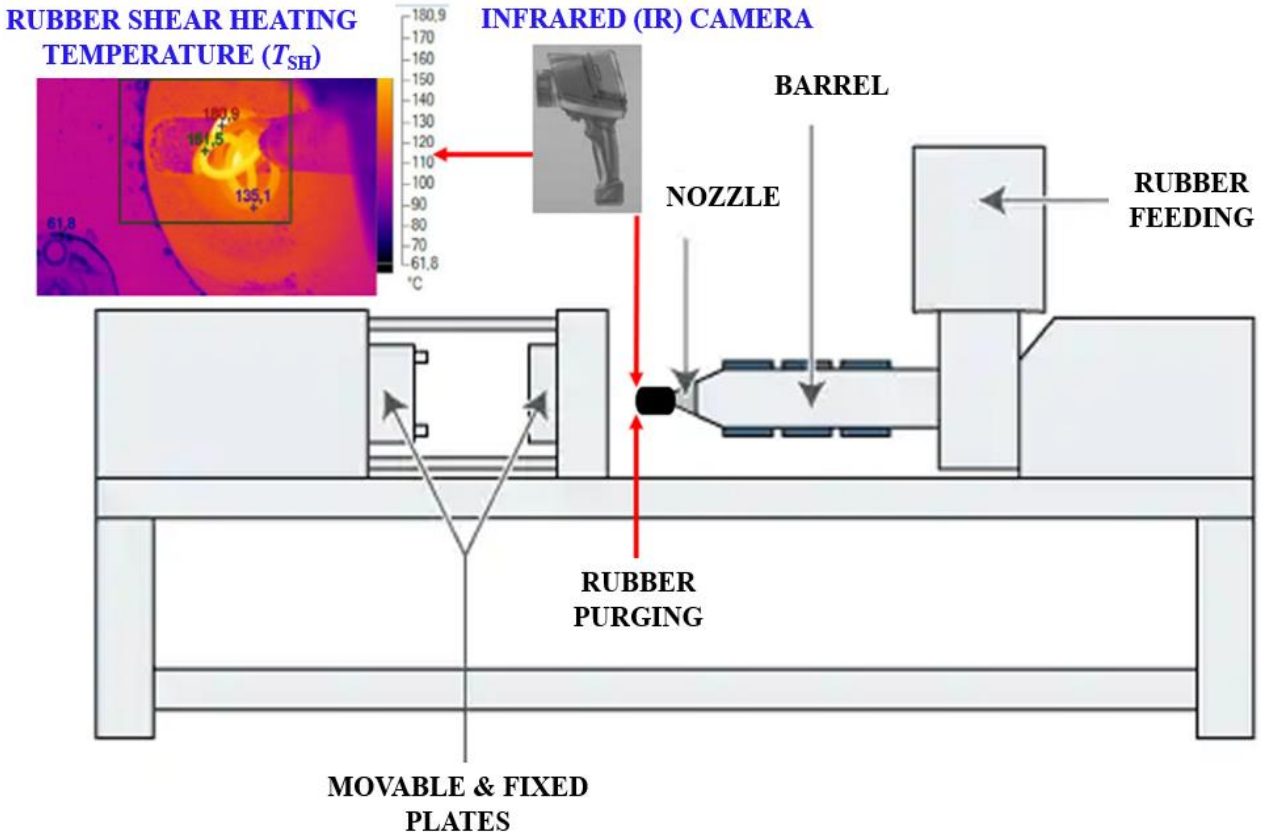

Fig.31. Online monitoring scheme of rubber surface temperature control proposed in this thesis [27].

A thermal imaging camera, Diacam C.A 1882, *Chauvin Arnoux Group, having* ± 2°C of accuracy and 0.08°C of thermal sensitivity, was used to control rubber surface temperature (T_{SH}) as it leaves the extruder barrel of the injection molding machine (Figure 31). The IR thermal camera was used to measure the rubber surface temperature by detecting the emitted electromagnetic radiation. The rubber emissivity was set to 0.95 in accordance with the software material database, and image analysis was provided by the software tools (Figure 32). The accuracy and sensitivity were selected in order to be lower than 5°C, which is an acceptable temperature oscillation during stable production run, on the basis of industrial experience [28].

In addition, CAm Report®, the software needed to create the measurement report, displays the temperature profile along line traced by technician following the rubber purging (see Figure 65a). Furthermore, using the software it is possible to obtain an automatic display of minimum, maximum, and average temperatures on a line profile, where conservatively the maximum temperature is considered equal to T_{SH}.

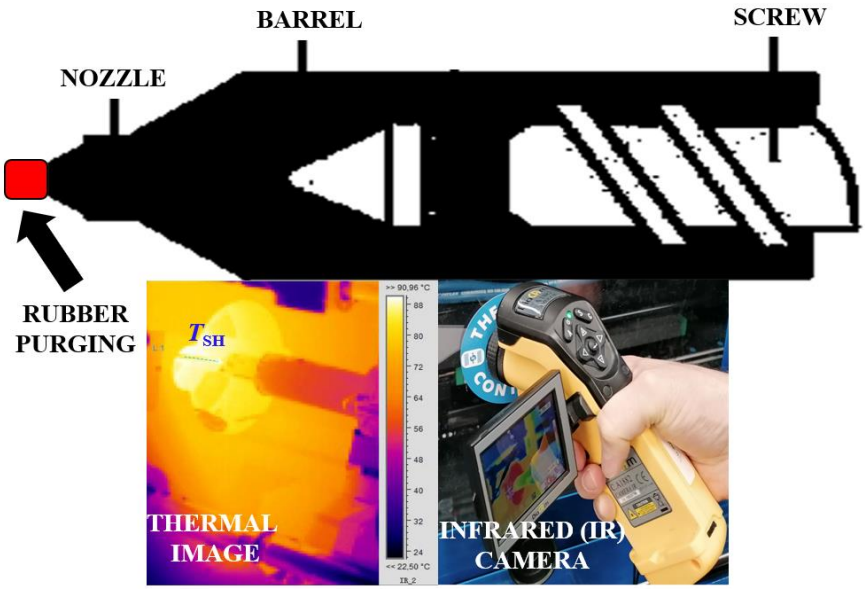

Fig.32. IR thermal camera used for online monitoring of T_{SH} [28].

5.1.3.1 Process parameters vs T_{SH}

An industrial production run of O-rings based on DIA-AEM60-2 was selected to investigate and to understand the process parameters setup effects on the rubber shear heating temperature (T_{SH}). For this analysis, a 300 Ton Maplan from *MAPLAN GmbH* having FIFO screw, L/D ratio of about 14 was used to produce O-rings based on DIA-AEM60-2. These O-rings after stabilization, deburring, post-curing for 4 hours at 175°C, and final controls, were used as gaskets in the automotive industry.

Therefore, the relationships between T_{SH} measured by an infrared camera vs injection pressure, vs injection speed and vs screw speed rotation were investigated, respectively. The effect of each parameter is investigated by varying the level of the parameter itself, and keeping constant all the other parameters.

Furthermore, a relationship between T_{SH} vs screw L/D ratio was investigated by using the same DIA-AEM60-2 rubber compound, but processed in different injection molding machines: a 300 Ton Maplan (FIFO screw L/D≈14), 300 Ton Engel (FIFO screw L/D≈ 6), a 190 Ton MIR (reciprocating screw L/D≈16) and a 190 Ton MIR (reciprocating screw L/D≈18), respectively.
The thermal measure DIA-AEM60-2 rubber compound was performed every hour, 3 measures at each time, for the purpose of controlling the shear heating effect during the injection stage.

5.1.3.2 T_{SH} and η_{SH} vs rubber shelf life

A 300 Ton Engel horizontal injection molding machine was also used to produce O-rings (80 x 4 mm) based on DIA-AEM70-1, 70 Shore-A and black colored.
Therefore, an industrial production run of O-rings (80 x 4 mm) based on DIA-AEM70-1 were selected to investigate the AEM material shelf life effect on the rubber shear heating temperature (T_{SH}). In particular, the calculation of the corresponding shear heating parameter (η_{SH}), by Equation (10), then correlated with minimum torque M_L results from MDR measurements, was performed [10, 26-28]. Furthermore, it was very interesting to understand the AEM rubber compound properties variation due to exceeding the shelf life.
DIA-AEM70-1 based O-rings (80 x 4 mm) affected by scorch problems, mold fouling and thermal degradation due to loss plasticizer and / or processing aids, were investigated. The mold fouling especially, once AEM the rubber compound exceeded shelf life, was continuously monitored.
The molded O-rings (80 x 4 mm), after stabilization, deburring, post-curing for 4 hours at 175°C, and final controls were used as gaskets in the automotive industry [28].

5.1.3.3 T_{SH} and η_{SH} in daily production runs

Five horizontal injection molding machines were selected for the daily industrial production runs processing characterization of the following eight rubber compounds. A 300 Ton Engel from *Engel Austria GmbH*, with FIFO screw, L/D ratio of about 6, was used to produce O-rings based on DIA-AEM60-1, and two different frame gaskets based on PO-EPDM60 and PO-FKM60, respectively. A 190 Ton MIR with reciprocating screw, L/D ratio of about 16, was used to produce technical rubber items based on DIA-AEM60-2. Furthermore, a 190 Ton MIR from *IMG Srl* with reciprocating screw, L/D ratio of about 15, was used to produce sealing rings based on DIA-AEM60-3. Another 190 Ton MIR with reciprocating screw, L/D ratio of about 18, was used to produce intake manifold gaskets based on DIA-HNBR60-1 and DIAHNBR60-2. A 450 Ton IMG from *IMG Srl* with FIFO screw, L/D ratio of about 12, was used to produce bellows based on S-EPDM60.
Figure 33 shows the images of O-ring based on DIA-AEM60-1, two different frame gaskets based on PO-EPDM60 and PO-FKM60, respectively, a sealing ring based on DIA-AEM60-3, and intake manifold gasket based on DIA-HNBR60-1 and DIAHNBR60-2, respectively and bellow based on S-EPDM60.

Daily production runs of each rubber compound were investigated and, after the start-up stage, the thermal control tests were performed. Also in this investigation the thermal measurement for each rubber compound and respective production run was performed every hour, three measures at each time, in order to control the rubber flow temperature and shear heating effect for each rubber compound during the injection stage [10, 26-27]. Furthermore, the molded parts, after stabilization, deburring, post-curing (if required), and final controls were used as gaskets in the automotive industry.

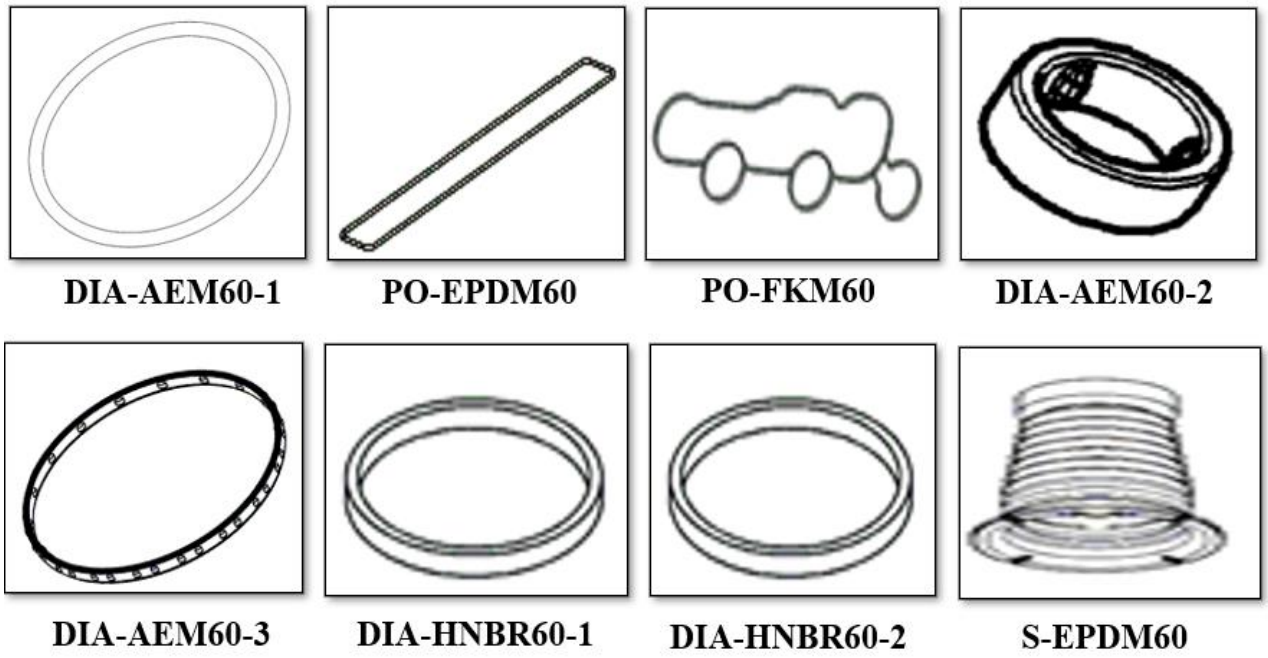

Fig.33. Molded parts investigated during the daily industrial production runs.

Table 3 reports the eight rubber compounds, the gasket type, and the corresponding horizontal injection molding machines classified as producers and screw L/D ratio.

Table 3. Rubber compounds, gasket type and their horizontal injection molding machine.

Rubber compound	Gasket type	Machine	Screw L/D
DIA-AEM60-1	O-ring	300 Ton Engel	6
DIA-AEM60-2	Technical item	190 Ton MIR	16
DIA-AEM60-3	Sealing ring	190 Ton MIR	15
PO-EPDM60	Frame	300 Ton Engel	6
S-EPDM60	Bellow	450 Ton IMG	12
DIA-HNBR60-1	Intake manifold	190 Ton MIR	18
DIA-HNBR60-2	Intake manifold	190 Ton MIR	18
PO-FKM60	Frame	300 Ton Engel	6

5.1.3.4 T_{SH} and η_{SH} for CAE simulation

The research activity is also focused on the possibility to use the shear heating temperature, T_{SH}, and shear heating parameter, η_{SH}, in the setup of CAE process simulations. More specifically, η_{SH} was used to derive flow curves (viscosity vs shear rate) of the material, and T_{SH} was used as melt temperature instead of barrel temperature (T_{barrel}), usually adopted in simulations. The case study of the 3D finite element simulation of the injection molding process was a sealing ring used in automotive industry (Figure 34). The simulations were carried out including both filling and curing stages, and using the *Moldex3D* CAE software.

Fig.34. 3D finite element CAE simulation sealing ring.

An FKM rubber compound black colored with 70 Shore-A hardness was characterized for CAE simulation. Therefore, the Pressure - Volume - Temperature curves (PVT), viscosity curves (viscosity vs shear rate), specific heat capacity and curing kinetics were experimentally obtained. As above-mentioned the specific heat capacity was measured by DSC referring to *ASTM E1269-11(2018)*. In addition also the curing kinetics were obtained by DSC: 10 mg of uncured samples were measured with heating rate of 10°C/min in nitrogen atmosphere from 45°C to 245°C. Furthermore, other measurements were performed, at 20, 40, 60°C/minutes of heating rate, respectively.

The viscosity used as input for CAE simulation was the shear heating parameter, η_{SH}. The latter was calculated by using a shear heating temperature, T_{SH}, of 110°C, obtained from a processing trial with a 190 Ton MIR with reciprocating screw, L/D ratio of about 18. Therefore, the rubber flow curve in logarithmic scale, log η_{SH}, was obtained by using Equation (10), and varying the flow rate parameter v in the range of 1.0 to 10,000 s^{-1}, at ΔT_{SH} (in this case 90°C) [10, 96].

Two process simulation runs were carried out with different values of "melt temperature" input, and by keeping the other inputs fixed (filling time, curing time, maximum injection pressure, mold temperature, and cycle

time). In the first simulation run (Run 1) the barrel temperature setup (T_{barrel}) of 80°C was set, in the second one (Run 2) the shear heating temperature, T_{SH} of 110°C, was used: in both cases experimental data coming from the above-mentioned processing trial [96]. Table 4 summarizes the main input data of the two process simulation runs.

Table 4. Input data of two process simulation runs.

Parameter	Run 1	Run 2
Filling time (s)	4.0	4.0
Curing time (s)	120.0	120.0
Maximum injection pressure (MPa)	250.0	250.0
Mold temperature (°C)	190.0	190.0
Cycle time (s)	129.0	129.0
Melt temperature (°C)	80.0	110.0

5.1.3.5 T_{SH} and η_{SH} for "green" rubber compounds

Three bisphenol cured FKM rubber compounds black colored with 75 Shore-A hardness, FKM-REF, and two recycled compounds, FKM-A and FKM-B, containing 10 and 20 wt.% of TT-FKM respectively, were investigated by processing trials. Figure 35 shows a simple scheme of the sequential steps: grinded FKM-REF (5-7 mm granules), twin screw corotating extruder and obtained TT-FKM strip.

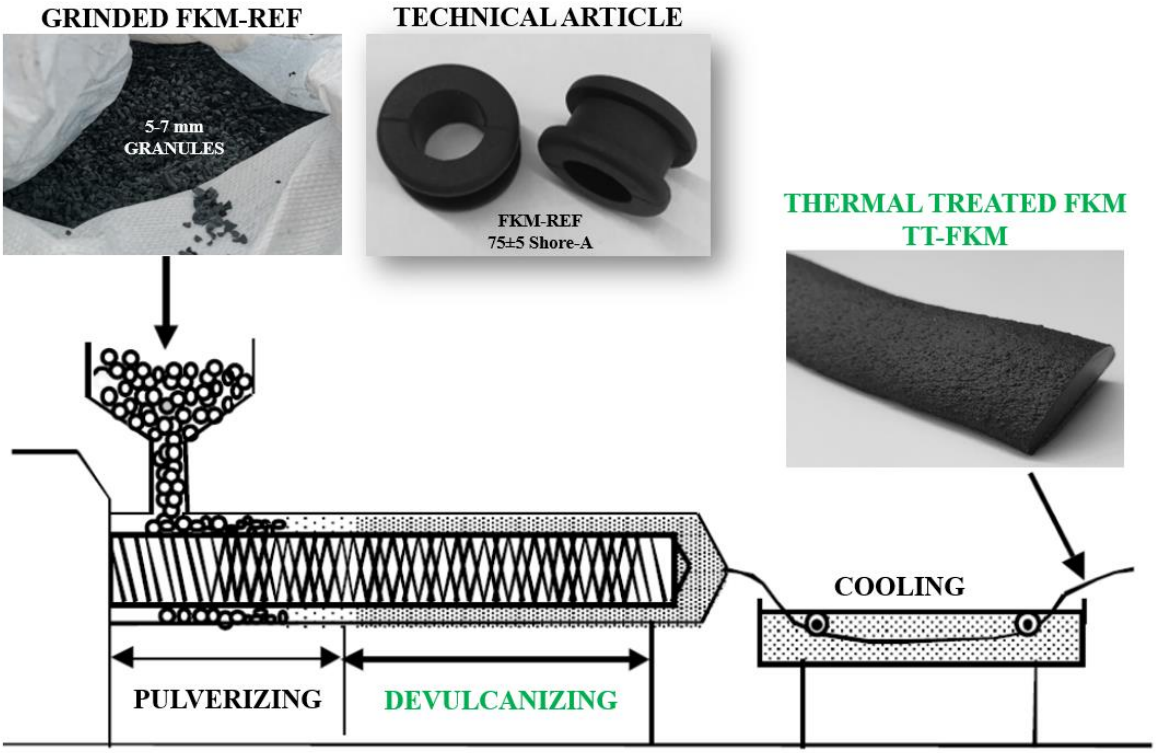

Fig.35. Simple scheme of TT-FKM production by devulcanization of FKM-REF.

Therefore, the TT-FKM of FKM-REF was considered as a new functional raw material for corresponding compounds FKM-A and FKM-B. TT-FKM, with 30 w% of soluble fraction, was obtained from the collected scraps and exploited to prepare two different bisphenol-curable FKM, 75 Shore-A hardness, black compounds: FKM-A and FKM-B containing 10 and 20 w% of TT-FKM respectively. A reference compound FKM-REF was also prepared with 100% of virgin elastomer. Recipes were studied in order to reach comparable curing behavior, hardness, density and composition (in terms of volatile, organic, oxidable and ash content) for the three different samples.

Industrial 75 kg batches of FKM-REF, FKM-A and FKM-B rubber compounds were prepared mixing the ingredients using a *Banbury* mixer followed by an open mill. Mechanical and chemical properties were tested on 200×200×2 mm slabs molded for 10 minutes at 180°C by laboratory compression molding press and oven post-curing for 24 hours at 230°C.

All the rubber compounds were used for the production of a technical article (used in automotive industry) via injection molding to verify the effect of TT-FKM on processability. This technical article (Figure 35) was chosen because its geometry can be very interesting to understand how the TT-FKM affects the mold fouling and the hot tear resistance, typical weaknesses of FKM compound.

The products are processed by using a horizontal 190 Ton MIR with reciprocating screw, L/D ratio of about 15. The mold is equipped with 32 cavities having a single nozzle injection system.

The same process parameters were used for all the rubber compounds. Table 5 summarizes the main process parameters set used for FKM-REF, FKM-A and FKM-B compounds processing trials.

Table 5. Process parameters setup used for FKM-REF, FKM-A and FKM-B.

Parameter	FKM-REF	FKM-A	FKM-B
Injection pressure, *P*i (bar)	140.0	140.0	140.0
Injection speed, *v*i (%)	85.0	85.0	85.0
Screw speed rotation (rpm)	30.0	30.0	30.0
Barrel temperature, T_{barrel} (°C)	85.0	85.0	85.0
Fixed plate temperature (°C)	195.0	195.0	195.0
Movable plate temperature (°C)	195.0	195.0	195.0
Curing time (s)	65.0	65.0	65.0

The online monitoring by T_{SH} measurements for each rubber compound and respective production run was performed every hour, three measures at each time, in order to control the rubber flow temperature and shear heating effect for each rubber compound during the injection stage [10, 26-27]. In this case it was very interesting to investigate the potential variation of shear heating effect due to the TT-FKM and the possible plasticizer effect of TT-FKM content in FKM-A and FKM-B recycled compounds. Moreover, the shear heating parameter was calculated for each rubber compound according to Equation (10) [108].

Finally, it was investigated the processability by injection molding of rubber compounds based on NBR filled with EAF slag as a total or partial substitution of carbon black (CB). NBR-REF with 60 Shore-A hardness, NBR-EAF100 filled with EAF slag at the same volume content as CB, having 45 Shore A hardness and NBR-EAF50, filled with a mixture of 50 vol% of CB and 50 vol% of EAF slag with 50 Shore-A hardness were studied.

About 5 kg batches of NBR-REF, NBR-EAF100 and NBR-EAF50 rubber compounds were prepared mixing the ingredients using a laboratory mixer followed by an open mill. Mechanical and chemical properties were tested on 200×200×2 mm slabs molded for 12 minutes at 177°C by laboratory compression molding press.

The three rubber compounds were used for the production of O-rings (internal diameter x section diameter: 13 x 2 mm) via injection molding to verify the effect of EAF slag on processability. The O-ring gasket type was chosen because it was the simplest geometry to understand the processing behavior of poorly known rubber compounds.

The rubber compounds were tested by using a horizontal 190 Ton MIR with reciprocating screw, L/D ratio of about 16. The mold is equipped with 174 cavities having a single nozzle injection system. The NBR-REF was the first processed rubber compound, then followed by NBR-EAF50 and NBR-EAF100. Injection molding process parameters such as injection pressure and injection speed were selected to appropriately setup the processing trials. The T_{SH} measurements for each rubber compound were performed in order to control the shear heating effect for each rubber compound during the injection stage [10, 26-27]. In this case was remarkable to understand the potential variation of shear heating effect due to the EAF slag. Finally, the shear heating parameter was calculated for each rubber compound according to Equation (10).

6 RESULTS & DISCUSSION

In this chapter the results of the work are reported and commented. Here is an overview of the contents.

Initially, the effects of process parameters setup such as injection pressure (Pi), injection speed (vi), screw speed rotation and screw L/D on the measured T_{SH} for DIA-AEM60-2 rubber compound are described.

Additionally, for the rubber compound DIA-AEM70-1, the AEM material shelf life effect on the rubber shear heating temperature (T_{SH}), was explained. In particular, the calculation of the corresponding shear heating parameter (η_{SH}), by Equation (10), then correlated with minimum torque M_L results from MDR measurements, was reported.

With the aim of understanding the T_{SH} variation effect on the final properties of the DIA-AEM70-1 based O-rings (80 x 4 mm), the results of glass transition temperature (T_g) from DSC, ATR-FTIR spectra, swelling ratio test, friction test, and storage modulus (G'), loss modulus (G'') , and mechanical energy dissipation (tan $\delta = G''/ G'$) as a function of strain amplitude from DMA, were reported.

Furthermore, the integrated approach based on the correlation between two technological parameters, η_{SH} vs M_L (operating roadmap) was explained and applied to industrial applications. Therefore, eight different rubber compounds based on AEM, HNBR, FKM, and EP(D)M elastomers and eight industrial production runs with long process stability were tested.

To show the potentiality of the operating roadmap, a case study is shown where this roadmap is successfully applied to optimize the injection molding of industrial production of DIA-AEM60-2 rubber compound affected by scorching and thermal degradation issues. In particular, various production runs of DIA-AEM60-2 rubber compound, where stable, unstable, and also the intermediate production runs were investigated. Scorching and thermal degradation phenomena on DIA-AEM60-2 parts were analysed by DSC, ATR-FTIR, TGA, hardness and compression set analyses.

In this chapter the results about the implementations of T_{SH} and η_{SH} in the setup of CAE simulations (case study: sealing ring based on FKM 70 Shore-A hardness), were also reported. Especially the output of two process simulation runs carried out using the same process parameters setup except the “melt temperature”, was highlighted. The use of T_{SH} as “melt temperature” is proposed instead of using the barrel temperature (T_{barrel}).

Finally, on the basis of sustainability focus, remarks about the application of T_{SH} and η_{SH} in the processing trials of recycled FKM rubber compounds (FKM-A and FKM-B containing 10 and 20 wt.% of TT-FKM respectively), and NBR rubber compounds containing EAF slag as reinforcing filler (NBR-EAF100 and NBR-EAF50, EAF slag 100% and 50% of total filler content, respectively), were reported.

6.1. Effect of process parameters on T_{SH}

The study of the effects of process parameters setup on the rubber shear heating temperature, was carried out on DIA-AEM60-2 rubber compound processed with a 300 Ton Maplan (FIFO screw L/D≈14) horizontal injection molding machine, producing O-rings. The effect of each parameter was investigated by varying the level of the parameter itself and keeping constant all the other parameters.

These O-rings after stabilization, deburring, post-curing for 4 hours at 175°C, and final controls, were used in the automotive industry.

The first process parameter investigated was the injection pressure (*P*i). Therefore, Figure 36 shows the relationship between T_{SH} measured by infrared camera vs injection pressure.

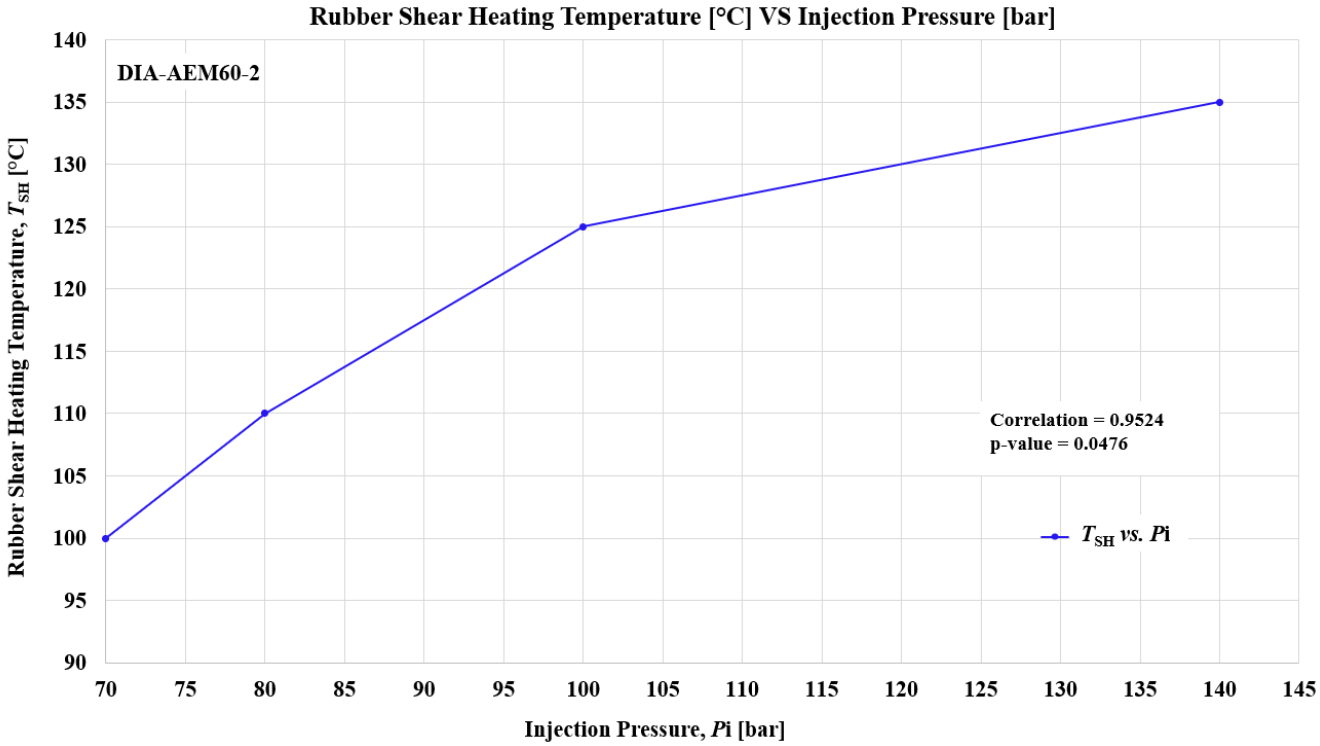

Fig.36. Relationship between temperature T_{SH} and injection pressure for DIA-AEM60-2 [28].

The Pearson correlation coefficient is also reported in the Figure 36 and the correlation test gives p-value lower than 0.05 (0.0476), thus the correlation is significant.

Reasonably, a reduction of injection pressure decreased the shear heating effect during the injection stage. The injection pressure reduction, from 140 to 70 bar, allowed a T_{SH} reduction of about 35°C, though maintaining a stable rubber compound processability with a negligible filling time variation. The trend is qualitatively expected because the shear heating temperature is by definition proportional to pressure drop in adiabatic conditions (Equation (1)). The second process parameter investigated was the screw speed rotation.

Consequently, Figure 37 shows the relationship between T_{SH} measured by infrared camera vs screw speed rotation, in which a similar proportional trend to the previous case of injection pressure was observed.

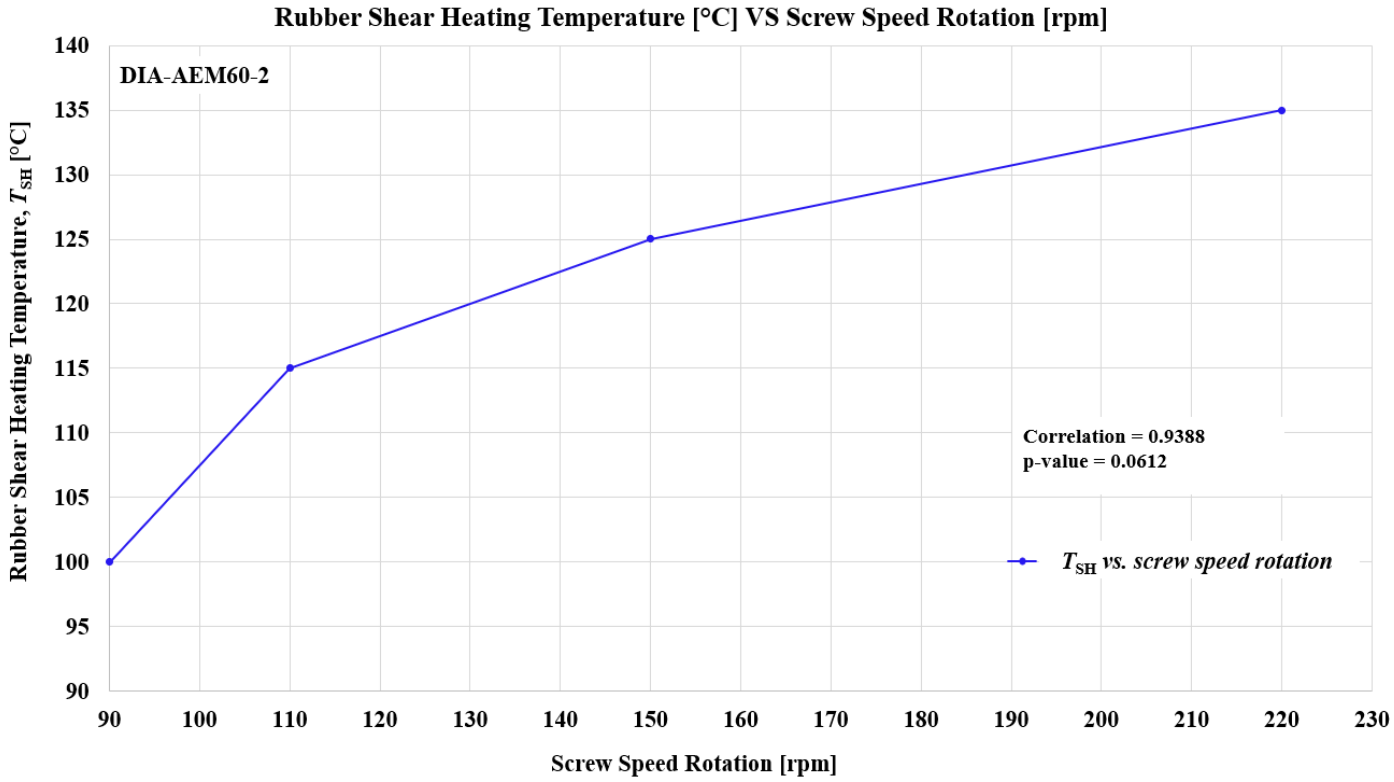

Fig.37. Relationship between temperature T_{SH} and screw speed rotation for DIA-AEM60-2 [28].

The Pearson correlation coefficient is also reported in the Figure 37 and the correlation test gives p-value higher than 0.05 (0.0612), probably due to the low number of data. Therefore, this trend cannot be statistically generalized outside the data sample. However this trend could be made significant by increasing the number of data. Also in this case, a screw speed rotation reduction, from 220 to 90 rpm, allowed a T_{SH} reduction of about 35 °C, though maintaining a stable rubber compound processability with a negligible filling time variation. The proportional trend can be explained by the fact that by increasing the screw speed rotation, the shear rate of rubber compound is increased along the screw direction. This results in a rapid shear heating effect (internal friction between different rubber compound layers inside the flow) and possibility to increase the risk of scorching in the injection unit, if it is not immediately detected and corrected.

The third process parameter investigated was the injection speed (*vi*) as shown in Figure 38. The Pearson correlation coefficient is also reported in the figure and the correlation test gives p-value higher than 0.05 (0.1283), probably due to the low number of data.

Figure 38 shows the relationship between T_{SH} measured by infrared camera vs injection speed, where a proportional trend similar to the previous cases of injection pressure and screw speed rotation was observed. However this trend could be made significant by increasing the number of data.

The injection speed reduction, from 40 to 15 mm/s, allowed a T_{SH} reduction of about 30°C; however, the largest T_{SH} decrease (about 20°C) was measured between 20 mm/s and 15 mm/s. On the other hand, only 10°C of T_{SH} decrease was measured between 40 mm/s and 20 mm/s.

Moreover, also in this case an injection speed reduction did not significantly affect the rubber compound processability. Increasing the injection speed causes an increase in shear rate especially in the extruder head, and thus, T_{SH} increases.

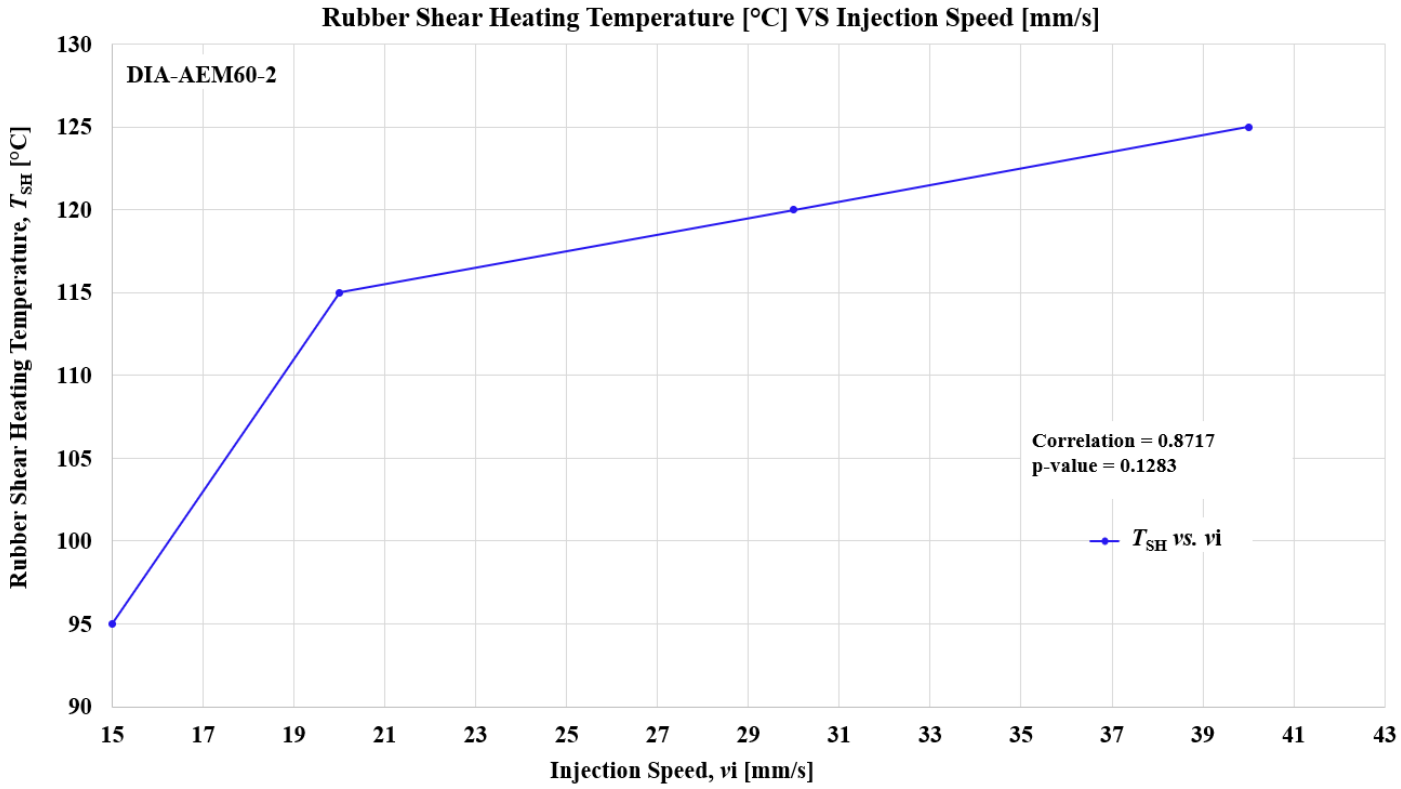

Fig.38. Relationship between temperature T_{SH} and injection speed for DIA-AEM60-2 [28].

Furthermore, a relationship between T_{SH} vs screw L/D ratio was investigated by using the same DIA-AEM60-2 rubber compound, but processed in different injection molding machines: a 300 Ton Maplan (FIFO screw L/D≈14), 300 Ton Engel (FIFO screw L/D≈ 6), a 190 Ton MIR (reciprocating screw L/D≈16) and a 190 Ton MIR (reciprocating screw L/D≈18), respectively.

Therefore, Figure 39 shows the relationship between T_{SH} measured by infrared camera vs screw L/D ratio, in which an interesting quasi-linear trend was observed.

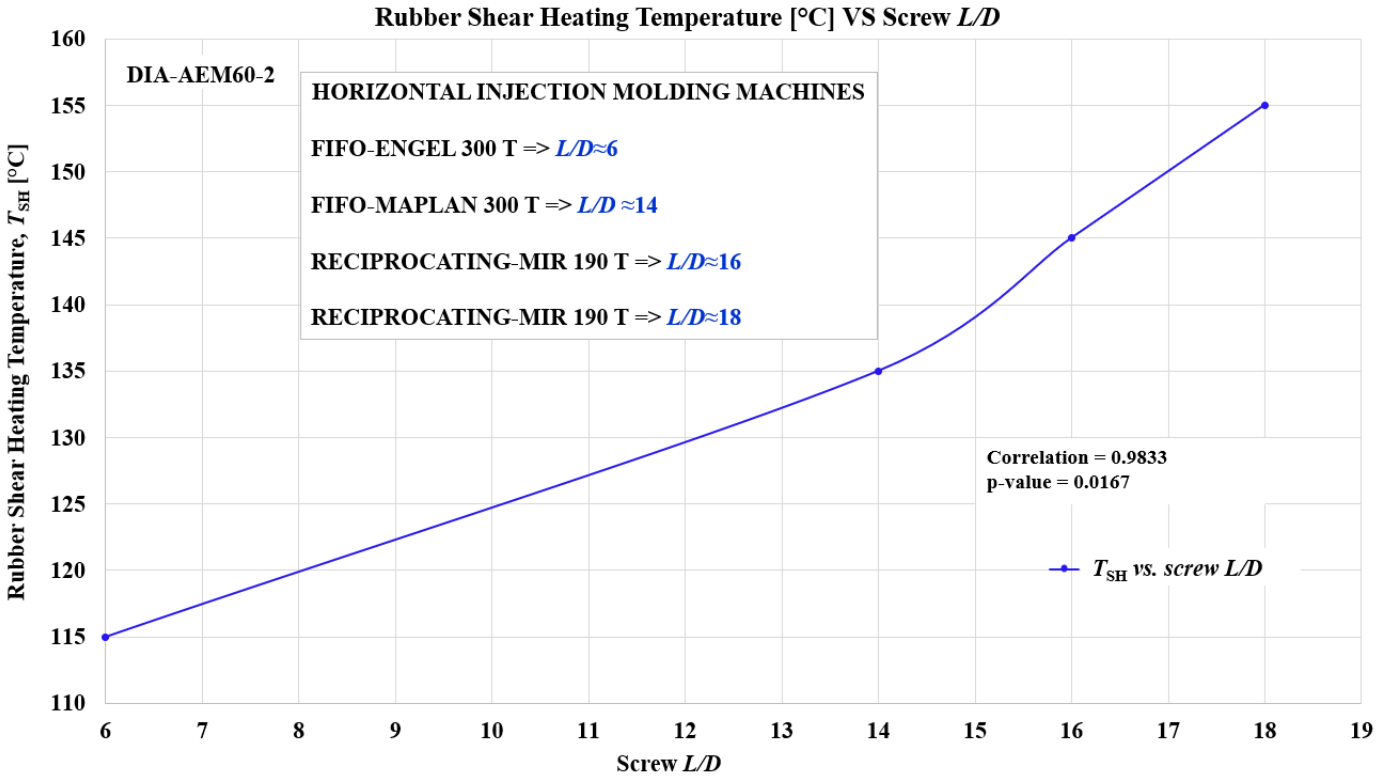

Fig.39. Relationship between temperature T_{SH} and scew L/D ratio for DIA-AEM60-2 [28].

The Pearson correlation coefficient is also reported in the Figure 39 and the correlation test gives p-value lower than 0.05 (0.0167), thus the correlation is significant.

Clearly, from the 190 Ton MIR (reciprocating screw L/D≈18) to the 300 Ton Engel (FIFO screw L/D≈6), a T_{SH} reduction of about 40°C was measured. Also in this case, a very stable rubber compound processability was observed with all the different injection molding machines used. Thus, production runs were carried out without relevant variations of cure rate, cure state (physical properties, *e.g.*, hardness) and with minor quality issue. Therefore, for the DIA-AEM60-2 rubber compound, and by using comparable process parameters setup as injection pressure, injection speed and screw speed rotation, the injection molding machines with higher screw L/D ratio showed the most significant shear heating effect T_{SH}. The main reason for the increase of T_{SH} of the rubber compound with increasing the screw L/D ratio can be ascribed the longer residence time.

Considering the results as a whole, for DIA-AEM60-2 rubber compound T_{SH} is manly influenced by the screw L/D ratio. Nevertheless, also the process parameters such as injection pressure and screw speed rotation clearly showed that they contribute consistently to the T_{SH} increase, especially if they are set to higher levels. Finally, also the injection speed has provided its most relevant contribution to the T_{SH} increase, if it is set to lower levels (Figure 38).

Normally in the industrial practice the most easy and intuitive parameter which is fine tuned to reduce T_{SH} is the screw speed rotation. On the other hand, the injection speed is the least effective parameter to reduce T_{SH} [28].

6.2. Effect of rubber shelf life on T_{SH} and η_{SH}

Besides the effect of setup parameters, also the effects of rubber properties variation on T_{SH} were interesting to be showed in this research activity. At this aim, a single rubber compound was studied, DIA-AEM70-1, and its properties varied due to exceeding the shelf life. It is well known that rubber compounds change their properties with storage time and temperature. Even under proper storage conditions, after some weeks the incubation time decreases, thus causing a risk of scorching, and the viscosity increases. This is reflected in deteriorated mechanical properties of the cured rubber [28, 61]. Typically, the AEM rubber compounds are characterized by a shelf life of about 1 month (Figure 11), obviously if properly stored according to *ISO 2230:2002—Rubber products—Guidelines* for storage [138, 139]. Therefore, the DIA-AEM70-1 rubber compound was processed both within the shelf life (2 weeks after the compounding) and off of it (5 weeks after the compounding), in a 300 Ton Engel by producing O-rings (80 x 4 mm), and the differences in processability were examined with particular care [28].

In this chapter, DIA-AEM70-1 based O-rings (80 x 4 mm) affected by scorch problems, mold fouling and thermal degradation due to plasticizer loss were analyzed as follows.

Figure 40a, b shows the cavities of movable plate during the DIA-AEM70-1 production runs, DIA-AEM70-1-OK (within the material shelf life) and DIA-AEM70-1-KO (out of the material shelf life), respectively. These production runs were chosen as a case study to show how the rubber compound shelf life, once exceeded, affects negatively on the rubber shear heating temperature, processing behavior and mold fouling.

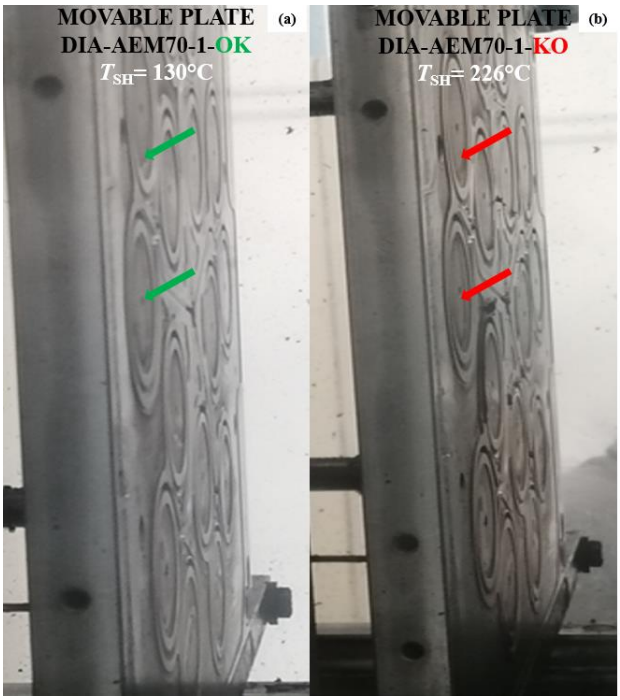

Fig.40. a Cavities of movable plate during the DIA-AEM70-1-OK production run. **b** Cavities of movable plate during the DIA-AEM70-1-KO production run. Green arrows indicate clean cavities, and red arrows indicate some fouled cavities [28].

Particularly, Figure. 40a shows the movable mold plate of DIA-AEM70-1-OK, where a not excessively fouling, even after a week of production run, was found. Instead Figure 40b shows the movable mold plate of DIA-AEM70-1-KO, where a significant fouling, just after 2 days of production run, was found, as pointed out by red arrows in the figure.

About the DIA-AEM70-1-OK production run, an average T_{SH} of 130°C was measured during the daily process control and, after injection molding, stabilization, deburring, and post-curing for 4 hours at 175°C, no relevant quality issue of final parts was found, including IRHD M hardness value of 71.1 ± 0.1 points according to *ISO 48-2-2018*, (70.0 ± 5 required specification) [28, 135]. Whereas in the case of DIA-AEM70-1-KO production run, an average T_{SH} of 226°C was measured during the daily process control and, after injection molding, stabilization, deburring and post-cure for 4 hours at 175°C, some surface hardened and cracked parts, 0.2–0.3% of the overall production (about 110,000 O-rings), were obtained. This amount of scraps, and especially this type of defect, is relevant because the automotive industry requires "zero defected" parts. A IRHD M hardness value of 82.4 ± 0.1 points was measured, thus out of the required specification.

The effect of exceeding rubber shelf life produced an increase of shear heating effect by T_{SH} of 96°C, which largely outcomes the effects produced by the variation of process setup parameters, at least within the range explored in this thesis. This suggests that the rubber compound properties have a considerable effect on T_{SH}.

The significant increase of T_{SH} was the first indicator of DIA-AEM70-1 processability change due to its shelf life variation. A further important indicator was the quick mold fouling increase in the DIA-AEM70-1-KO production run, after only 2 days of industrial production. The last condition obviously has negatively affected the productivity of DIA-AEM70-1-KO, thus subjected to extraordinary cleaning [28]. Thus, by impacting on an additional industrial cost of the mold cleaning phase, and delays in final products shipment to automotive customers.

Besides, even modifying injection pressure, injection speed and screw rotation speed, no reduction in this excessive shear heating was found. Therefore, T_{SH} is already a useful tool to guarantee a very fast online process control, that is, to collect information concerning the risk of scorching and thermal degradation, leading, for example, to the diffusion of compound ingredients (low volatile chemicals), stickiness, mold fouling and also color variation [26-28].

Nevertheless, monitoring also η_{SH} allowed to get an added value in terms of quantitative and precise indication of the quality of molded parts, as will be shown in Chapter 6.3.

Afterwards, in order to understand the effect of T_{SH} variation on the final properties of the DIA-AEM70-1 based O-rings (80 x 4 mm), a laboratory physical-mechanical characterization was performed. Calorimetric glass transition temperature (T_g) measurements on the final O-rings with T_{SH} of 130°C and 226°C, were performed. The O-ring samples were prepared in order to measure by DSC both bulk and surface sections. The T_g was measured also in O-rings after post-curing for 4 hours at 175°C.

Figure 41 shows as an example the DSC curve for O-ring (80 x 4 mm)-1, surface section, with T_g value of -37.0°C.

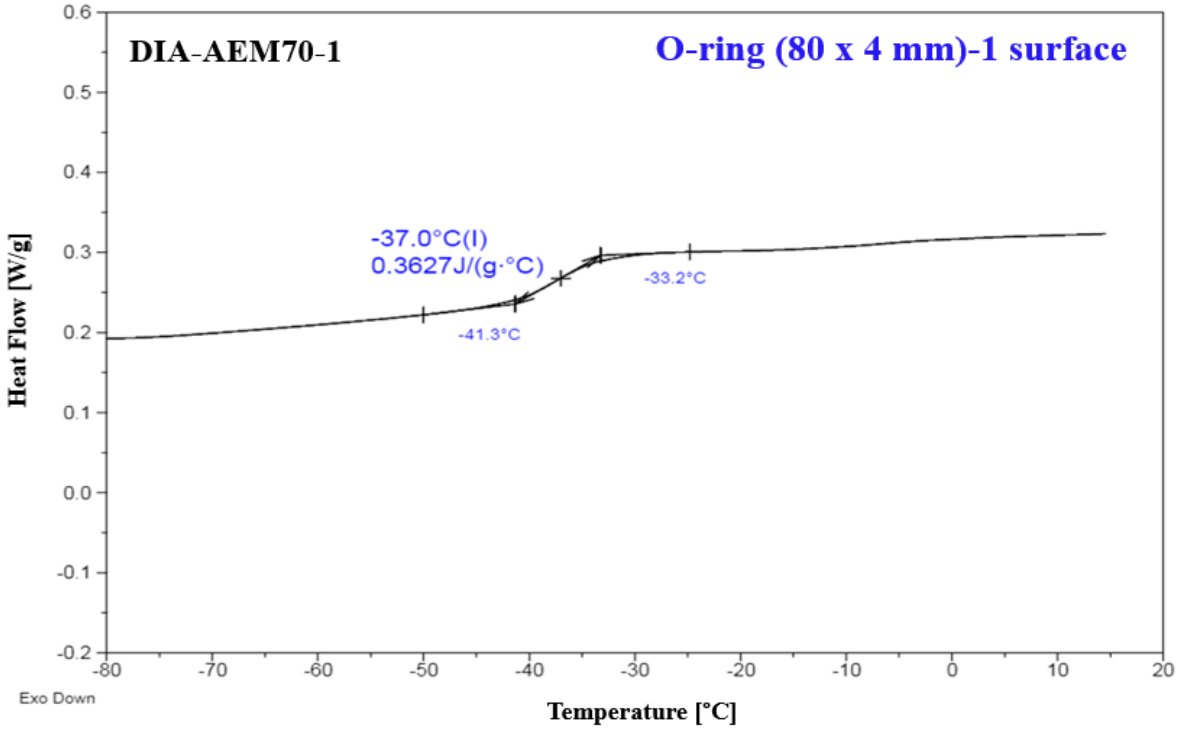

Fig.41. DSC curve for O-ring (80 x 4 mm)-1, surface section, with T_g value of -37.0°C.

Table 6 reports T_g values of two O-rings, both bulk and surface sections, with T_{SH} of 130°C and 226°C.

Table 6. Glass transition temperature (T_g): O-ring at 130°C and O-ring at 226°C of T_{SH}.

Rubber compound	T_{SH} °C	Sample number	T_g °C *Bulk*	T_g °C *Surface*
DIA-AEM70-1-OK	130.0	O-ring (80 x 4 mm)-1	-36.4	-37.0
DIA-AEM70-1-KO	226.0	O-ring (80 x 4 mm)-2	-37.2	-36.9

After post-curing the glass transition temperature of O-ring (80 x 4 mm)-2 was once again -36.9°C. There weren't noteworthy variations of T_g, neither between bulk and surface sections, nor with different T_{SH}, and not even after oven post-curing stage. Therefore, this result suggested that plasticizer loss did not occur.

Furthermore, bulk and surface sections of the O-rings (80 x 4 mm) based on DIA-AEM70-1 rubber compound with different shear heating temperatures, were immersed in ethyl acetate for swelling test at room temperature for 48 h. Therefore, the swelling ratio (SR) was calculated according to Equation (12).

Table 7 reports the average data of swelling ratio of six compounds, with samples taken both from bulk and surface sections, with the following shear heating temperatures: 130°C, 147°C, 209°C, 213°C, 226°C, and after post-curing for 4 hours at 175°C (DIA-AEM70-1-OK-PC).

In this case, samples at intermediate T_{SH} values at 130°C and 226°C were also investigated with the purpose to understand if significant swelling variations could also occur at intermediate temperatures.

Table 7. Average SR data for O-rings at 130°C, 147°C, 209°C, 213°C and 226°C of T_{SH}, and post-cured.

Rubber compound	T_{SH} °C	SR *Bulk*	SR *Surface*
DIA-AEM70-1-OK	130.0	2.51 ± 0.19	2.07 ± 0.23
DIA-AEM70-1-OK	147.0	2.41 ± 0.07	2.17 ± 0.01
DIA-AEM70-1-KO	209.0	2.26 ± 0.10	2.11 ± 0.14
DIA-AEM70-1-KO	213.0	2.40 ± 0.08	2.15 ± 0.08
DIA-AEM70-1-KO	226.0	2.23 ± 0.10	2.20 ± 0.34
DIA-AEM70-1-OK-PC	130.0	2.15 ± 0.03	2.12 ± 0.08

Figure 42 shows the average data of swelling ratio (SR) for the above-mentioned O-rings in both bulk and surface sections. In the O-rings with T_{SH} of 130°C and 147 °C (both DIA-AEM70-1-OK) there was a slight swelling difference between bulk and surface sections, where the bulk section was appeared less cross-linked. However, this slight swelling difference disappeared in the O-rings with higher T_{SH} (above 200°C), and especially after post-curing. Therefore, T_{SH} above 200°C may have accelerated the curing reaction progress, that for diamine curing system should be completed in a second stage which takes place in oven post-curing for 4 hours at 175°C (a relatively long thermal treatment).

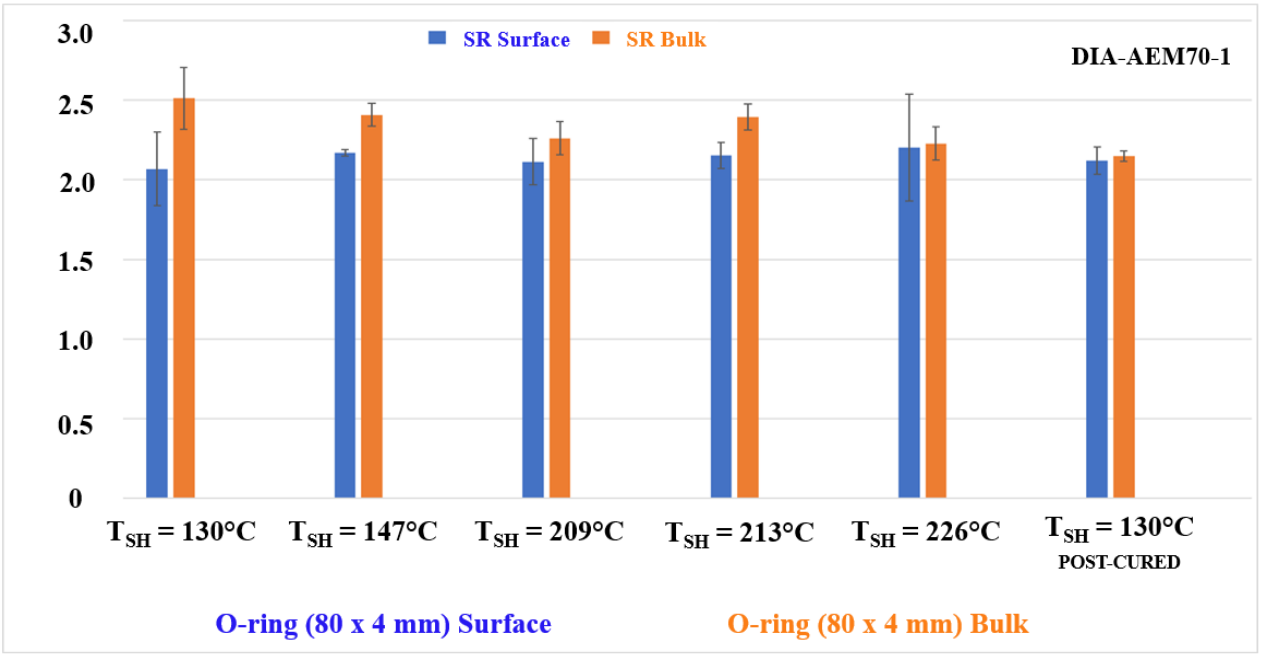

Fig.42. Average SR data for several O-rings (80 x 4 mm) in both bulk and surface sections.

As above-mentioned for some DIA-AEM70-1 based O-rings (80 x 4 mm) from the injection molding and post-curing stages, and characterized by different shear heating temperatures, ATR-FTIR was used with the

purpose to detect the absorption frequencies of imide groups (a weak band of C=O stretching vibration near 1700 cm^{-1}) [127]. The imide groups should be formed in the relatively long thermal treatment in oven post-curing for 4 hours at 175°C.

Therefore, the DIA-AEM70-1 based O-rings (80 x 4 mm) with shear heating temperature of 130°C, 226°C, and with post-curing for 4 hours at 175°C, and the uncured compound as well, were analyzed by ATR-FTIR spectroscopy, with the aim to verify whether a higher T_{SH} led to a too significant progress in cross-linking. Significant differences were not detected, except in the region at wavenumber values between 1600 and 1800 cm^{-1}. For this reason, Figure 43 shows a comparison of spectra between 1600 and 1800 cm^{-1} of DIA-AEM70-1 based O-rings with 130°C of T_{SH} (green spectrum), 226°C of T_{SH} (light blue spectrum), with post-curing (red spectrum), and uncured DIA-AEM70-1 rubber compound (violet spectrum), respectively.

However, by providing a peak ratio (Figure 44), between the lowest peak segment with lower absorbance (set at 1700 cm^{-1} for all the specimens) and highest peak segment with higher absorbance, some interesting differences were observed.

The least intense peak at 1700 cm^{-1} is associated to imide groups, (C=O stretching vibration), and its peak ratio increased from uncured sample (peak ratio: 16%) to molded O-ring (peak ratio: 26%, both with 130°C and 226°C of T_{SH}), and also from molded O-rings to post-cured O-rings (peak ratio: 28%). However, between the molded O-rings there weren't significant variations. Therefore, the T_{SH} didn't influence the imide peak absorbance of molded O-rings with 130°C and 226°C.

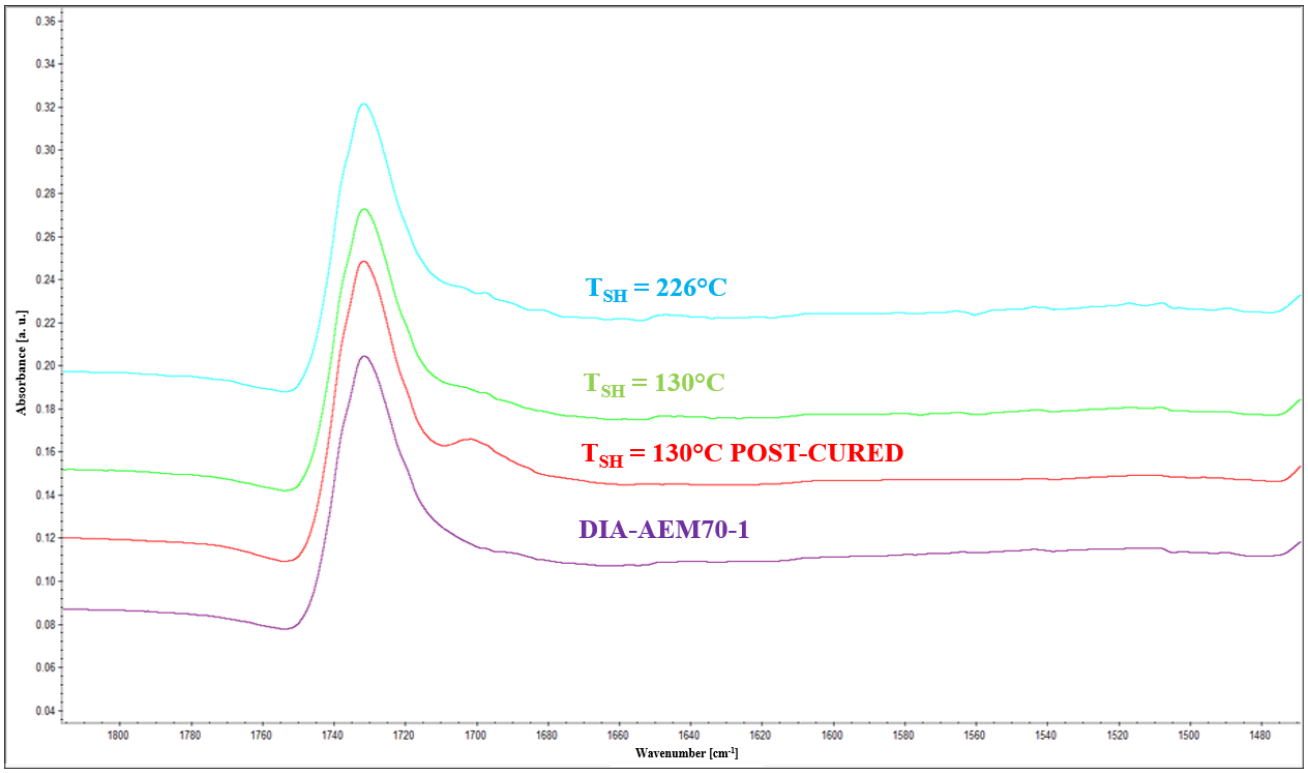

Fig.43. ATR-FTIR spectra comparison between O-rings with 130°C (green), 226°C (light blue), with post-curing (red), and uncured DIA-AEM70-1 rubber compound (violet).

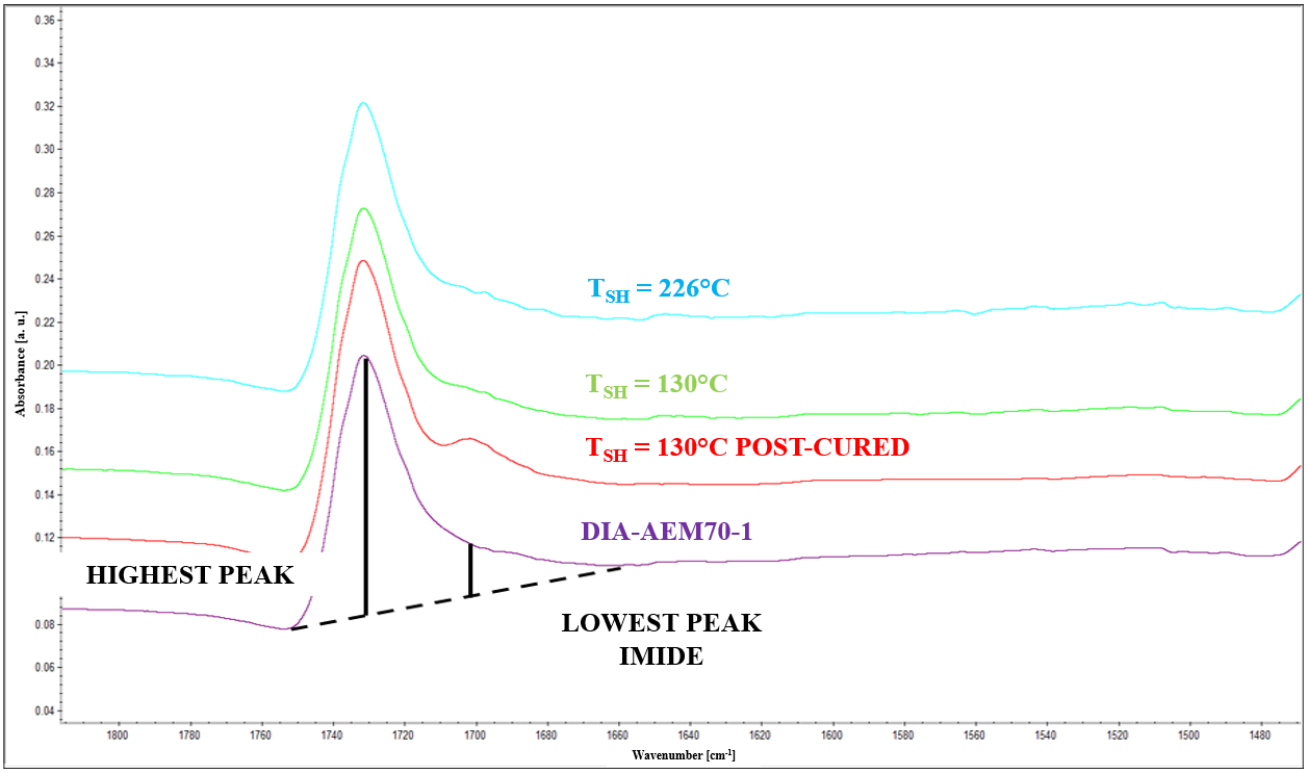

Fig.44. ATR-FTIR peak area ratio between the lowest peak segment and highest peak segment.

Furthermore, friction tests were carried out to investigate effects of T_{SH} on surface characteristics of O-rings. DIA-AEM70-1 based O-rings (80 x 4 mm) were directly tested to determine the friction force, F_f, (N) after 10 mm and 100 mm of sliding, and the mean force between these two levels of slide (i.e. the average of force data recorded between 10 and 100 mm of displacement).

Therefore, Figure 45 shows as example of force-displacement curve obtained from a friction test carried out on an O-ring with shear heating temperature of 130°C. F_f, at 10 mm and 100 mm of sliding, and the mean force are displayed on the graph.

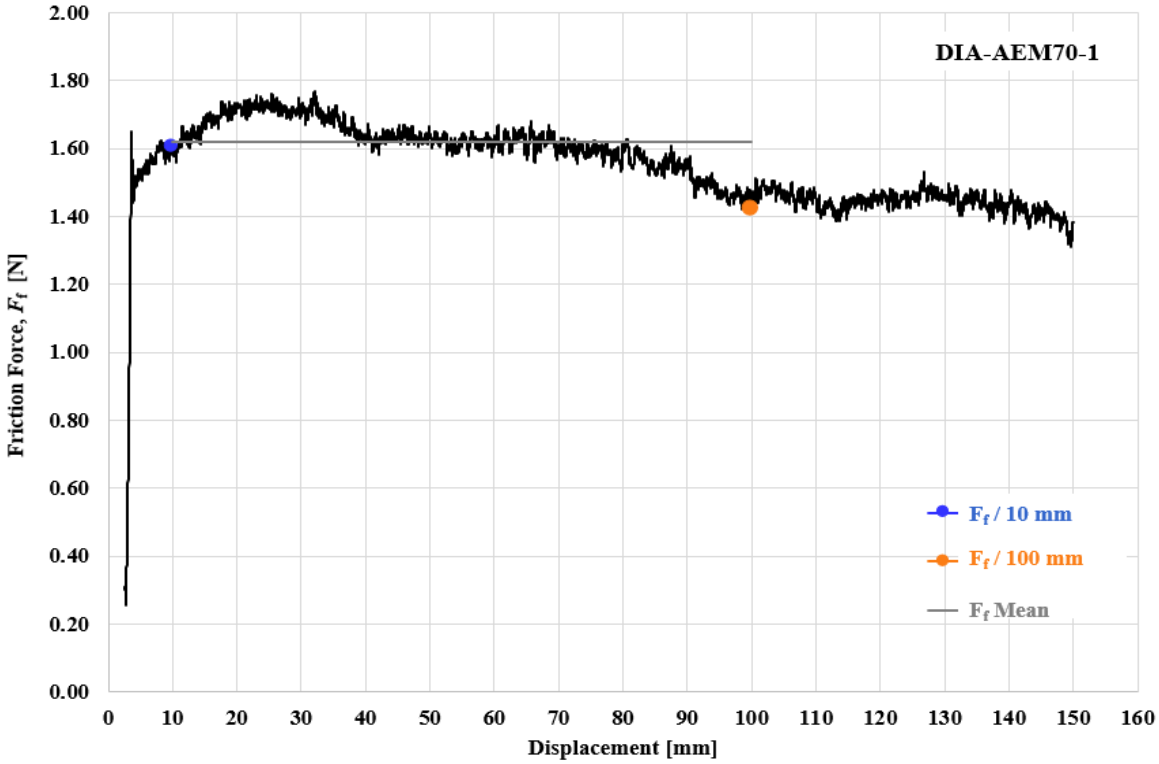

Fig.45. Friction force calculation for O-rings (80 x 4 mm) with T_{SH} of 130°C.

Figure 46 instead, shows the friction force values for the following T_{SH}: 130°C, 147°C, 209°C, 213°C and 226°C.

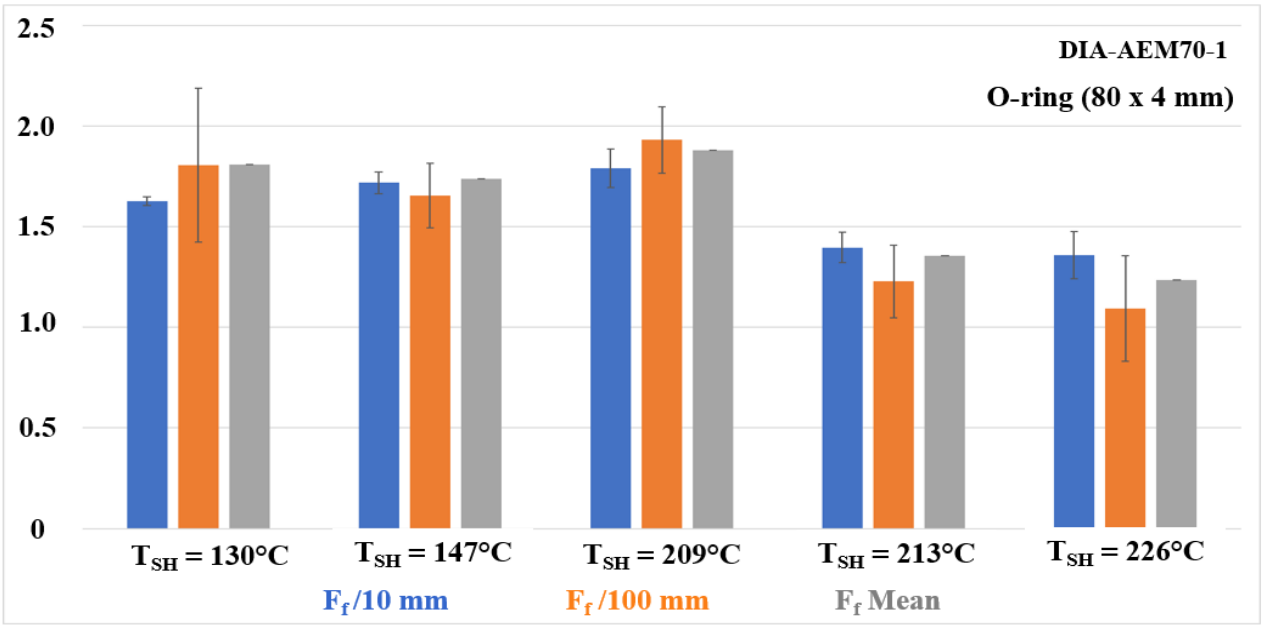

Fig.46. Friction force for O-rings (80 x 4 mm) with T_{SH} of 130°C, 147°C, 209°C, 213°C and 226°C.

The friction forces obtained for O-rings with T_{SH} of 213°C and 226°C were lower than those of O-rings with T_{SH} 130°C and 209°C. This can be attributed to an increase in surface roughness or the presence of lubricants on the surface at higher shear heating temperatures.

The most reasonable explanation is that at higher shear heating temperatures volatile organic compounds, such as processing aids, diffuse and accumulate on the surface.

Finally, O-ring circular sections with T_{SH} of 130°C and 226°C were also measured by DMA with the purpose to evaluate the Payne effect, in shear sandwich configuration. Storage modulus (G'), loss modulus (G''), and tan δ were measured as a function of strain amplitude between 0.003% and 28% as shear strain amplitude. At least four repetitions are carried out for each material. The storage modulus is a measure of the elastic response of a rubber material, instead loss modulus is a measure of the viscous response. The moduli are indicative of the average cross-linking degree of the specimen, and the Payne effect (drop of storage modulus with strain amplitude) is indicative of filler networking phenomena.

Figure 47, 48 and 49 show the storage modulus, loss modulus, and tan δ for the above-mentioned two O-rings. Along with a shear heating temperature increasing, the values of storage modulus, loss modulus, and tan δ, especially for low deformations, were increased. Therefore, the O-ring portion with T_{SH} of 226°C showed a higher storage modulus (G'), or stiffness, at low deformations, corresponding to slightly higher cross-linking degree, than the O-ring portion with T_{SH} of 130°C (Figure 47). However, at higher deformations both the O-ring portions with T_{SH} of 130°C and 226°C showed the same storage modulus level. Thus the moduli reduction due to Payne effect was more significant with T_{SH} of 226°C, in accordance with a higher value of loss modulus (Figure 48), or dissipation (G'' max). This can be due to increased interactions between elastomer macromolecules (cross-linking) or interactions between filler and elastomer.

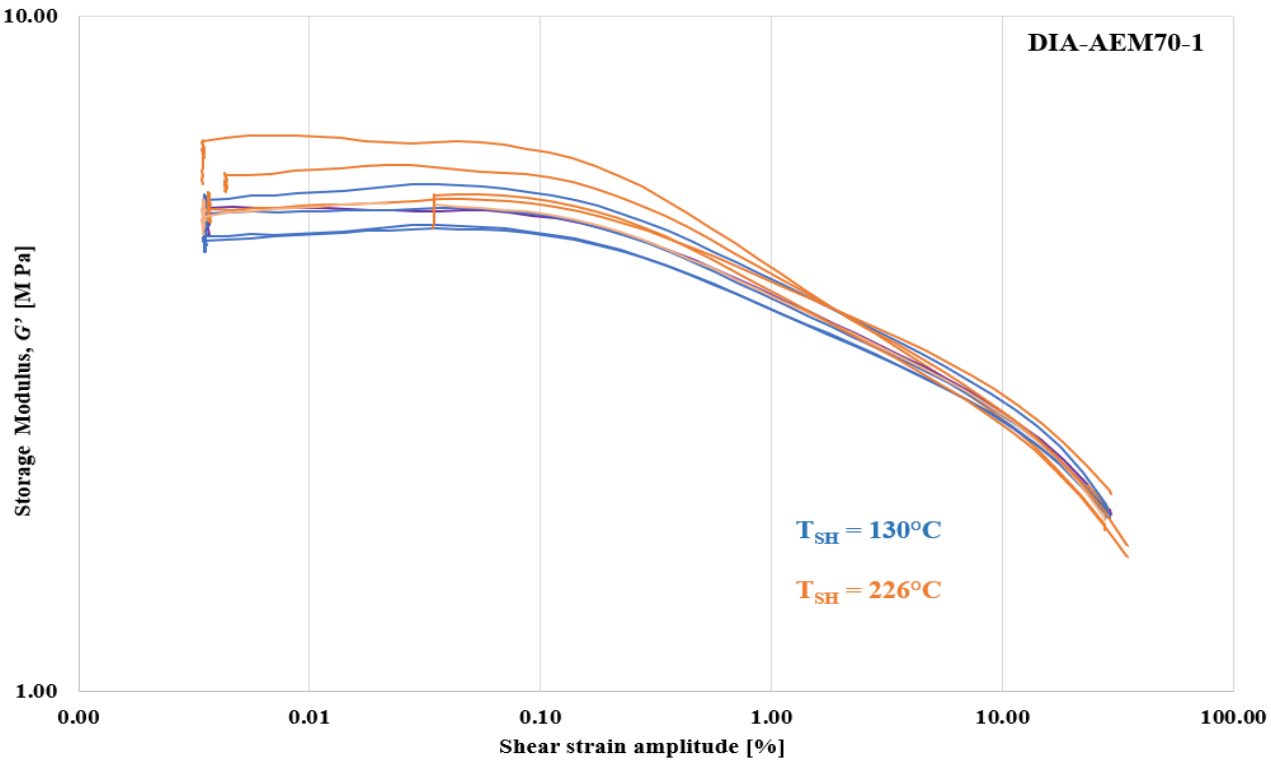

Fig.47. Storage modulus (G') for O-rings (80 x 4 mm) with T_{SH} of 130°C and 226°C.

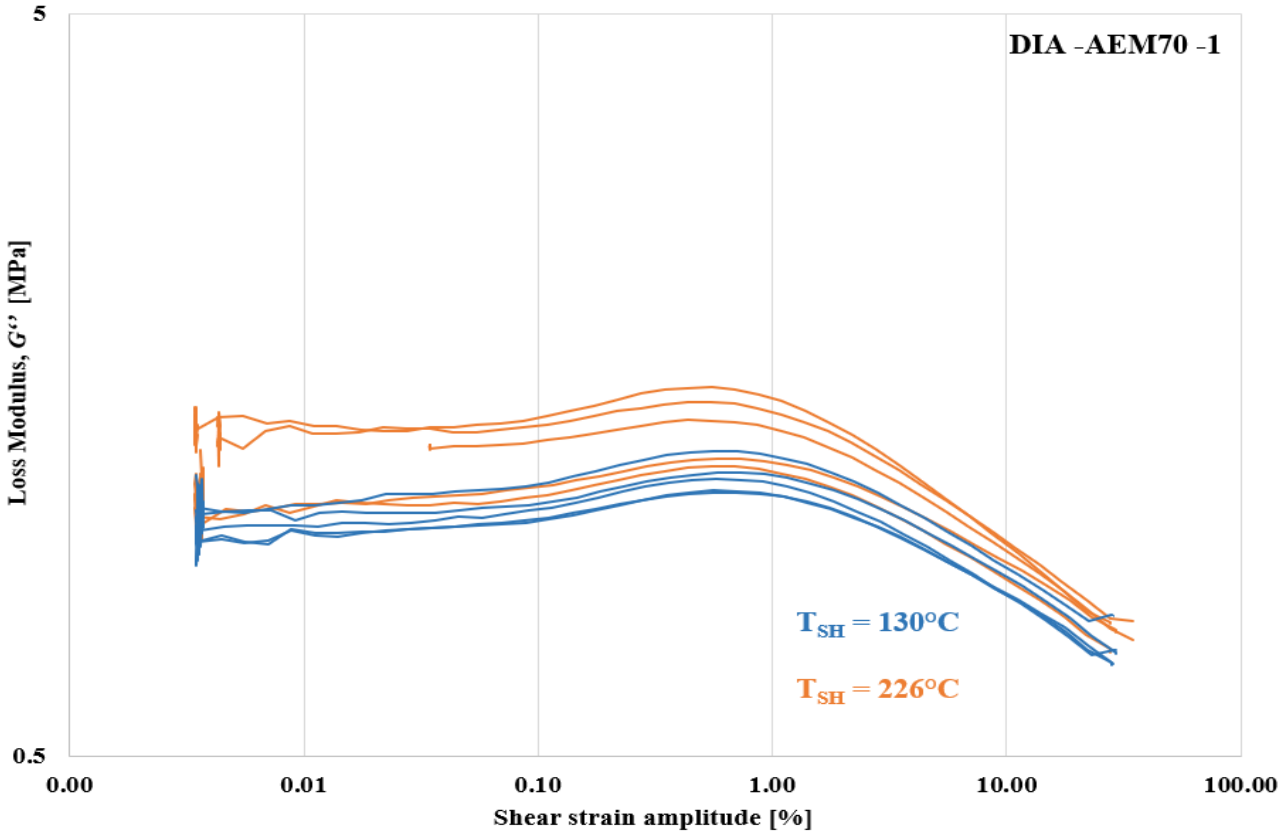

Fig.48. Loss modulus (G'') for O-rings (80 x 4 mm) with T_{SH} of 130°C and 226°C.

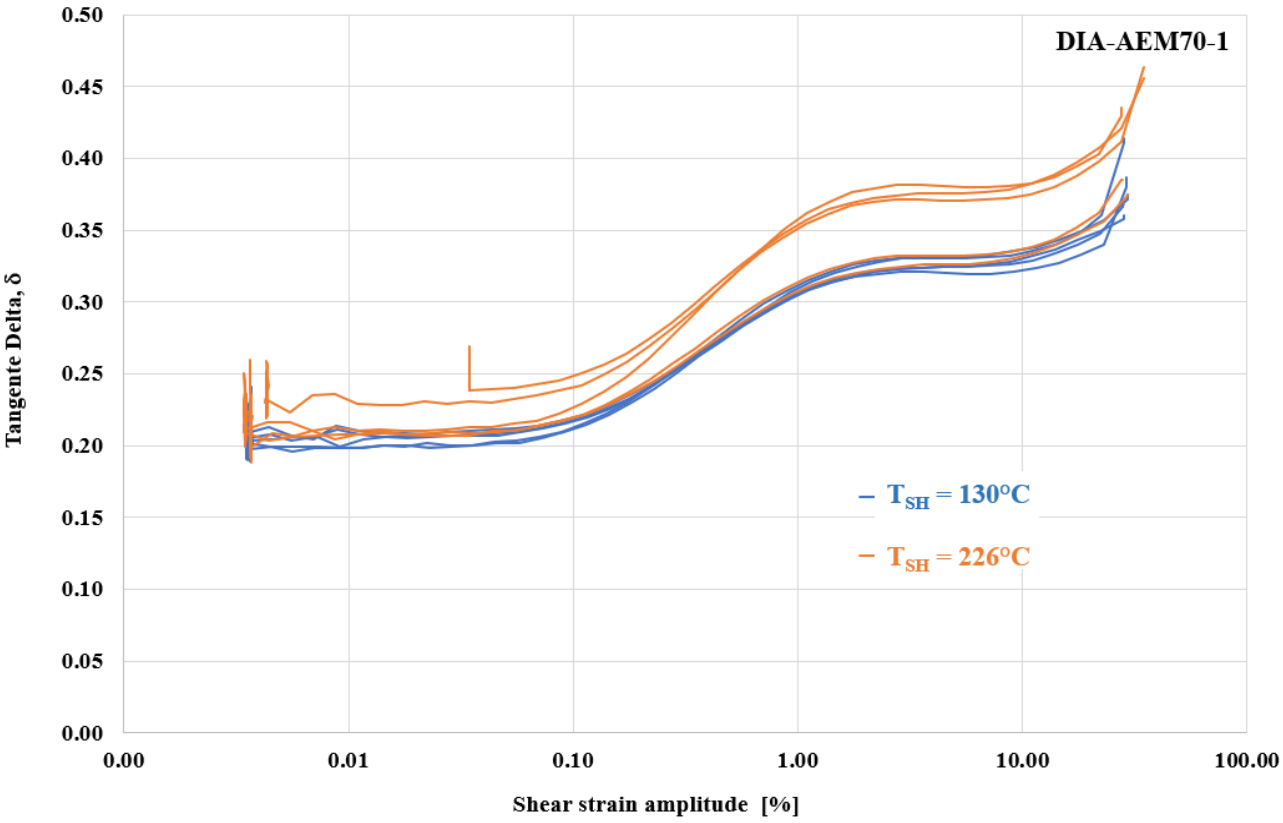

Fig.49. Tan δ for O-rings (80 x 4 mm) with T_{SH} of 130°C and 226°C.

6.3. Operating roadmap use in daily production runs

Therefore, eight different rubber compounds based on AEM, HNBR, FKM, and EP(D)M elastomers were monitored. Eight rubber compounds and eight industrial production runs with long process stability without significant deviations of set parameters and with very little scrap were investigated.

Table 8 reports the average experimental data from laboratory characterization.

Table 8. Average experimental data from laboratory characterization.

Rubber compound	Density (ρ) kg/m^3	Specific heat capacity (C_p)* J/kg/°C	Minimum torque (M_L)** dN m
DIA-AEM60-1	1267 ± 1	2930 ± 3	1.24 ± 0.011
DIA-AEM60-2-OK#,§	1243 ± 1	2931 ± 4	0.40 ± 0.011
DIA-AEM60-3	1389 ± 2	1459 ± 3	0.38 ± 0.017
PO-EPDM60	1090 ± 1	4180 ± 2	1.40 ± 0.015
S-EPDM60	1140 ± 1	4150 ± 3	0.93 ± 0.023
DIA-HNBR60-1	1273 ± 2	3240 ± 3	0.58 ± 0.018
DIA-HNBR60-2	1331 ± 1	2770 ± 3	0.47 ± 0.036
PO-FKM60	2029 ± 1	1345 ± 2	0.69 ± 0.018

* At T_{SH}.
** At 177°C.
# MIR 190 tons machine process parameter setup: injection speed = 70%; screw speed rotation = 80 rpm, curing time = 85 s, barrel temperature = 75 ± 5°C and both fixed and movable plate temperature = 195 ± 5°C.
§ injection pressure = 70 bar.

Process parameter setup common to all the systems investigated was injection speed of 70%, the screw rotation speed of 80 rpm, curing time of 85 s, barrel temperature of 75 ± 5°C, and both fixed and movable plate temperature of 195 ± 5°C. About laboratory characterization, the data of density (ρ), specific heat capacity (C_p), and minimum torque (M_L) at 177°C were also reported in Table 7.

Figure 50 shows the curing curve for each rubber compound performed for 12 minutes at 177 °C by MDR according to *ASTM D5289-95* [34]. The M_L values reported in Table 7 were obtained from these curves as the minimum torque values reached after the initial transient stage.

It is worth pointing out that curing curves show large differences among rubber compounds in terms of rheological and curing behavior. Therefore, this heterogeneity is intentionally sought to develop a robust correlation (the roadmap) with a phenomenological approach.

The curing curves were measured on standard samples collected from the same rubber compounds used for the processing investigation. Furthermore, the selected rubber compounds were fresh material within their shelf life, where the measured M_L and the calculated shear heating parameter are subject to negligible variation.

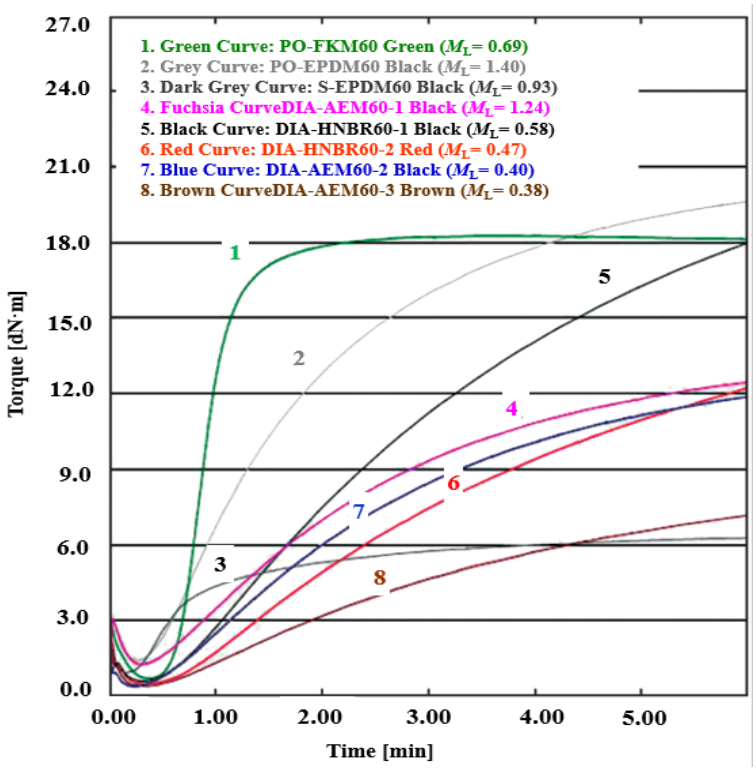

Fig.50. Curing curves performed for 12 minutes at 177°C by MDR [27].

Instead, Table 9 reports the average experimental data from processing characterization of the eight different rubber compounds, and screw L/D ratio of the used horizontal injection molding machines. About the processing characterization, the data of barrel temperature setup (T_{Barrel}), measured shear heating temperature (T_{SH}) of the rubber by infrared thermal camera and the temperature difference in shear heating (ΔT_{SH}) considering 20°C as initial temperature are reported.

Table 9. Average experimental data from processing characterization.

Rubber compound	Screw L/D	Barrel temperature (T_{Barrel}) °C	Shear heating temperature (T_{SH}) °C	Temperature difference in shear heating (ΔT_{SH})* °C
DIA-AEM60-1	6	80.0	114.0 ± 2.5	94.0
DIA-AEM60-2-OK#,§	16	75.0	115.0 ± 3.0	95.0
DIA-AEM60-3	15	75.0	125.0 ± 2.5	105.0
PO-EPDM60	6	95.0	105.0 ± 2.5	85.0
S-EPDM60	12	70.0	155.0 ± 3.0	135.0
DIA-HNBR60-1	18	75.0	136.0 ± 2.5	116.0
DIA-HNBR60-2	18	75.0	132.0 ± 3.0	112.0
PO-FKM60	6	80.0	110.0 ± 2.5	90.0

* Considering 20°C as initial temperature.
# MIR 190 tons machine process parameter setup: injection speed = 70%; screw speed rotation = 80 rpm, curing time = 85 s, barrel temperature = 75 ± 5°C and both fixed and movable plate temperature = 195 ± 5°C.
§ injection pressure = 70 bar.

Eventually, Table 10 reports the average data of calculated shear heating parameter (η_{SH}) at 10 s^{-1} and the corresponding logarithmic values for the rubber compounds reported in Tables 8 and 9.

To use the log η_{SH} parameter as a tool for improvement of process control, data from different rubber compounds and production runs were compared and correlated with M_L values, thus obtaining a common correlation, operating roadmap.

Table 10. Average data of calculated shear heating parameter (η_{SH}) at 10 s^{-1}.

Rubber compound	Shear heating parameter (η_{SH})* Pa s	Log shear heating parameter Log(η_{SH})* Log Pa s
DIA-AEM60-1	1.50×10^6	6.18
DIA-AEM60-2-OK#,§	5.37×10^5	5.73
DIA-AEM60-3	3.64×10^5	5.56
PO-EPDM60	1.67×10^6	6.22
S-EPDM60	1.31×10^6	6.12
DIA-HNBR60-1	6.69×10^5	5.83
DIA-HNBR60-2	5.77×10^5	5.76
PO-FKM60	1.06×10^6	6.02

* At 10 s^{-1} and ΔT_{SH}.
# MIR 190 tons machine process parameter setup: injection speed = 70%; screw speed rotation = 80 rpm, curing time = 85 s, barrel temperature = 75 ± 5°C and both fixed and movable plate temperature = 195 ± 5°C.
§ injection pressure = 70 bar.

Figure 51 shows the relationship between log η_{SH} at 10 s^{-1} and M_L from 12 minutes at 177 °C by MDR, giving a comparison between the eight rubber compounds investigated and the eight industrial production runs with long process stability without the relevant quality issue of final parts, including the DIA-AEM60-2-OK run. A proportional trend was observed with R^2 of 0.935 according to a power regression law. The Pearson correlation coefficient is also reported in the Figure 51 and the correlation test gives p-value lower than 0.05 (0.00083), thus the correlation is significant. Therefore, a good correlation was established between the results of the laboratory test, M_L, and the technological parameter, η_{SH}.

The advantage of monitoring also the η_{SH} parameter, and not only M_L values, is that it takes into account both rubber composition effects and the effect of operating conditions, thus providing information about the thermal history of the rubber injection and process safety. The eight industrial production runs were characterized by different injection molding machines, different molded part geometries, and by very stable production runs, with very little scrap after molded part stabilization, deburring and post-curing.

Therefore, a robust correlation between η_{SH} and M_L, labelled roadmap, was obtained by considering various rubber compounds having different elastomeric matrices, different curing systems, different injection molding machines and process parameter setups, by producing different geometries of the molded parts (both O-rings and technical rubber items). This heterogeneity is intentionally sought to develop a robust correlation η_{SH} vs

M_L with a phenomenological approach. Therefore, the values of log η_{SH} and M_L (operating roadmap) represent the reference points with the function to support, the process engineer and plant operator in the improvement of the process control by online thermal measurements [26-28].

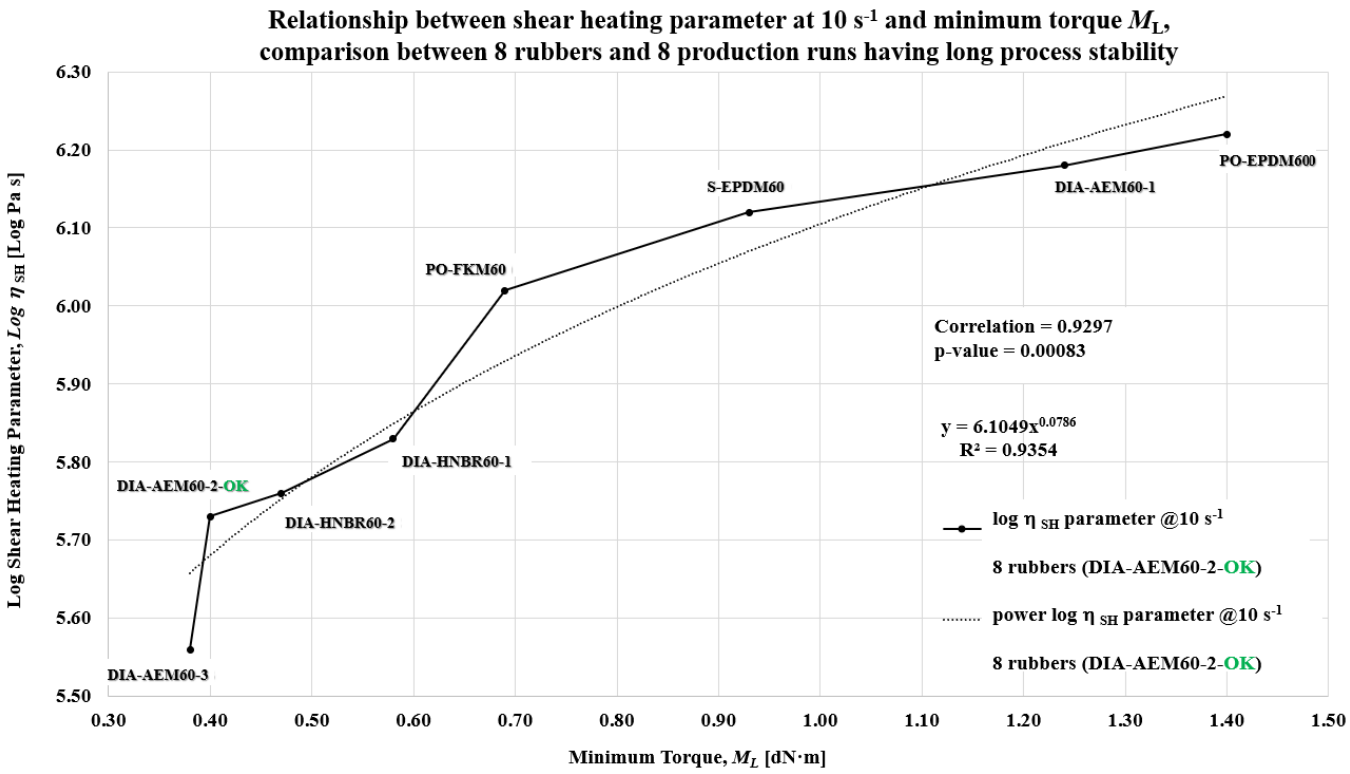

Fig.51. Relationship η_{SH} at 10 s^{-1} and M_L, comparison between 8 rubbers and 8 production runs having long process stability [27].

In this chapter, the operating roadmap was used to investigate the effect of shelf life variation for the DIA-AEM70-1 rubber compound during its industrial production run in a 300 Ton Engel by producing O-rings (80 x 4 mm).

Table 11 reports the results for both the processing investigations of DIA-AEM70-1: a stable production run, within the material shelf life, designated DIA-AEM70-1-OK, and an unstable production run, out of the material shelf life, designated DIA-AEM70-1-KO. About laboratory test, the data of density (ρ), specific heat capacity (C_p) and minimum torque (M_L) at 177 °C are reported.

Table 11. Average experimental data from laboratory characterization of DIA-AEM70-1.

Rubber compound	Density (ρ) kg/m^3	Specific heat capacity (C_p)* J/kg/°C	Minimum torque (M_L)** dN m
DIA-AEM70-1-OK	1240 ± 1	1650 ± 3	0.77 ± 0.010
DIA-AEM70-1-KO	1240 ± 1	1920 ± 3	0.84 ± 0.010

* At T_{SH}.
** At 177°C.

Table 12 reports the average experimental data from processing characterization for both the investigated DIA-AEM70-1-OK and DIA-AEM70-1-KO. About the processing characterization the screw L/D ratio of the used horizontal injection molding machines, and the data of barrel temperature setup (T_{Barrel}), measured shear heating temperature (T_{SH}) of the rubber by infrared thermal camera and the temperature difference in shear heating (ΔT_{SH}) considering 20°C as initial temperature are reported.

Table 12. Average experimental data from processing characterization of DIA-AEM70-1.

Rubber compound	Screw L/D	Barrel temperature (T_{Barrel}) °C	Shear heating temperature (T_{SH}) °C	Temperature difference in shear heating (ΔT_{SH})* °C
DIA-AEM70-1-OK	6	75.0	130.0 ± 2.5	110.0
DIA-AEM70-1-KO	6	75.0	226.0 ± 3.0	206.0

* Considering 20°C as initial temperature.

Eventually, Table 13 reports the average data of calculated shear heating parameter (η_{SH}) at 10 s^{-1} and the corresponding logarithmic values for the rubber compounds reported in Tables 10 and 11.

Table 13. Average data of calculated shear heating parameter (η_{SH}) at 10 s^{-1} of DIA-AEM70-1.

Rubber compound	Shear heating parameter (η_{SH})* Pa s	Log shear heating parameter Log(η_{SH})* Log Pa s
DIA-AEM70-1-OK	9.68×10^5	5.99
DIA-AEM70-1-KO	2.11×10^6	6.32

* At 10 s^{-1} and ΔT_{SH}.

The η_{SH} was calculated by using Equation (10), where the flow rate parameter v (s^{-1}) is directly related to the shear rate. Therefore, a conventional value of flow rate of 10 s^{-1} was chosen based on the commonly achievable order of magnitude of shear rate in the plasticizing extruder of the injection molding machine.

The results of calculated η_{SH} for DIA-AEM70-1-OK production run, reported in Table 13, were compared with minimum torque, M_L, from MDR routine rheometric laboratory measurements (Table 11), and along with the eight rubber compounds with very stable industrial production runs (Tables 8 and 10).

Figure 52 shows the relationship between log η_{SH} at 10 s^{-1} and M_L from 12 minutes at 177 °C by MDR, giving a comparison between the nine rubber compounds investigated and the nine industrial production runs having long process stability without the relevant quality issue of final parts, including the DIA-AEM70-1-OK production run.

Therefore, a good correlation was established between the results of the laboratory characterization, M_L, and the technological parameter (η_{SH}) and described by a proportional trend with R^2 of 0.936 according to a power regression law.

The Pearson correlation coefficient is also reported in the Figure 52 and the correlation test gives p-value lower than 0.05 (0.00033), thus the correlation is significant.

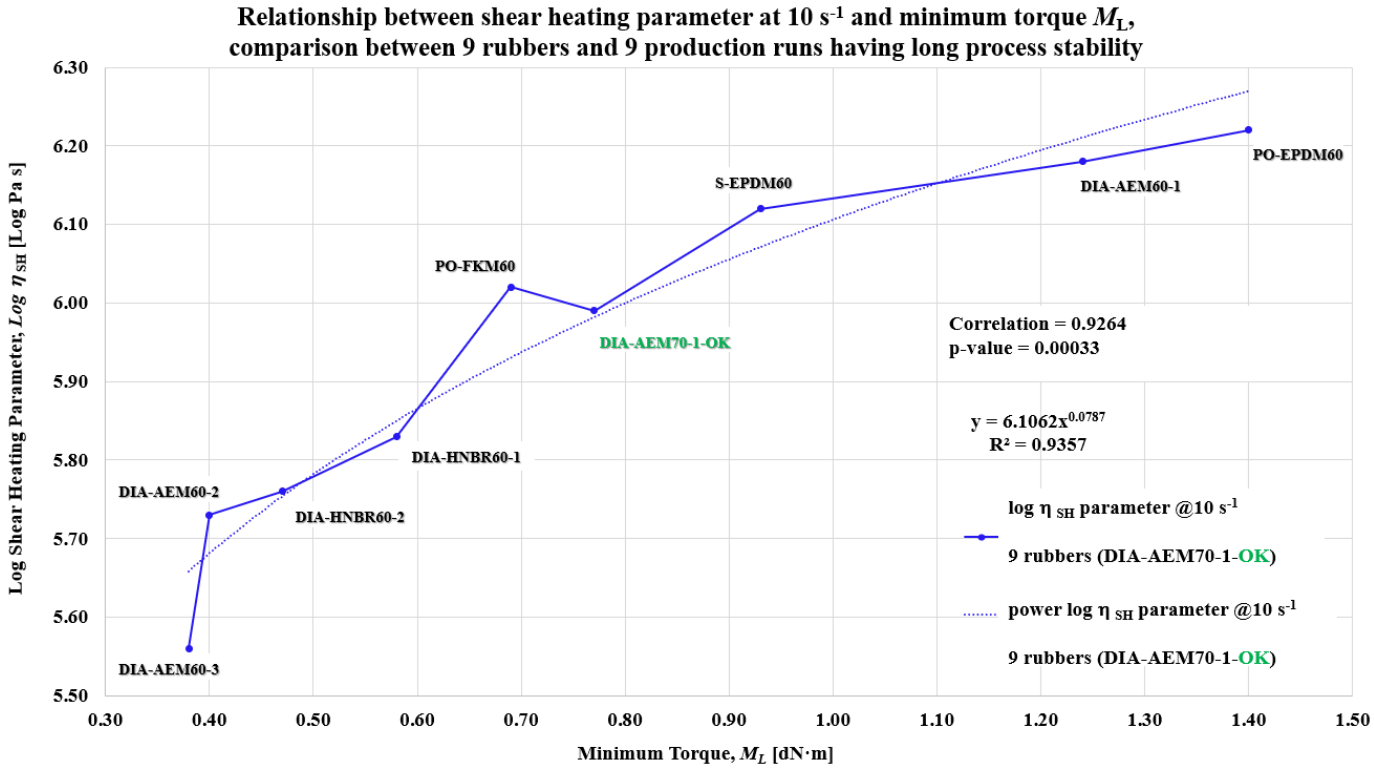

Fig.52. Relationship η_{SH} at 10 s^{-1} and M_L, comparison between 9 rubbers and 9 production runs having long process stability (including DIA-AEM70-1-OK) [28].

It was interesting to remark that the introduced DIA-AEM70-1-OK compound has a higher hardness compared to the others: This seems to indicate that the validity of such correlations is not strictly related to rubber of the same hardness degree. The nine industrial production runs investigated in this work are characterized by different injection molding machines, different molded part geometries and by very stable production runs, with very little scrap after molded part stabilization, deburring and post-curing.

Therefore, the integrated approach based on the correlation between two technological parameters η_{SH} vs M_L, (operating roadmap) was found to be useful for process control and allows to make predictions on different rubber compounds, with the purpose of supporting the process engineer and the plant operator, in the improvement of process control by thermal online measurements.

By introducing η_{SH} of a new production run into the data of η_{SH} vs M_L correlation, the processability of the newly introduced production run can be inferred from the coefficient of determination R^2 [27]. Furthermore, η_{SH} and the use of the above-mentioned roadmap could provide information also about new compounds, whose T_{SH} limit for the obtainment of good quality parts is not known a priori, unless process trials are performed. Therefore, log η_{SH} was introduced to allow the comparison of process outputs between DIA-AEM70-1 and the other rubber compounds.

Figure 53 shows the relationship between log η_{SH} at 10 s^{-1} and M_L from 12 minutes at 177 °C by MDR for the eight rubber compounds with very stable industrial production runs, and the DIA-AEM70-1-KO production run (R^2 of 0.797 and p-value of 0.00479).

In more detail, new curve was created, starting from the roadmap reported in Figure 52, by introducing the values log η_{SH} at 10 s^{-1} and M_L of DIA-AEM70-1-KO, while keeping the values of the other eight productions runs constant. By introducing the point of DIA-AEM70-1-KO, a significant deviation from the previous proportional trend was observed, with decreased R^2 from 0.936 to 0.797, according to the power regression model. Therefore, the coefficient of determination of η_{SH} vs M_L curves provides a good indication of process stability of DIA-AEM70-1 production runs. For this reason the DIA-AEM70-1-KO run, out of the material shelf life, with M_L of 0.84 ± 0.07 dN·m, an average T_{SH} of 226°C (+ 96°C) and log η_{SH} at 10 s^{-1} of 6.32 ± 0.33 Pa·s, didn't allowed a stable production cycle, where hardened and cracked parts, 0.2-0.3% of final scraps, were produced.

Figure 53 also clearly shows how log η_{SH} values of a production run, combined with M_L values, give indication of the "real output" of the injection molding process by comparison of this data with a well-established roadmap, obtained from stable production runs of different rubber compounds and process conditions.

Therefore, this monitoring has the advantage of being fast and provides information about the stability of the process, while it is running, well before completing the production run [28].

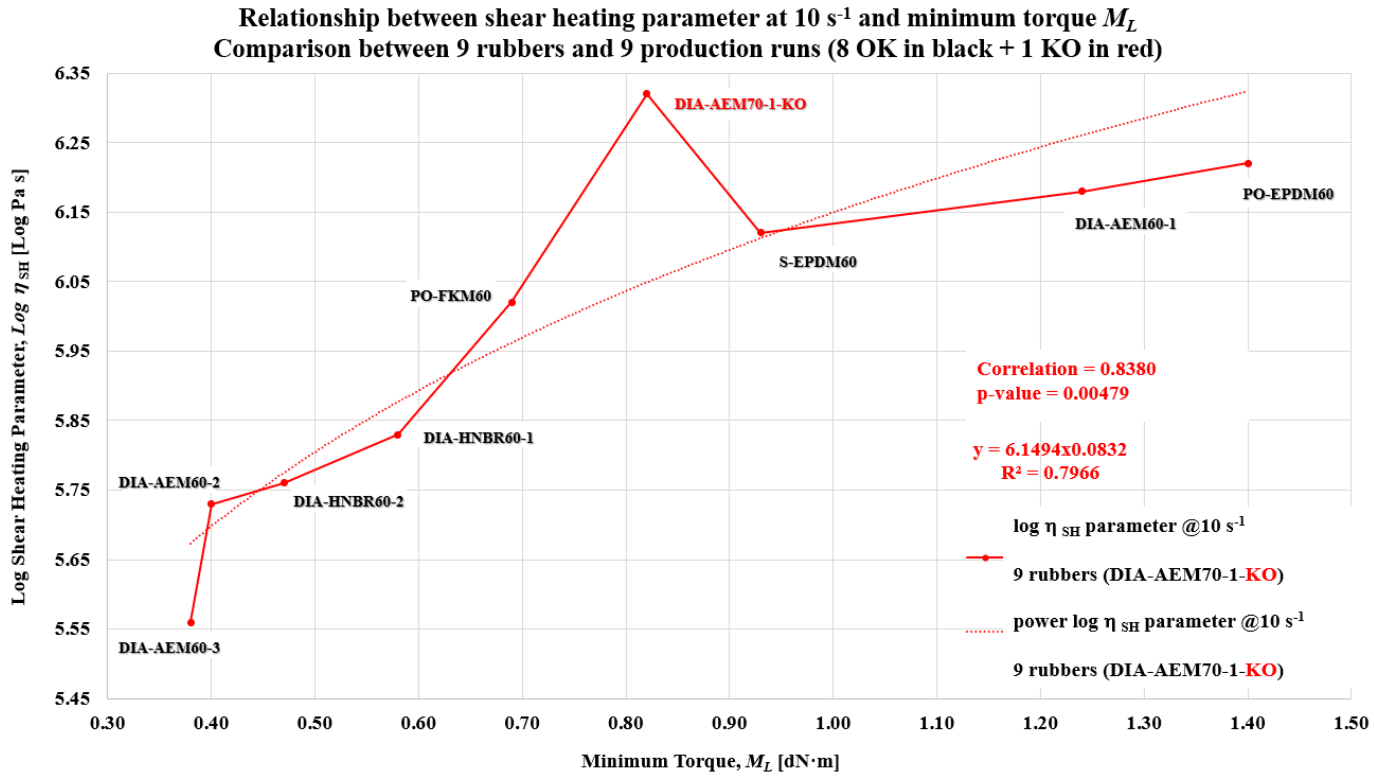

Fig.53. Relationship η_{SH} at 10 s^{-1} and M_L, comparison between 9 rubbers and 9 production runs: 8 OK runs and 1 KO run (DIA-AEM70-1-KO).

The integrated approach based on the correlation between η_{SH} vs M_L, (operating roadmap) was used to optimize the injection molding of industrial production of DIA-AEM60-2 rubber compound affected by scorching and thermal degradation issues.

Furthermore various production runs of DIA-AEM60-2 rubber compound, where stable, unstable, and also the intermediate production runs were also investigated with particular attention. Table 14 reports the average experimental data from laboratory characterization of various production runs of DIA-AEM60-2: both a very stable production run and an unstable production run are reported, designated DIA-AEM60-2-OK and DIA-AEM60-2-KO, respectively. In addition, the intermediate production runs necessary to restore the process stability are reported and designated DIA-AEM60-INT1 and DIA-AEM60-INT2, respectively.

Table 14. Average experimental data from laboratory characterization of DIA-AEM60-2.

Rubber compound	Density (ρ) kg/m^3	Specific heat capacity (C_p)* J/kg/°C	Minimum torque (M_L)** dN m
DIA-AEM60-2-OK$^{\#,\S}$	1243 ± 1	2931 ± 4	0.40 ± 0.011
DIA-AEM60-2-INT2$^{\#,\Phi}$	1243 ± 1	3075 ± 4	0.40 ± 0.011
DIA-AEM60-2-INT1$^{\#,\Psi}$	1243 ± 1	3255 ± 4	0.40 ± 0.011
DIA-AEM60-2-KO$^{\#,\lambda}$	1243 ± 1	3290 ± 4	0.40 ± 0.011

* At T_{SH}.
** At 177°C.
# MIR 190 tons machine process parameter setup: injection speed = 70%; screw speed rotation = 80 rpm, curing time = 85 s, barrel temperature = 75 ± 5°C and both fixed and movable plate temperature = 195 ± 5°C.
§ injection pressure = 70 bar.
Φ injection pressure = 80 bar.
Ψ injection pressure = 100 bar.
λ injection pressure = 140 bar.

Table 15 reports the average experimental data from processing characterization for the investigated DIA-AEM60-2-OK, DIA-AEM60-2-KO, DIA-AEM60-INT1 and DIA-AEM60-INT2, respectively.

Table 15. Average experimental data from processing characterization of DIA-AEM60-2.

Rubber compound	Screw L/D	Barrel temperature (T_{Barrel}) °C	Shear heating temperature (T_{SH}) °C	Temperature difference in shear heating (ΔT_{SH})* °C
DIA-AEM60-2-OK$^{\#,\S}$	16	75.0	115.0 ± 3.0	95.0
DIA-AEM60-2-INT2$^{\#,\Phi}$	16	75.0	162.0 ± 3.0	142.0
DIA-AEM60-2-INT1$^{\#,\Psi}$	16	75.0	223.0 ± 3.0	203.0
DIA-AEM60-2-KO$^{\#,\lambda}$	16	75.0	235.0 ± 3.0	215.0

* Considering 20°C as initial temperature.
# MIR 190 tons machine process parameter setup: injection speed = 70%; screw speed rotation = 80 rpm, curing time = 85 s, barrel temperature = 75 ± 5°C and both fixed and movable plate temperature = 195 ± 5°C.
§ injection pressure = 70 bar.
Φ injection pressure = 80 bar.
Ψ injection pressure = 100 bar.
λ injection pressure = 140 bar.

Figure 54 shows an example of the thermal image taken of the rubber as it emerged from the reciprocating screw nozzle outlet, from which T_{SH} values reported in Table 15 were obtained. This figure shows thermal image of KO run for DIA-AEM60-2 black rubber compound (DIA-AEM60-2-KO), and emerging from the reciprocating screw nozzle outlet.

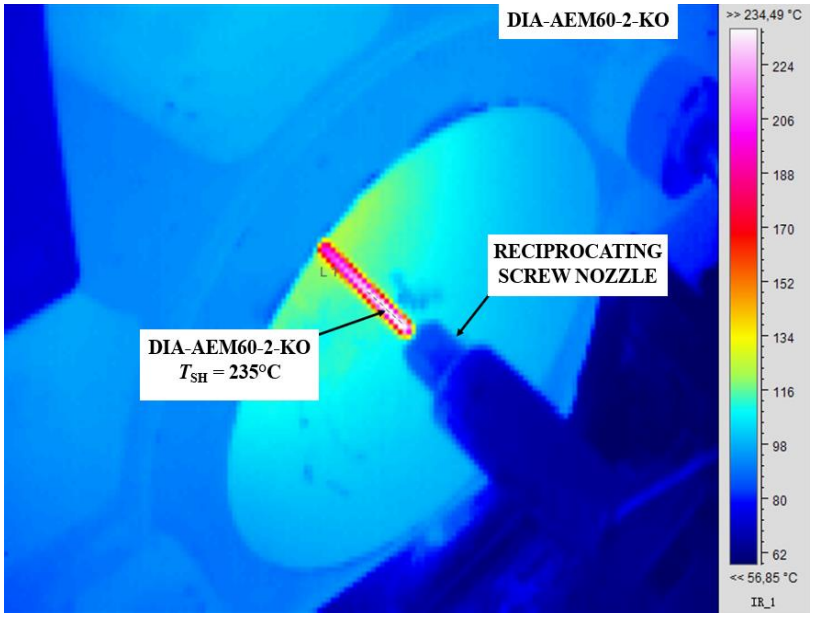

Fig.54. Image of DIA-AEM60-2-KO emerging from the reciprocating screw nozzle outlet [27].

Eventually, Table 16 reports the average data of calculated shear heating parameter (η_{SH}) at 10 s^{-1} and the corresponding logarithmic values for the rubber compounds reported in Tables 14 and 15.

Table 16. Average data of calculated shear heating parameter (η_{SH}) at 10 s^{-1} of DIA-AEM60-2.

Rubber compound	Shear heating parameter (η_{SH})* Pa s	Log shear heating parameter Log(η_{SH})* Log Pa s
DIA-AEM60-2-OK$^{\#,\S}$	5.37×10^5	5.73
DIA-AEM60-2-INT2$^{\#,\Phi}$	8.45×10^5	5.93
DIA-AEM60-2-INT1$^{\#,\Psi}$	1.28×10^6	6.11
DIA-AEM60-2-KO$^{\#,\lambda}$	1.37×10^6	6.14

* At 10 s^{-1} and ΔT_{SH}.
\# MIR 190 tons machine process parameter setup: injection speed = 70%; screw speed rotation = 80 rpm, curing time = 85 s, barrel temperature = 75 ± 5°C and both fixed and movable plate temperature = 195 ± 5°C.
§ injection pressure = 70 bar.
Φ injection pressure = 80 bar.
Ψ injection pressure = 100 bar.
λ injection pressure = 140 bar

With the aim of showing the industrial application of this roadmap as a 'calibration curve' for the fast control of successful setting up of process parameters, the process optimization of AEM rubber parts affected by

scorch problems and thermal degradation due to plasticizer loss is reported as follows. The thermal image in Figure 54 was taken during a DIA-AEM60-2-KO production run, in which about 450, 000 parts were produced. This production run was chosen as a case study for this work to show how the proposed integrated approach helps to improve the process control of rubber injection molding.

An average rubber surface temperature of 235°C was measured during the daily process control and, after injection molding, stabilization, deburring, and post-curing for 4 hours at 175°C, some surface cracked parts were obtained, thus 8 cracked parts/1000 sampled parts. These DIA-AEM60-2-KO cracked parts were detected during the automatic sorting control, and they are characterized by IRHD M hardness values of 25-30 points higher than the required level, thus very out of specification.

Furthermore, AEM hardened parts (12 hardened parts/1000 sampled parts) were detected, characterized by both hardness and compression set values out of the required specification, even if less than the cracked parts. From laboratory characterization of both cracked parts and in-specification parts, cracked parts clearly showed higher hardness (+30 IRHD M points) than the required standard, higher T_g (+9°C) from DSC (see Table 18), and plasticizer loss from TGA and ATR-FTIR spectroscopy.

Figure 55 shows the comparison between ATR-FTIR spectra of DIA-AEM60-2-OK and DIA-AEM60-2-KO parts. This comparison provides qualitative information about differences of the two parts. The black spectrum shows the main absorption frequencies of the DIA-AEM60-2-OK rubber, while the red spectrum shows intensity reduction of the absorption frequencies of DIA-AEM60-2-KO rubber with the change of some peaks, mainly in the fingerprint region (from about 1500 to 500 cm^{-1}). This spectral comparison indicates a very large variation of the sample composition, then quantitatively confirmed by TGA.

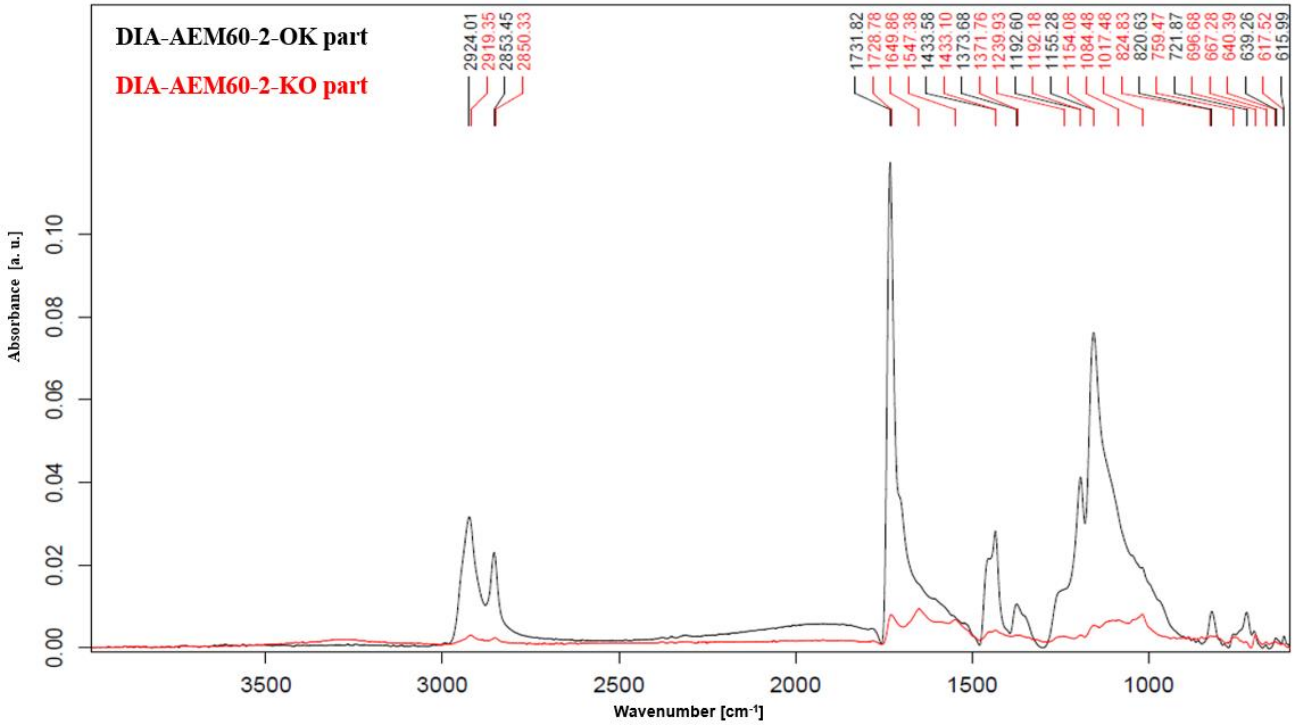

Fig.55. ATR-FTIR spectra DIA-AEM60-2-OK part (black) vs DIA-AEM60-2-KO part (red) [27].

Figure 56 and 57 show the TGA thermograms of DIA-AEM60-2-OK and DIA-AEM60-2-KO parts, respectively. Figure 56 (DIA-AEM60-2-OK) shows a plasticizer content of about 4.71 wt.% (identified as weight loss between RT and 440°C), while Figure 57 (DIA-AEM60-2-KO) shows the absence of plasticizer, demonstrating plasticizer loss in the final parts.

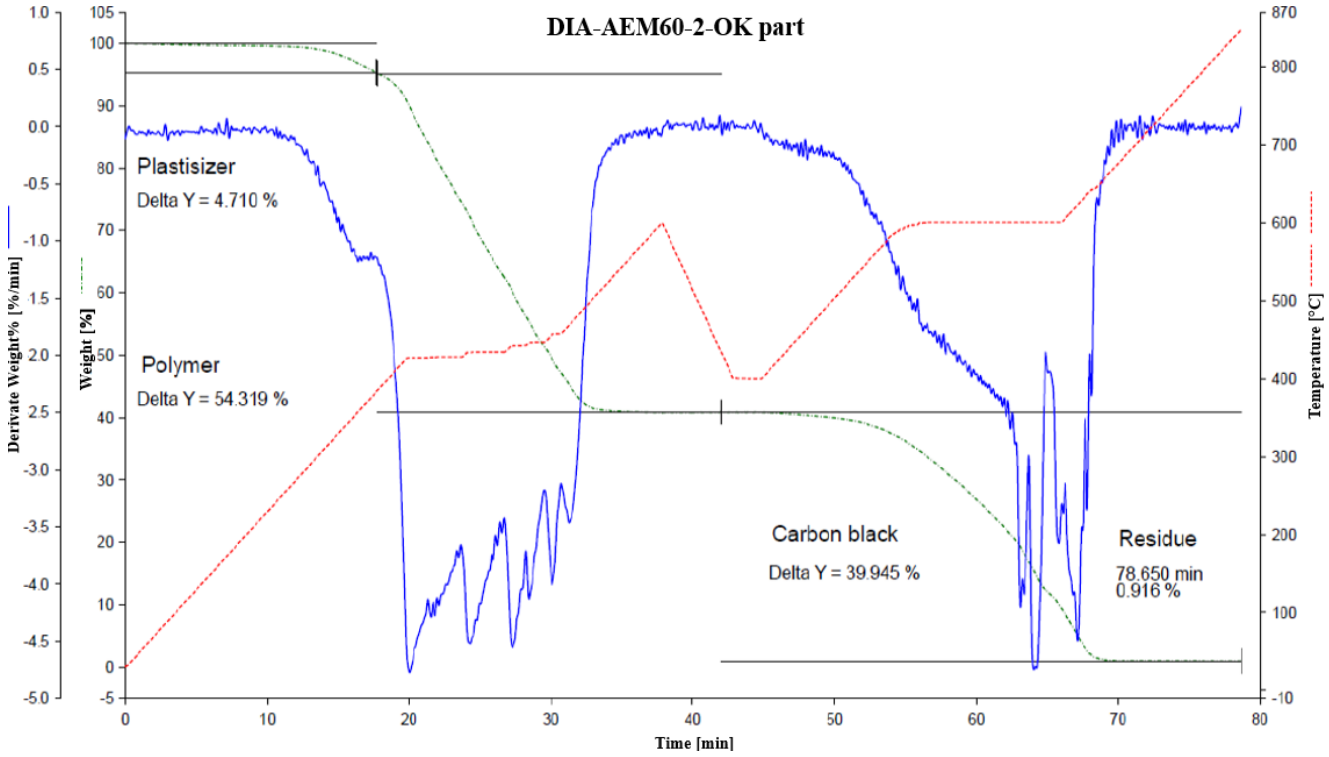

Fig.56. TGA thermogram of DIA-AEM60-2-OK part [27].

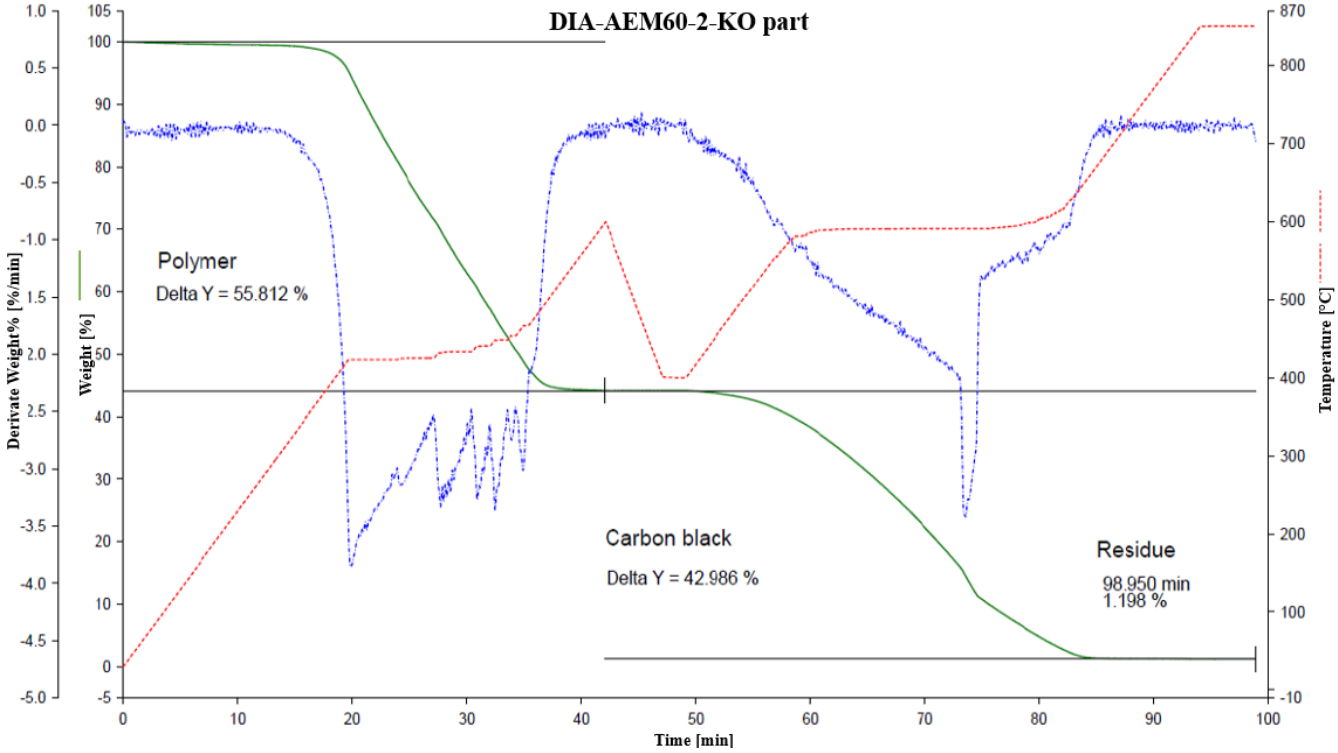

Fig.57. TGA thermogram of DIA-AEM60-2-KO part [27].

During the injection molding, the rubber flow is laminar according to shear-thinning theory; thus a relevant shear rate can produce a high shear heating effect and, as a consequence, the rubber surface temperature increases. Therefore, it was hypothesized that plasticizer diffusion and evaporation started during the injection stage, caused by excessive shear heating measured at the reciprocating screw nozzle outlet, T_{SH} = 235°C (Figure 54).

From preliminary process parameter fine-tuning performed on injection speed, screw rotation speed, and barrel temperature, it was verified that injection pressure was the process parameter that mostly reduced this excessive shear heating.

Table 17 reports the investigated injection pressure setup (Pi) for DIA-AEM60-2 production runs.

Table 17. Injection pressure setup (Pi) for DIA-AEM60-2 production runs.

DIA-AEM60-2	Injection pressure# (P_I) bar
DIA-AEM60-2-KO run	140.0
DIA-AEM60-2-INT1 run	100.0
DIA-AEM60-2-INT2 run	80.0
DIA-AEM60-2-OK run	70.0

MIR 190 tons machine process parameter setup: injection speed = 70%; screw speed rotation = 80 rpm, curing time = 85 s, barrel temperature = 75 ± 5°C and both fixed and movable plate temperature = 195 ± 5°C.

Each selected injection pressure setup was maintained constant for the whole production lot of about 450,000 parts. Four production runs were investigated: KO run, INT1 run, INT2 run and OK run, where the process parameters other than injection pressure were maintained constant.

Figure 58 shows the relationship between the measured temperature, T_{SH}, of rubber shear heating by thermal camera and the injection pressure setup, Pi. Clearly, a reduction of injection pressure decreased the shear heating effect during the injection stage, maintaining the AEM rubber in a thermal condition away from high temperatures likely to produce plasticizer diffusion and evaporation. Unlike Figure 36, where the same rubber compound was processed (DIA-AEM60-2), in this case a higher shear heating temperature is due to the fact that a different injection molding machine with different injection unit (in this case reciprocating) having different screw L/D ratio (in this case higher) was used.

T_{SH} is already a very useful parameter to guarantee very fast online process control, that is, to collect information concerning the risk of scorching and thermal degradation, leading, for example, to the diffusion of compound ingredients (low volatile chemicals), stickiness, and mold fouling, and also color variation [26-28]. However, T_{SH} values obtained for different rubber compounds cannot be directly compared since each material has different thermal behavior. Therefore, log η_{SH} was introduced to allow the comparison of process outputs between DIA-AEM60-2 and the other rubber compounds.

Figure 59 shows the relationship between the log of the shear heating parameter at 10 s^{-1}, log η_{SH}, and injection pressure setup, *P*i. Log η_{SH} at 10 s^{-1} was calculated by using the data for ΔT_{SH} (°C), ρ (kg/m^3), C_p (J/kg/°C), and screw L/D ratio reported in Tables 13 and 14 respectively.

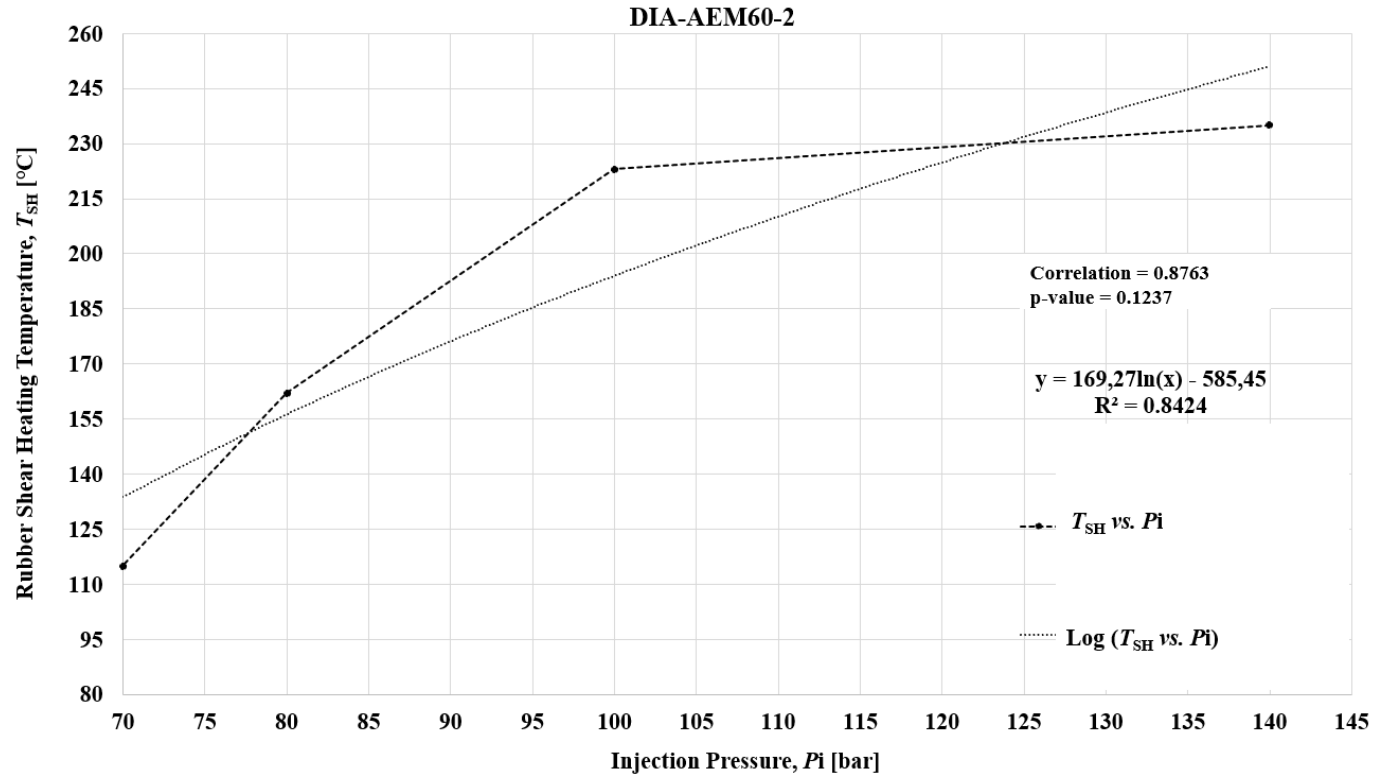

Fig.58. Relationship between temperature T_{SH} and injection pressure for DIA-AEM60-2 runs [27].

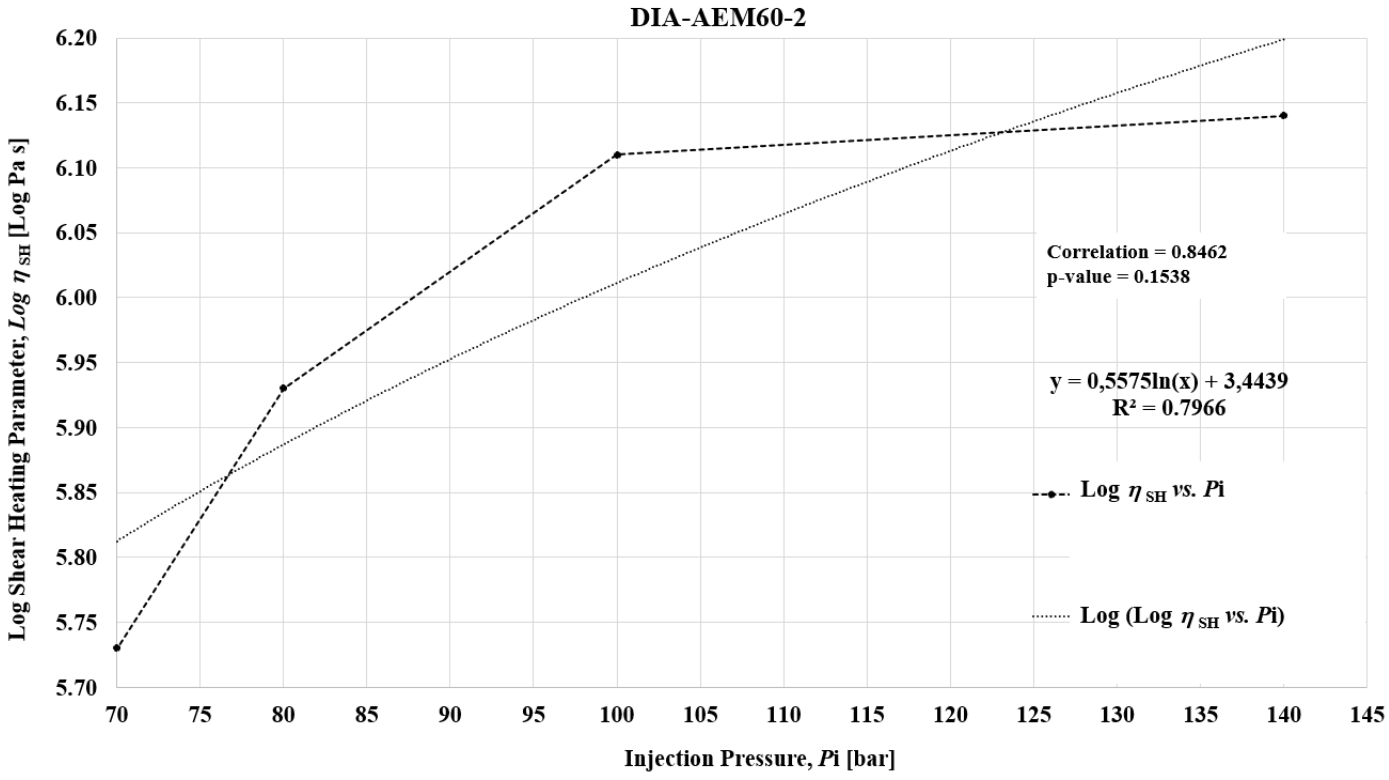

Fig.59. Relationship between log η_{SH} at 10 $s^{-1}$and injection pressure for DIA-AEM60-2 runs [27].

Therefore, working with injection pressure setup of 140 bar and the DIA-AEM60-2-KO run, an average T_{SH} of 235°C was measured online, and a log η_{SH} at 10 s^{-1} of 6.14 Pa·s was calculated. Moreover, in this production run, eight cracked parts and 12 hardened parts in 1000 sampled parts were collected. As mentioned previously, the cracked parts showed an average hardness value of 87.0 IRHD M according to *ISO 48-2-2018* due to plasticizer evaporation, thus about 30 IRHD points more than the required specification of 60±5 (molded parts had low thickness; therefore IRHD M hardness was used instead of Shore A) [27, 135]. The hardened parts showed an average hardness value of 71.0 IRHD M, thus also out of specification, and compression set of 55.0%, performed for 94 hours at 150°C after post-cure for 4 hours at 175°C. Hence, the compression set was also out of the required specification of ≤50.0%, according to *PV3330* (see Table 18) [27, 136].

On the contrary, working with injection pressure setup of 70 bar and the DIA-AEM60-2-OK run, a lower rubber shear heating temperature was measured online, average T_{SH} of 115°C, and a lower shear heating parameter was calculated, log η_{SH} at 10 s^{-1} of 5.73 Pa·s. Therefore, this production run guaranteed a thermal condition away from high temperatures likely to produce plasticizer diffusion and evaporation.

Table 18 also reports the hardness and compression set results for the DIA-AEM60-2-OK run, where average values of 58.0 IRHD M and 40.0%, respectively, were reported, both within the required specification.

Table 18. Physical-mechanical data for DIA-AEM60-2, comparison between OK and KO runs [27].

Parameter*	DIA-AEM60-2-OK	DIA-AEM60-2-KO
Hardness after post-curing**, IRHD M, (point)	58.0	71.0
Compression set (94 hrs. at150°C) after post-curing (%)	40.0	55.0
Glass transition temperature (DSC), T_g (°C)	-35.7	-26.7

* Required specification: IRHD M (*ISO 48-2-2018*) = 60±5 and compression set 94 hours at 150°C (*PV3330*) ≤50%.
** 4 hours at 175°C.

With the aim of showing the roadmap application for fast control of successful setup of process parameters, Figure 60 shows the relationship between log η_{SH} at 10 s^{-1} and M_L from 12 minutes at 177 °C by MDR for the seven rubber compounds with very stable industrial production runs and DIA-AEM60-2-KO run (R^2 of 0.526 and p-value of 0.04855), DIA-AEM60-2-INT1 run (R^2 of 0.562 and p-value of 0.03994) and DIA-AEM60-2-INT2 run (R^2 of 0.788 and p-value of 0.01196).

In more detail, new curves were created, starting from the roadmap reported in Figure 51, by replacing the data of DIA-AEM60-2-OK with values of either DIA-AEM60-2-KO run (Figure 60a), INT1 run (Figure 60b) or INT2 run (Figure 60c), while keeping the values of the other seven productions runs constantly. Only the log η_{SH} values of DIA-AEM60-2 were modified, whereas M_L was always the same since it is a laboratory property, not influenced by process parameters. By introducing the curves of the KO run, INT1 run, and INT2 run, some relevant deviations from the previous proportional trend were observed, especially in Figure 60a (red curve) with R^2 of 0.526 according to the power regression model.

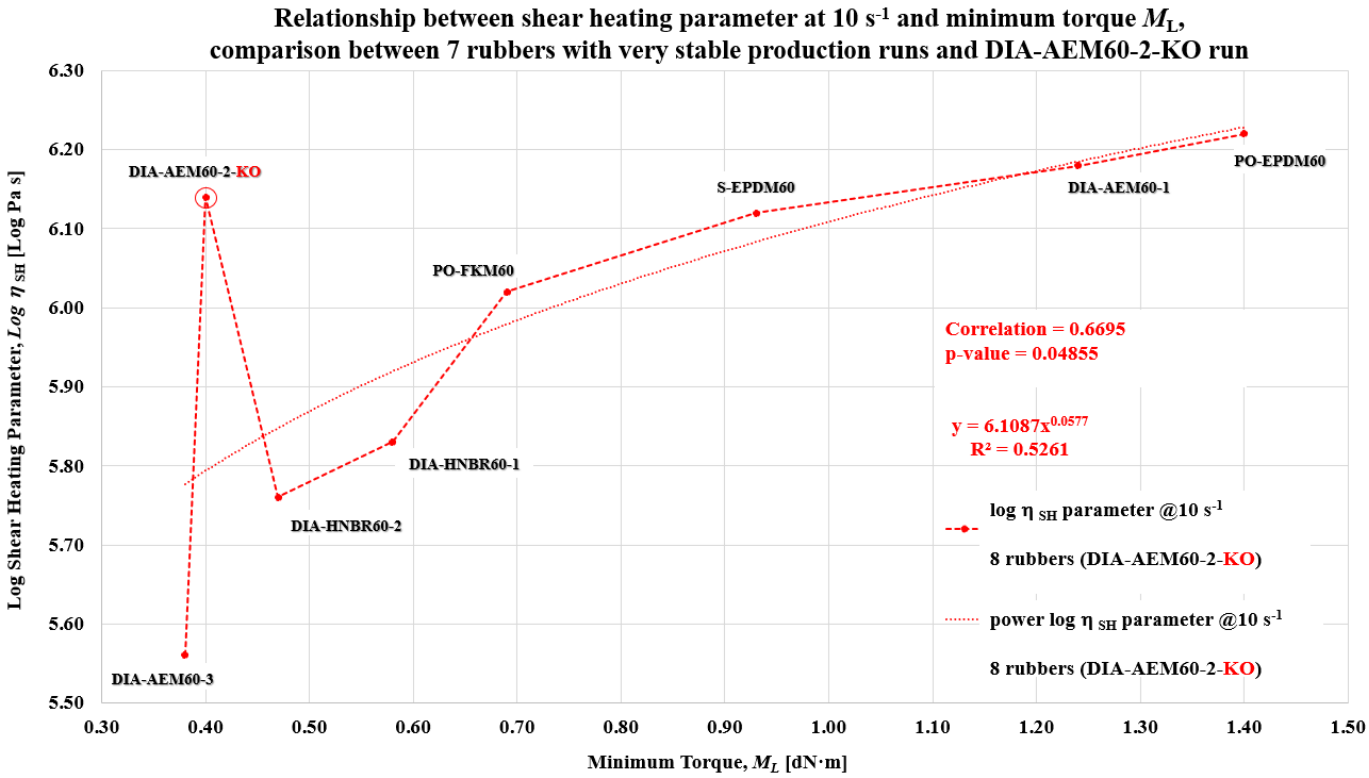

Fig.60 a. Relationship η_{SH} at 10 s^{-1} and M_L, comparison between 7 rubbers and 7 production runs having long process stability and DIA-AEM60-2-KO run [27].

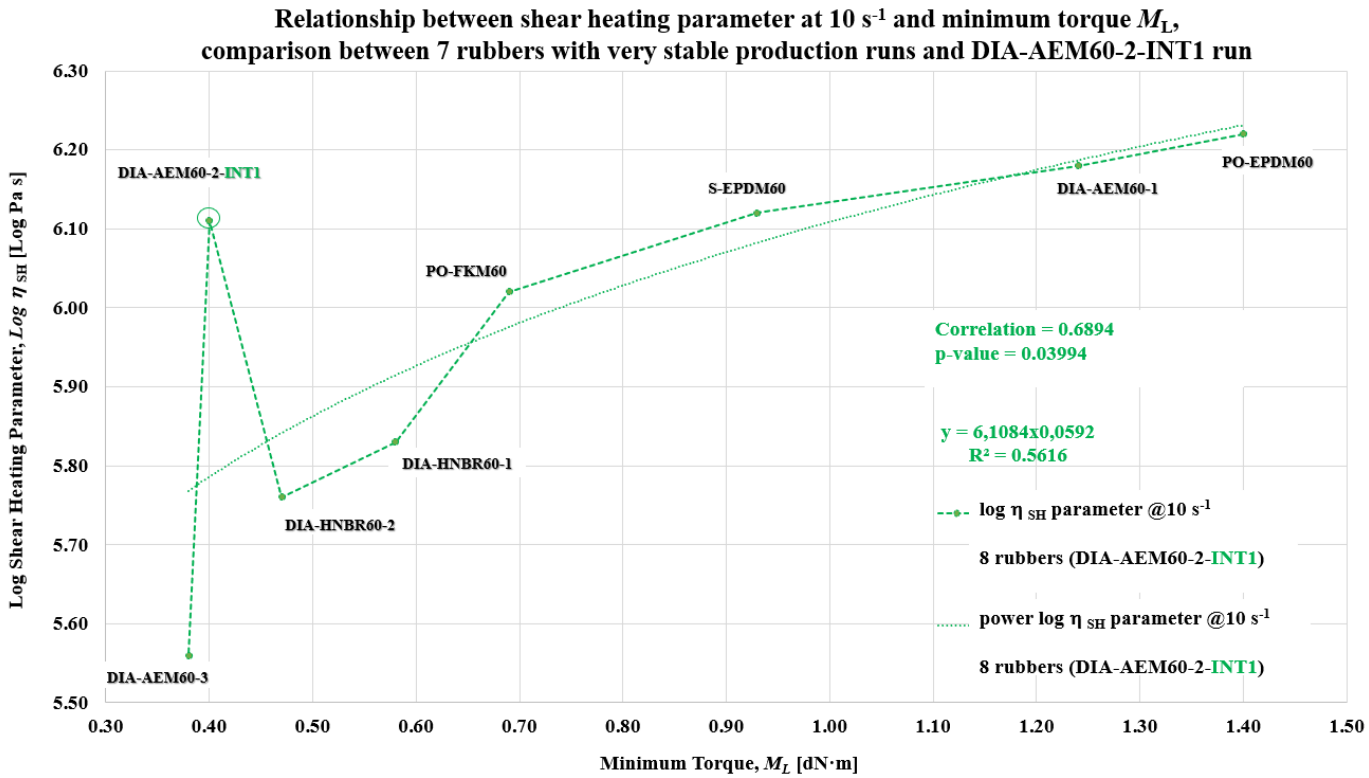

Fig.60 b. Relationship η_{SH} at 10 s^{-1} and M_L, comparison between 7 rubbers and 7 production runs having long process stability and DIA-AEM60-2- INT1 run [27].

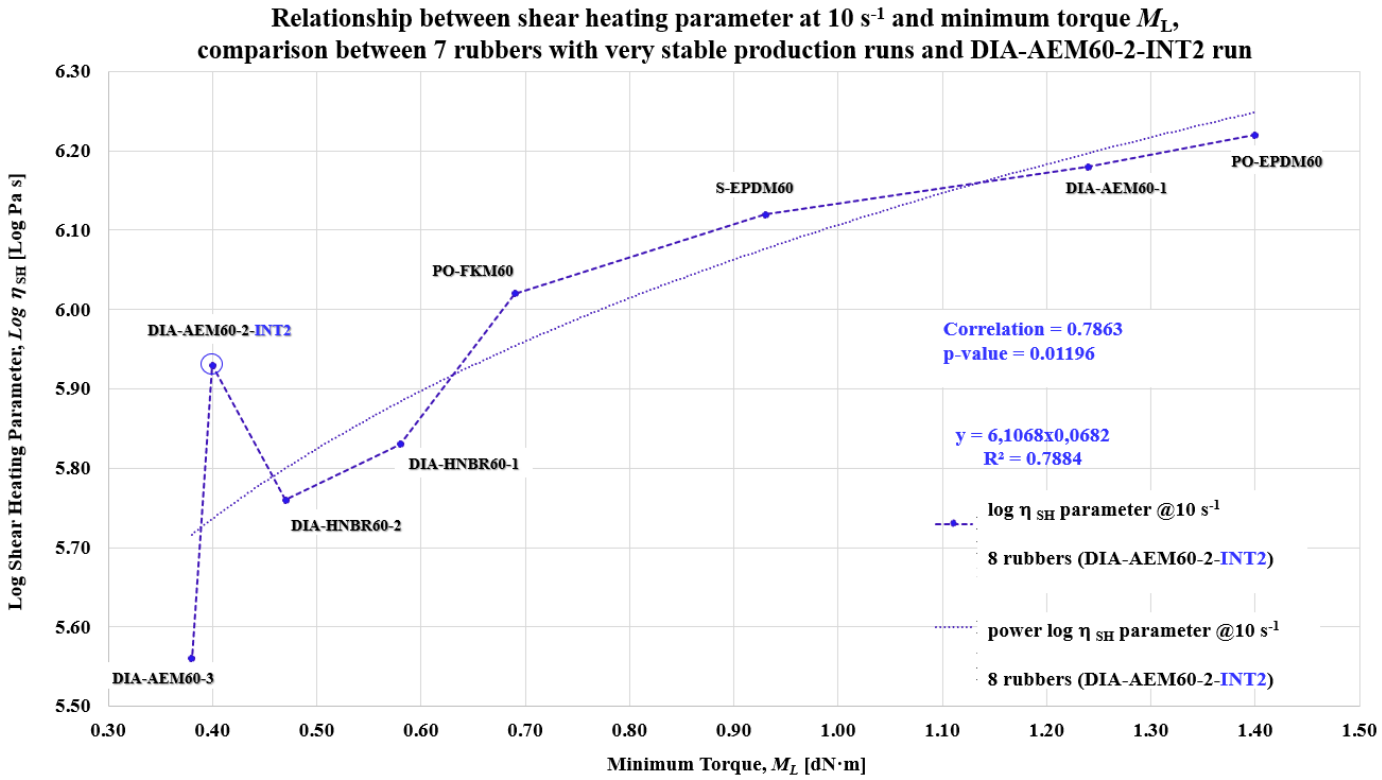

Fig.60 c. Relationship η_{SH} at 10 s^{-1} and M_L, comparison between 7 rubbers and 7 production runs having long process stability and DIA-AEM60-2- INT2 run [27].

Accordingly, the DIA-AEM60-2-KO run, based on injection pressure setup of 140 bar, average T_{SH} of 235 °C, and log η_{SH} at 10 s^{-1} of 6.14 Pa·s, didn't allow a stable production cycle, where hardened and cracked parts were produced. Furthermore, DIA-AEM60-2-INT1 and DIA-AEM60-2-INT2 runs were used to fine-tune the injection pressure setup from KO to OK runs, thus in this case also the log η_{SH} at 10 s^{-1} values deviated from the proportional trend with R^2 of 0.562 and 0.788, respectively.

Finally, the DIA-AEM60-2-OK run, based on injection pressure setup of 70 bar, average T_{SH} of 115 °C, and log η_{SH} at 10 s^{-1} of 5.73 Pa·s, allowed a very stable production cycle without hardened and cracked parts.

In this process setup, the log η_{SH} value was within the proportional trend with R^2 of 0.935 according to the power regression model (see Figure 51). Therefore, the coefficient of determination of log η_{SH} vs M_L curves (operating roadmap) provides a good indication of process stability of DIA-AEM60-2 runs. Figure 51 and Figure 60 clearly show how log η_{SH} values of a production run, combined with M_L values, give indication of the successful output of the injection molding process by comparison of this data with a well-established roadmap obtained from stable production runs of different rubber compounds and process conditions. This monitoring has the advantage of being fast, and provides information about the stability of the process while it is running, well before completing the production run. The proposed integrated approach, obtained for a very heterogeneous sample of rubber compounds and operating conditions, was found to be successful and useful in industrial applications, taking into account that type of defects such as hardened and cracked parts cannot be accepted in the automotive industry, because requires "zero defected" parts [27-28].

6.4. Effect of T_{SH} and η_{SH} in CAE simulation setup

This chapter reports the results about the implementations of T_{SH} and η_{SH} in the setup of CAE simulations.
A sealing ring typically used in automotive industry (Figure 34) was selected as case study for the 3D finite element process simulation. About the material, an FKM rubber compound black colored with 70 Shore-A hardness was chosen. Practically, the simulations were carried out including both filling and curing stages, and using the *Molded 3D* CAE software.
The FKM rubber setup has taken into account PVT curves, specific heat capacity and curing kinetics, the last two obtained from DSC measurements, experimentally measured on the studied material [96].
Typically, the viscosity data used as input for CAE simulation is the dynamic complex viscosity, η*, determined by rheological measurements performed with Rubber Process Analyzer (RPA), from 80-100°C in the range of 1.0 to 10,000 s^{-1}.
However, this research activity had as its purpose the implementation of the shear heating parameter, η_{SH}, as viscosity input of CAE simulation setup. The shear heating parameter was calculated by using a shear heating temperature, T_{SH}, of 110°C, obtained from processing trial by a 190 Ton MIR with reciprocating screw, L/D ratio of about 18. Therefore, the FKM 70 Shore-A hardness flow curve in logarithmic scale, log η_{SH}, is obtained by using Equation (10), and varying the flow rate parameter v in the range of 1.0 to 10,000 s^{-1}, at ΔT_{SH} of 90°C. [10, 96].
Two process simulation runs were carried out using the same setup of filling time, curing time, maximum injection pressure, mold temperature, and cycle time, except the "melt temperature". In the first simulation run (Run 1) the barrel temperature setup (T_{barrel}) of 80°C was used as "melt temperature", in the second one (Run 2) the shear heating temperature, T_{SH}, of 110°C, was used: in both cases experimental data coming from the above-mentioned processing trial. Figure 61 summarizes the main input data of the two process simulation runs.

PROCESS SIMULATION SETUP	Run-1 FKM 70 Shore-A T_{barrel} = 80°C	Run-2 FKM 70 Shore-A T_{SH} = 110°C
[Filling]		
Filling time (sec)	4	4
Melt Temperature (oC)	80	110
Mold Temperature (oC)	190	190
Maximum injection pressure (MPa)	250	250
Injection volume (cm^3)	11.7923	11.7923
[Curing]		
Curing time (sec)	120	120
Maximum curing pressure (MPa)	250	250
[Miscellaneous]		
Cycle time (sec)	129	129

Fig.61. Input setup data of two process simulations with T_{barrel} and T_{SH} respectively [96].

By comparing the two simulations according to the filling stage, no substantial differences were found between the two runs. Therefore, the temperature of shear heating didn't significantly affect the filling stage, Figure 62 shows the melt front time, where a same filling time output of about 3.8 s was obtained.

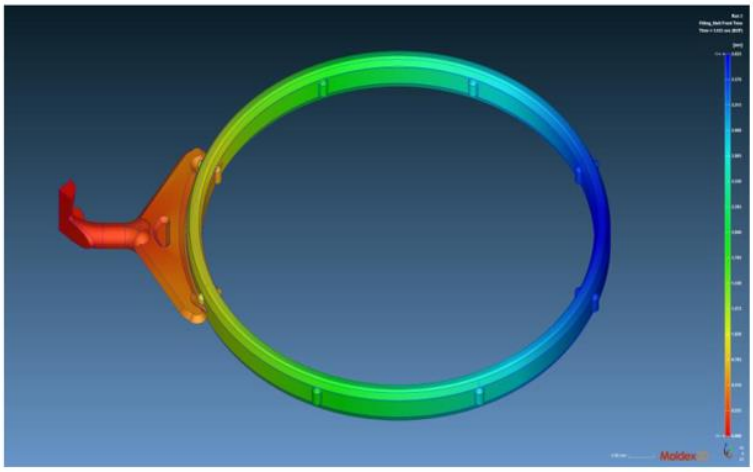

Run-1 FKM 70 Shore-A T_{barrel} = 80°C	Run-2 FKM 70 Shore-A T_{SH} = 110°C
MAX MELT FRONT TIME [S]	MAX MELT FRONT TIME [S]
3.825	3.853

Fig.62. Melt front time output of two process simulations with T_{barrel} and T_{SH} respectively [96].

Furthermore, even the melt front temperature in the filling stage didn't provide considerable differences (Figure 63). However, the Run-2 with T_{SH} as input showed obviously a higher average melt front temperature, because 110°C was the set point, but with lower dispersion of the obtained results (lower standard deviation). Therefore, the Run-1 (T_{barrel} = 80°C) showed an average melt front temperature of 131 ± 18°C, instead the Run-2 (T_{SH} = 110°C) showed an average melt front temperature of 148 ± 13°C.

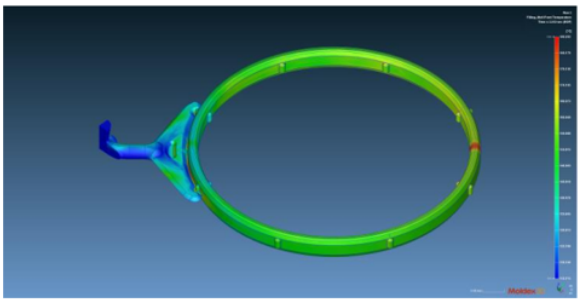

Run-1 FKM 70 Shore-A T_{barrel} = 80°C	Run-2 FKM 70 Shore-A T_{SH} = 110°C

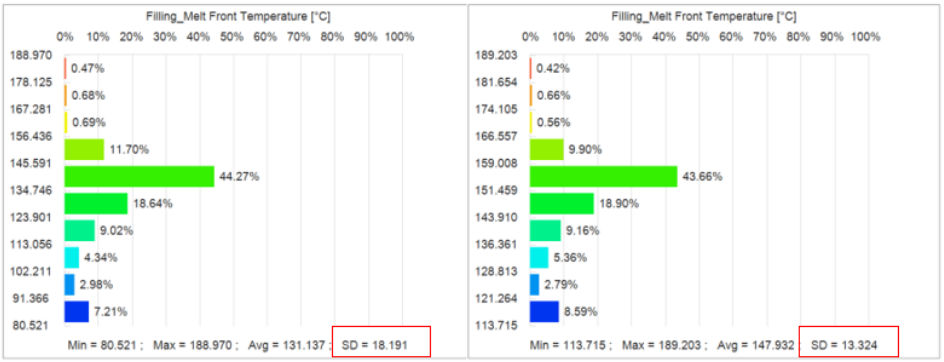

AVERAGE MELT FRONT TEMPERATURE [°C] 131 ± 18°C

AVERAGE MELT FRONT TEMPERATURE [°C] 148 ± 13°C

Fig.63. Melt front temperature output of two process simulations with T_{barrel} and T_{SH} respectively [96].

Finally, by comparing the two simulations according to the curing stage, very interesting differences were obtained. Therefore, the temperature of shear heating significantly affected the curing conversion expressed in percentage (Figure 64), where different percentages of conversion were obtained between the Run-1(T_{barrel} = 80°C) and Run-2 (T_{SH} = 110°C). The Run-1(T_{barrel} = 80°C) showed an average curing conversion of 70 ± 17%, instead the Run-2 (T_{SH} = 110°C) showed an average curing conversion of 78 ± 12%. Increased curing conversion will allow a higher cross-linking density on the final parts.

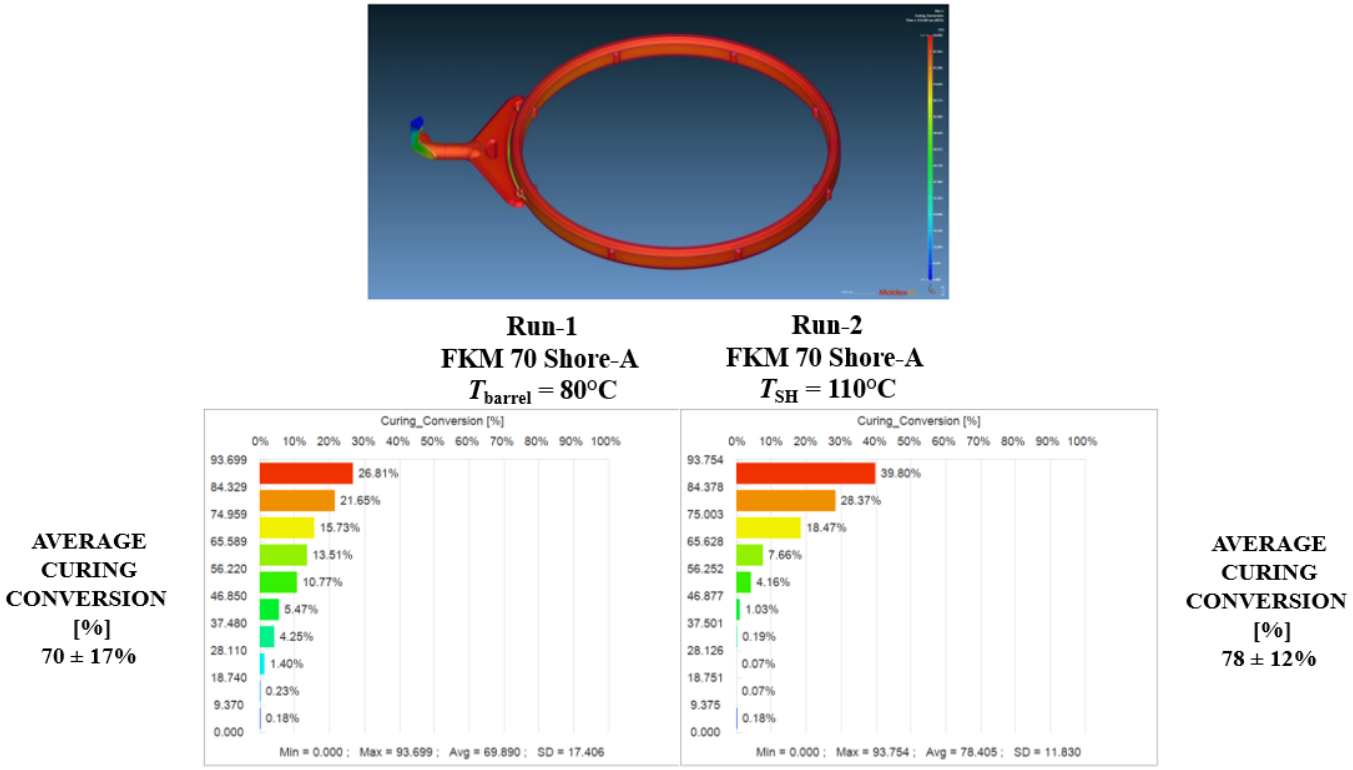

Fig.64. Curing conversion output of two process simulations with T_{barrel} and T_{SH} respectively [96].

In summary, the use of T_{SH} did not significantly affect the simulation of the filling stage, most likely due to the slight sensitivity of viscosity characteristics to temperature, compared to plastics. Furthermore, it is important to emphasize that a case study with relatively simple geometry (without significant variations in section) is considered.

However, T_{SH} has impacted mostly the simulation run of the curing stage: in particular the average curing conversion was higher and more homogeneous than the result obtained with T_{barrel}, with a lower standard deviation (Figure 64). Furthermore, these results have described how the reliability of simulation results depend on the input parameters, and has highlighted the importance of using a real value of rubber material's inlet temperature on the simulation outputs.

Therefore, by using the real measured shear heating temperature, T_{SH}, as "melt temperature", input of *Moldex 3D* CAE process simulator, instead of barrel temperature, T_{barrel}, more realistic results were obtained [96].

6.5. Effect of "green compounds" on T_{SH} and η_{SH}

Finally, this chapter reports the results and remarks about the application of T_{SH} and η_{SH} in the processing trials of recycled FKM rubber compounds from devulcanization process, and NBR rubber compounds containing EAF slag, a by-product of steel industry, as reinforcing filler.

6.5.1. Recycled FKM rubber compounds

Three bisphenol cured, black colored FKM rubber compounds with 75 Shore-A hardness, FKM-REF, and two recycled compounds, FKM-A and FKM-B, containing 10 and 20 wt.% of TT-FKM respectively, were processed by injection molding. TT-FKM was obtained by thermo-mechanical treatment of cured scraps of FKM-REF black colored with 75 Shore-A hardness. Therefore, the TT-FKM of FKM-REF was considered as a new functional raw material for corresponding compounds FKM-A and FKM-B.

Industrial 75 kg batches of FKM-REF, FKM-A and FKM-B rubber compounds were prepared in *Banbury* type internal mixer, followed by an open mill.

Table 19 reports the physical and mechanical data of the compounds, obtained from laboratory characterization performed on 200×200×2 mm slabs molded for 10 minutes at 180°C by laboratory compression molding press and air oven post-cured for 24 hours at 230°C [108]. About laboratory characterization, Shore-A hardness, density (ρ), specific heat capacity (C_p), minimum torque (M_L) at 177°C, tensile properties and compression set were measured. Tensile strength and elongation at break were measured according to *ASTM D412-16(2021)*, instead the compression set for 24 hours at 200°C in accordance with *ASTM D395-18-B* [34, 108].

Table 19. Experimental data from laboratory characterization of FKM-REF, FKM-A and FKM-B, after post-curing for 24 hours at 230°C [108].

Property	Reference standard	FKM-REF	FKM-A	FKM-B
Hardness (Shore-A)	*ASTM D2240-15*	76.0 ± 1	76.0 ± 1	76.0 ± 1
Density, ρ (kg/m^3)	*ASTM D297-15*	1890 ± 1	1890 ± 1	1890 ± 1
Specific heat capacity at T_{SH}, C_p (J/kg/°C)	*ASTM E1269-11*	2200 ± 3	1805 ± 3	2100 ± 3
Minimum torque, M_L (dN m)	*ASTM D5289-95*	0.80 ± 0.05	0.70 ± 0.05	0.70 ± 0.05
Tensile strength (MPa)	*ASTM D 412-16*	11.5 ± 0.5	11.0 ± 0.5	10.9 ± 0.5
Elongation at break (%)	*ASTM D 412-16*	205.0 ± 10	195.0 ± 10	190.0 ± 10
Compression set (%) (24 hours at 200°C)	*ASTM D395-18-B*	12.0 ± 2	13.0 ± 2	14.0 ± 2

Table 19 doesn't show significant difference of hardness, density, tensile strength, elongation at break and compression set results between the three samples, thus demonstrating that a proper devulcanization procedure together with proper compounding, has enabled for the use of recycled rubber without detrimental effects on compound properties. Nevertheless, the introduction of TT-FKM has reduced both the minimum torque, M_L, by MDR and specific heat capacity, especially in the compound containing 10 wt.% of TT-FKM. Furthermore, the same result of M_L at 177°C was obtained for both FKM-A and FKM-B.

The industrial 75 kg batches of FKM-REF, FKM-A and FKM-B rubber compounds were processed by using a horizontal 190 Ton MIR with reciprocating screw, L/D ratio of about 15. The mold is equipped with 32 cavities having a single nozzle injection system. All the rubber compounds were used for the production of a technical article, used in automotive industry to verify the effect of TT-FKM on processability by injection molding. This technical article (Figure 35) was chosen because its geometry can be very interesting to understand how the TT-FKM affects the mold fouling and the hot tear resistance, typical FKM compound weaknesses. The online monitoring by T_{SH} measurements for each rubber compound and respective production run was performed every hour, three measures at each time, in order to control the rubber flow temperature and shear heating effect for each rubber compound during the injection stage [10, 26-27].

Table 20 report the experimental data from processing characterization of the FKM-REF, FKM-A and FKM-B. The setup parameters, already reported in Table 5, were the same for all the rubber compounds. About the processing characterization, the data of measured shear heating temperature (T_{SH}) of the rubber by infrared thermal camera and the temperature difference in shear heating (ΔT_{SH}) considering 20°C as initial temperature were reported. Moreover, the shear heating parameter (η_{SH}) at 10 s^{-1} and the corresponding logarithmic values were therefore calculated for FKM-REF, FKM-A and FKM-B rubber compounds according to Equation (10) [108].

Table 20. Experimental data from processing characterization of FKM-REF, FKM-A and FKM-B [108].

Parameter	FKM-REF	FKM-A	FKM-B
Injection pressure, *P*i (bar)	140.0	140.0	140.0
Injection speed, *v*i (%)	85.0	85.0	85.0
Screw speed rotation (rpm)	30.0	30.0	30.0
Barrel temperature, T_{barrel} (°C)	85.0	85.0	85.0
Shear heating temperature, T_{SH} (°C)	140.0	130.0	135.0
Temperature difference in shear heating, ΔT_{SH} (°C)	120.0	110.0	115.0
Fixed plate temperature (°C)	195.0	195.0	195.0
Movable plate temperature (°C)	195.0	195.0	195.0
Injection time (s)	7.0	4.0	4.0
Curing time (s)	65.0	65.0	65.0
Cycle time (s)	90.0	89.0	89.0
Shear heating parameter, η_{SH} (Pa s)	8.52×10^5	6.40×10^5	7.80×10^5
Log shear heating parameter, Log η_{SH} (Log Pa s)	5.93	5.81	5.89

Figure 65 shows the three thermal images for FKM-REF (Figure 65a), FKM-A (Figure 65b) and FKM-B (Figure 65c) rubber compounds, taken to the rubber as it emerged from the reciprocating screw nozzle outlet, from which T_{SH} values reported in Table 20 were obtained.

Therefore, compared to FKM-REF (Figure 65a), a lower shear heating effect was measured on the recycled compounds: about 10°C less for FKM-A (Figure 65b), and about 5°C less for FKM-B (Figure 65c). However

the FKM-B showed an higher shear heating effect than FKM-A (5°C more). These data were in agreement with the obtained results of specific heat capacity from DSC and the calculated shear heating parameter according to Equation (10).

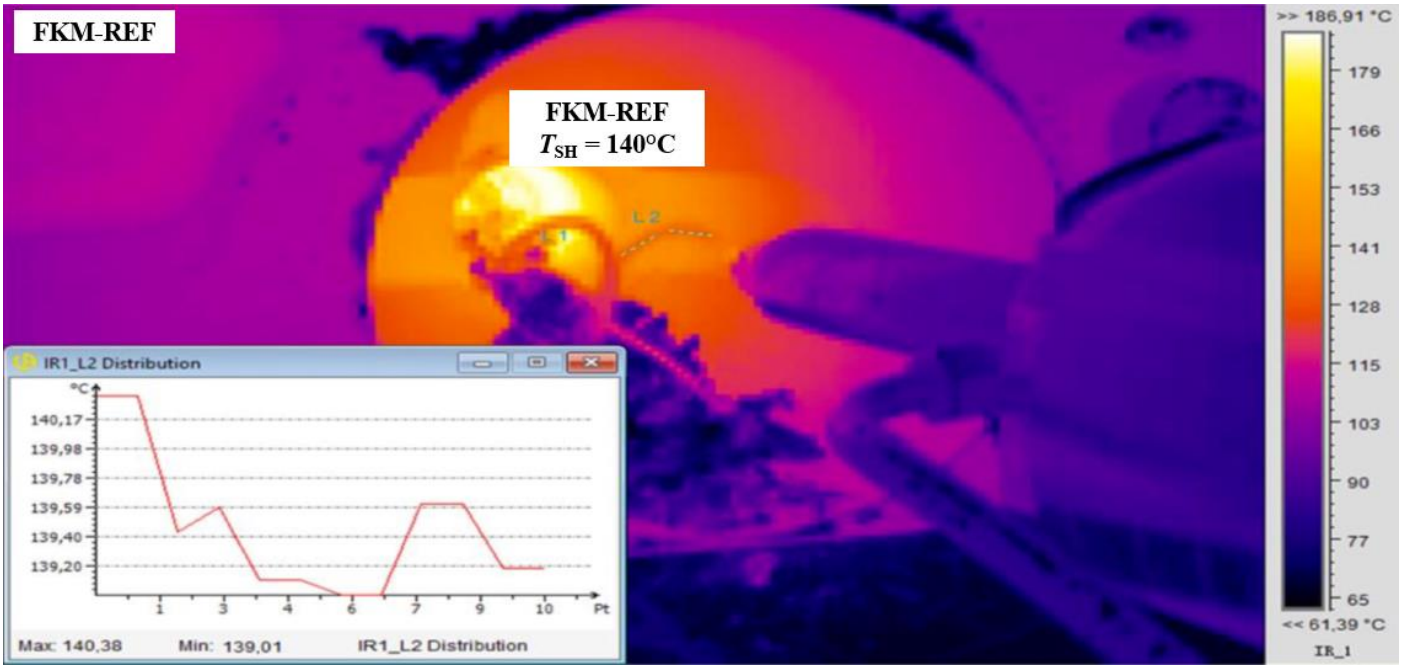

Fig.65 a. Image of FKM-REF emerging from the reciprocating screw nozzle outlet, T_{SH} = 140°C [108].

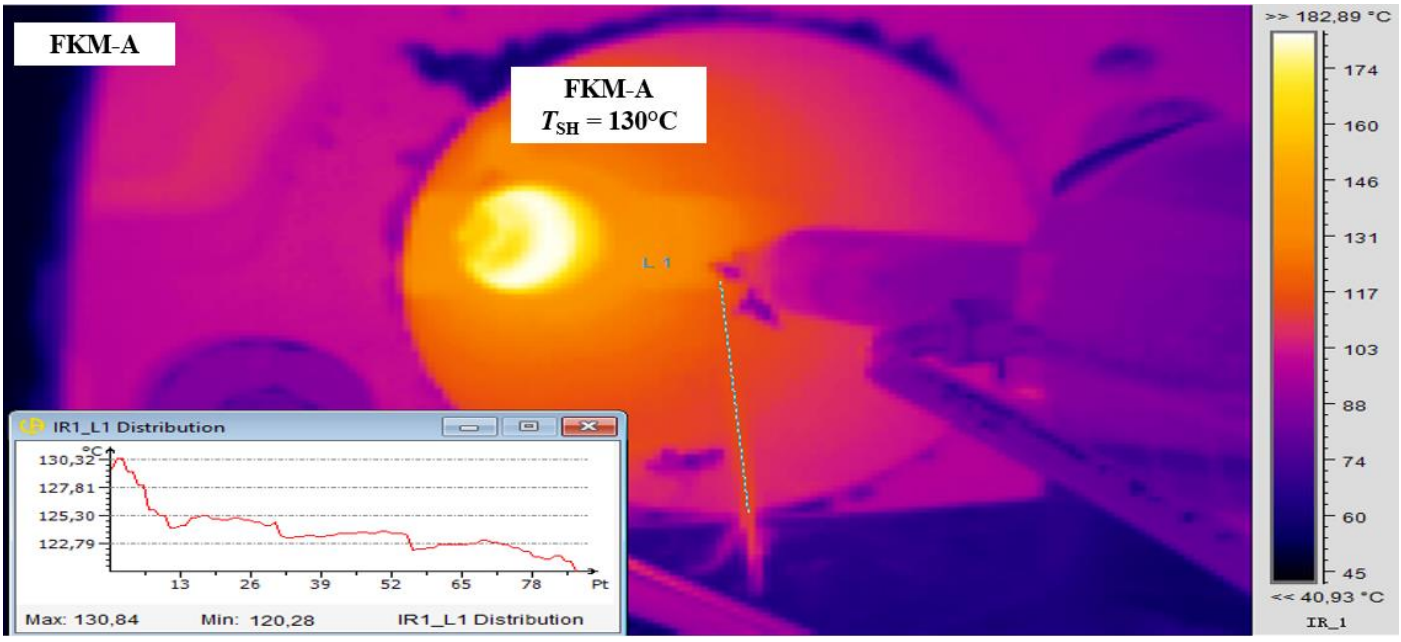

Fig.65 b. Image of FKM-A emerging from the reciprocating screw nozzle outlet, T_{SH} = 130°C [108].

Furthermore, both FKM-A and FKM-B rubber compounds have exhibited the faster injection time with respect to FKM-REF, (4.0 s vs 7.0 s, see Table 20), thanks to the soluble fraction of TT-FKM that acted as a plasticizer. The TT-FKM is constituted by two different fractions: soluble and insoluble in common FKM solvents like methylethylketone or tetrahydrofuran. These fractions are separated via solvent extraction and

characterized. Soluble fraction consists in medium to low molecular weight FKM while insoluble fraction is a network of FKM strictly bonded to the fillers which can be compared to “carbon gel” or “bound rubber” [108, 113, 121].

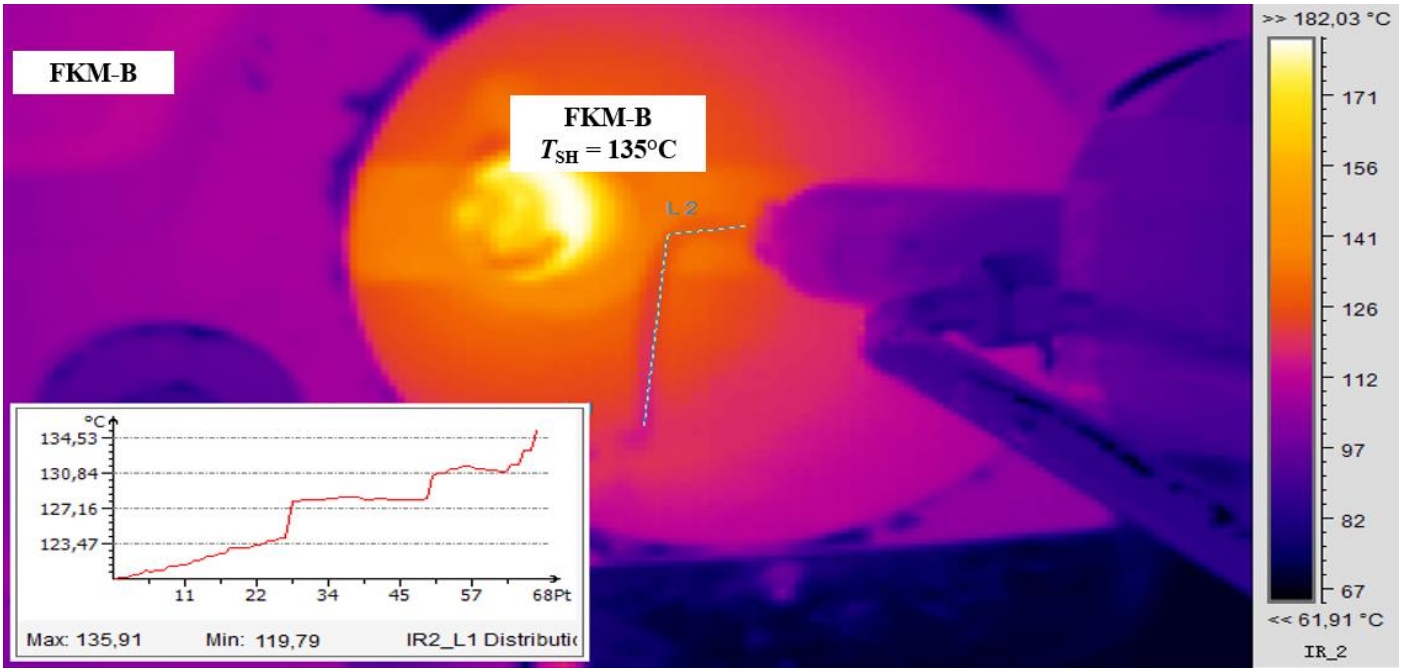

Fig.65 c. Image of FKM-B emerging from the reciprocating screw nozzle outlet, T_{SH} = 135°C [108].

FKM-A especially has possessed the lower shear heating effect (T_{SH} = 130°C) measured by infrared thermal camera at the nozzle outlet of the injection moulding machine extruder, and confirmed by the calculated shear heating parameter (log η_{SH} at 10 s^{-1} of 5.81). Therefore, the use of TT-FKM has facilitated the injection stage by improving the FKM rubber compounds processability.

Moreover, during the processing trials the FKM-A and FKM-B showed an improved mold release with reduced mould fouling than FKM-REF, due to the insoluble fraction of TT-FKM. These insoluble fraction being a micro-cross-linked fraction has allowed a better hot tear resistance (resistance to tearing during demolding) with relevant reduction of molded parts fracture. These molded parts after stabilization and deburring, were post-cured with two different operating conditions: 24 hours at 230°C and 12 hours at 230°C in air industrial oven. Table 21 reports the average IRHD M hardness values of the final parts, before and after post-curing for 12 and 24 hours at 230°C, respectively [108]. The hardness were measured by IRHD M durometer and according to *ISO 48-2-2018*, (75.0 ± 5 required specification) [28, 135].

Table 21. IRHD M hardness average data before and after post-curing for 12 and 24 hours at 230°C [108].

Type of Treatment	FKM-REF	FKM-A	FKM-B
Before post-curing	69.4 ± 0.7	65.8 ± 1.0	66.3 ± 0.8
After post-curing for 12 hours at 230°C	70.0 ± 1.1	67.0 ± 1.0	66.9 ± 1.1
After post-curing for 24 hours at 230°C	72.4 ± 1.0	69.7 ± 0.7	69.0 ± 0.9

The use of TT-FKM could help in reducing post-curing treatment time with production cost reduction in terms of energy saving and productivity optimization. Nevertheless, the rubber compound recipes FKM-A and FKM-B will need to be finely tuned, by adding some phr of carbon black to align the hardness values in accordance with the specification tolerance. The final parts of FKM-REF, FKM-A and FKM-B were also measured by quantitative thermogravimetric analysis (TGA). In this case about 10 mg of FKM parts were placed in a platinum crucible and heated in a thermo-balance; the measurements were run in an N_2 atmosphere heating from RT to 150°C at 20°C/min, and from 150°C to 850°C at 10°C/min, then heating from 850°C to 950°C at 20°C/min in an oxygen atmosphere. This schedule of temperature was used to investigate potential compositive differences in the area of elastomers and fillers between FKM-REF and two are recycled compounds.

Figure 66 shows the comparison between thermograms of FKM-REF (green), FKM-A (red) and FKM-B (blue) final parts after post-curing for 24 hours at 230°C, where no significant compositive differences were observed. Especially, in the area of elastomers, the weight loss difference between the three samples was below 1.0 wt.%, thus negligible.

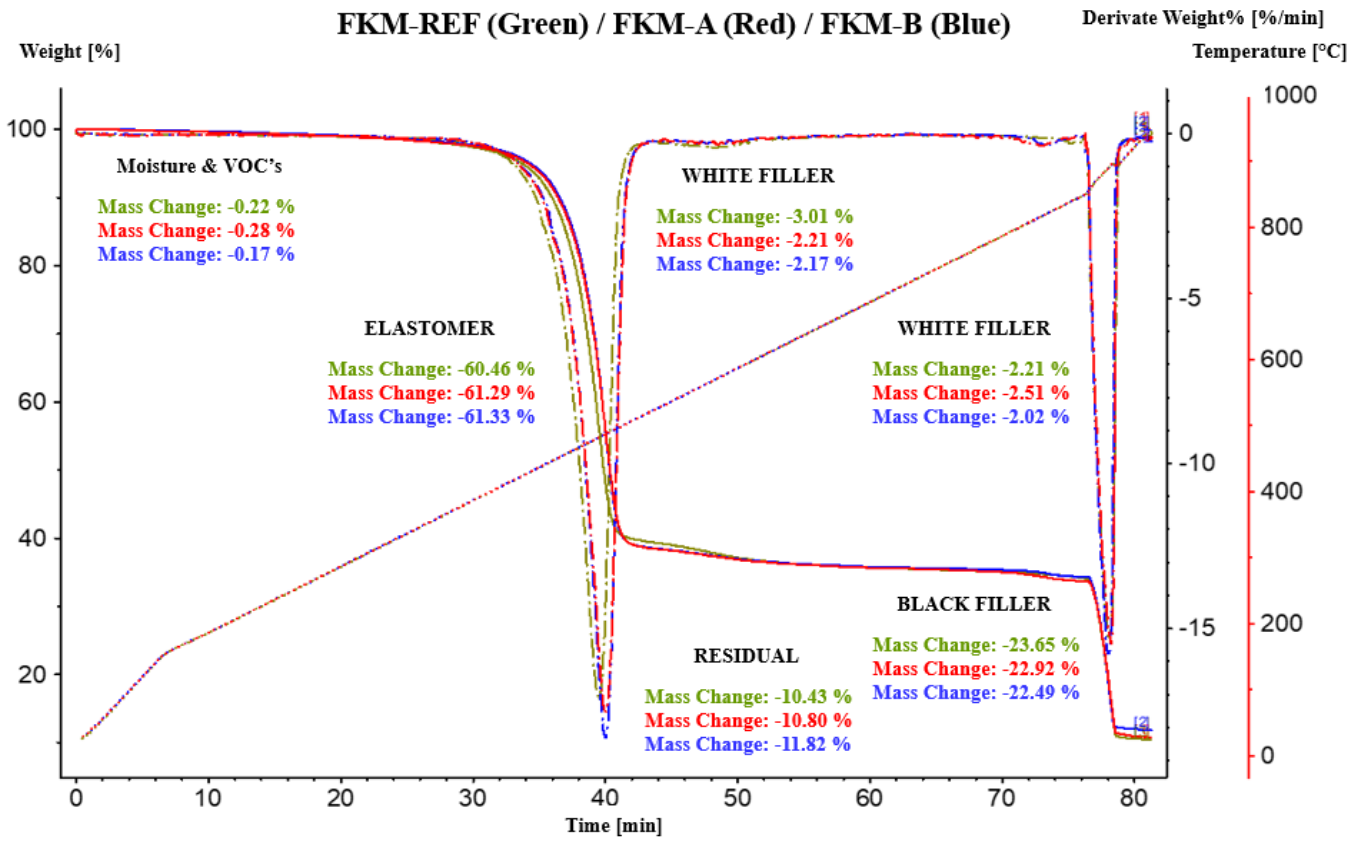

Fig.66. TGA thermograms final parts of FKM-REF (green), FKM-A (red) and FKM-B (blue) [108].

The scraps amount after final sorting was comparable between the three production runs, even if in FKM-A and FKM-B production runs a lower level of fractured parts were detected.

As already mentioned, TT-FKM is constituted by both soluble and insoluble fractions. The soluble fraction acted as a plasticizer for the rubber compound improving processability, mold flow and reducing undesired mold fouling because it reacts upon curing. The measure of T_{SH} and the calculation of η_{SH} quantitively confirmed this plasticizer effect. The insoluble fraction, on its turn, behaved as a reinforcing filler since it is already a micro-cross-linked fraction. The result was an increase in hot tear resistance with easy mold release, especially found in the reduction of detected fractured parts. Soluble to insoluble fraction ratio can be driven acting on devulcanization process parameters and different TT-FKM grades can be produced depending on specific applications and desired properties. TT-FKM cannot be considered as a mere filler, it behaves as an active new ingredient able to impart unusual properties and special characteristics and this aspect can play a very important role in HPE compounding [108].

6.5.2. NBR rubber compounds with EAF slag

Finally, the rubber compounds based on NBR filled with EAF slag were investigated via injection molding trials aimed to understand the processing behavior by T_{SH} measurements and η_{SH} calculation. In detail the three sulfur cured NBR rubbers black colored were: one NBR filled with carbon black (NBR-REF) with 60 Shore-A hardness, and the same NBR were the filler volume of CB was totally (NBR-EAF100) or half substituted by EAF slag (NBR-EAF50), with 45 and 50 Shore-A, respectively, as reported in Table 2. The main components of EAF slag used as filler in this study are iron oxide (Fe_2O_3) and calcium oxide (CaO), with maximum particles size of 100 μm [118-119]. About 5 kg batches of NBR-REF, NBR-EAF100 and NBR-EAF50 rubber compounds were prepared by mixing the ingredients using a laboratory mixer followed by an open mill. Table 22 reports the physical and mechanical data from laboratory characterization performed on 200×200×2 mm slabs molded for 12 minutes at 177°C by laboratory compression molding press. About laboratory characterization, the Shore-A hardness, density (ρ), specific heat capacity (C_p), minimum torque (M_L) at 177°C, tensile properties and compression set were performed. Tensile strength and elongation at break were measured according to *DIN 53 504-S2*, instead the compression set for 24 hours at 100°C in accordance with *ISO 815-1:2019*, method A (type B) [137, 140].

Table 22. Experimental data from laboratory characterization of NBR-REF, NBR-EAF100 & NBR-EAF50.

Property	Reference standard	NBR-REF	NBR-EAF100	NBR-EAF50
Hardness (Shore-A)	*ASTM D2240-15*	60.5	49.2	53.9
Density, ρ (kg/m^3)	*ASTM D297-15*	1206	1654	1433
Specific heat capacity at T_{SH}, C_p (J/kg/°C)	*ASTM E1269-11*	1883	1641	1601
Minimum torque, M_L (dN m)	*ASTM D5289-95*	0.46	0.27	0.27
Tensile strength (MPa)	*DIN 53 504-S2*	14.8	1.9	9.0
Elongation at break (%)	*DIN 53 504-S2*	433.0	363.0	451.0
Compression set (%) (24 hours at 100°C)	*ISO 815-1:2019*	10.8	12.9	11.6

The laboratory characterization showed considerable differences in hardness, density and specific heat capacity values, in NBR-EAF100 rubber compound, especially. Therefore, the EAF slag added as filler in the NBR compound has definitely modified the elastomer/filler ratio.

Figure 67 shows the trend of the specific heat capacity as a function of the temperature for the three investigated rubber compounds. Clearly, a different thermal behavior was observed, where the NBR-REF showed the higher C_p values, and also the greater specific heat capacity data, which in this graph is represented by the slope of the specific heat capacity vs. temperature trend. However, the introduction of EAF slag decreased the specific heat capacity values, in particular if added at 50%. This reduction can be attributed to the high level of metal oxides contained in the slag.

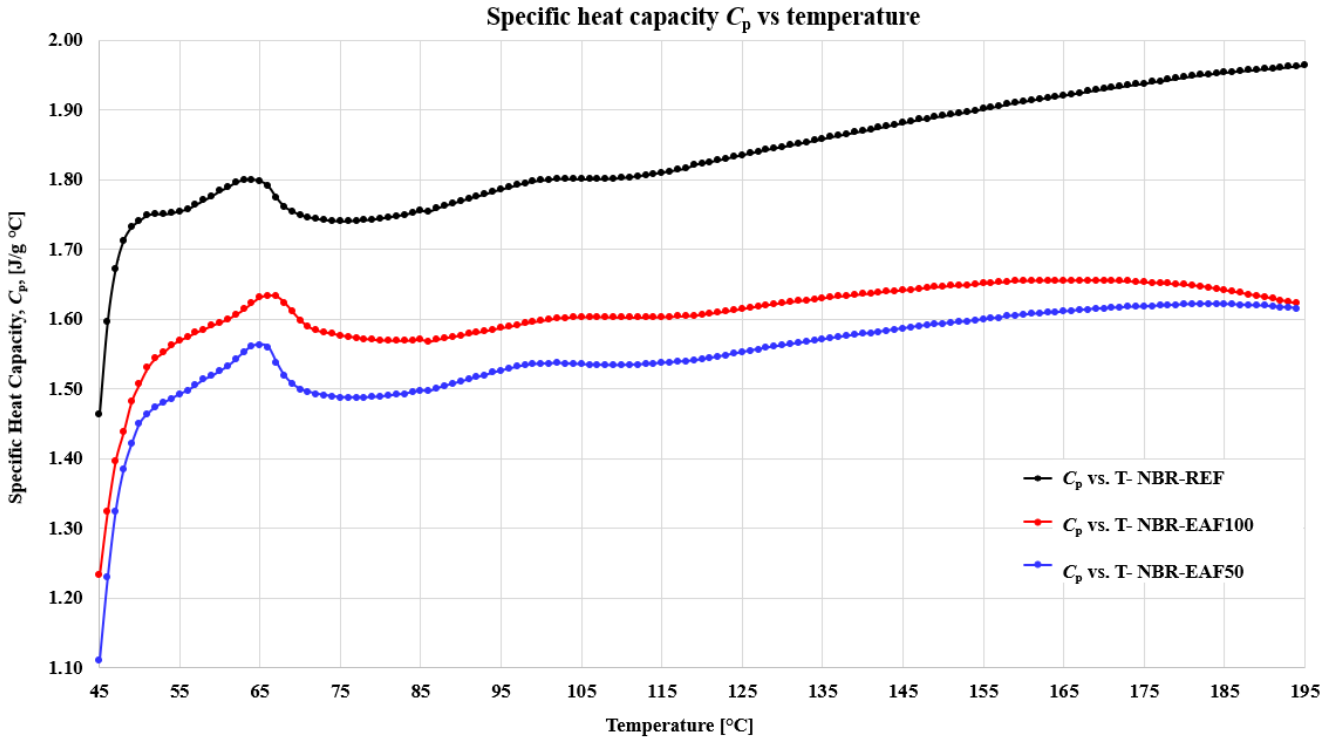

Fig.67. Specific heat capacity (C_p) vs. temperature for NBR-REF, NBR-EAF100 and NBR-EAF50.

Furthermore, the presence of EAF slag has reduced the minimum torque, M_L, by MDR, where the same result of M_L at 177°C, 0.27 dN m, was obtained for both NBR-EAF100 and NBR-EAF50.

About mechanical properties, the addition of EAF slag has decreased the tensile strength to very low values, especially at 100%, and this condition may be primarily related to the larger particle size of slag compared to carbon black, where the slag has negatively interfered. Nevertheless, the addition of EAF slag didn't change the strain properties such as elongation at break and compression set. Therefore, NBR-REF, NBR-EAF100 and NBR-EAF50 rubber compounds showed quite similar results.

The three rubber compounds were used to produce O-rings (13 x 2 mm) via injection molding to verify the effect of EAF slag on processability. The O-ring gasket type was chosen because it was the simplest geometry to understand the processing behavior of poorly known rubber compounds.

The 5 kg batches rubber compounds were tested by using a horizontal 190 Ton MIR (Figure 68a) with reciprocating screw, L/D ratio of about 16. The mold is equipped with 174 cavities having a single nozzle injection system. (Figure 68b).

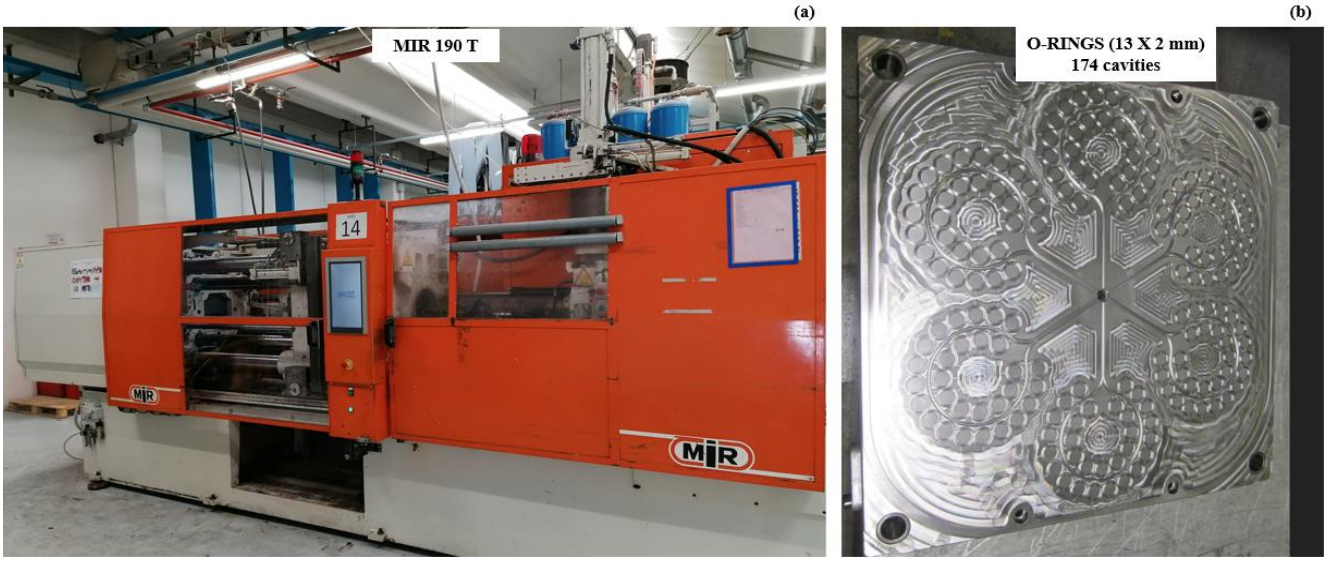

Fig.68. a Horizontal injection molding 190 Ton MIR. **b** Mold of O-rings (13 x 2 mm) with 174 cavities.

The NBR-REF was the first processed rubber compound, then followed by NBR-EAF50 and NBR-EAF100. The process parameters setup was 120 bar of injection pressure, 80% of injection speed, 20 rpm of screw speed rotation, 65°C of barrel temperature, 190°C of both fixed and movable plate temperature and 85 s of curing time. The T_{SH} measurements were performed to measure the shear heating effect during the injection stage [10, 26-27]. Thus, Figure 69, 70 and 71 show the thermal image with average T_{SH} for NBR-REF, NBR-EAF50 and NBR-EAF100, respectively. NBR-REF had an average T_{SH} value of 146°C.

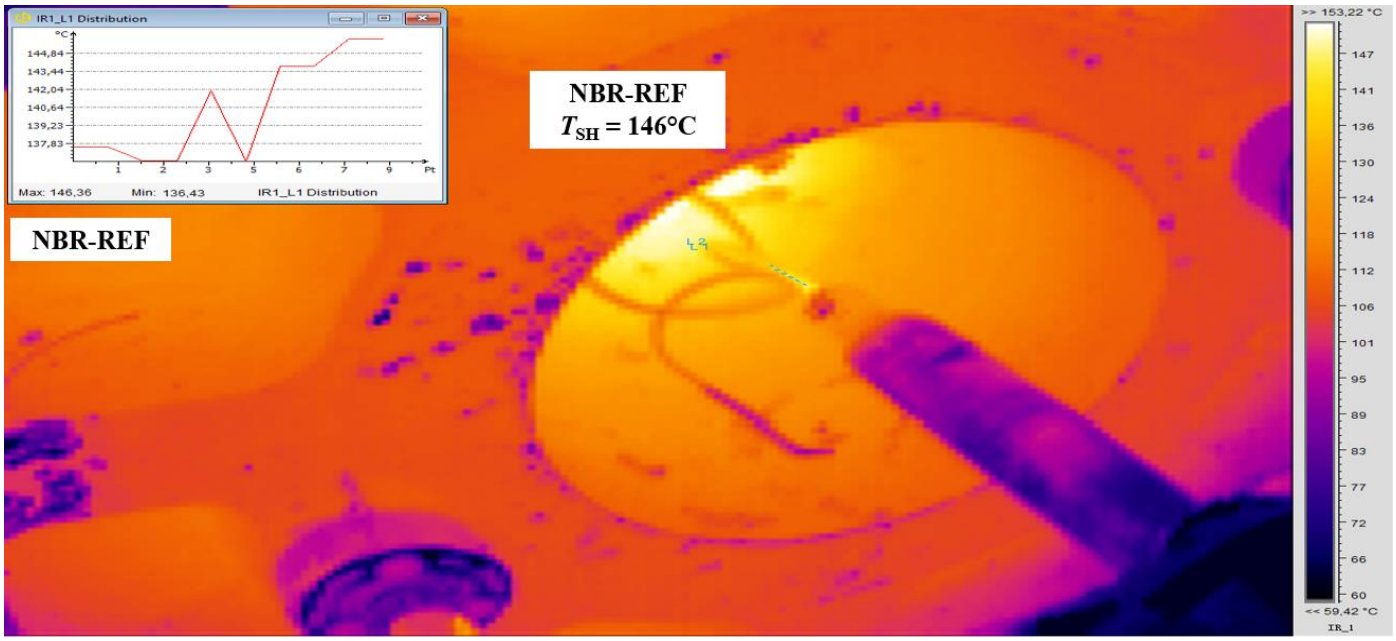

Fig.69. Image of NBR-REF emerging from the reciprocating screw nozzle outlet, T_{SH} = 146°C.

The 5 kg of NBR-REF were processed very quickly without any problem about injection and curing stages, mold release and deburring by hand as well, with 5 s of injection time and 114 s of cycle time of in automatic mode (Figure 72a).

The NBR-EAF50 was the second processed rubber compound, by setting the same process parameter of NBR-REF. In this case the T_{SH} measurements were performed to understand the potential variation of shear heating effect due to the EAF slag addition.

Figure 70 shows the thermal image with average T_{SH} value of 156°C, which is about 10°C higher with respect to NBR-REF. This shear heating temperature increase wasn't attributable to EAF slag addition, but it was reasonably attributable to the injection pressure and injection speed increases, carried out to improve the injection stage. However, by processing the NBR-EAF50 with the same parameters of NBR-REF the injection time was increased up to 15 s (injection system went into alarm). Furthermore, while increasing both injection pressure and injection speed to 125 bar and 90%, respectively, it's processability wasn't improved.

The main processing problem of NBR-EAF50 was the difficulty to fill in the parts (Figure 72b), therefore, it wasn't processable by injection molding.

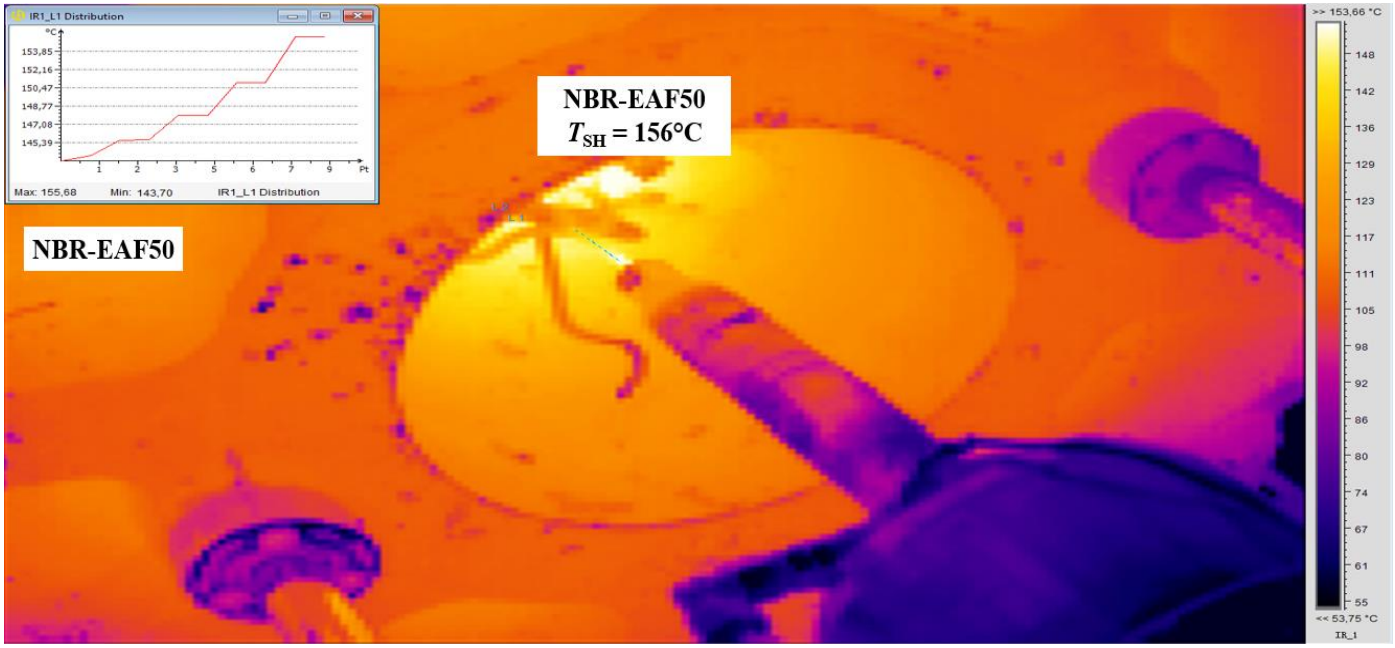

Fig.70. Image of NBR-EAF50 emerging from the reciprocating screw nozzle outlet, T_{SH} = 156°C.

The NBR-EAF100 was the last processed rubber compound, by setting the same process parameter of NBR-REF. Also in this case the T_{SH} measurements were performed to understand the potential variation of shear heating effect due to the EAF slag addition.

Figure 71 shows the thermal image with average T_{SH} value of 146°C, thus very similar to NBR-REF. Therefore, a high percentage of EAF slag didn't affect the temperature of shear heating, T_{SH}. Moreover, even with NBR-EAF100 the difficulty of injection occurred again, confirming the same injection system went into alarm, and in this case an injection time of 30 s was reached.

Furthermore, once again increasing both injection pressure and injection speed to 140 bar and 95%, respectively, it processability wasn't improved on the contrary has worsened (Figure 72c).

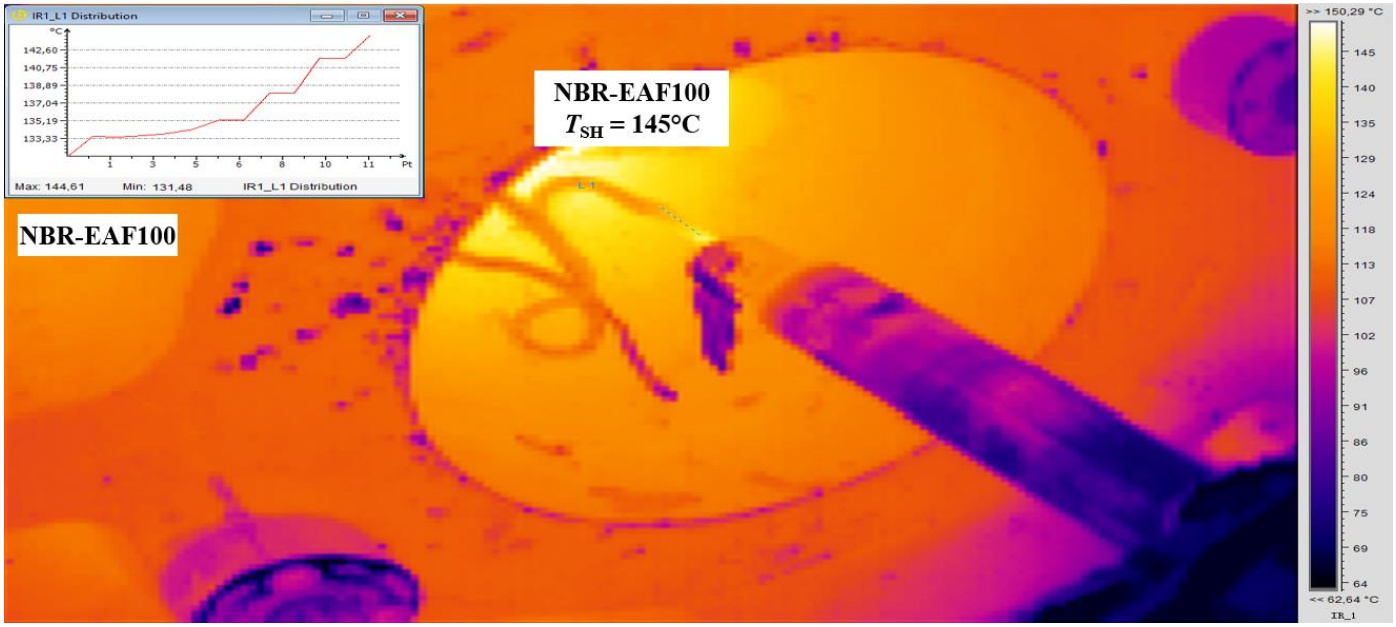

Fig.71. Image of NBR-EAF100 emerging from the reciprocating screw nozzle outlet, T_{SH} = 145°C.

Figure 72 shows the pictures of molded rubber parts before demolding, where NBR-REF (Figure 72a) has demonstrated it processability without any issue, instead NBR-EAF50 (Figure 72b) showed unbalanced filling stage and NBR-EAF100 (Figure 72c) showed uncomplete mold filling, thus were not processable by injection molding.

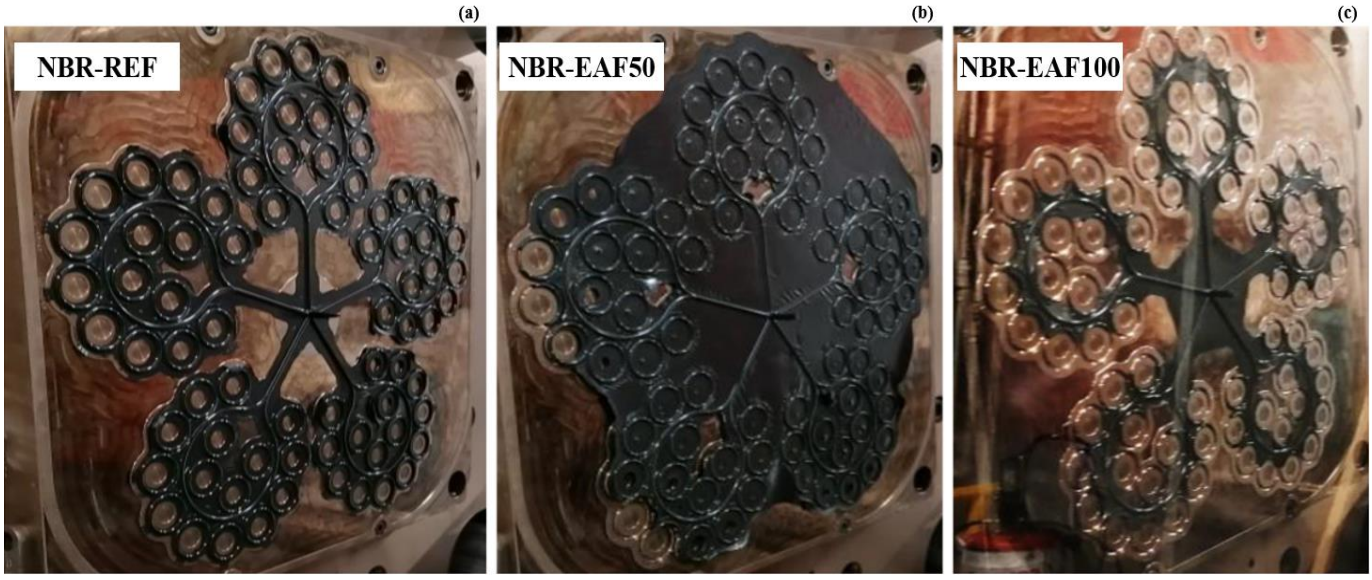

Fig.72. a Molded parts of NBR-REF. **b** Molded parts of NBR-EAF50. **c** Molded parts of NBR-EAF100.

Although the shear heating temperature, T_{SH}, wasn't affected by the addition of EAF slag, the shear heating parameter, η_{SH}, was therefore calculated for each rubber compound according to Equation (10).

Therefore, the shear heating temperature, T_{SH}, wasn't affected by the addition of EAF slag. The shear heating parameter, η_{SH}, was calculated for each rubber compound according to Equation (10).

Table 23 reports the experimental data from processing characterization of the NBR-REF, NBR-EAF50 and NBR-EAF100. About the processing characterization, the data of measured shear heating temperature (T_{SH}) of the rubber by infrared thermal camera and the temperature difference in shear heating (ΔT_{SH}) considering 20°C as initial temperature were reported. Moreover, the shear heating parameter (η_{SH}) at 10 s^{-1} and the corresponding logarithmic values were therefore calculated for NBR-REF, NBR-EAF50 and NBR-EAF100 rubber compounds according to Equation (10).

Table 23. Experimental data from processing characterization of NBR-REF, NBR-EAF100 & NBR-EAF50.

Parameter	NBR-REF	NBR-EAF100	NBR-EAF50
Injection pressure, Pi (bar)	120.0	140.0	125.0
Injection speed, vi (%)	80.0	95.0	90.0
Screw speed rotation (rpm)	20.0	20.0	20.0
Barrel temperature, T_{barrel} (°C)	65.0	65.0	65.0
Shear heating temperature, T_{SH} (°C)	146.0	145.0	156.0
Temperature difference in shear heating, ΔT_{SH} (°C)	126.0	125.0	136.0
Fixed plate temperature (°C)	190.0	190.0	190.0
Movable plate temperature (°C)	190.0	190.0	190.0
Injection time (s)	5.0	30.0	15.0
Curing time (s)	85.0	85.0	85.0
Cycle time (s)	114.0	Not Processable	Not Processable
Shear heating parameter, η_{SH} (Pa s)	4.47×10^5	5.30×10^5	4.88×10^5
Log shear heating parameter, Log η_{SH} (Log Pa s)	5.65	5.72	5.69

The shear heating parameter, η_{SH}, at 10 s^{-1} resulted equal to 5.65 Pa·s for NBR-REF, 5.69 Pa·s for NBR-EAF50, and 5.72 Pa·s for NBR-EAF100. Therefore, the use of EAF slag in NBR rubber compounds has increased η_{SH}. Nevertheless, this η_{SH} increase was not directly related to shear heating temperature (not significantly increased), but it was mainly due to the data of density and specific heat caused by the introduction of EAF slag.

Despite the minimum torque, M_L, by MDR of NBR-EAF50 and NBR-EAF100 was reduced (see Table 22), the processing characterization highlighted some critical issues. NBR-EAF50 shows an unbalanced molding shot, while regarding the NBR-EAF100 it was difficult to completely fill the mold cavities. Therefore, the increase of the parameter of shear heating has confirmed the non-processability of the two NBR-EAF50 and NBR-EAF100 rubber compounds. The advantage of η_{SH} parameter is that it considers both rubber compositional effects (density and specific heat capacity), and the effect of operating conditions, and also in this experiment, it proved to be much more reliable than M_L in providing indication about processability.

7 CONCLUSIONS

This research activity aimed to improve the process control for optimal injection molding of technical rubber parts by introducing a new tool for online monitoring of the shear heating phenomenon.

A very fast process control was proposed by using an infrared thermal camera, and it allowed to take into account the shear heating effect before injection of the rubber into the mold cavities. The online monitoring is based on direct measurement of the surface rubber temperature (shear heating temperature, T_{SH}) by an infrared thermal camera at the nozzle outlet of the injection molding machine extruder (see Figure 31).

This measured temperature led to the calculation of a technological parameter designated shear heating parameter, η_{SH}, which also takes into account physical material properties (density and specific heat capacity) and process conditions (screw L/D ratio).

Therefore, a very fast process control was applied to industrial cases to investigate the processing behavior of several rubber compounds. In particular, industrial production runs based on AEM rubber compounds were investigated, because they are materials highly susceptible to scorching, mold fouling and thermal degradation issues, as well as of large application in the automotive industry.

The first investigation concerned the effects of process parameters setup such as injection pressure (Pi), injection speed (vi), screw speed rotation and screw L/D on the measured T_{SH} for DIA-AEM60-2 rubber compound. The setup level of the four parameters is varied close to the limit of the operativity range, by ensuring the rubber compound processability without relevant cycle time variation. About DIA-AEM60-2, T_{SH} was mainly influenced by the screw L/D ratio, followed by injection pressure and screw speed rotation (especially if set to higher levels), whereas the injection speed is the least effective parameter to reduce T_{SH}.

The second investigation focused on the rubber properties variation due to exceeding the shelf life for the DIA-AEM70-1 rubber compound, processed both within the shelf life (DIA-AEM70-1-OK, 2 weeks after the compounding) and off of it (DIA-AEM70-1-KO, 5 weeks after the compounding). T_{SH} is highly influenced by AEM material shelf life, and increased from 130°C for a stable production run within the material shelf life, to 226°C for an unstable production run out of the material shelf life, with a T_{SH} increase of 96°C. This suggested that the rubber compound properties have a considerable effect on T_{SH}. A further important indicator was the quick mold fouling increase in the DIA-AEM70-1-KO production run, after only 2 days of industrial production. The last condition obviously has negatively affected the productivity of DIA-AEM70-1-KO, thus subjected to extraordinary cleaning.

Besides, even modifying injection pressure, injection speed and screw rotation speed, no reduction in this excessive shear heating was found. Therefore, T_{SH} is already a useful tool to guarantee a very fast online process control, that is, to collect information concerning the risk of scorching and thermal degradation, leading, for example, to the diffusion of compound ingredients (low volatile chemicals), stickiness, mold fouling and also color variation.

Additionally, a technological parameter was developed in this thesis, the shear heating parameter, η_{SH}, which can be calculated from T_{SH} values by Equation (10) and which also takes into account physical material properties (density and specific heat capacity) and process conditions (L/D ratio). This parameter was then correlated with minimum torque M_L results from MDR measurements, in order to provide a tool for online monitoring of the injection molding process. Eight different rubber compounds, based on different base elastomer (AEM, EP(D)M, HNBR and FKM elastomers), having eight industrial production runs with long process stability, without significant deviations of set parameters and with very little scrap were investigated. These additional eight different rubber compounds provided the data to build a robust correlation between the shear heating parameter (η_{SH}), calculated by Equation (10), and minimum torque value (M_L) from MDR measurements for stable production runs, that was the operating roadmap useful to evaluate the processability of other compounds. Therefore, by introducing η_{SH}, of a new production run into the data of η_{SH} vs M_L correlation (roadmap), the processability of the newly introduced production run can be inferred from the coefficient of determination R^2 and p-value.

Therefore, by introducing the data of DIA-AEM70-1-OK production run into the operating roadmap, a good correlation was established between the results of the laboratory characterization, M_L, and the technological parameter, η_{SH}, and described by a proportional trend with R^2 of 0.936 according to a power regression law. Instead for DIA-AEM70-1-KO production run a significant deviation from the proportional trend was observed, with decreased R^2 from 0.936 to 0.797, according to the power regression model. Therefore, monitoring also η_{SH} allowed to get an added value in terms of quantitative and precise indication of the quality of molded part. Furthermore, log η_{SH} values of a production run, combined with M_L values, give indication of the "real output" of the injection molding process by comparison of this data with a well-established roadmap, obtained from stable production runs of different rubber compounds and process conditions.

Moreover, this integrated approach (operating roadmap) based on the laboratory data and process data, has the advantage of being fast and provides information about the stability of the process, while it is running, well before completing the production run. Therefore, the operating roadmap allows to realistically predict the rubber processing behavior, with the purpose to promptly reduce defects and scraps amount.

Furthermore, to show the integrated approach potentiality, it has been successfully used to optimize the injection molding of industrial production of DIA-AEM60-2 rubber compound affected by scorching and thermal degradation issues (production of hardened and cracked parts). Various production runs of DIA-AEM60-2 rubber compound, where stable (DIA-AEM60-2-OK), unstable (DIA-AEM60-2-KO), and also the intermediate production runs (DIA-AEM60-2-INT1 and DIA-AEM60-2-INT2), were investigated. The only one difference between the production runs was the injection pressure: 70 bar, 140 bar, 100 bar and 80 bar, respectively.

The correlation between log η_{SH} and M_L for the eight rubber compounds with long process stability, including the DIA-AEM60-2-OK run, showed a proportional trend, with R^2 of 0.935 according to the power regression

model. During the DIA-AEM60-2-OK run an average rubber surface temperature of 115°C was measured during the daily process control, and no hardened and cracked parts were produced. Thus, this proportional trend represented the operating roadmap to support the process engineer and plant operator in the improvement of the process control by thermal online measurements.

However, including the DIA-AEM60-2-KO run an average rubber surface temperature of 235°C was measured during the daily process control, and some surface cracked parts were obtained after stabilization, deburring and post-curing for 4 hours at 175°C. From laboratory characterization cracked parts clearly showed higher hardness (+30 IRHD M points) than the required standard, higher Tg (+9°C) from DSC, and plasticizer loss from TGA and ATR-FTIR spectroscopy. Therefore, it was reasonable that plasticizer diffusion and evaporation started during the injection stage, caused by excessive shear heating measured at the reciprocating screw nozzle outlet, T_{SH} = 235°C. In this case, the correlation between log η_{SH} and M_L for the seven rubber compounds with long process stability, and the DIA-AEM60-2-KO run, showed a significant deviation from the proportional trend, with decreased R^2 from 0.935 to 0.526, according to the power regression model. Therefore, the coefficient of determination of the operating roadmap, log η_{SH} vs M_L curves, provided a good indication of process stability of DIA-AEM60-2 runs. The proposed integrated approach, obtained for a very heterogeneous sample of rubber compounds and operating conditions, was found to be successful and useful in industrial applications, taking into account that type of defects such as hardened and cracked parts that cannot be accepted in the automotive industry, because "zero defected" parts are required.

The results showed that the shear heating parameter is a very suitable tool because it considers not only the rubber compositional effects based on density and specific heat capacity measurements but also the effect of operating conditions setup. The η_{SH} gives more information than M_L about the thermal history and process safety; thus it can be used in industrial practice to improve the process control by improving the knowledge of rubber behavior and its shear heating effect during the injection stage.

Therefore, this knowledge can help the process engineer, plant operator, and mold designer to:

- provide suitable process parameter setup and mold design to avoid scorch problems and thermal degradation, preventing the production of out of specification rubber parts;
- optimize processes for new materials where information about thermal behavior is lacking because, differently from T_{SH}, log η_{SH} is able to correlate data obtained from different rubber compounds;
- select the injection molding machine, taking into account the rubber compound rheological behavior.

This operating roadmap (Figure 73) thus can support the process engineer and plant operator in the improvement of process control by thermal online measurements, allows defining the suitable process parameters setup, and optimizing the injection molding process for rubbers where knowledge about thermal history is lacking.

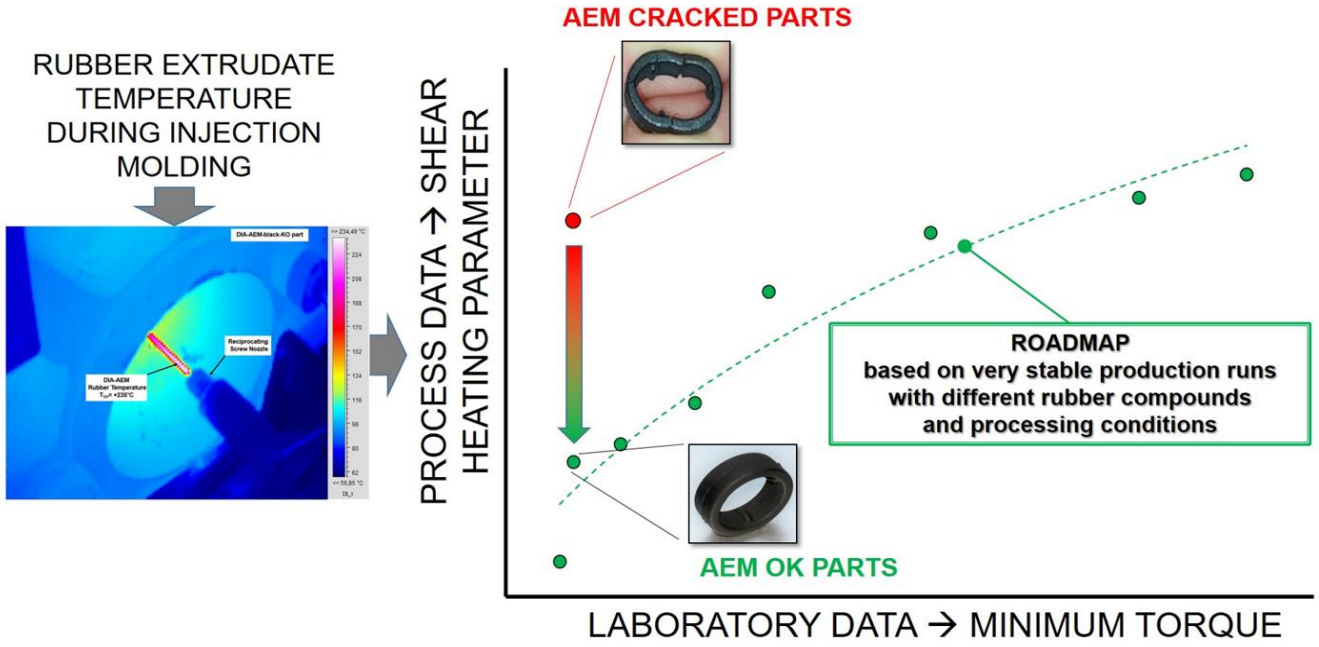

Fig.73. Operating roadmap to support the process engineer in the improvement of process control [27].

Furthermore, η_{SH} and the use of the above-mentioned roadmap could provide information also about new compounds, whose T_{SH} limit for the obtainment of good quality parts is not known a priori, unless process trials are performed.

The integrated approach should be as general as possible, potentially applicable to any rubber compound processable by injection molding. It was therefore validated not only for industrial compounds, but also for two types of innovative compounds, characterized by a high level of sustainability: recycled rubbers coming from devulcanization process, such as FKM on one side, and NBR rubber compounds containing EAF slag, a by-product of steel industry, studied as possible substitute for CB, on the other side.

About recycled FKM rubber compounds, FKM-A and FKM-B containing 10 and 20 wt.% of devulcanized scraps of FKM-REF (called TT-FKM) respectively, were investigated. During the online monitoring a lower shear heating effect was measured on the recycled FKM-A and FKM-B, about 10°C less comparing the FKM-REF. However, the FKM-B showed an higher shear heating effect than FKM-A (5°C more). These data were in agreement with the obtained results of specific heat capacity from DSC and the calculated shear heating parameter according to Equation (10).

Furthermore, both FKM-A and FKM-B rubber compounds exhibited the faster injection time respect to FKM-REF, thanks to the soluble fraction of TT-FKM that acted as a plasticizer. The measure of T_{SH} and the calculation of η_{SH} quantitively confirmed this plasticizer effect. Therefore, the use of TT-FKM has facilitated the injection stage by improving the FKM rubber compounds processability. TT-FKM cannot be considered as a mere filler, it behaves as an active new ingredient able to impart unusual properties and special characteristics and this aspect can play a very important role in HPE compounding.

About NBR rubber compounds containing EAF slag, one NBR filled with carbon black (NBR-REF), and the same NBR were the filler volume of CB was totally (NBR-EAF100) or half substituted by EAF slag (NBR-EAF50), were investigated. Figure 72 shows the pictures of molded rubber parts previous demolding, where NBR-REF (Figure 72a) has demonstrated it processability without any issue, instead NBR-EAF50 (Figure 73b) and NBR-EAF100 (Figure 72c) weren't processable by injection molding. Although the shear heating temperature, T_{SH}, wasn't affected by the addition of EAF slag, the shear heating parameter, instead was increased mainly due to the data of density and specific heat caused by the introduction of EAF slag. Despite the minimum torque, M_L, by MDR of NBR-EAF50 and NBR-EAF100 was reduced, the increase of the parameter of shear heating has confirmed the non-processability of the two NBR-EAF50 and NBR-EAF100 rubber compounds. Therefore, the advantage of η_{SH} parameter with respect to M_L was confirmed again, because it takes into account both rubber compositional effects (density and specific heat capacity), and the effect of operating conditions.

Finally, the research activity is also focused on the possibility to use the shear heating temperature, T_{SH}, in the setup of computer-aided engineering simulations (CAE) useful for mold design and injection molding process optimization. Therefore, a sealing ring typically used in automotive industry (Figure 34) was selected as case study for the 3D finite element process simulation. About the material, an FKM rubber compound black colored with 70 Shore-A hardness was chosen. The shear heating parameter, η_{SH}, was used to derive the viscosity curves for the CAE simulation setup. The shear heating parameter was calculated at increasing values of flow rate parameter v by using a shear heating temperature, T_{SH}, of 110°C, obtained from processing trial.

Two process simulation runs were carried out using the same setup of filling time, curing time, maximum injection pressure, mold temperature, and cycle time, with the exception of the "melt temperature". In the first simulation run the barrel temperature setup (T_{barrel}) of 80°C was input, in the second one the shear heating temperature, T_{SH}, of 110°C: in both cases experimental data coming from the above-mentioned processing trial. The comparison between the two simulations showed no substantial differences in the filling stage, most likely due to the slight sensitivity of viscosity characteristics to temperature, compared to plastics. However, T_{SH} has impacted mostly the simulation run of the curing stage: in particular the average curing conversion was higher and additionally more homogeneous than the result obtained with T_{barrel}, with a lower standard deviation.

Therefore, these results described how the simulation results depend on the input parameters, and has highlighted the importance of using a real value of rubber material's inlet temperature on the simulation outputs. Furthermore, the shear heating parameter can be used as viscosity input of CAE simulation, thus a suitable alternative to the conventional laboratory instruments such as RPA.

In conclusion, this research activity firstly proposed a very fast tool for the online rubber temperature measurement, T_{SH}, secondly it introduced the technological parameter, η_{SH}, thirdly it correlated η_{SH} with another

technological parameter, M_L, with the purpose to improve the injection molding process control, via an integrated approach based on the operating roadmap suitable for industrial practice.

Table 24 summarizes the utilization and the advantage of this integrated approach in some significant production runs processed in *Italian Gasket* plant in the year 2022. Therefore, here below are reported ten of the main production runs with higher turnover and also very expensive rubber compounds. This table shows how this rational approach has considerably reduced the percentage value of the scraps amount, consequently its economic value as well, taking into account that the year 2022 was characterized by relevant increase of both the raw materials and energy cost.

Table 24. Integrated approach used in *Italian Gasket* plant: plant: scraps % 2021 vs scraps % 2022.

Rubber compound	Gasket type	Scraps 2021 (%)	Scraps 2022 (%)
AEM 70 Black (diamine cured)	O-ring	13.0	8.0
AEM 70 Black (diamine cured)	O-ring	15.0	7.0
FKM 80 Black (bisphenol cured)	Frame	25.0	7.0
FKM 70 Green (peroxide cured)	O-ring	30.0	5.0
FKM 60 Green (peroxide cured)	Frame	10.0	6.0
VMQ 30 Red (peroxide cured)	Sealing ring	10.0	7.0
EP(D)M 60 Black (peroxide cured)	Technical item	15.0	8.0
EP(D)M 60 Black (sulfur cured)	Grommet	5.0	3.0
NBR 60 Black (sulfur cured)	O-ring	14.0	3.0
HNBR 70 Black (peroxide cured)	Frame	10.0	3.0

Looking to the future, the integrated approach showed in Figure 1 could be turned into a predictive algorithm of Artificial Intelligence (AI). The data from T_{SH} measurements and from laboratory characterization could be constantly collected during production and implemented together with a specific database directly in the injection molding machine. The first objective will be to increase the interconnection between the laboratory and the injection molding machine, by providing tools able to combine the data coming from the laboratory characterization and process parameters continuously monitored by suitable probes. After a sufficiently large database is built, an automated control based on AI would be even faster and more efficient than the practice implemented so far, dependent on the data collection and judgement of the operator. Thanks to the adaptive learning abilities of AI, with time the process control would become even more efficient to detect potentially risky variations of the process at the very first symptoms of deviation.

8 REFERENCES

[1] Fazli, A.; Rodrigue, D. Waste Rubber Recycling: A review on the evolution and properties of thermo plastic Elastomers, *Materials*, 13, 782, 2020.
https://doi.org/10.3390/ma13030782

[2] Monge I.V., Serrano N. A., Izquierdo S., Vallejo I. C., Zambrano V., Grijota L.A.G.: Reduced order models for uncertainty management and zero-defect control in seal manufacturing. *17th International Conference on Industrial Informatics*, 22-25 July, Helsinki, Finland (2019).
10.1109/INDIN41052.2019.8972097

[3] Cheremisinoff, N. P: Elastomer technology handbook. CRC Press (1993).
https://doi.org/10.1201/9780138758851

[4] Godec D., Rujnic Havstad M., Šercer M.: Processing parameters influencing energy efficient injection moulding of plastics and rubbers, *Polimeri*, 33, 112–117 (2012).

[5] Abraham E., Cherian B. M., A1 E. P., Pothen L. A., Thomas S.: Recent advances in the recycling of rubber waste. T Transworld Research Network 37/661 (2), Fort P.O. Trivandrum-695 023 Kerala, India (2011).

[6] Baldassarre, B., Maury, T., Mathieux, F., Garbarino, E., Antonopoulos, I., Sala, S.: Drivers and barriers to the circular economy transition: the case of recycled plastics in the automotive sector in the european union, *Procedia CIRP*, 105, 37–42 (2022).
https://doi.org/10.1016/j.procir.2022.02.007

[7] Formela, K.; Kurańska, M.; Barczewski M.: Recent advances in development of waste-based polymer materials: a review, *Polymers*, 14, 1050 (2022).
https://doi.org/10.3390/polym14051050

[8] Skrobaka A,. Senkerik V,. Janostik V,: The effect of injection molding on physical properties of EPDM rubber. *MATEC Web of Conferences* 210, 02039 (2018).
https://doi.org/10.1051/matecconf/201821002039

[9] Ramini M.: Process control philosophy during injection molding of rubber compounds, *Sealing material development for critical industrial applications forum*, Berlin 16 – 17 May 2019.

[10] Ramini M., Agnelli S.: Shear heating parameter of rubber compounds useful for process control in injection molding machine, *Rubber Chemistry & Technology*, 93, 729–737 (2020).
https://doi.org/10.5254/rct.20.79954

[11] Restrepo-Zapata N. C., Eagleburger B., Saari T., Osswald T. A., Hernández-Ortiz J. P.: Chemorheo logical time-temperature-transformation-viscosity diagram: Foamed EPDM rubber compound, *Journal of Applied Polymer Science*, 133 (38), (2016).
DOI: 10.1002/app.43966

[12] Stanek M., Manas D., Manas M., Ovsik M., Senkerik V., Skrobak A.: Injection molding of rubber compound influenced by injection mold surface roughness, *Advanced Materials Research*, 1025–1026, 283–287 (2014).
https://doi.org/10.4028/www.scientific.net/AMR.1025-1026. 283

[13] Proske M., Bhogesra H.: Evaluating the root causes of rubber molding defects through virtual molding, *Rubber World*, 255, 20–26 (2016).

[14] Anderson A., Jones M.: Using low viscosity HNBR to increase productivity in high shear molding methods, *Rubber World* 245, 25–32 (2011).

[15] Long H.: Basic compounding and processing of rubber. Rubber Division of the ACS, Akron (1985).

[16] Nishizawa H.: Heat controls and rubber flow behaviour in screw of extruder and injection machine and the problems occurring in these processes, *International Polymer Science & Technology*, 43, 41–50 (2016).
https://doi.org/10.1177/0307174X1604300409

[17] Dick J. S.: Compound processing characteristics and testing, Rubber Technology, 2, 17–45(200).
https://doi.org/10.3139/9783446439733.002

[18] Stritzke B.: Custom molding of thermoset elastomers a comprehensive approach to materials, mold design, and processing. Hanser, Munich (2009).

[19] Cox H. W., Macosko C. W.: Viscous dissipation in die flows, *AIChE Journal*, 20, 785–795 (1974).
https://doi.org/10.1002/aic.690200421

[20] Winter H. H.: Temperature fields in extruder dies with circular, annular, or slit cross- section. *Polymer Engineering & Science*, 15, 84–89 (1975).
https://doi.org/10.1002/pen.760150206

[21] Tadmor Z., Gogos C. G.: Principles of polymer engineering. Wiley, Hoboken (2006).

[22] Ramini M., Viola G. T., Paganin L., Battisti M.: Saving post-cure of FPM processed by injection molding, *Europe rubber industry Forum - All about rubber compounding*, Vienna 7–9 May 2019.

[23] Paganin L., Viola G. T., Battisti M,. Ramini M.: Optimization of peroxide curable FPM compound in injection molding, *Europe rubber industry Forum - All about rubber compounding*, Vienna 7–9 May 2019.

[24] Ramini M., Viola G. T., Paganin L., Battisti M.: Achieving savings in the post-curing process of fluoroelastomer compounds prepared by injection molding, *Rubber World*, 261, 46–51 (2019).

[25] Traintinger M., Kerschbaumer C., Lechner B., Friesenbichler W., Lucyshyn T.: Temperature profile in rubber injection molding: Application of a recently developed testing method to improve the Process simulation and calculation of curing kinetics, *Polymers*, 13, 380 (2021). https://doi.org/10.3390/polym13030380

[26] Ramini M., Agnelli S.: Process control in injection molding machine by using shear heating parameter of rubber compounds, *All about rubber compounding*, May 6 2021, (virtual event), knowhow webinars forum by Technobiz.

[27] Ramini M., Agnelli S., Ramorino G.: Applications of shear heating parameter for injection molding process optimization of AEM rubber compounds, *Express Polym Lett* 16(4):354–367 (2022). https://doi.org/10.3144/expresspolymlett.2022.27

[28] Ramini, M., Agnelli, S.: Monitoring of shear heating effects during injection molding of rubber to improve the process control, *Polym. Bull* (2022). https://doi.org/10.1007/s00289-022-04376-y

[29] Brown R.: Physical test methods for elastomers. Springer, New York (2018).

[30] Viola G.T., Bacchelli F., Fabbri A.: Encyclopaedia of hydrocarbons, Vol. 2, refining and petrochem icals, elastomers, 791–835, Istituto della Enciclopedia Italiana, G. Treccani (2006).

[31] Ciesielski A.: An Introduction to Rubber Technology. iSmithers Rapra Publi shing (1999).

[32] Nagdi K.: Manuale della gomma. Tecniche Nuove (1987).

[33] Shrivastava A.: Introduction to plastics engineering, Plastics Design Library, 17–48 (2018). https://doi.org/10.1016/B978-0-323-39500-7.00002-2

[34] ASTM book of standards: Rubber, natural and synthetic, general test methods, carbon black (2007).

[35] Furniss B. S.: Vogel's textbook of practical organic chemistry. Prentice Hall (1989).

[36] Mark J., Erman B., Eirich F. R.: Science and technology of rubber. 3rd Edition, Elsevier (1995).

[37] Immergut E. H., Mark H.F.: Principles of Plasticization, *American Chemical Society* (1965). DOI: 10.1021/ba-1965-0048.ch001

[38] Hertz D. L.: Theory & practice of vulcanization. Seals Eastern Inc., Red Bank, NJ 07701.

[39] Vergnaud J. M.: Rubber curing and properties. Taylor & Francis Group (2009).

[40] Noordermeer J. W. M.: Encyclopedia of Polymer Science and Technology. Vol. 6, 179–195. John Wiley & Sons (2002).

[41] Orza R. A., Magusin P. C. M. M., Litvinov V. M., van Duin M., and Michels M. A. J.: Solid-state ^{1}H NMR study on chemical cross-links, chain entanglements, and network heterogeneity in peroxide-cured EPDM rubbers, *Macromolecules*, 40 (25), 8999-9008 (2007). https://doi.org/10.1021/ma0710151

[42] Bukhina M.F., Morozov Y.L., van de Ven P.M., Noordermeer J.W.M.: Mold fouling of EPDM rubber compounds, *Kautschuk und Gummi Kunststoffe*, 56, 4, 172–183 (2003).

[43] McBride E.: Press cure and post cure options for AEM terpolymers. in *'17th Fall Technical Meeting of the Rubber Division*, American Chemical Society 2008, Louisville, USA' 86 (2008).

[44] McBride E., Christopher S. G.,: HT-AEM solution for high performance turbocharger hoses, *Rubber World*, May 2012.

[45] McBride E.: Processing of AEM compounds: scorch issues. in '*19th Fall Technical Meeting of the Rubber Division*, American Chemical Society 2018, Louisville, USA' 1289 (2018).

[45] McBride E.: Processing of AEM compounds: Scorch issues, *Rubber World*, 256, 32–38 (2019).

[47] Öztürk S., Cömez E. E., Hoşgün H. L.: The rheological, mechanical and aging properties of AEM/EPDM rubber blends, *Journal of Rubber Research*, 24, 61–67 (2021). https://doi.org/10.1007/s42464-020-00073-5

[48] Moore A. L.: Fluoroelastomers handbook. Delaware (2011).

[49] Arnold R. G., Barney A. L., Thompson D. C.: Fluoroelastomers, *Rubber Chemistry & Technology*, 46:625, (1973).

[50] Schmiegel W.W.: *Kautschuk Gummi Kunstoffe*, 31:127, (1978).

[51] Schmiegel W.W.: Crosslinking of elastomeric vinylidene fluoride copolymers with nucleophiles, Die Angewandte *Makromolekulare Chemie*, 76/77, 39-65, (1979). https://doi.org/10.1002/apmc.1979.050760103

[52] Lückmann M., Steinhoff W.: Crosslinking of fluoroelastomers and the influence on final properties, (2014).

[53] Morton M.: Rubber technology. Springer Science & Business Media, (2012).

[54] Brydson J.A.: Speciality rubbers. Rapra Technology (1994).

[55] Klingender R. C.: Handbook of Specialty Elastomers. Taylor & Francis Group (2008). https://doi.org/10.1201/9781420017670

[56] Carr, J. and Ginn, A., Ethylene/acrylic elastomers - new candidates for sealing applications. SAE Technical Paper 780403 (1978). https://doi.org/10.4271/780403

[57] Carr J., Ginn A.: Ethylene/acrylic elastomers (EAE): sealing application candidates for the automo tive industry, *Automot. Eng*., 87, 19790101, 66, (1979).

[58] Bonnie L. S., Boyd K., Czomba P., Freeman B., McBride E., Uminska A., Domi.: A new curative for ethylene acrylic elastomers, *Rubber World*, 236, 14–18 (2007).

[59] Kammerer K.: High viscosity AEM rubbers for increased demands on seals in the automotive industry. *International Polymer Science &Technology*, 40, 1–8 (2013).

[60] Smith P.M.: Diamine cured HNBR for improved long term compression set on thin sectioned articles, *Rubber World*, 264, 31–40 (2021).

[61] Fasching M., Friesenbichler W., Berger G. R.: Change of processing behavior of rubbers in injection molding caused by material storage. *AIP Conf Proc.*, (2015). https://doi.org/10.1063/1.4965537

[62] Vamac® Influence of Mixing, Ingredients and Storage Conditions on Compound Viscosity, ®Trade mark of E.I. duPont de Nemours & Co.

[63] Lindsay J. A.: Rubber injection moulding: A practical guide. iSmithers Rapra Publishing (2000).

[64] Sommer J., Troubleshooting rubber problems. Carl Hanser Verlag, Munich (2013).

[65] Arrillaga A., Zaldua A. M., Atxurra R. M., Farid A. S.: Die pressure losses during injection molding of rubber mixes, *Rubber Chemistry & Technology*, 82, 62–93 (2009). https://doi.org/10.5254/1.3557007

[66] Sezna J. A., DiMauro P. J.: Processability testing of injection molding rubber compounds, *Rubber Chemistry & Technology* 57, 826–842 (1984). https://doi.org/10.5254/1.3536037

[67] Beaumont J. P., Young J. H., Jaworski M. J.: Mold filling imbalances in geometrically balanced runner, *Journal of Reinforced Plastics & Composites*, 18, 572–590 (1999). https://doi.org/10.1177/073168449901800609

[68] Costa, A. and Macedonio, G.: Viscous heating in fluids with temperature-dependent viscosity: imply cations for magma flows, *Nonlin. Processes Geophys.,* 10, 545–555 (2003). https://doi.org/10.5194/npg-10-545-2003

[69] Graf H-J., Hellberg G., Lauhus W. P., Werner H., Prozessnahe Pruefung der Verarbeitbarkeit von Elastomermischungen; Einsatz einer zur Laboreinheit modifizierten Standardspritzgiess Maschine vertikaler Bauweise, *Kunststoffe* 79, 5(1989).

[70] Röthemeyer F., Sommer F.: Kautschuk Technologie. Hanser 6.3, ISBN: 978-3-446-43776-0, (2013).

[71] Pahl, M. H.: Rheologie der Rohrströmung, Praktische Rheologie der Kunststoffe, VDI Verlag, Düsseldorf (1978).

[72] Graf H-J., Issel H. M., Kühnberger A.: Einsatz, Leistngsspektrum und Wirkmechanismus von Verarbeitungswirkstoffen in Katuschukmischungen, *KGK* (1996).

[73] Nakashima K., Fukuta H., Mineki M.: Anisotropic shrinkage of injection-molded rubber, *Journal of Applied Polymer Science*, 17, 769–778 (1973). https://doi.org/10.1002/app.1973.070170309

[74] Byam J. D., Colbert G. P: An integrated approach to efficient polymer processing. paper n.317, pre sensed at the conference on practical rheology in polymer processing, Loughborough University, U.K. (1980).

[75] Leblanc J. L., Polet R., Andrietti S., Vincent M. and Agassant J-F.: Kgk, *Kautsch. Gummi Kunstst*. 44, 690 (1991).

[76] Karam S.: Modélisation de l'injection des élastomères chargés: approche expérimentel et théorique. Ph.D Thesis, L'école Nationale Supérieure des Mines de Paris (1995).

[77] Hoster B., Jaunich M., Stark W.: Monitoring of the vulcanisation process by ultrasound during inject tion moulding, *e-Journal of Nondestructive Testing* (NDT) ISSN 1435-4934 (2009).

[78] Hutterer T., Berger G. R. , Praher B., Friesenbichler W.: Determination of the temperature of an in dustrial rubber compound after dosing, A new ultrasound based method, Poster *DKT Conference* (2018).

[79] Ramorino G., Girardi M., Agnelli S., Franceschini A., Baldi F., Riccò T.: Injection molding of engi neering rubber components: a comparison between experimental results and numerical simulation. *Int J Mater Form*, 551–554 (2010).
https://doi.org/10.1007/s12289-010-0829-6

[80] Javadi M., Moghiman M., Erfanian M. R., Hosseini N.: Numerical investigation of curing process in reaction injection molding of rubber for quality improvements, *Key Engineering Materials*, 462–463, 1206–1211, (2011).
doi:10.4028/www.scientific.net/KEM.462-463.1206

[81] Stanek M., Manas D., Manas M, Javorik J.: Simulation of injection molding process, Conference: Proceedings of the 13th WSEAS international conference on Automatic control, modelling & simula tion, May 2011.

[82] Kyas K., Cerny J., Stanek M., Manas M., Manas D., Senkerik V., Skrobak A.: Measuring of temper ature and pressure in injection mold, *International Journal of Mathematics & Computers in Simula tion*, 6, 600–607 (2012).

[83] Khang, T. H., Ariff Z. M.: Mold filling simulation dependence on material data input for injection molding process of natural rubber compound, *International Polymer Processing*, 29, 3, 325–331 (2014).
https://doi.org/10.3139/217.2934

[84] Zhang N., Gilchrist M. D.: Characterization of thermorheological behavior of polymer melts during the micro injection moulding process. *Polymer Testing Journal*, 31, 748–758 (2012). https://doi.org/10.1016/j.polymertesting.2012.04.012

[85] Fasching M., Berger G., Friesenbichler W., Filz P., Helbich B.: Robust process control for rubber injection moulding with use of systematic simulations and improved material data, 42, 1–6 (2015).
https://doi.org/10.1177/0307174X1504200301

[86] Friesenbichler, W., Neunhäuserer, A. & Duretek, I.: Rheometry of polymer melts using processing machines, *Korea-Aust. Rheol. J*. 28, 167–174 (2016).
https://doi.org/10.1007/s13367-016-0016-5

[87] Mitsoulis E.; Battisti M,; Neunhäuserer A.; Perko L.; Friesenbichler W.; Ansari M.; Hatzikiriakos S.G.: Flow behaviour of rubber in capillary and injection moulding dies, *Macromolecular Engineer ing*, 46, 110–118 (2017).
http://dx.doi.org/10.1080/14658011.2017.1298207

[88] Friesenbichler W.: Viscoelasticity and processing of rubber in injection molding with cold runner, *Europe rubber industry Forum - All about rubber compounding*, Vienna 7– 9 May 2019.

[89] Rochman A., Zahra K.: Development and performance analysis of static mixing nozzle for injection molding of thermoset elastomers, *Polymer Engineering & Science*, 58, 521–527 (2018). https://doi.org/10.1002/pen.24763

[90] Stieger S.: Flow visualization of rubber compounds in molding, *Europe rubber industry Forum - All about rubber compounding*, 7–9 May 2019, Vienna.

[91] Farahani S., Brown N., Loftis J., Krick C., Pichl F., Vaculik R., Pilla S.: Evaluation of in-mold sen sors and machine data towards enhancing product quality and process monitoring via industry 4.0, *International Journal of Advanced Manufacturing Technology*, 105, 1371–1389 (2019). https://doi.org/10.1007/s00170-019-04323-8

[92] Chen J-Y., Tseng C-C., Huang M-S.: Quality indexes design for online monitoring polymer injection molding, *Advances in Polymer Technology*, 3720127 (2019). https://doi.org/10.1155/2019/3720127

[93] Ramorino G., Agnelli S., Guindani M.: Analysis of reactive injection compression molding by numerical simulations and experiments, *Advances in Polymer Technology*, (2020). https://doi.org/10.1155/2020/1421287

[94] Traintinger M., Kerschbaumer C., Lechner B., Friesenbichler W., Lucyshyn T.: Temperature profile in rubber injection molding: application of a recently developed testing method to improve the process simulation and calculation of curing kinetics, *Polymers* 13:380 (2021). https://doi.org/10.3390/polym13030380

[95] Traintinger M., Kerschbaumer R.C., Lechner B., Friesenbichler W.: Cycle time reduction in rubber injection molding – a numerical approach, *DKG Elastomer Symposium*, 28 June – 01 July 2021. DOI: 10.13140/RG.2.2.17306.36802

[96] Agnelli S., Ramini M., Ramorino G.: Injection molding process of rubber components: improving the process design with the shear heating parameter, *15th International Conference on Advance Compu tation Engineering*, Florence 3–7 July 2022.

[97] Saito T., Satoh I., Kurosaki Y.,: A new concept of active temperature control for an injection molding process using infrared radiation heating, *Polymer Engineering & Science*, 42, 2418–2429, (2002).

[98] Vera-Sorroche J., Kelly A. L., Brown E. C., Coates P. D.: Infrared melt temperature measurement of single screw extrusion, *Polymer Engineering & Science*, 55, 1059–1066 (2015). https://doi.org/10.1002/pen.23976

[99] Straka K., Praher B., Hettrich-Keller M., Steinbichler G.: To the measurement and influences of pro cess parameters variations on the axial melt temperature profile in the screw chamber of an injection molding machine, *SPE ANTEC 2017*, Anaheim, USA, 1645–1651 (2017).

[100] Ageyeva T., Horváth S., Kovács J. G.: In-mold sensors for injection molding: on the way to industry 4.0, *Sensors*, 19, 3551 (2019).
https://doi.org/10.3390/s19163551

[101] Silva A., Silva F. J. G.,.Campilho R. D.S.G., Nevesa P. M.P.F.: A new approach to temperature control in the extrusion process of composite tire products, *Journal of Manufacturing Processes*, 65, 80–96 (2021).
DOI :10.1016/j.jmapro.2021.03.022

[102] Noordermeer J. W. M., Dierkes W., Blume A., van Hoek H., Reuvekamp L., Dijkhuis K., Saiwari S.: Cradle-to-cradle devulcanization options for various elastomer types, *Rubber World*, 262, 20–28 (2020).

[103] Beckman J. A., Crane G., Kay E. I., Laman J. R.: Scrap tire disposal.
Rubber Chemistry & Technology, 47, 597–624 (1974).

[104] Myhre M., MacKillop D.A.: Rubber recycling, *Rubber Chemistry & Technology*, 75, 429–474 (2002).

[105] Myhre M., Saiwari S., Dierkes W.K., Noordermeer J.W.M.: Rubber recycling: chemistry, pro cessing, and applications, *Rubber Chemistry & Technology*, 85, 408–449 (2012).

[106] De S. K, Isayev A.I, Khait K.: Rubber recycling. Taylor & Francis Group (2005).
https://doi.org/10.1201/9780203499337

[107] Dijkhuis K. A. J.: Recycling of vulcanized EPDM-rubber : mechanistic studies into the development of a continuous process using amines as devulcanization aids. PhD Thesis, Research UT, University of Twente, Print ISBNs 978-90-365-2643-2, Published, 17 April 2008.

[108] Paganin L., Viola G. T., Ramini M., Battisti M., Agnelli S.: From fluoroelastomers scraps to high performing gaskets: devulcanization, compounding and moulding, *DKG Elastomer Symposium*, online conference, 28 June – 01 July 2021.

[109] D. B. de Sousa, F., Devulcanization of elastomers and applications. Nevin Cankaya (2017).
DOI: 10.5772/intechopen.68585

[110] Markl, E.; Lackner, M. Devulcanization technologies for recycling of tire-derived rubber: a review, *Materials*, 13, 1246 (2020).
https://doi.org/10.3390/ma13051246

[111] Asaro, L., Gratton, M., Seghar, S., Ait Hocine, N.: Recycling of rubber wastes by devulcanization, *Resources, Conservation & Recycling* 133, 250–262 (2018).
https://doi.org/10.1016/j.resconrec.2018.02.016

[112] D. B. de Sousa, F.; Zanchet, A.; H. Scuracchio, C.: From devulcanization to revulcanization: challenges in getting recycled tire rubber for technical applications, *ACS Sustainable Chem. Eng*., 7 (9), 8755–8765 (2019). https://doi.org/10.1021/acssuschemeng.9b00655

[113] Cervellati A, Viola G.T.: Process for devulcanizing vulcanized fluoroelastomers, fluoroelastomers thereof and their use, *WO2013132523A8 WIPO (PCT)*. Application filed by Dott. Viola & Partners Chemical Research S.R.L., 2013-02-28.

[114] Schuster J., Johannes L., Shaik Y. P., Yadav V. R.: Recycling of fluorocarbon elastomers – a review, *Advanced Industrial & Engineering Polymer Research* (2022). https://doi.org/10.1016/j.aiepr.2022.08.002

[115] Peterson C., Chandrasekaran S. R., Sharma B. K.: Birchwood biochar as partial carbon black replacement in styrene-butadiene rubber composites, *J. Elastomers Plast*., 48, 4, 305–316 (2016). doi: 10.1177/0095244315576241.

[116] Fan Y., Fowler G. D., Zhao M.: The past, present and future of carbon black as a rubber reinforcing filler – a review, *Journal of Cleaner Production*, 247 (2020). doi: 10.1016/j.jclepro.2019.119115.

[117] Athanassiades E.: Waste tyre pyrolysis: sustainable recovery and reuse of a valuable resource. PQDT - UK Irel (2013).

[118] Gobetti A., Cornacchia G., Ramorino G.: Innovative reuse of electric arc furnace slag as filler for different polymer matrixes, *Minerals*, 11(8), 832 (2021). https://doi.org/10.3390/min11080832

[119] Gobetti A., Cornacchia G., Ramorino G.: Reuse of electric arc furnace slag as filler for nitrile butadiene rubber, *JOM* 74, 1329–1339 (2022). https://doi.org/10.1007/s11837-021-05135-6

[120] Macosko, C:. W. Rheology principles, measurements, and applications. Wiley-VCH (1996).

[121] Dannenberg, E. M.: Bound rubber and carbon black reinforcement, *Rubber Chemistry & Technology*, 59 (3), 512–524 (1986). https://doi.org/10.5254/1.3538213

[122] ASTM Standards, E1269-11: *Standard test method for determining specific heat capacity by Differential Scanning Calorimetry*. (2018).

[123] ASTM Standards, D3418-21: *Standard test method for transition temperatures and enthalpies of fusion and crystallization of polymers by Differential Scanning Calorimetry*. (2021).

[124] Forrest M. J.: Rubber analysis - polymers, compounds and products. Smithers Rapra Technology, (2001).

[125] Smith B. C.: Infrared spectral interpretation, a systematic approach, CRC Press (1998). https://doi.org/10.1201/9780203750841

[126] Coates J.: Interpretation of infrared spectra, a practical approach. Encyclopedia of Analytical Chemistry R.A. Meyers (Ed.), John Wiley & Sons Ltd (2000). https://doi.org/10.1002/9780470027318.a5606

[127] Uno T., Machida K.: Infrared spectra of acyclic imides. II. the characteristic absorption bands of saturated acyclic imides in the crystalline state, *Bulletin of the Chemical Society of Japan* (1961). https://doi.org/10.1246/bcsj.35.1226

[128] Gaisford S.; Kett, V.; Haines P.: Principles of thermal analysis and calorimetry. Royal Society of Chemistry, Cambridge (2016).

[129] Plasticizers for Vamac®Trademark of E.I. duPont de Nemours and Co 2013.

[130] DuPont™ Vamac® Injection Moulding, Technical Bulletin, ®Trademark of E.I. duPont de Nemours & Co.

[131] Payne A. R.: The dynamic properties of carbon black-loaded natural rubber vulcanizates. part I", *J.Appl. Polym. Sci*. 6 (19): 57–63 (1962). doi:10.1002/app.1962.070061906.

[132] Medalia A. I.: Effect of carbon black on dynamic properties of rubber vulcanizates, *Rubber Chemistry &Technology*. 51: 437–523 (1978). doi:10.5254/1.3535748.

[133] Fletcher W. P., Gent A.: Non-linearity in the dynamic properties of vulcanised rubber compounds, *Trans. Inst. Rubber Ind*. 29: 266–280 (1953). doi:10.5254/1.3543472.

[134] Wang, M. J.: The role of filler networking in dynamic properties of filled rubber, *Rubber Chemistry & Technology*. 72 (2): 430–448 (1999). doi:10.5254/1.3538812.

[135] ISO Standards, 48-2:2018: *Rubber, vulcanized or thermoplastic — determination of hardness — part 2: Hardness between 10 IRHD and 100 IRHD*. (2018).

[136] VW Standards, PV 3330: *Elastomer round seals compression set (permanent deformation)*.

[137] ISO Standards, ISO 815-1:2019: *Rubber, vulcanized or thermoplastic — determination of compres sion set — part 1: At ambient or elevated temperatures*. (2019).

[138] DuPont™ Vamac® Influence of mixing, ingredients and storage conditions on compound viscosity of E.I. duPont de Nemours& Co.

[139] ISO Standards, ISO 2230:2002 *Rubber products — Guidelines for storage*. (2002).

[140] DIN Standards, DIN 53504, *Testing of rubber — determination of tensile strength at break, tensile stress at yield, elongation at break and stress values in a tensile test*. (2017).

9 APPENDIXES

The appendix reports the original papers published on refereed international journals covering the following aspects of the PhD thesis:

Publication I: presentation of the shear heating parameter useful for process control in injection molding process [10].

Publication II: applications of shear heating parameter for injection molding process optimization of AEM rubber compounds [27].

Publication III: influence of process parameters on shear heating effects during injection molding of rubber [28].

- Frontiers -

SHEAR HEATING PARAMETER OF RUBBER COMPOUNDS USEFUL FOR PROCESS CONTROL IN INJECTION MOLDING MACHINE

MATTIA RAMINI,[1,2,*] SILVIA AGNELLI[2]

[1]ITALIAN GASKET S.P.A., VIA TENGATTINI N.9, 25030 PARATICO (BS), ITALY
[2]UNIVERSITÀ DEGLI STUDI DI BRESCIA, DEPARTMENT OF MECHANICAL AND INDUSTRIAL ENGINEERING, VIA BRANZE 38, 25123 BRESCIA (BS), ITALY

RUBBER CHEMISTRY AND TECHNOLOGY, Vol. 93, No. 4, pp. 729–737 (2020)

ABSTRACT

Control of the injection molding process of rubber is made complex by the influence of many parameters. Shear heating, heat generation due to viscous dissipation, is a phenomenon largely exploited in rubber to lower compound viscosity, particularly in the extrusion phase, but it is impossible to predict it from laboratory tests. With the aim of providing useful tools for process control, a parameter for on-line monitoring of shear heating phenomenon is proposed. This parameter is based on direct measurement of rubber surface temperature by infrared thermal camera at the nozzle outlet of the injection molding machine extruder. The measured rubber temperature is a process indicator to give the thermal history of the rubber injection and process safety. Measured temperature increase is then converted into a parameter having dimensions of viscosity, the shear heating parameter, η_{SH}. Four different rubber compounds are investigated. The η_{SH} results are compared to minimum torque (*ML*) from routine rheometric laboratory measurement. The calculated η_{SH} values increase with increasing *ML* values. The *ML* value is a rough indication of the rubber compound viscosity, where its relevant variations affect the rubber processability. Meanwhile η_{SH} is more sensitive to small processability variations and more accurate because it takes into account the thermal history during the injection stage. The found relationship provides deeper insights into the behavior of rubber, compared to laboratory tests, and how it can be used in the industrial practice to improve the process control by monitoring the shear heating effect during the injection stage. [doi:10.5254/rct.20.79954]

INTRODUCTION

Rubber processing by extrusion or injection molding is a complex process, influenced by many parameters, such as temperature, pressure, and shear rate.[1,2] The control of this process is crucial to obtaining high quality rubber parts. In industrial practice, the typical control parameters for rheological behavior like vulcanization curve are obtained from laboratory tests carried out with a moving die rheometer (MDR). However, these technological parameters are not accurate in describing the physics occurring in process machines. There is a need to develop tests which realistically predict the process behavior.[3] Establishing correlations between process parameters and the rheological behavior provides a more accurate and reliable approach to process optimization.

One of the most important control parameters is temperature. A traditional injection molding machine relies on both controlled heating system and internal shear heat generation to provide the necessary heat to bring the polymer up to the necessary temperature in a plasticizing extruder.[4] Temperature increase during the injection stage reduces rubber compound viscosity. Shear heating, that is, heat generation due to viscous dissipation resulting in significant temperature rises,[1,4–7] is largely present in industrial processing of polymers and particularly of rubbers and makes it complicated to control the temperature and therefore the viscosity. Optimal temperature values must ensure a balance between not excessive viscosity (reduced injection time), scorch safety (avoiding curing reaction before complete mold filling), and thermal degradation (plasticizer and processing aids loss). Therefore excessively high rubber temperature can cause the underfilling of mold cavities due to scorching, and in the worst case it can damage rubber parts due to plasticizer

*Corresponding author. Ph: +39 035924553; email: mattia.ramini@italiangasket.com

diffusion and evaporation. Instead small rubber temperature fluctuations can be attributed to small minimum torque (*ML*) value variations due to the rubber storage conditions and shelf life. Moreover in cases with peroxide cured rubber this temperature can be very interesting because, above the peroxide temperature activation limit, the cross-linking and mold fouling phenomena can occur.

Shear heating is a processing phenomenon not taken into consideration in laboratory tests. Moreover, in spite of the importance of the shear heating phenomenon, few producers pay attention to it, because it is very difficult to measure and to control; thus no one really knows to which temperature profile the rubber was actually exposed.

On-line process control and rheological characterization can help the plant operator and process engineer to properly understand the rubber flow behavior during the injection molding process.[7–10] This work aims to introduce a new parameter for on-line control of rubber rheology behavior during the injection molding process. The new parameter is based on direct measurement of rubber surface temperature by infrared thermal camera at the nozzle outlet of the injection molding machine extruder. According to shear-thinning theory the rubber compound flowing in the channel is characterized by laminar flow. Therefore in the injection unit, cold rubber block, or in the mold, the rubber can reach relatively higher temperatures near the outer wall. This is because the flowing material experiences a higher shear rate in this region; in contrast, the flowing material in the center region of the bulk has a much lower shear rate. Although the temperature of the rubber purging section is not homogeneous, it can be more conservative to measure the rubber temperature on the surface where temperature itself is higher.[1]

The infrared technique is a noncontact method which does not disturb the flow and which is characterized by a fast response. An infrared thermal camera was already used as a tool for monitoring the extrusion process of polymers[11–13] and rubber.[7]

Temperature rise (ΔT, K) due to shear heating of rubber itself in an extruder may be related to rubber viscosity (η, Pa·s) by the following equation[1]:

$$\Delta T = \eta \cdot \frac{4\dot{\gamma}L}{\rho C_p D} \tag{1}$$

where $\dot{\gamma}$ (s^{-1}) is the shear rate, ρ is the rubber density (kg/m^3), C_p is the specific heat capacity (J/kg/K), and L/D is the screw length over diameter ratio. First of all it is known that the shear heating effect depends on several factors, such as screw speed rotation, injection pressure, injection speed, injection time, and barrel temperature setup. Nevertheless the authors considered Eq. 1 only as reference, by obtaining in the reverse manner a parameter having dimensions of viscosity, here labeled shear heating parameter, η_{SH}. Therefore the equation is generalized by introducing a parameter α, which is a function of the several factors mentioned above:

$$\eta_{SH} = \Delta T_{SH} \cdot \frac{\rho C_p}{4\dot{\gamma}} \alpha \tag{2}$$

where, generally, α is a function of D/L; screw speed rotation; injection pressure, speed, and time; barrel temperature setup; and other factors.

In this work the authors assumed a first approximation and used $\alpha = D/L$, because it is one of the relevant effects to be considered, according to the authors' experimental experience. In the future the authors will investigate the effect of other abovementioned factors and will include them in the definition of α, depending on their actual influence. However both temperature increase and, for the first time, also η_{SH} are obtained for four different rubber compounds during on-line measurements.

The results are compared to *ML* values, from routine MDR laboratory measurement. Advantages and potentialities of shear heating parameters for process control are highlighted.

TABLE I
FILLER CONTENT ACCORDING TO IMDS DATA

Rubber	Hardness, Shore A	Fillers content, wt%	Filler type
BP-FKM	60 ± 5	8.0–13.0	Carbon black
PO-FKM	60 ± 5	18.0–23.0	Barium sulfate
PO-EPDM	60 ± 5	28.0–33.0	Carbon black
S-EPDM	60 ± 5	26.3–33.5	Carbon black

EXPERIMENTAL

Two ethylene–propylene–diene monomer rubbers, EP(D)Ms, one sulfur and one peroxide cured, and two fluoroelastomers (FKMs), one ionic and one peroxide cured, are investigated. These rubber compounds are characterized both by laboratory measurements and by processing tests during the injection molding stage.

MATERIALS

The rubber compounds investigated are the following:

- BP-FKM: ionic cured and black colored FKM
- PO-FKM: peroxide cured and green colored FKM
- PO-EPDM: peroxide cured and black colored EP(D)M
- S-EPDM: sulfur cured and black colored EP(D)M

These industrial grade rubber compounds were designed and developed in accordance with automotive industry specifications, and their recipes cannot be disclosed because they are confidential. They are characterized by 60 ± 5 Shore A of hardness according to ASTM D 2240-15e1, and by a fillers content according to available International Material Data System (IMDS) data as shown in Table I.

LABORATORY CHARACTERIZATION OF RUBBER COMPOUNDS

The rubber compounds characterization was performed in the R&D laboratory of *Italian Gasket* (Italian plant). The laboratory measurements were performed by using uncured and cured standard samples.

The four rubber compounds were characterized by laboratory measurements collecting the data for the η_{SH} calculation (see Eq. 1). Several 200 mm × 200 mm × 2 mm slabs were molded by a laboratory compression molding press. After stabilization the cured standard samples were used to measure the density (ρ) by digital densimeter from Doss, (accuracy: 0.001 g) and according to ASTM D 297-15. Density was measured at room temperature under the hypothesis that it is not significantly different from density at higher temperatures. The cured samples were also used to measure C_p by differential scanning calorimetry, 214 Polyma, from Netzsch and according to ASTM E 1269-11(2018). The C_p data were recorded from 45 to 245 °C by setting 20 °C/min of heating rate.

Instead the uncured samples were used to measure the *ML* data, by MDR 2000 from Alpha Technologies and according to ASTM D 5289-95, at a frequency of 1.7 Hz and 3° of oscillation amplitude. The vulcanization curve was performed for 12 min at 177 °C for each rubber compound, the usual operating condition used in industrial practice.

TABLE II
EXPERIMENTAL DATA

Rubber	BP-FKM	PO-FKM	PO-EPDM	S-EPDM
L/D	6	6	6	12
ρ, kg/cm^3	1859	2029	1090	1140
C_p at T_{SH}, J/kg/°C	2225	1345	4180	4150
ML at 177 °C, dNm	5.77	0.69	1.40	0.93
T_{Barrel}, °C	95.00	80.00	95.00	70.00
T_{SH}, °C	135.00	110.00	105.00	155.00
ΔT_{SH}, °C	115.00	90.00	85.00	135.00
η_{SH} at 10 s^{-1} and ΔT_{SH}, Pa·s	2.05×10^6	1.06×10^6	1.67×10^6	1.31×10^6
log (η_{SH}) at 10 s^{-1} and ΔT_{SH}	6.31	6.02	6.22	6.12

PROCESSING CHARACTERIZATION OF RUBBER COMPOUNDS

The four rubber compounds also were characterized from a processing point of view; thus injection tests were performed by using two horizontal injection molding machines located in the Italian Gasket plant. About 30 kg for each rubber compound were used for processing characterization, and the molded parts, after post-cure stage, and final controls were used in the automotive industry.

The injection molding machines combine an extruder, able to heat and to extrude the rubber, with a reservoir and a mold. In this case two injection molding machines with the extruder characterized by first-in-first-out (FIFO) screw are used. The first injection molding machine, a 300 Ton Engel, was used for the processing tests of BP-FKM, PO-FKM, and PO-EPDM rubber compounds, and is characterized by a length (*L*) over diameter (*D*) ratio, *L/D*, of about 6. The second one, a 450 Ton IMG, was used for processing test of S-EPDM rubber compound, and is characterized by an *L/D* ratio of about 12. The barrel temperature, T_{Barrel}, setup was varied from rubber to rubber (Table II), in order to optimize the balance between flow and curing behavior and to ensure the best compromise between cure rate, cure state, and cycle time, thus avoiding scorch problems. Figure 1 shows the image of rubber purging at the FIFO screw nozzle outlet extruding S-EPDM, as an example. A thermal camera, Diacam C.A 1882 Camera IR-Chauvin Arnoux Group (accuracy, ±2 °C; thermal sensitivity, 0.08 °C), was used to control rubber temperature at the FIFO screw nozzle outlet on the surface of the rubber extrudate during purging.

The thermal control was done to check the rubber flow temperature and shear heating effect for each rubber compound. Figure 2 shows the thermal image of rubber purging at the FIFO screw nozzle outlet extruding S-EPDM, where an average rubber temperature before the injection in the mold cavity, T_{SH}, is 155 ± 2 °C. This thermal control was performed every hour, three measures at a time, to check the shear heating effect and, thus, the rheological behavior of rubber during the injection stage. The average of such values gives T_{SH} temperatures, reported in Table II. The same philosophy was applied for each rubber compound. The same plant operator processed all the materials tested.

RESULTS AND DISCUSSION

Table II reports the experimental data from laboratory and processing characterization. Thus the data of density (ρ), specific heat capacity (C_p) at the temperature of rubber shear heating (T_{SH}) measured by infrared thermal camera at the FIFO screw nozzle outlet (Figure 2), minimum torque

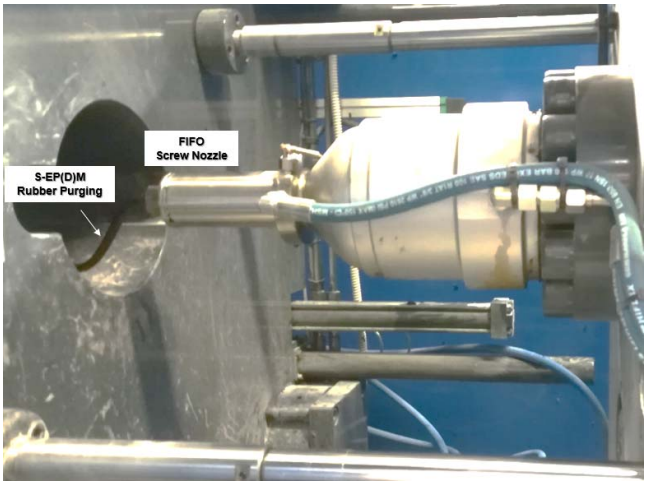

FIG. 1. — Image of S-EPDM rubber purging at FIFO screw nozzle outlet.

(*ML*) at 177 °C, barrel temperature setup (T_{Barrel}), measured T_{SH} by infrared thermal camera, temperature difference in shear heating (ΔT_{SH}) considering 20 °C as initial temperature, and calculated shear heating parameter (η_{SH}) at 10 s^{-1} in logarithmic scale are reported as well. The shear rate choice of 10 s^{-1} was based on the common magnitude order achievable in the plasticizing extruder of the injection molding machine. T_{SH} is achieved both by conduction from the heated barrel wall and by shear heating, but since it is difficult to separate the two contributions, at first approximation the temperature increase has been attributed to shear heating effect only, and it was used for the calculation of η_{SH}. T_{SH} is already a very useful parameter to process control, that is, to collect information about the risk of scorching and thermal degradation, leading for example to diffusion of compound ingredients (low volatile chemicals), stickiness, and color variation. Table II also reports the ratio *L/D* of the two injection molding machines using for the processing tests. Figure 3 shows the vulcanization curve for each rubber compound performed for 12 min at 177 °C

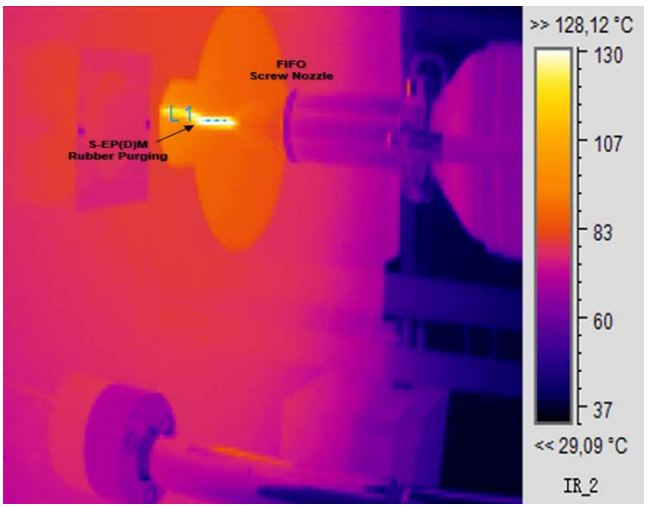

FIG. 2. — Thermal image of S-EPDM rubber purging at the FIFO screw nozzle outlet.

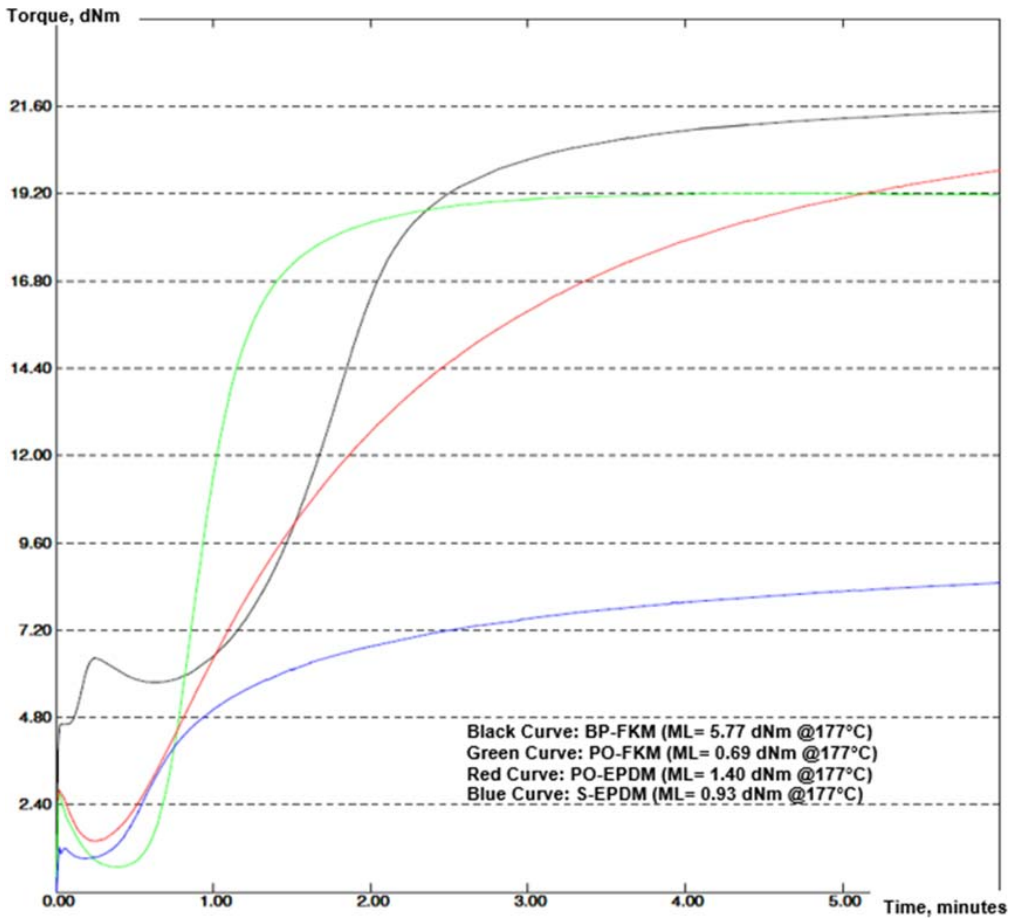

FIG. 3. — Vulcanization curves performed for 12 min at 177 °C by MDR.

by MDR according to ASTM D 5289-95. *ML* values are obtained from such curves as the minimum torque values achieved after the initial transient stage.

Figure 4 shows flow curves in logarithmic scale for each rubber compound. The log (η_{SH}) is calculated by using Eq. 2 and varying $\dot{\gamma}$, at ΔT_{SH}. A shear rate range from 1.0 to 100 s^{-1} is considered, which is a common range for extrusion processes. Such curves graphically show η_{SH} values, which can be obtained from Eq. 2 and their relative ranking, which depends on real operating conditions. BP-FKM turned out to be the compound with the higher η_{SH}, followed by PO-EPDM, S-EPDM, and PO-FKM. Shear heating parameter values are therefore influenced not only by temperature, but also by thermal properties (C_p) and density of the materials.

Figure 5 shows the relationship between log (η_{SH}) at 10 s^{-1} calculated by using ΔT_{SH} and *ML* data from 12 min at 177 °C by MDR, which are also reported in Table II. The η_{SH} is influenced by measured shear heating effect, whereas minimum torque data are obtained from routine laboratory measurements. Although the data are obtained from different rubber compounds, Figure 5 shows a proportional trend, characterized by η_{SH} increasing with the increase of *ML* values. Therefore the relationship between typical laboratory data, as minimum torque, and rheological process data, as shear heating parameter from measured rubber temperature, can be very interesting from the operating point of view. In fact, companies producing rubber goods have a wide database of *ML*

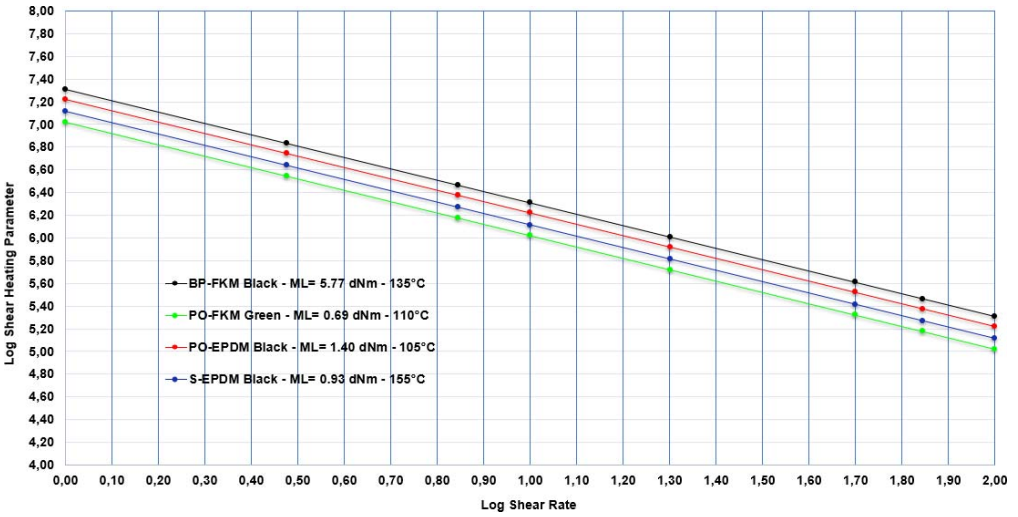

FIG. 4. — Flow curves in logarithmic scale from 1 to 100 s^{-1} by using ΔT_{SH}.

values, which are used to select whether a compound is suitable to be processed with a specific machine. When a compound is out of the specified range, companies know that the compound will not be properly processed. However this laboratory check parameter is sensitive only to compound composition, not to operating conditions. Therefore the *ML* value is a rough indication of the rubber compound viscosity, where its relevant variation affects the rubber processability. Meanwhile the shear heating parameter is more sensitive to small processability variations and is more accurate because it takes into account the thermal history during the injection process. A typical industrial example is when the *ML* value of a rubber compound considerably increases due to improper storage conditions and the processing window changes; thus the injection stage can become difficult. In some cases an increase in barrel temperature setup will decrease the viscosity of the

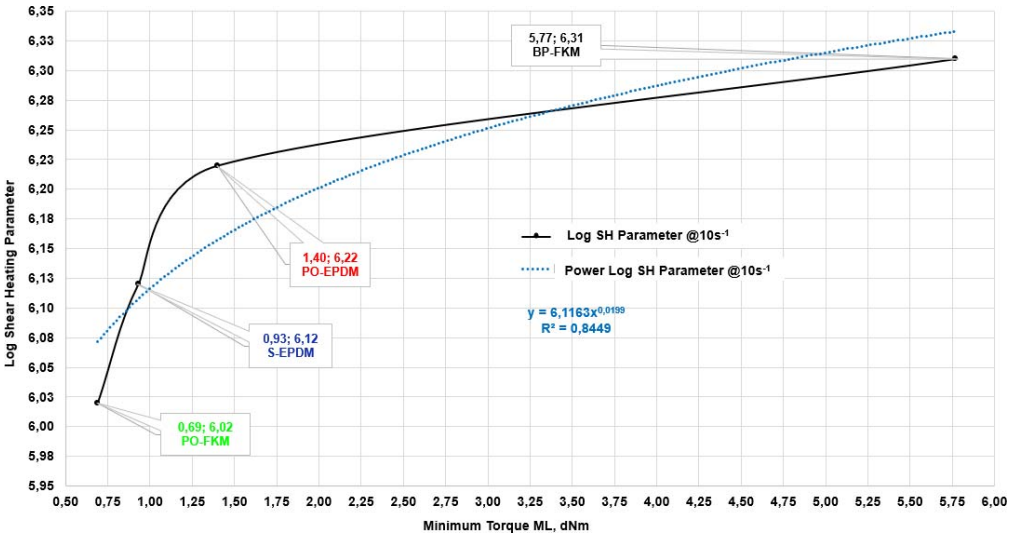

FIG. 5. — Relationship between ΔT_{SH} parameter at 10 s^{-1} and *ML*.

rubber compound by improving the processability. Nevertheless a higher *ML* value could cause an increased injection time and possible scorching risk due to viscous dissipation increasing. This condition can be adjusted by improving the rubber compound recipe formulation, for instance by increasing the plasticizer concentration. Therefore the shear heating parameter monitoring will allow an understanding both of the operating risk and of the limit by which the main process parameters can be maintained constant.

It also should be pointed out that the found relationship is valid for two different injection molding machines: it seems therefore that shear heating parameter is able to take into account not only physical and thermal properties of rubber, but also the screw geometry (*L*/*D*). Since η_{SH} is found proportional to *ML*, this could be used, for example, to define an operating range, inside which rubber materials can be properly processed, this also time taking into account actual operating conditions.

CONCLUSIONS

This study aims to improve the process control for optimal injection molding of technical rubber parts. A very fast process control was performed by using an infrared thermal camera, and it allowed the authors to take into account the shear heating effect before the rubber injection in the cavities mold. The on-line control allowed measurement of the surface rubber temperature by an infrared thermal camera at the nozzle outlet of the injection molding machine extruder and led to calculation of a new parameter for on-line control of rubber rheology behavior, η_{SH}. Four different rubber compounds were tested. The results are compared with *ML* from MDR laboratory measurement. The calculated η_{SH} values were correlated to *ML*, showing a pathway almost in accordance with a proportional trend. The advantage of the η_{SH} parameter is that it takes into account not only rubber compositional effects, but also the effect of operating conditions, to give the thermal history of the rubber injection and process safety. Therefore, this relationship can be used to improve the process control by improving the knowledge of rubber behavior and its shear heating effect during the injection stage. Furthermore this knowledge can help the process engineer, plant operator, and mold designer to provide the suitable process parameters setup and mold design to avoid scorch problems and thermal degradation, preventing the production of rubber parts out of specification. The abovementioned correlation also can be used to properly select the injection molding machine, taking into account the rubber compound rheology behavior.

This work introduces for the first time the η_{SH} parameter and shows an example of its application. However much work still has to be done to understand its physical meaning and further potentialities. Investigations will be carried out to generalize this new parameter and to study its relationship with process parameters other than screw *L*/*D* ratio, and with rubber compound composition. Moreover, the possibility of using such data, measured on-line, to implement quantitative analysis of the injection molding process by computer-aided engineering simulations will be also explored.

ACKNOWLEDGEMENTS

This paper is the result of a collaboration created by Italian Gasket S.p.A and the Department of Mechanical and Industrial Engineering of the University of Brescia. The rubber compounds characterization and the processing tests were performed in the Italian Gasket plant. The authors wish to thank Germana Bergomi, CEO of Italian Gasket, for starting the collaboration between Italian Gasket S.p.A and University of Brescia.

REFERENCES

[1]H. Nishizawa, *Int. Polym. Sci. Technol*. **43**, T41 (2016).

[2]*Custom Molding of Thermoset Elastomers—A Comprehensive Approach to Materials, Mold Design, and Processing*, B. Stritzke, Ed., Carl Hanser Verlag, Munich, 2009.

[3]*Physical Testing of Rubber*, R. Brown, Ed., Springer Science+Business Media, New York, 2006.

[4]H. W. Cox and C. W. Macosko, *AIChE J*. **20**, 785 (1974).

[5]H. H. Winter, *Polym. Eng. Sci*. **12**, 84 (1975).

[6]*Principles of Polymer Engineering*, Z. Tadmor and C. G. Gogos, Eds., John Wiley & Sons, Hoboken, NJ, 2006.

[7]M. Ramini, G. T. Viola, L. Paganin, and M. Battisti, *Rubber World* **261**, 46 (2019).

[8]S. Farahani, N. Brown, J. Loftis, C. Krick, F. Pichl, R. Vaculik, and S. Pilla, *Int. J. Adv. Manuf. Technol*. **105**, 1371 (2019).

[9]J. Y. Chen, C. C. Tseng, and M. S. Huang, *Adv. Polym. Technol.* 2019, 3720127, 20 p.

[10]N. Zhang and M. D. Gilchrist, *Polym. Testing* **31**, 748 (2012).

[11]J. Vera-Sorroche, A. L. Kelly, E. C. Brown, and P. D. Coates, *Polym. Eng. Sci*. **55**, 1059 (2015).

[12]K. Straka, B. Praher, M. Hettrich-Keller, and G. Steinbichler, "To the Measurement and Influences of Process Parameters Variations on the Axial Melt Temperature Profile in the Screw Chamber of an Injection Molding Machine," presented at *SPE ANTEC*® Anaheim, CA, May 2017, pp. 1645–1651.

[13]T. Ageyeva, S. Horváth, and J. G. Kovács, *Sensors* **19**, 3551 (2019).

[*Received May 2020, Revised September 2020*]

Express Polymer Letters Vol.16, No.4 (2022) 354–367
Available online at www.expresspolymlett.com
https://doi.org/10.3144/expresspolymlett.2022.27

express polymer letters

Research article

Applications of shear heating parameter for injection molding process optimization of AEM rubber compounds

Mattia Ramini[1,2*], *Silvia Agnelli*[2], *Giorgio Ramorino*[2]

[1]Italian Gasket S.P.A., Via Tengattini N.9, 25030 Paratico (Bs), Italy
[2]University of Brescia, Department of Mechanical and Industrial Engineering, Via Branze 38, 25123 Brescia (Bs), Italy

Received 19 July 2021; accepted in revised form 13 November 2021

Abstract. Shear heating phenomena during injection molding of rubber compounds greatly affect product quality but are difficult to control and replicate with laboratory tests. In this work, a very fast online process control of industrial injection molding is proposed, based on the measurement of surface temperature by infrared thermal camera of the rubber as it leaves the extruder barrel. Moreover, a new technological parameter (shear heating parameter, η_{SH}) is calculated from the measured temperature. A robust correlation between η_{SH} and viscosity from rheometric laboratory measurements was achieved for different rubber compounds. This represents an operating roadmap to support the process engineer in the improvement of process control. To show the potential of this tool, it was successfully used to optimize the injection molding of industrial production of AEM rubber compound affected by scorching and thermal degradation issues. η_{SH} was found to be suitable for industrial practice and able to provide accurate information about thermal history and process safety.

Keywords: *industrial applications, processing technologies, rubber, AEM rubber, shear heating*

1. Introduction

Nowadays, the automotive industry requires rubber parts of very high quality. Therefore, it is advisable to improve control of the injection molding process, especially in the machine. Injection molding is one of the most commonly used rubber processing technologies enabling the manufacture of final products [1]. The quality of the final product is the result of a combination of factors, including the rubber, mold design, the process, and injection molding machine capability. Consequently, rubber processing by injection molding is very complex and influenced by several parameters, such as temperature, pressure, and shear rate. One of the most important control parameters is temperature. Even though the mold temperature is very easy to control by using thermocouples or other in-mold sensors, on the contrary, the rubber temperature is very difficult to control because it varies according to parameters such as injection pressure, injection speed and screw rotation speed. In particular, the rubber temperature is not only critical for the curing stage but also for the filling stage. If the rubber temperature increases too much, it can start to cure during cavity filling, which can generate defects in the molded parts with possible elongation decrease because the cure progressed too quickly, causing scorch [2]. On the other hand, if the curing reaction occurs while rubber is flowing, viscosity increases sharply, and flow will virtually stop, so that some areas of the mold may not fill properly. Therefore, the mold cavity should be filled completely with rubber before curing commences [2, 3]. Nevertheless, it will be important to guarantee a suitable rubber temperature, a compromise between scorch safety and cure commencing, to improve the cycle time and productivity. When rubber flows too fast into one

*Corresponding author, e-mail: m.ramini@unibs.it

specific cavity, faster than the cavity immediately beside it, there is a shear rate difference. The higher the shear rate, the greater the shear heating and the larger the effect on viscosity. The problem is that the viscosity is not affected uniformly everywhere, but it is only affected in the material at the higher shear rate, whereas the lower viscosity rubber flows more easily under pressure and a filling imbalance is created [2]. Other molding problems due to rubber temperature being too high are mold fouling and sticking phenomena, mainly due to diffusion of rubber compound ingredients [4].

Furthermore, the shrinkage in the parallel direction is larger than in the perpendicular direction, and anisotropic shrinkage increases with the increase of vulcanization temperature and flow distance. The shrinkage is independent of the 'expanded orientation' (*i.e.*, macromolecular orientation due to material thermal expansion and perpendicular to rubber flow), but is strongly associated with the shear orientation, while the mechanical properties are affected by the expanded orientation [5].

Three main sources of heat can increase the rubber temperature in the injection molding process: the heating system of the machine, the exothermal curing reaction, and shear heating. The last factor is a phenomenon where internal friction within the rubber, while it is flowing, generates heat and locally reduces the viscosity [1–12]. This phenomenon is often present in the industrial processing of rubbers and, although it is advantageous to increase the temperature of the rubber by saving energy, it complicates the control of the temperature and also of the viscosity [4].

In this article, the processing behavior of ethylene acrylate rubber (AEM) by injection molding is investigated, with a focus on scorch and thermal degradation issues. Ethylene acrylate elastomers were first introduced to the market more than 40 years ago. They are non-crystalline copolymers of ethylene and methyl acrylate. Both monomers are responsible for giving high-temperature stability and the completely saturated polymer chains that impart excellent resistance to ozone, oxidation, and weathering. The nonpolar ethylene contributes to the good low-temperature flexibility. Most of the polymer grades contain a small amount of acidic cure site monomer for diamine crosslinking, while the polar methyl acrylate monomer provides the oil and fluid resistance. Since its introduction by DuPont under the trade name Vamac® in 1975, it has been used in the automotive industry, in particular, for example, for turbocharger hoses, transmission oil cooler hoses, positive crankcase ventilation hoses, and exhaust gas recovery hoses. Furthermore, AEM is a suitable material for seals and gaskets for automatic transmissions and engines [13–16].

A high percentage of AEM parts used in the automotive industry are made from AEM terpolymer compounds cured with diamines. As reported in literature works by McBride from DuPont [13–15], these compounds are more prone to scorch than most elastomeric compounds; thus, suitable process control has to be provided in order to prevent it. The diamine curative reacts with the cure site monomer in a two-step curing process: the first step involves the formation of an amide (relatively fast step, which occurs in the mold); the second step involves the conversion of the amide to an imide (this reaction is slow and requires a long post-cure step to finish the cure, usually 4 hours at 175 °C). After the injection molding process, the part has dimensional stability, but the compression set is high (70 to 90% after one week at 150 °C), and the hardness and modulus are relatively low. The post-cure stage increases the hardness until the required specification is met, and the compression set drops to about 20–30%.

The first step is the source of the scorch. Scorch issues can cause molding problems such as underfilling the mold cavity and problems at knit lines, which necessitate extra processing aids to lower viscosity. Scorch reactions are a function of time and temperature, and they become an issue for AEM compounds at temperatures above 100 °C. Therefore, for AEM compounds, the processing temperatures (mixing, molding and/or extrusion) should be kept under 100 °C [13–15], which is very difficult to maintain, for instance, in the injection molding machine extruder due to shear heating. However, as the temperature further increases, there will be a point at which the viscosity starts to increase due to the scorching of the compound. Furthermore, in the worst cases, if the rubber temperature increases too much due to higher shear rates, thermal degradation by loss of plasticizer and processing aids can start.

An optimal rubber temperature must ensure a balance between not having excessively high viscosity, scorch safety, and thermal degradation. The actual rubber temperature in an injection molding machine, mostly generated by shear heating, is very difficult

to replicate in the laboratory by typical instruments such as a moving die rheometer (MDR), because the MDR does not reproduce properly the physical process occurring in the injection stage of the molding machine extruder. The shear heating generated inside the injection molding machine extruder depends on the screw length to diameter ratio L/D, and mostly on the process parameter setup, such as screw rotation speed, injection pressure, speed and time, barrel temperature setup and other factors [4, 17].

This work puts forward an approach to improve the control of industrial injection molding of technical rubber parts based on the measurement of rubber temperature. The approach is based on very fast online process control, which is suggested in order to be used in industrial practice, and consists of the direct measurement of rubber surface temperature (T_{SH}) by the infrared thermal camera at the nozzle outlet of the injection molding machine extruder. Although the temperature of the rubber leaving the extruder is not homogeneous, it can be more conservative in measuring the rubber temperature on the surface where the temperature is higher (according to shear-thinning theory) [3]. The use of an infrared thermal camera does not disturb the rubber flow and is a noncontact method characterized by a very fast response [4, 11, 18–20]. The measured rubber shear heating temperature (T_{SH}) is then used to calculate a technological parameter designated shear heating parameter and labeled η_{SH}. The results of η_{SH} were compared with minimum torque, M_L, from MDR routine rheometric laboratory measurements for eight different industrial rubber compounds, based on AEM, hydrogenated acrylonitrile butadiene rubber (HNBR), fluorocarbon rubber (FKM) and ethylene-propylene-diene monomer rubber (EP(D)M). The measured M_L value is a rough indication of the rubber compound viscosity; hence variations of M_L affect the rubber processability. Instead, the calculated η_{SH} value combines both rubber composition and operating condition effects, giving more information about the thermal history of the rubber injection stage and process safety [4].

A robust correlation between η_{SH} and M_L, labeled roadmap, was sought and is shown in this work by considering various rubber compounds having different elastomeric matrices, AEM, HNBR, FKM, and EP(D)M, different geometries of the molded parts (both O-rings and technical rubber items), and also different injection molding machines and process parameter setups. This heterogeneous pattern of rubber compounds was chosen to develop a phenomenological approach based on a robust roadmap, with the purpose of supporting the process engineer in the improvement of process control by thermal online measurements [4, 11, 21–23]. To show its potential, this work shows how this roadmap can be successfully used to improve the process control of AEM rubber compound industrial production affected by scorch problems and thermal degradation due to plasticizer loss [24].

2. Theoretical background

Starting from the online measured shear heating temperature (T_{SH}) of the rubber, the shear heating parameter, η_{SH}, is calculated according to the Equation (1) [4]:

$$\eta_{SH} = \Delta T_{SH} \frac{\rho C_p}{4v} \alpha \tag{1}$$

where ΔT_{SH} [°C] is the temperature difference between T_{SH} and the initial temperature (considering 20 °C as initial temperature), ρ is the rubber density [kg/m^3], C_p is the specific heat capacity [J/kg/K], v [s^{-1}] is a flow rate parameter, and α is a function of process parameters such as D/L, screw rotation speed, injection pressure, speed and time, barrel temperature setup and other factors. Due to the complexity of the injection molding process, a thorough investigation needs to be performed to define α and its dependence on the process parameters. However, in this work, α is approximated as equal to D/L because, according to experimental data (not yet published), it is one of the most relevant factors contributing to shear heating during the injection stage. Therefore, η_{SH} is a technological parameter having dimensions of viscosity [Pa·s] [4].

Equation (1) is inspired by the equation reported below, where the temperature rise (ΔT, [K]) due to shear heating of rubber in an extruder is related to rubber viscosity [4, 6] (Equation (2)):

$$\Delta T = \eta \frac{4\dot{\gamma} L}{\rho C_p D} \tag{2}$$

Equation (2) is derived for a simple cylindrical channel, a tube with dimensions L (length) and D (diameter), where a Newtonian fluid is flowing with a stationary laminar flow with $\dot{\gamma}$ as wall shear rate,

therefore, assumptions such as no wall slip, Newtonian fluid, and adiabatic flow (no heat transfer to the surroundings) were considered [8].
The authors are aware that most of these assumptions do not apply to rubber. Nevertheless, they were inspired by Equation (2) to derive the technological parameter η_{SH} in Equation (1), which is proposed with the purpose of providing a suitable process parameter setup during the injection phase [4].

3. Experimental

Eight different rubber compounds were investigated: two EP(D)Ms, one sulfur and one peroxide cured, three AEM rubbers, all diamine cured, two HNBR, both diamines cured, and one FKM, peroxide cured. These industrial-grade rubber compounds were developed in accordance with automotive industry standard specifications, and their formulations cannot be disclosed for confidentiality reasons. They are characterized by 60±5 Shore A hardness according to *ASTM D2240-15*, and by a filler type and content according to available *International Material Data System* (IMDS) data, as reported in Table 1. The black filler was usually carbon black type N 990. Black and white filled rubber compounds were characterized by both laboratory tests and processing injection trials in the molding machine during daily production runs.

3.1. Materials

The eight rubber compounds investigated were the following:

- PO-EPDM-black: peroxide cured and black colored EP(D)M,
- S-EPDM-black: sulfur cured and black colored EP(D)M,
- Two types of DIA-AEM-black: diamine cured and black colored AEM,
- DIA-AEM-brown: diamine cured and brown colored AEM,
- DIA-HNBR-black: diamine cured and black colored HNBR,
- DIA-HNBR-red: diamine cured and red-colored HNBR,
- PO-FKM-green: peroxide cured and green-colored FKM.

Table 1. Filler content according to IMDS data.

Rubber	Hardness [Shore A]	Fillers content [wt%]	Filler type
PO-EPDM-Black	60±5	28.0–33.0	Carbon black
S-EPDM-Black	60±5	26.3–33.5	Carbon black
DIA-AEM-Black	60±5	40.0–46.0	Carbon black
DIA-AEM-Black	60±5	35.0–45.0	Carbon black
DIA-AEM-Brown	60±5	38.0–46.0	Silicon dioxide
DIA-HNBR-Black	60±5	44.5–48.5	Carbon black
DIA-HNBR-Red	60±5	40.0–48.0	Calcined kaolin
PO-FKM-Green	60±5	18.0–23.0	Barium sulfate

3.2. Laboratory characterization

The eight rubber compounds were characterized by using uncured and cured standard samples and the equipment located in the R&D laboratory of *Italian Gasket* (Italian plant). The laboratory results collected for each rubber compound were used to calculate the corresponding shear heating parameter (η_{SH}) by Equation (1), then correlated with minimum torque M_L results.
The uncured samples were used to measure the minimum torque M_L data by an MDR 2000 from *Alpha Technologies* (Cinisello Balsamo, MI – Italy).according to *ASTM D5289-95* at a frequency of 1.7 Hz and 3° oscillation amplitude. The vulcanization curve of each rubber compound was measured for 12 minutes at 177 °C because this is a historical and well-established internal methodology. The Monsanto MDR usually has 350 °F as the test temperature, corresponding to 177 °C. Moreover, this temperature can be easily reached in an injection molding machine to achieve the cure of a rubber compound.
A laboratory compression molding press from *Gibitre Instruments Srl* (Bergamo, BG – Italy) was used to mold 200×200×2 mm slabs. After 24 hours of stabilization, the cured standard samples were used for density (ρ) measurements, performed at room temperature, by a digital densimeter from *Doss* (For Lab Italia, Stezzano, BG – Italy) (accuracy: 0.001 g) in accordance with *ASTM D297-15*. The density value to be used for Equation (1) should be measured at the temperature and pressure in the injection molding machine extruder. However, to use an applicable industrial method, the density at room temperature and pressure was considered to be a reasonable approximation of density at higher temperature and pressure. This approximation is supported by the rubber material data reported in the CAE simulation software database, where a typical density variation is 5% with temperature increase from *RT* to 100 °C and pressure increase from 0 to 200 MPa.

Moreover, the cured samples were used for specific heat capacity (C_p) measurements by differential scanning calorimetry (DSC) in a 214 Polyma from N*ETZSCH Geraetebau GmbH* (Selb – Germany). The C_p results were recorded from 45 to 245 °C with a heating rate of 20 °C/min and referring to *ASTM E1269-11(2018)*.

DSC was also used to measure the T_g of AEM parts, both OK and KO (cracked), recording the first and the second heating from –80 to 40 °C with a heating rate of 10 °C/min and referring to *ASTM D3418-21*.

AEM parts, both OK and KO (cracked), were used to qualitatively analyze their specific IR absorption frequencies by total reflection-Fourier transform infrared (ATR-FTIR) spectroscopy, using an ALPHA II FT-IR spectrometer from *Bruker Italia Srl* (Milano, MI – Italy) equipped with a Ge ATR crystal. The sample measurements were run at a resolution of 4 cm^{-1} and applied 24 scans from 400 to 4000 cm^{-1}.

Furthermore, AEM parts, both OK and KO (cracked), were used to quantitatively analyze their composition (*e.g.*, elastomers, plasticizers, and fillers) by thermogravimetric analysis (TGA), using a TG 209 F3 Tarsus® from *Netzsch Geraetebau GmbH* (Selb – Germany). The sample measurements were run in an N_2 atmosphere heating from *RT* to 600 °C at 20 °C/min, cooling from 600 to 400°C at 40 °C/min, holding for 2 minutes at 400 °C, then heating from 600 to 850 °C at 20 °C/min in an oxygen atmosphere and holding for 5 minutes at 850 °C.

3.3. Processing characterization

The processing injection tests were performed using horizontal injection molding machines located in the Italian plant of *Italian Gasket*. Five horizontal injection molding machines were selected for the processing investigation.

A 190 Ton MIR from *IMG Srl* (Capriano del Colle, BS – Italy) with reciprocating screw, *L*/*D* ratio of about 15, was used to produce sealing rings based on DIA-AEM-brown. A 190 Ton MIR with reciprocating screw, *L*/*D* ratio of about 16, was used to produce technical rubber items based on DIA-AEM-black. Another 190 Ton MIR with reciprocating screw, *L*/*D* ratio of about 18, was used to produce intake manifold gaskets based on DIA-HNBR-black and DIA-HNBR-red.

A 300 Ton Engel from *Engel Austria GmbH* (Schwertberg – Austria), with First In First Out (FIFO) screw, *L*/*D* ratio of about 6, was used to produce O-rings based on another DIA-AEM-black, and two different frame gaskets based on PO-EPDM-black and PO-FKM-green, respectively.

A 450 Ton IMG from *IMG Srl* (Capriano del Colle, BS – Italy), with FIFO screw, *L*/*D* ratio of about 12, was used to produce bellows based on S-EPDM-black.

Daily production runs of each rubber compound were investigated and, after the start-up stage, the thermal control tests were performed. Figure 1 shows the online monitoring scheme of rubber surface temperature control.

The thermal measurement for each rubber compound and respective production run was performed every hour, three measures at each time, in order to control the shear heating effect during the injection stage. A thermal imaging camera, Diacam C.A 1882, *Chauvin Arnoux Group* (Asnières-sur-Seine – France) (±2 °C accuracy and 0.08 °C thermal sensitivity), was used to control rubber surface temperature at the

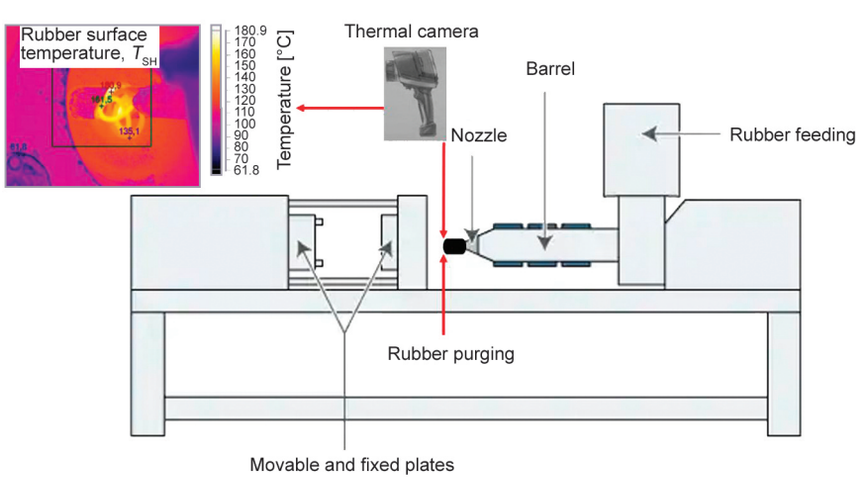

Figure 1. Online monitoring scheme of rubber surface temperature control.

screw nozzle outlet of the injection molding machine extruder. The infrared thermal camera was used to measure the temperature of the rubber by detecting the emitted electromagnetic radiation. The rubber emissivity was set to 0.95 in accordance with the software material database, and image analysis was provided by the software tools. The advantage of using a commercial brand is to improve the availability of the technology in the rubber industry.

The molded parts, after stabilization, deburring, post-cure (if required), and final controls were used as gaskets in the automotive industry.

4. Results and discussion

Table 2 reports the setup of the most important process parameters and the summary of average experimental data from both laboratory and injection molding process characterizations for each rubber compound investigated and their respective daily production runs (average data).

Therefore, eight rubber compounds and eight industrial production runs with long process stability, without significant deviations of set parameters and with very little scrap were investigated. Table 2 also reports the results of the investigation of various production runs of DIA-AEM-black: both a very stable production run and an unstable production run are reported, designated DIA-AEM-black-OK and DIA-AEM-black-KO, respectively. In addition, the intermediate production runs necessary to restore the process stability are reported and designated DIA-AEM-black-INT1 and DIA-AEM-black-INT2, respectively.

Process parameter setup common to all the systems investigated was: injection speed of 70%, the screw rotation speed of 80 rpm, injection time of 10 s, cure time of 85 s, barrel temperature of 75±5 °C, and both fixed and movable plate temperature of 195±5 °C. $L/_D$ ratio of the five injection molding machines used for the processing trials and barrel temperature setup (T_{Barrel}) are reported in Table 2 for each system. About laboratory characterization, the data of density (ρ), specific heat capacity (C_p), and minimum torque (M_L) at 177 °C are reported. Finally, the processing characterization data, such as measured shear heating temperature (T_{SH}) of the rubber by infrared thermal camera, the temperature difference in shear heating (ΔT_{SH}) considering 20 °C as initial temperature, and the calculated shear heating parameter (η_{SH}) on a logarithmic scale is reported. The shear heating

Table 2. Process parameters setup and experimental data.

Rubber		PO-EPDM-black	S-EPDM-black	DIA-AEM-black	DIA-AEM-brown	DIA-HNBR-black	DIA-HNBR-red	PO-FKM-green	DIA-AEM-black-KO[a,b]	DIA-AEM-black-INT1[a,c]	DIA-AEM-black-INT2[a,d]	DIA-AEM-black-OK[a,e]
ρ	[kg/m^3]	1090±1	1140±1	1267±1	1389±2	1273±2	1331±1	2029±1	1243±1	1243±1	1243±1	1243±1
C_p at T_{SH}	[J/kg/°C]	4180±2	4150±3	2930±3	1459±3	3240±3	2770±3	1345±2	3290±4	3255±4	3075±4	2931±4
M_L at 177 °C	[dN·m]	1.40±0.02	0.93±0.02	1.24±0.01	0.38±0.02	0.58±0.02	0.47±0.04	0.69±0.02	0.40±0.01	0.40±0.01	0.40±0.01	0.40±0.01
L/D		6	12	6	15	18	18	6	16	16	16	16
T_{Barrel}	[°C]	95.0	70.0	80.0	75.0	75.0	75.0	80.0	75.0	75.0	75.0	75.0
T_{SH}	[°C]	105.0±2.5	155.0±3.0	114.0±2.5	125.0±2.5	136.0±2.5	132.0±3.0	110.0±2.5	235.0±3.0	223.0±3.0	162.0±3.0	115.0±3.0
ΔT_{SH}	[°C]	85.0	135.0	94.0	105.0	116.0	112.0	90.0	215.0	203.0	142.0	95.0
η_{SH} at 10 s^{-1} and ΔT_{SH}	[Pa·s]	$1.67 \cdot 10^6$	$1.31 \cdot 10^6$	$1.50 \cdot 10^6$	$3.64 \cdot 10^5$	$6.69 \cdot 10^5$	$5.77 \cdot 10^5$	$1.06 \cdot 10^6$	$1.37 \cdot 10^6$	$1.28 \cdot 10^6$	$8.43 \cdot 10^5$	$5.37 \cdot 10^5$
Log η_{SH} at 10 s^{-1} and ΔT_{SH}		6.22	6.12	6.18	5.56	5.83	5.76	6.02	6.14	6.11	5.93	5.73

[a]MIR 190 tons injection molding machine, process parameter setup: injection speed = 70%; screw speed rotation = 80 rpm, injection time = 10 s, curing time = 85 s, barrel temperature = 75±5 °C and both fixed and movable plate temperature = 195±5 °C.
[b]Injection pressure = 140 bar.
[c]Injection pressure = 100 bar.
[d]Injection pressure = 80 bar.
[e]Injection pressure = 70 bar

parameter was calculated using Equation (1), where the flow rate parameter v [s^{-1}] is directly related to shear rate. Therefore, a conventional value of flow rate of 10 s^{-1} was chosen based on the commonly achievable order of magnitude of shear rate in the plasticizing extruder of the injection molding machine.

Figure 2 shows the curing curve for each rubber compound performed for 12 minutes at 177 °C by MDR according to *ASTM D5289-95*. The M_L values reported in Table 2 were obtained from these curves as the minimum torque values reached after the initial transient stage. It is worth pointing out that curing curves show large differences among rubber compounds in terms of rheological and curing behavior. Once again, this heterogeneity is intentionally sought to develop a robust correlation (the roadmap) with a phenomenological approach.

The curing curves were measured on standard samples collected from the same rubber compounds used for the processing investigation. Furthermore, the selected rubber compounds were fresh material within their shelf life, where the measured M_L and the calculated shear heating parameter are subject to negligible variation.

Figure 3 shows an example of the thermal images taken of the rubber as it emerged from the reciprocating screw nozzle outlet, from which T_{SH} values reported in Table 2 were obtained.

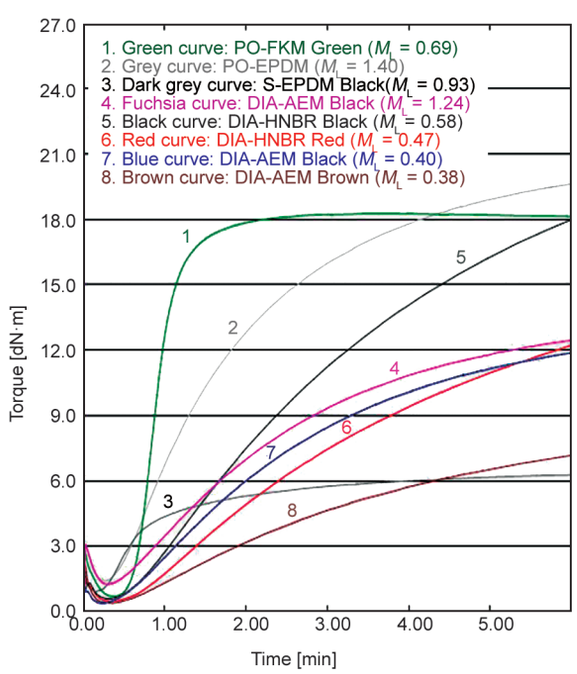

Figure 2. Vulcanization curves performed for 12 minutes at 177 °C by MDR.

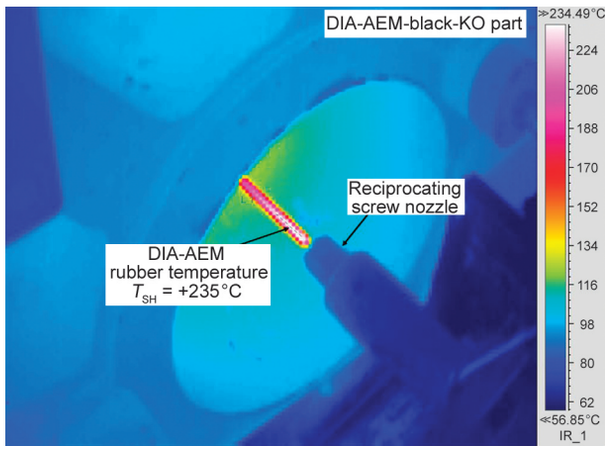

Figure 3. Image of KO run for DIA-AEM black rubber emerging from the reciprocating screw nozzle outlet.

In order to use the log η_{SH} parameter as a tool for improvement of process control, data from different rubber compounds and production runs were compared and correlated with M_L values, thus obtaining a common correlation, a sort of roadmap.

Figure 4 shows the relationship between log η_{SH} at 10 s^{-1} and M_L from 12 min at 177 °C by MDR, giving a comparison between the eight rubber compounds investigated and the eight industrial production runs with long process stability without the relevant quality issue of final parts, including the DIA-AEM-black-OK run.

A proportional trend was observed with R^2 of 0.935 according to a power regression law. Therefore, a good correlation was established between the results of the laboratory test, M_L, and the technological parameter (η_{SH}). The advantage of also monitoring the η_{SH} parameter is that it takes into account both rubber composition effects and the effect of operating conditions, thus providing information about the thermal history of the rubber injection and process safety. A similar correlation curve was previously shown by the authors [4] for three rubber systems (PO-FKM-green, PO-EPDM-black, and S-EPDM-black). In the present work, the previous investigation was extended, and further rubber systems were investigated to obtain the correlation in Figure 4. The existence of such a correlation is, therefore, confirmed and strengthened by the new data. The eight industrial production runs investigated in this work are characterized by different injection molding machines, different molded part geometries, and by very stable production runs, with very little scrap after molded part stabilization, deburring and post-cure. Therefore, the

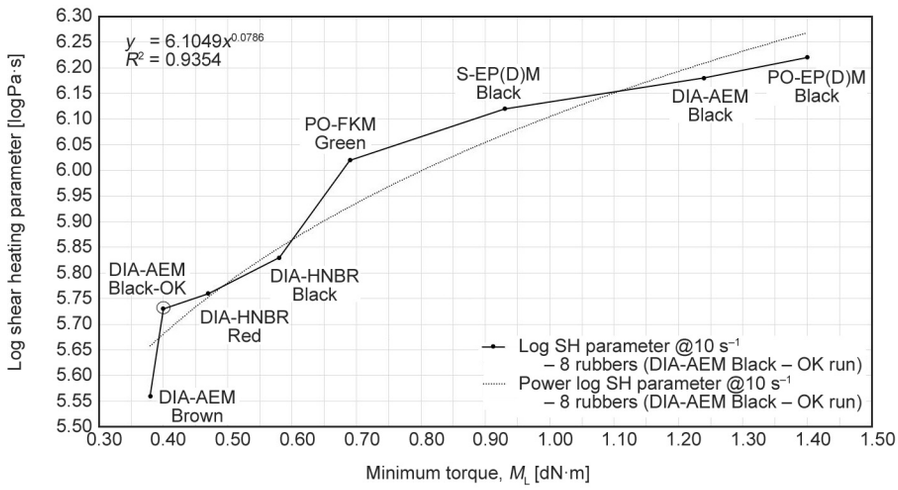

Figure 4. Relationship between shear heating parameter at 10 s^{-1} and minimum torque M_L, comparison between 8 rubbers and 8 production runs having long process stability.

values of $\log \eta_{SH}$ and M_L represent the reference points to achieve a robust correlation with the molding function to support, by an operating roadmap, the process engineer and plant operator in the improvement of the process control by online thermal measurements.

With the aim of showing the industrial application of this roadmap as a 'calibration curve' for the fast control of successful setting up of process parameters, the process optimization of AEM rubber parts affected by scorch problems and thermal degradation due to plasticizer loss is reported as follows.

The image in Figure 3 was taken during a DIA-AEM-black-KO production run, in which about 450 000 parts were produced. This production run was chosen as a case study for this work to show how the proposed approach helps to improve the process control of rubber injection molding. An average rubber surface temperature of 235 °C was measured during the daily process control and, after injection molding, stabilization, deburring, and post-cure of 4 hours at 175 °C, some surface cracked parts were obtained (8 cracked parts/1000 sampled parts). These AEM cracked parts were detected during the automatic sorting control, and they are characterized by IRHD M hardness values of 25–30 points higher than the required level, thus very out of specification. Furthermore, AEM hardened parts (12 hardened parts/1000 sampled parts) were detected, characterized by both hardness and compression-set values out of the required specification, even if less than the cracked parts. From laboratory characterization of both cracked parts and in-specification parts, cracked parts clearly showed higher hardness (+30 IRHD M points) than the standard, higher T_g (+9 °C) from differential scanning calorimetry (see Table 4), and plasticizer loss from thermogravimetric analysis (TGA) and attenuated total reflection-Fourier transform infrared (ATR-FTIR) spectroscopy.

Figure 5 shows qualitative information of the ATR-FTIR spectra comparison between DIA-AEM-black-OK and DIA-AEM-black-KO parts. The black spectrum shows the main absorption frequencies of the OK AEM rubber, while the red spectrum shows intensity reduction of the absorption frequencies of KO AEM rubber with the change of some peaks, mainly in the fingerprint region (from about 1500 to 500 cm^{-1}). This spectral comparison indicates a very large variation of the sample composition, then quantitatively confirmed by TGA.

Figure 6a and 6b show the TGA plots of DIA-AEM-black-OK and DIA-AEM-black-KO parts, respectively. Figure 6a shows a plasticizer content of about 4.71 wt%, while Figure 6b shows the absence of plasticizer, demonstrating plasticizer loss in the final parts.

During the injection molding, the rubber flow is laminar according to shear-thinning theory; thus a relevant shear rate can produce a high shear heating effect and, as a consequence, the rubber surface temperature (T_{SH}) increases. Therefore, it is hypothesized that plasticizer diffusion and evaporation started during the injection stage, caused by excessive shear heating measured at the reciprocating screw nozzle outlet, T_{SH} = 235 °C (Figure 3).

From preliminary process parameter fine-tuning performed on injection speed, screw rotation speed, and barrel temperature, it was verified that injection

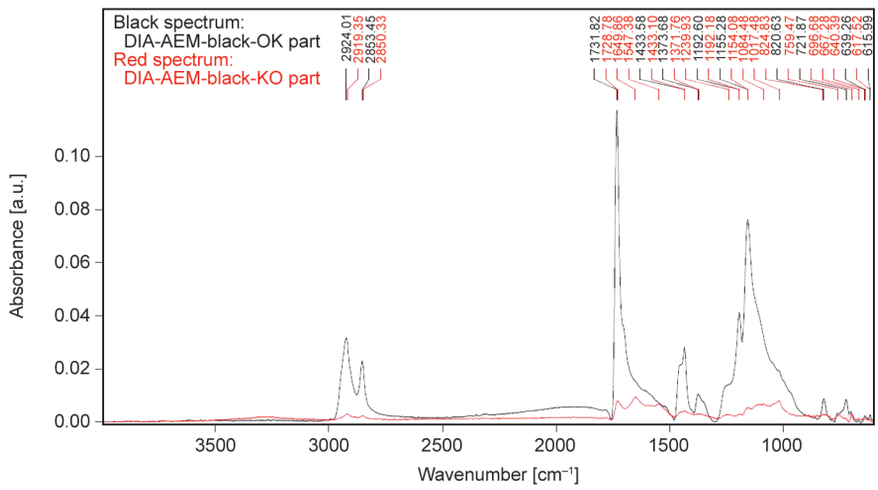

Figure 5. ATR-FTIR spectra comparison between DIA-AEM-black-OK part (black) and DIA-AEM-black-KO part (red).

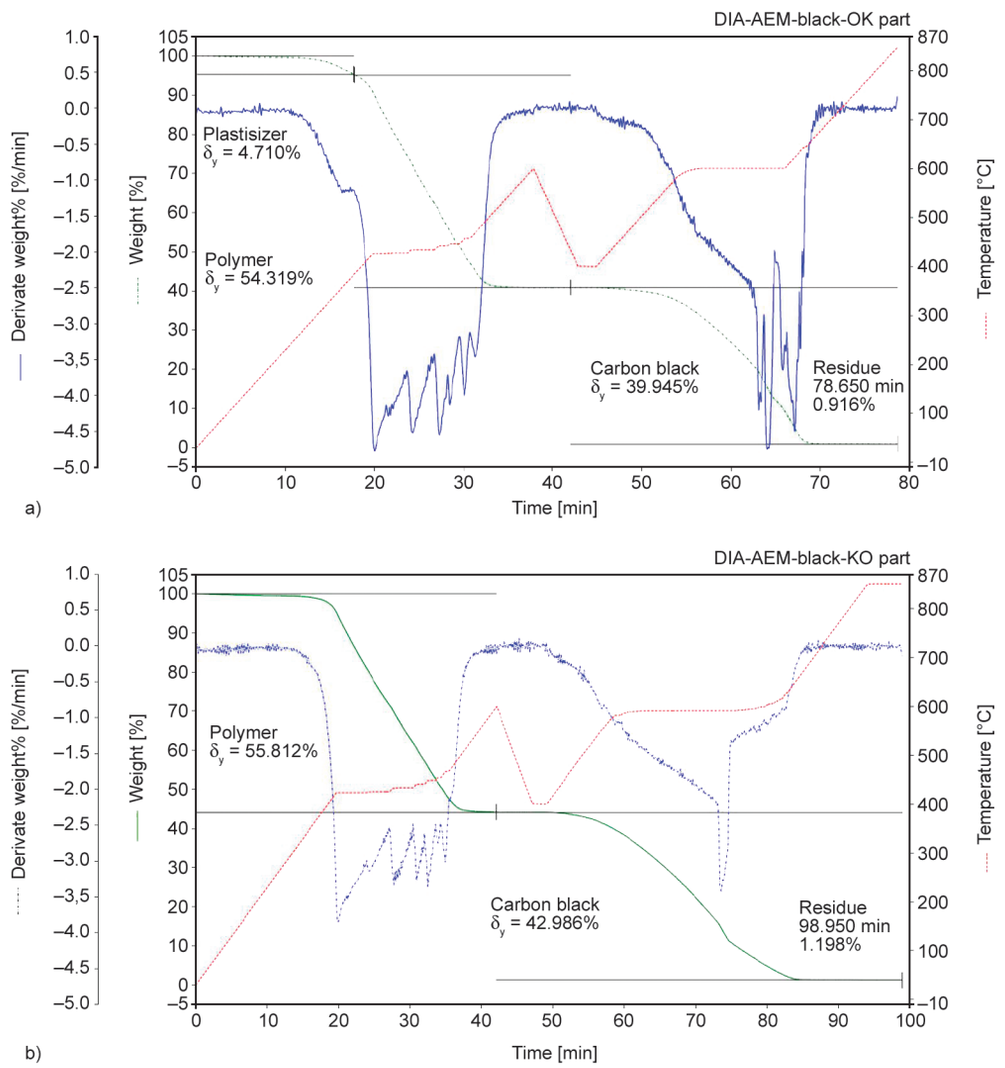

Figure 6. a) TGA plot of DIA-AEM-black-OK part. b) TGA plot of DIA-AEM-black-KO part.

pressure is the process parameter that mostly reduced this excessive shear heating.

Table 3 reports the investigated injection pressure setup (P_i) for DIA-AEM-black production runs. Each selected injection pressure setup was maintained constant for the whole production lot of about 450 000 parts. Four production runs were investigated: KO run, INT1 run, INT2 run and OK run, where

Table 3. Injection pressure setup for DIA-AEM-black production runs.

DIA-AEM-black	Production run injection pressure[a] [bar]
KO run	140
INT1 run	100
INT2 run	80
OK run	70

[a]MIR 190 tons injection molding machine process parameter setup: injection speed = 70%; screw rotation speed = 80 rpm, injection time = 10 s, cure time = 85 s, barrel temperature = 75 °C and both fixed and movable plate temperature = 195 °C.

the process parameters other than injection pressure were maintained constant.

Figure 7 shows the relationship between the measured temperature, T_{SH}, of rubber shear heating by thermal camera and the injection pressure setup, P_i. Clearly, a reduction of injection pressure decreased the shear heating effect during the injection stage, maintaining the AEM rubber in a thermal condition away from high temperatures likely to produce plasticizer diffusion and evaporation.

T_{SH} is already a very useful parameter to guarantee very fast online process control, that is, to collect information concerning the risk of scorching and thermal degradation, leading, for example, to the diffusion of compound ingredients (low volatile chemicals), stickiness, and mold fouling, and also color variation. However, T_{SH} values obtained for different rubber compounds cannot be directly compared since each material has different thermal behavior.

Therefore, $\log \eta_{SH}$ was introduced to allow the comparison of process outputs between DIA-AEM-black and the other materials.

Figure 8 shows the relationship between the log of the shear heating parameter at 10 s^{-1}, $\log \eta_{SH}$, and injection pressure setup, P_i. $\text{Log}\,\eta_{SH}$ at 10 s^{-1} was calculated by using the data for ΔT_{SH} [°C], ρ [kg/m^3],

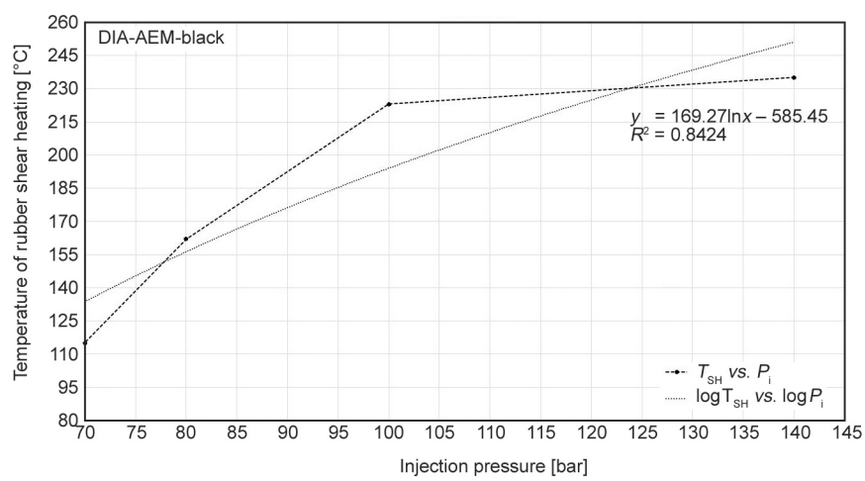

Figure 7. Relationship between temperature of rubber shear heating T_{SH} and injection pressure P_i for DIA-AEM-black production runs.

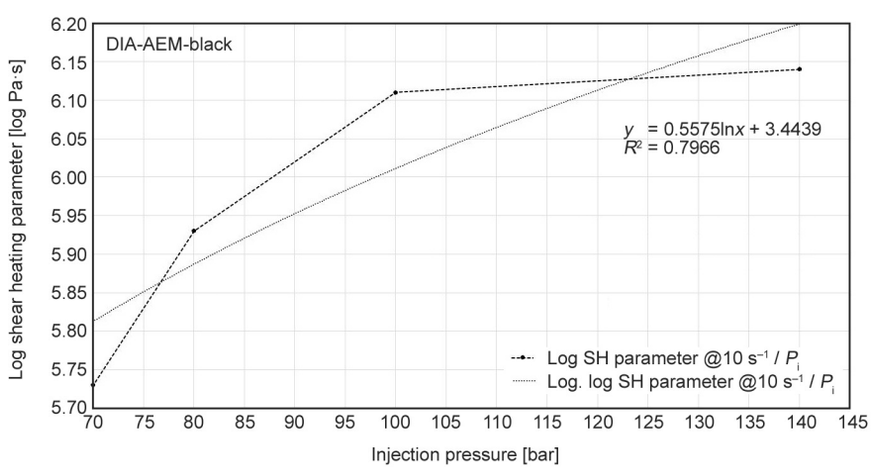

Figure 8. Relationship between log shear heating parameter at 10 s^{-1}, $\log \eta_{SH}$ and injection pressure P_i for DIA-AEM-black production runs.

C_p [J/kg/K], and L/D reported in Table 2. Therefore, working with injection pressure setup of 140 bar and the DIA-AEM-black-KO run, an average T_{SH} of 235°C was measured online, and a $\log \eta_{SH}$ at 10 s^{-1} of 6.14 Pa·s was calculated.

In this production run, eight cracked parts and 12 hardened parts in 1000 sampled parts were collected. As mentioned previously, the cracked parts showed an average hardness value of 87.0 *IRHD M* according to ISO 48 due to plasticizer evaporation, thus about 30 *IRHD* points more than the required specification of 60±5 (molded parts had low thickness; therefore *IRHD M* hardness was used instead of Shore A). The hardened parts showed an average hardness value of 71.0 *IRHD M*, thus also out of specification, and compression set of 55.0%, performed for 94 hours at 150 °C after post-cure of 4 hours at 175 °C. Hence, the compression set was also out of the required specification of ≤50.0%, according to *PV3330* (Table 4).

On the contrary, working with injection pressure setup of 70 bar and the DIA-AEM-black-OK run, a lower rubber shear heating temperature was measured online, average T_{SH} of 115 °C, and a lower shear heating parameter was calculated, $\log \eta_{SH}$ at 10 s^{-1} of 5.73 Pa·s. Therefore, this production run guaranteed a thermal condition away from high temperatures likely to produce plasticizer diffusion and evaporation. Table 4 also reports the hardness and compression set results for the DIA-AEM-black-OK run, where average values of 58.0 *IRHD M* and 40.0%, respectively, are reported, both within the required specification.

With the aim of showing the use of the roadmap for fast control of successful setup of process parameters, Figure 9 shows the relationship between $\log \eta_{SH}$ at 10 s^{-1} and M_L from 12 min at 177 °C by MDR for the seven rubber compounds with very stable industrial production runs and DIA-AEM-black-KO run (R^2 of 0.526), DIA-AEM-black-INT1 run (R^2 of 0.562) and DIA-AEM-black-INT2 run (R^2 of 0.788). In more detail, new curves were created, starting from the roadmap reported in Figure 4, by replacing the data of DIA-AEM-black-OK with values of either DIA-AEM-black-KO run (Figure 9a), INT1 run (Figure 9b) or INT2 run (Figure 9c), while keeping the values of the other seven productions runs constantly. Only the $\log \eta_{SH}$ values of DIA-AEM-black were modified, whereas M_L was always the same since it is a laboratory property, not influenced by process parameters.

By introducing the curves of the KO run, INT1 run, and INT2 run, some relevant deviations from the previous proportional trend were observed, especially in Figure 9a (red curve) with R^2 of 0.526 according to the power regression model. Accordingly, the DIA-AEM-black-KO run, based on injection pressure setup of 140 bar, average T_{SH} of 235 °C, and $\log \eta_{SH}$ at 10 s^{-1} of 6.14 Pa·s, did not allow a stable production cycle, where hardened and cracked parts were produced. Furthermore, DIA-AEM-black-INT1 and INT2 runs were used to fine-tune the injection pressure setup from KO to OK runs, thus in this case also the $\log \eta_{SH}$ at 10 s^{-1} values deviated from the proportional trend with R^2 of 0.562 and 0.788, respectively. Finally, the DIA-AEM-black-OK run, based on injection pressure setup of 70 bar, average T_{SH} of 115 °C, and $\log \eta_{SH}$ at 10 s^{-1} of 5.73 Pa·s, allowed a very stable production cycle without hardened and cracked parts. In this process setup, the $\log \eta_{SH}$ value was within the proportional trend with R^2 of 0.935 according to the power regression model (see Figure 4). Therefore, the coefficient of determination of $\log \eta_{SH}$ *vs* M_L curves provides a good indication of process stability of DIA-AEM-black runs.

Figure 4 and Figure 9 clearly show how $\log \eta_{SH}$ values of a production run, combined with M_L values, give indication of the successful output of the injection molding process by comparison of this data with a well-established roadmap obtained from stable production runs of different rubber compounds and process conditions. This monitoring has the advantage of being fast, and provides information about the stability of the process while it is running, well before completing the production run.

Table 4. Physical-mechanical data for DIA-AEM-Black, comparison between OK and KO runs.

Parameter[a]		DIA-AEM-black-OK	DIA-AEM-black-KO
Hardness after post-cure 4 hrs. at 175 °C, IRHD M	[–]	58.0	71.0
Compression set (94 hrs. at150 °C) after post-cure 4 hrs. at 175 °C	[%]	40.0	55.0
Glass transition temperature (DSC), T_g	[°C]	–35.7	–26.7

[a]Required specification: *IRHD M* (ISO 48) = 60±5 and compression set 94 hrs. at 150 °C (PV3330) ≤50%.

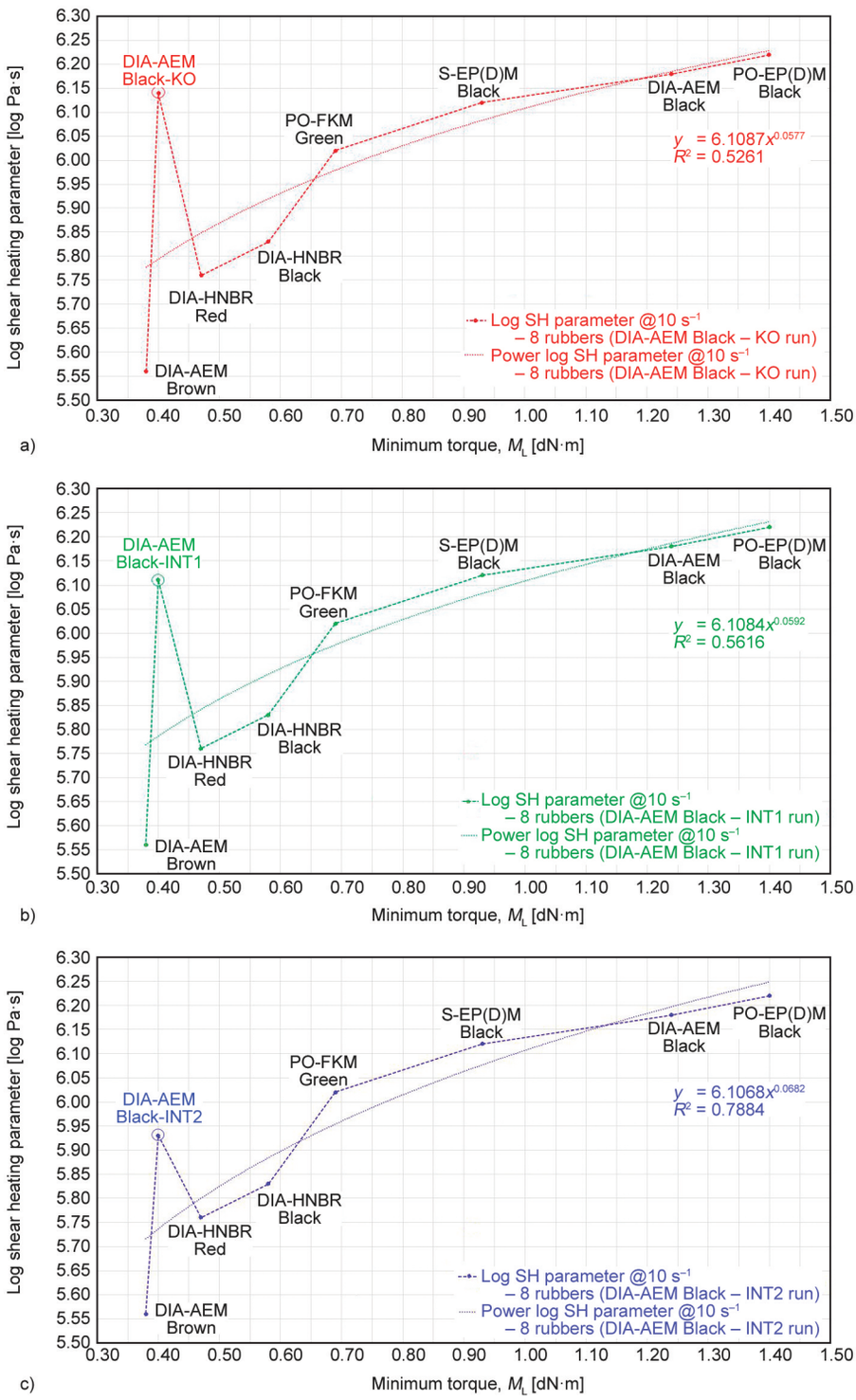

Figure 9. a) Relationship between shear heating parameter at 10 s^{-1} and minimum torque M_L, comparison between 7 rubber compounds with very stable production runs and DIA-AEM-black-KO run. b) Relationship between shear heating parameter at 10 s^{-1} and minimum torque M_L, comparison between 7 rubber compounds with very stable production runs and DIA-AEM-black-INT1 run. c) Relationship between shear heating parameter at 10 s^{-1} and minimum torque M_L, comparison between 7 rubber compounds with very stable production runs and DIA-AEM-black-INT2 run.

The proposed approach, obtained for a very heterogeneous sample of rubber compounds and operating conditions, was found to be successful and useful. It is worth pointing out that the roadmap in the present work was obtained for rubber compounds having similar hardness. In principle, it is possible to extend this approach to other types of rubber compounds, but the limits of validity of the roadmap still need to

be investigated. In the meantime, to apply it to a new rubber compound, preliminary tests in good operating conditions must be performed to demonstrate that the new data are in accordance to the established operating roadmap.

5. Conclusions

This study aimed to improve the process control for optimal injection molding of technical rubber parts by introducing a new tool for online monitoring of the shear heating phenomenon. Specifically, very fast process control of injection molding is proposed and applied to an industrial case study to improve the processing behavior of AEM with a focus on its scorch and thermal degradation issues. The online monitoring is based on direct measurement of the surface rubber temperature (T_{SH}) by an infrared thermal camera at the nozzle outlet of the injection molding machine extruder. This measure provides very fast online process control and provides information about rubber behavior and its shear heating effect before injection of the rubber into the mold cavities. This measured temperature led to the calculation of a technological parameter designated shear heating parameter, η_{SH}, which also takes into account physical material properties (density and specific heat capacity) and process conditions (L/D ratio).

Eight different rubber compounds based on AEM, HNBR, FKM, and EP(D)M elastomers were tested. In particular, eight rubber compounds and eight industrial production runs with long process stability and various production runs of DIA-AEM-black, where stable, unstable, and also the intermediate production runs were investigated. The results of η_{SH} were correlated with M_L from MDR laboratory measurements. The relationship between $\log \eta_{SH}$ and M_L for the 8 rubber compounds with long process stability, including the DIA-AEM-black-OK run, showed a proportional trend, with R^2 of 0.935 according to the power regression model. Thus, this proportional trend represented a reference point to achieve a robust correlation with the molding function to support, by an operating roadmap, the process engineer and plant operator in the improvement of the process control by thermal online measurements. The operating roadmap was successfully used to improve the process control of industrial productions based on AEM rubber compounds affected by scorch problems and thermal degradation due to plasticizer loss. The results show that the shear heating parameter is a very suitable tool because it considers not only the rubber compositional effects based on density and specific heat capacity measurements but also the effect of operating conditions setup, especially based on T_{SH} online measurements. The η_{SH} gives more information than M_L about the thermal history and process safety; thus it can be used in industrial practice to improve the process control by improving the knowledge of rubber behavior and its shear heating effect during the injection stage. Therefore, this knowledge can help the process engineer, plant operator, and mold designer to:

i) provide suitable process parameter setup and mold design to avoid scorch problems and thermal degradation, preventing the production of out of specification rubber parts;
ii) optimize processes for new materials where information about thermal behavior is lacking because, differently from T_{SH}, $\log \eta_{SH}$) is able to correlate data obtained from different rubber compounds;
iii) select the injection molding machine, taking into account the rubber compound rheological behavior.

In this article, the operating roadmap based on two technological parameters, η_{SH} and M_L, is proposed as a new tool very suitable for industrial practice. However, some insights concerning its physical meaning and further applications still need to be explored. Therefore, further investigations will be carried out to study its relationship with α, such as the effects of nozzle type, L/D of nozzle, and residence time. Finally, the possibility to use the shear heating parameter in the setup of computer-aided engineering simulations useful for mold design and injection molding process optimization can also be investigated.

Acknowledgements

This paper is the result of a collaboration created by Italian Gasket S.p.A and the Department of Mechanical and Industrial Engineering of the University of Brescia. The rubber compound characterization and the processing tests were performed in the Italian plant of Italian Gasket. The authors wish to thank Germana Bergomi, board member of Italian Gasket, for starting the collaboration between Italian Gasket S.p.A and the University of Brescia.

References

[1] Stanek M., Manas D., Manas M., Ovsik M., Senkerik V., Skrobak A.: Injection molding of rubber compound influenced by injection mold surface roughness. Advanced Materials Research, **1025–1026**, 283–287 (2014). https://doi.org/10.4028/www.scientific.net/AMR.1025-1026.283

[2] Proske M., Bhogesra H.: Evaluating the root causes of rubber molding defects through virtual molding. Rubber World, **255**, 20–26 (2016).

[3] Long H.: Basic compounding and processing of rubber. Rubber Division of the ACS, Akron (1985).

[4] Ramini M., Agnelli S.: Shear heating parameter of rubber compounds useful for process control in injection molding machine. Rubber Chemistry and Technology, **93**, 729–737 (2020). https://doi.org/10.5254/rct.20.79954

[5] Nakashima K., Fukuta H., Mineki M.: Anisotropic shrinkage of injection-molded rubber. Journal of Applied Polymer Science, **17**, 769–778 (1973). https://doi.org/10.1002/app.1973.070170309

[6] Nishizawa H.: Heat controls and rubber flow behaviour in screw of extruder and injection machine and the problems occurring in these processes. International Polymer Science and Technology, **43**, 41–50 (2016). https://doi.org/10.1177/0307174X1604300409

[7] Stritzke B.: Custom molding of thermoset elastomers a comprehensive approach to materials, mold design, and processing. Hanser, Munich (2009).

[8] Cox H. W., Macosko C. W.: Viscous dissipation in die flows. AIChE Journal, **20**, 785–795 (1974). https://doi.org/10.1002/aic.690200421

[9] Winter H. H.: Temperature fields in extruder dies with circular, annular, or slit cross- section. Polymer Engineering and Science, **15**, 84–89 (1975). https://doi.org/10.1002/pen.760150206

[10] Tadmor Z., Gogos C. G.: Principles of polymer engineering. Wiley, Hoboken (2006).

[11] Ramini M., Viola G. T., Paganin L., Battisti M.: Achieving savings in the post-curing process of fluoroelastomer compounds prepared by injection molding. Rubber World, **261**, 46–51 (2019).

[12] Traintinger M., Kerschbaumer C., Lechner B., Friesenbichler W., Lucyshyn T.: Temperature profile in rubber injection molding: Application of a recently developed testing method to improve the process simulation and calculation of curing kinetics. Polymers, **13**, 380 (2021). https://doi.org/10.3390/polym13030380

[13] McBride E.: Press cure and post cure options for AEM terpolymers. in '174th Fall Technical Meeting of the Rubber Division, American Chemical Society 2008, Louisville, USA' 86 (2008).

[14] McBride E.: Processing of AEM compounds: Scorch issues. in '194th Fall Technical Meeting of the Rubber Division, American Chemical Society 2018, Louisville, USA' 1289 (2018).

[15] McBride E.: Processing of AEM compounds: Scorch issues. Rubber World, **256**, 32–38 (2019).

[16] Öztürk S., Cömez E. E., Hoşgün H. L.: The rheological, mechanical and aging properties of AEM/EPDM rubber blends. Journal of Rubber Research, **24**, 61–67 (2021). https://doi.org/10.1007/s42464-020-00073-5

[17] Brown R.: Physical test methods for elastomers. Springer, New York (2018).

[18] Vera-Sorroche J., Kelly A. L., Brown E. C., Coates P. D.: Infrared melt temperature measurement of single screw extrusion. Polymer Engineering and Science, **55**, 1059–1066 (2015). https://doi.org/10.1002/pen.23976

[19] Straka K., Praher B., Hettrich-Keller M., Steinbichler G.: To the measurement and influences of process parameters variations on the axial melt temperature profile in the screw chamber of an injection molding machine. in 'SPE ANTEC 2017, Anaheim, USA, 1645–1651 (2017).

[20] Ageyeva T., Horváth S., Kovács J. G.: In-mold sensors for injection molding: On the way to industry 4.0. Sensors, **19**, 3551 (2019). https://doi.org/10.3390/s19163551

[21] Farahani S., Brown N., Loftis J., Krick C., Pichl F., Vaculik R., Pilla S.: Evaluation of in-mold sensors and machine data towards enhancing product quality and process monitoring *via* Industry 4.0. International Journal of Advanced Manufacturing Technology, **105**, 1371–1389 (2019). https://doi.org/10.1007/s00170-019-04323-8

[22] Chen J-Y., Tseng C-C., Huang M-S.: Quality indexes design for online monitoring polymer injection molding. Advances in Polymer Technology, **2019**, 3720127 (2019). https://doi.org/10.1155/2019/3720127

[23] Zhang N., Gilchrist M. D.: Characterization of thermo-rheological behavior of polymer melts during the micro injection moulding process. Polymer Testing Journal, **31**, 748–758 (2012). https://doi.org/10.1016/j.polymertesting.2012.04.012

[24] Ramini M., Agnelli S.: Process control in injection molding machine by using shear heating parameter of rubber compounds, All about rubber compounding, May 6 2021, (virtual event), knowhow webinars forum by Technobiz.

Polymer Bulletin
https://doi.org/10.1007/s00289-022-04376-y

ORIGINAL PAPER

Monitoring of shear heating effects during injection molding of rubber to improve the process control

Mattia Ramini[1,2] · **Silvia Agnelli**[2]

Received: 18 May 2022 / Revised: 21 June 2022 / Accepted: 7 July 2022

Abstract

This work aims to get new insights into the "process monitoring tool" proposed by the authors for the online monitoring of the shear heating phenomenon during injection molding of technical rubber parts. The online monitoring is based on direct measurement of the surface rubber temperature (shear heating temperature, T_{SH}) by an infrared thermal camera of the rubber as it leaves the extruder barrel of the injection molding machine. The measured rubber temperature is a process indicator giving the thermal history of the rubber compound injection and process safety. Therefore, this fast process control is applied to industrial applications to investigate the processing behavior of ethylene acrylate (AEM) rubber compounds. In particular, the relationships between T_{SH} vs injection pressure, vs injection speed, vs screw speed rotation and vs screw length over diameter ratio (*L/D* ratio) and vs AEM rubber compound properties variation due to exceeding the shelf life are investigated. The results show that T_{SH} is manly influenced by the screw *L/D* ratio, followed by injection pressure and screw speed rotation (especially if are set to higher levels), whereas the injection speed is the least effective parameter to reduce T_{SH}. Furthermore, a previously found robust correlation between the shear heating parameter (η_{SH}) and the minimum torque measured in rheometric laboratory tests (M_L) is used to show the noteworthy deviation from the proportional trend when the AEM rubber compound exceeded it shelf life. Therefore, the coefficient of determination of $\log\eta_{SH}$ vs M_L curves provides a good indication of process stability, while it is running.

Keywords Industrial applications · Injection molding · Process control · Rubber · Shear heating · Viscosity

✉ Mattia Ramini
mattia.ramini@italiangasket.com

[1] Italian Gasket S.P.A., via Tengattini 9, Paratico, BS, Italy

[2] Department of Mechanical and Industrial Engineering, University of Brescia, via Branze 38, Brescia, Italy

Published online: 26 July 2022

Introduction

Injection molding is one of the most commonly used processing technologies enabling the manufacture of rubber technical parts [1, 2]. The injection molding machine is still seen as a black box, because the output, the quality of the final product, is influenced by many, interplaying, parameters, related to the rubber properties, mold design, process setup parameters and injection molding machine capability [2].

Once the parameters of the injection machine are set, the final quality of the product depends on the properties of the rubber compound, which are temperature, pressure and time dependent. The rubber temperature is therefore a very influencing parameter on the final parts quality. A rubber temperature increase during the injection stage reduces rubber compound viscosity, but it may trigger the curing reaction. If curing occurs when rubber is flowing, viscosity increases, and flow stops.

Therefore, an optimal rubber temperature during the injection process must ensure a balance between relatively low viscosity (therefore low injection time) and a scorch safety condition (curing starts after complete mold filling) [2–5]. In spite of its importance, the rubber temperature during flow cannot be directly controlled, because it is raised not only by the heating system of the machine and by the curing reaction (if by mistake it occurs during flow) but also by shear heating, i.e., temperature increase due to viscous heat dissipation [2–14]. For most rubber compounds, characterized by a viscosity higher than plastics, the latter phenomenon is predominant and it is very difficult to be replicated in the laboratory.

To improve the quality of the final parts and reduce waste production, with both economical and environmental advantages, a thorough monitoring and control of the injection molding process is required. Moreover, also the processability of the raw rubber needs to be continuously controlled, because it is subject to fluctuations, from batch to batch and with storage time and temperature. A longer storage time may cause an increase in viscosity and a reduction of incubation time, thus reducing the processing window [15]. In industrial practice, the control of the process is exerted through: setup of machine parameters and laboratory tests on compounds before production run, and/or sorting of faulty parts after production run. However, an online monitoring could potentially help the modification of machine setup parameters at the first symptoms of defect formation, thus minimizing the time between the occurrence of defects and the fast corrective measures implementation [16–18]. The authors recently proposed a method for the online monitoring of the industrial injection molding process based on the measurement of rubber surface temperature (T_{SH}) and showed how this can significatively improve the control of the process [6, 19]. More in the details, the surface temperature of the rubber, T_{SH}, is measured by an infrared camera during rubber purging at the nozzle outlet of the injection molding machine extruder, several times during a daily production run. The use of infrared thermal camera does not disturb the rubber flow, and it is a noncontact method characterized by

a very fast response [20–22]. This measure provides already an indication of the temperature of rubber at the mold entrance and could be used directly to monitor the risk of getting faulty parts. However, the temperature alone does not allow a comparison of the behavior of different rubber compounds, because the dependency on temperature of their properties is different for each compound. Therefore, the authors [6, 19] proposed, to convert T_{SH} into a technological parameter having the dimensions of a viscosity, the shear heating parameter (η_{SH}). This parameter is a combination of rubber material and machine properties:

$$\eta_{SH} = \Delta T_{SH} \cdot \frac{\rho C_p}{4v} \alpha \tag{1}$$

Where ΔT_{SH} (°C) is the temperature difference between T_{SH} and the initial temperature (considering 20 °C as initial temperature), ρ is the rubber density (kg/m^3), C_p is the specific heat capacity (J/kg/°C), v (s^{-1}) is a flow rate parameter, and α is a function of process parameters such as screw length over diameter (*L/D*), screw speed rotation, injection pressure, speed and time, barrel temperature setup and other factors [19]. In the present work, $\alpha = 1/(L/D)$.

The authors found a robust correlation between the shear heating parameter and the minimum torque measured in rheometric laboratory tests (M_L), a correlation valid for different rubber compounds and different injection molding machines and process parameters setup. Such a correlation can be used as a tool for process control and allows to predict the process parameter setup useful for molding of a new rubber compound.

The aim of the present work is to investigate the effects on T_{SH} of the main process parameters setup and the effects of variation of rubber properties due to exceeding the shelf life. Therefore, the relationships between T_{SH} measured by an infrared camera vs injection pressure, vs injection speed, vs screw speed rotation and vs *L/D* ratio were investigated. The effects of such parameters on the shear heating parameter (η_{SH}) are also shown.

Experimental

Materials

Nine different rubber compounds based on different elastomers were investigated: three types of diamine cured ethylene acrylate rubber (DIA-AEMs) black colored, two with 60 Shore-A and one with 70 Shore-A of hardness; one DIA-AEM brown colored, diamine cured with 60 Shore-A of hardness; two types of ethylene propylene diene monomer rubbers black colored, with 60 Shore-A of hardness, one peroxide cured (PO-EPDM), and one sulfur cured (S-EPDM); two types of diamine cured hydrogenated acrylonitrile rubbers (DIA-HNBRs) with 60 Shore-A of hardness, one black and one red colored; finally one peroxide cured fluoroelastomer (PO-FKM), green colored, with 60 Shore-A of hardness.

Table 1 Rubber compounds investigated with their filler type and content according to IMDS data

Rubber compound	Color	Hardness, Shore-A*	Filler content wt.%	Filler type
DIA-AEM60-1	Black	60 ± 5	40.0–46.0	Carbon black
DIA-AEM60-2	Black	60 ± 5	35.0–45.0	Carbon black
DIA-AEM70-1	Black	70 ± 5	30.0–40.0	Carbon black
DIA-AEM60-3	Brown	60 ± 5	38.0–46.0	Silicon dioxide
PO-EPDM60	Black	60 ± 5	28.0–33.0	Carbon black
S-EPDM60	Black	60 ± 5	26.3–33.5	Carbon black
DIA-HNBR60-1	Black	60 ± 5	44.5–48.5	Carbon black
DIA-HNBR60-2	Red	60 ± 5	40.0–48.0	Calcined kaolin
PO-FKM60	Green	60 ± 5	18.0–23.0	Barium sulfate

*According to *ASTM D2240-15*

These industrial grade rubber compounds were developed in accordance with automotive industry standard specifications, and their formulations cannot be disclosed for confidentiality reasons. The filler type and content are in accordance with available *International Material Data System* (IMDS) data and are reported in Table 1.

Both black and whitefilled rubber compounds were characterized by both laboratory tests and processing injection trials in the molding machine during daily production runs.

Laboratory tests

The above-mentioned rubber compounds were analyzed by using both uncured and cured standard samples, and the analytical instrumentation located in the R&D laboratory of *Italian Gasket* plant.

A laboratory compression molding press from *Gibitre Instruments Srl* was used to mold 200 × 200 × 2 mm standard rubber slabs. After 1 day of stabilization, the cured samples were used for density (ρ) measurements, performed at room temperature, by a digital densimeter from *Doss* (accuracy: 0.001 g), and according to *ASTM D297-15*. The density value to be used for Eq. 1 should be measured at the temperature and pressure in the injection molding machine extruder. However, to use an industrially applicable method, the density at room temperature and pressure was considered to be a reasonable approximation of density at higher temperature and pressure.

In addition, the cured standard samples were used for specific heat capacity (C_p) measurements by differential scanning calorimetry (DSC) in a 214 Polyma, from *NETZSCH GmbH*. The C_p data were recorded from 45 to 245 °C with a heating rate of 20 °C/min and referring to *ASTM E1269-11(2018)*.

The uncured standard samples were used to measure the minimum torque M_L data by an Moving Die Rheometer, MDR 2000 from *Alpha Technologies* according to *ASTM D5289-95* at a frequency of 1.7 Hz and 3° of oscillation amplitude. The

vulcanization curve of each rubber compound was measured for 12 min at 177 °C, thus by using an historical and "die-hard" internal methodology.

The processing trials, mainly focused on the injection stage of molding process, were performed by using horizontal injection molding machines located in the Italian plant of *Italian Gasket*. Six horizontal injection molding machines were selected for the daily production runs processing characterization.

Processing trials

Two 300 Ton Engel from *ENGEL AUSTRIA GmbH* both having first-in first-out (FIFO) screw, *L/D* ratio of about 6, were used to produce O-rings and technical items. In detail, one 300 Ton Engel was used to produce two kinds of O-rings having different sizes and based on DIA-AEM70-1 (70 Shore-A and black colored), and on DIA-AEM60-1 (60 Shore-A and black colored), respectively. The other one 300 Ton Engel was used to produce two different frame gaskets based on PO-EPDM60 (60 Shore-A and black colored) and PO-FKM60 (60 Shore-A and green colored), respectively.

A 450 Ton IMG from *IMG Srl*, with FIFO screw, *L/D* ratio of about 12, was used to produce bellows based on S-EPDM60 (60 Shore-A and black colored).

A 190 Ton MIR also this from *IMG Srl* with reciprocating screw, *L/D* ratio of about 15, was used to produce sealing rings based on DIA-AEM60-3 (60 Shore-A and brown colored). Furthermore, another 190 Ton MIR with reciprocating screw and with *L/D* ratio of about 16 was used to produce technical rubber items based on DIA-AEM60-2 (60 Shore-A and black colored). Finally, another 190 Ton MIR with reciprocating screw, but with *L/D* ratio of about 18, was used to produce intake manifold gaskets based on DIA-HNBR60-1 (60 Shore-A and black colored) and DIA-HNBR60-2 (60 Shore-A and red colored), respectively.

The processing trials have concerned daily production runs of each rubber compound, and after the start-up stage, the thermal controls by the infrared (IR) camera were performed.

Figure 1 shows a simple scheme for the rubber surface temperature control by IR thermal camera (online monitoring).

The thermal measure for each rubber compound and respective production run was performed every hour, 3 measures at each time, for the purpose of controlling the shear heating effect during the injection stage. A thermal imaging camera, Diacam C.A 1882, *Chauvin Arnoux Group*, having ± 2 °C of accuracy and 0.08 °C of thermal sensitivity, was used to control rubber surface temperature (T_{SH}) as it leaves the extruder barrel of the injection molding machine (Fig. 1).

The IR thermal camera was used to measure the rubber surface temperature by detecting the emitted electromagnetic radiation. The rubber emissivity was set to 0.95 in accordance with the software material database, and image analysis was provided by the software tools (Fig. 1). The accuracy and sensitivity were selected in order to be lower than a temperature difference of 5 °C during stable production run on the basis of industrial experience.

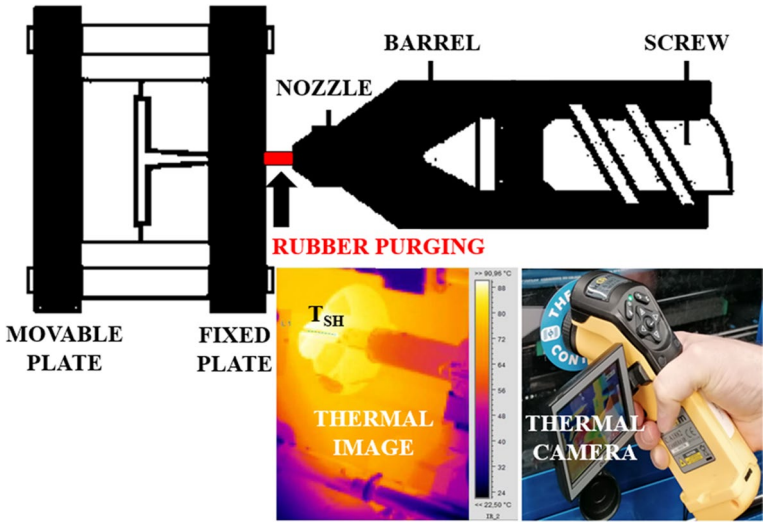

Fig. 1 Scheme for the rubber surface temperature control as it leaves the extruder barrel of the injection molding machine by IR thermal camera

The molded parts coming from each investigated production run, after stabilization, deburring, post-cure (if required) and final controls, were used as gaskets in the automotive industry.

The processing characterization was completed by investigating the process parameters setup effects on the rubber shear heating temperature. For this analysis, a 300 Ton Maplan from *MAPLAN GmbH* having FIFO screw, *L/D* ratio of about 14, was used to produce O-rings based on DIA-AEM60-2. Therefore, the relationships between T_{SH} measured by an infrared camera vs injection pressure, vs injection speed and vs screw speed rotation were investigated, respectively. The effect of each parameter is investigated by varying the level of the parameter itself, and keeping constant all the other parameters.

Furthermore, a relationship between $T_{SH\ vs}$ screw *L/D* ratio was investigated by using the same DIA-AEM60-2 rubber compound, but processed in different injection molding machines: a 300 Ton Maplan (FIFO screw $L/D \approx 14$), 300 Ton Engel (FIFO screw $L/D \approx 6$), a 190 Ton MIR (reciprocating screw $L/D \approx 16$) and a 190 Ton MIR (reciprocating screw $L/D \approx 18$), respectively.

Results and discussion

The processing characterization was partially focused on the effects of process parameters setup on the rubber shear heating temperature, and it was referred to the processing of DIA-AEM60-2 rubber compound in a 300 Ton Maplan (FIFO screw $L/D \approx 14$) horizontal injection molding machine, producing O-rings. Therefore, Fig. 2 shows the relationship between T_{SH} measured by an infrared camera vs injection pressure.

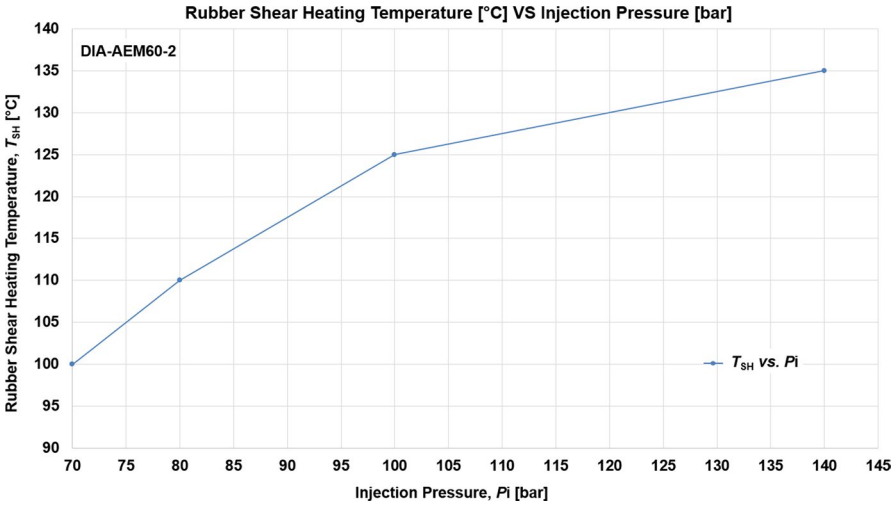

Fig. 2 Relationship between temperature T_{SH} and injection pressure for DIA-AEM60-2

Comprehensibly, a reduction of injection pressure decreased the shear heating effect during the injection stage. The injection pressure reduction, from 140 to 70 bar, allowed a T_{SH} reduction of about 35 °C, though maintaining a stable rubber compound processability with a negligible filling time variation. The trend is qualitatively expected because the shear heating temperature is by definition proportional to pressure drop in adiabatic conditions.

Figure 3 shows the relationship between T_{SH} measured by an infrared camera vs screw speed rotation, in which a similar proportional trend to the previous case of

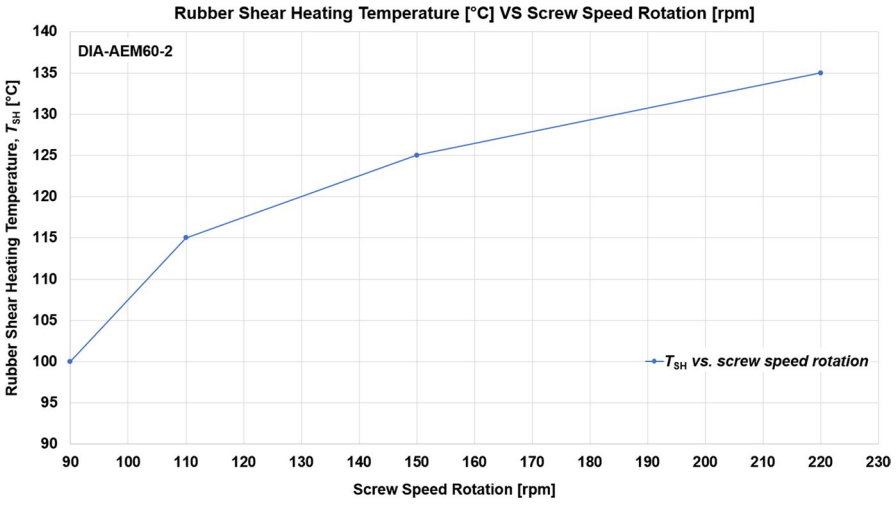

Fig. 3 Relationship between temperature T_{SH} and screw speed rotation for DIA-AEM60-2

injection pressure was observed. Also in this case, a screw speed rotation reduction, from 220 to 90 rpm, allowed a T_{SH} reduction of about 35 °C, though maintaining a stable rubber compound processability with a negligible filling time variation.

The proportional trend can be explained by the fact that by increasing the screw speed rotation, the shear rate of rubber compound is increased along the screw direction.

Figure 4 shows the relationship between T_{SH} measured by an infrared camera vs injection speed, where a proportional trend similar to the previous cases of injection pressure and screw speed rotation was observed. The injection speed reduction, from 40 to 15 mm/s, allowed a T_{SH} reduction of about 30 °C; however, the largest T_{SH} decrease (about 20 °C) was measured between 20 mm/s and 15 mm/s. On the contrary, only 10 °C of T_{SH} decrease was measured between 40 mm/s and 20 mm/s. Moreover, also in this case an injection speed reduction did not significantly affect the rubber compound processability. Increasing the injection speed causes an increase in shear rate especially in the extruder head, and thus, T_{SH} increases.

Figure 5 instead shows the relationship between T_{SH} measured by an infrared camera vs screw *L/D* ratio, in which a linear trend was observed. Clearly, from the 190 Ton MIR (reciprocating screw *L/D* ≈ 18) to the 300 Ton Engel (FIFO screw *L/D* ≈ 6), a T_{SH} reduction of about 40 °C was measured. Therefore for the DIA-AEM60-2 rubber compound, and by using the same philosophy of process parameters setup, the injection molding machines with higher screw *L/D* ratio showed the most significant shear heating effect T_{SH}. Furthermore also in this case, based on different injection molding machines with different screws, a very stable rubber compound processability was observed. Thus, production runs were carried out without relevant variations of cure rate, cure state (physical properties, e.g., hardness) and with minor quality issue. The main reason for the increase of T_{SH} of the rubber compound with increasing the screw *L/D* ratio can be ascribed the longer residence time.

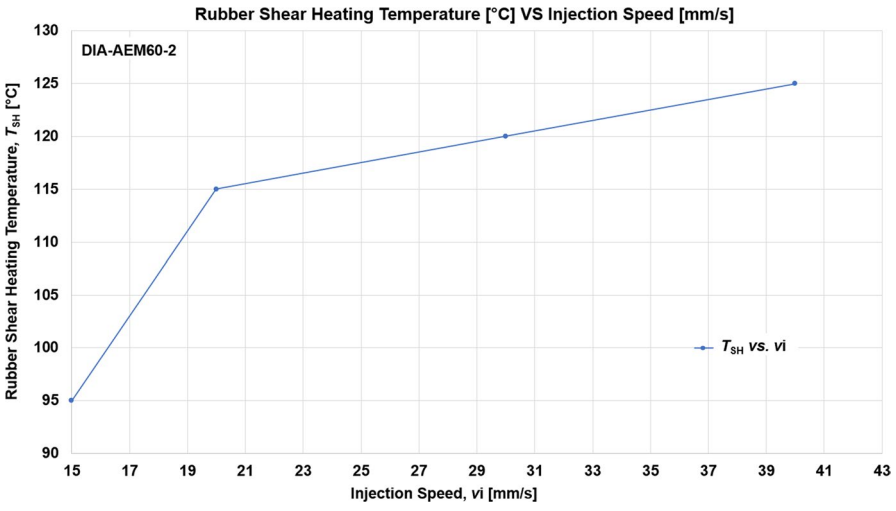

Fig. 4 Relationship between temperature T_{SH} and injection speed for DIA-AEM60-2

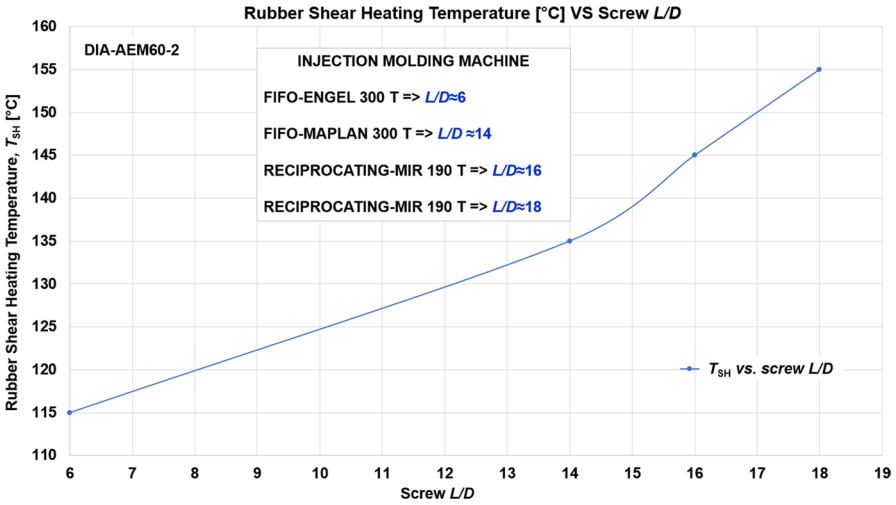

Fig. 5 Relationship between temperature T_{SH} and screw *L/D* ratio for DIA-AEM60-2

Therefore, for DIA-AEM60-2 rubber compound, T_{SH} is manly influenced by the screw *L/D* ratio. Nevertheless, also the process parameters such as injection pressure and screw speed rotation clearly showed that they contribute consistently to the T_{SH} increase, especially if they are set to higher levels. Finally, also the injection speed has provided its most relevant contribution to the T_{SH} increase, if it is set to lower levels (Fig. 4). Typically in the industrial practice the most easy parameter which is fine tuned to reduce T_{SH} is the screw speed rotation. On the contrary, the injection speed is the least effective parameter to reduce T_{SH}.

Besides the effect of setup parameters, also the effects of rubber properties variation on T_{SH} are shown in this work. At this aim, a single rubber compound was studied, DIA-AEM70-1, and its properties varied due to exceeding the shelf life. It is well known that rubber compounds change their properties with storage time and temperature. Even under proper storage conditions, after some weeks the incubation time decreases, thus causing a risk of premature start of curing reaction, and the viscosity increases. This is reflected in deteriorated mechanical properties of the cured rubber [15]. Typically, the AEM rubber compounds are characterized by a shelf life of about 1 month, obviously if properly stored according to *ISO 2230:2002—Rubber products—Guidelines for storage*. Therefore, the DIA-AEM70-1 rubber compound was processed both within the shelf life (2 weeks after the compounding) and off of it (5 weeks after the compounding) in a 300 Ton Engel by producing O-rings, and the differences in processability were investigated with particular care.

Table 2 reports the results for both the investigations of DIA-AEM70-1: a stable production run, within the material shelf life, designated DIA-AEM70-1-OK, and an unstable production run, out of the material shelf life, designated DIA-AEM70-1-KO. About laboratory test, the data of density (ρ), specific heat capacity (C_p) and minimum torque (M_L) at 177 °C are reported. Table 2 also reports the average experimental data from laboratory test of other eight different rubber

Table 2 Average experimental data from laboratory tests

Rubber compound	Density (ρ) kg/m^3	Specific heat capacity (C_p)* J/kg/°C	Minimum torque (M_L)** dN m
DIA-AEM60-1	1267 ± 1	2930 ± 3	1.24 ± 0.011
DIA-AEM60-2	1243 ± 1	2931 ± 4	0.40 ± 0.011
DIA-AEM70-1-OK	1240 ± 1	1650 ± 3	0.77 ± 0.010
DIA-AEM70-1-KO	1240 ± 1	1920 ± 3	0.84 ± 0.010
DIA-AEM60-3	1389 ± 2	1459 ± 3	0.38 ± 0.017
PO-EPDM60	1090 ± 1	4180 ± 2	1.40 ± 0.015
S-EPDM60	1140 ± 1	4150 ± 3	0.93 ± 0.023
DIA-HNBR60-1	1273 ± 2	3240 ± 3	0.58 ± 0.018
DIA-HNBR60-2	1331 ± 1	2770 ± 3	0.47 ± 0.036
PO-FKM60	2029 ± 1	1345 ± 2	0.69 ± 0.018

*At T_{SH}

**At 177 °C

compounds, based on different elastomer, having eight industrial production runs with long process stability, without significant deviations of set parameters and with very little scrap. These additional eight different rubber compounds provide the data to build the robust correlation between the shear heating parameter and M_L for stable production runs, which is used as a reference to evaluate the processability of DIA-AEM70-1-OK and DIA-AEM70-1-KO compounds.

Table 3 reports the average experimental data from processing characterization of the eight different rubber compounds, and screw *L/D* ratio of the used injection molding machines. About the processing characterization, the data of barrel temperature setup (T_{Barrel}), measured shear heating temperature (T_{SH}) of the

Table 3 Average experimental data from processing characterization

Rubber compound	*L/D*	Barrel temperature (T_{Barrel}) °C	Shear heating temperature (T_{SH}) °C	Temperature difference in shear heating (ΔT_{SH})* °C
DIA-AEM60-1	6	80.0	114.0 ± 2.5	94.0
DIA-AEM60-2	16	75.0	115.0 ± 3.0	95.0
DIA-AEM70-1-OK	6	75.0	130.0 ± 2.5	110.0
DIA-AEM70-1-KO	6	75.0	226.0 ± 3.0	206.0
DIA-AEM60-3	15	75.0	125.0 ± 2.5	105.0
PO-EPDM60	6	95.0	105.0 ± 2.5	85.0
S-EPDM60	12	70.0	155.0 ± 3.0	135.0
DIA-HNBR60-1	18	75.0	136.0 ± 2.5	116.0
DIA-HNBR60-2	18	75.0	132.0 ± 3.0	112.0
PO-FKM60	6	80.0	110.0 ± 2.5	90.0

*Considering 20 °C as initial temperature

rubber by infrared thermal camera and the temperature difference in shear heating (ΔT_{SH}) considering 20 °C as initial temperature are reported.

Table 3 also reports the results for both the investigated DIA-AEM70-1-OK and DIA-AEM70-1-KO.

Finally, Table 4 reports the average data of calculated shear heating parameter (η_{SH}) at 10 s^{-1} and the corresponding logarithmic values for the rubber compounds of Tables 2 and 3.

The η_{SH} was calculated by using Eq. 1, where the flow rate parameter v [s^{-1}] is directly related to the shear rate. Therefore, a conventional value of flow rate of 10 s^{-1} was chosen based on the commonly achievable order of magnitude of shear rate in the plasticizing extruder of the injection molding machine.

The results of calculated η_{SH} were compared with minimum torque, M_L, from MDR routine rheometric laboratory measurements for the nine different industrial rubber compounds. Therefore, a robust correlation between η_{SH} and M_L, labeled roadmap, was obtained by considering various rubber compounds having different elastomeric matrices, different injection molding machines and process parameter setups, by producing different geometries of the molded parts (both O-rings and technical rubber items).

In this work, the robust correlation between η_{SH} and M_L is used to investigate the effect of shelf life variation for the DIA-AEM70-1 rubber compound during its production run.

Figure 6 shows the relationship between logη_{SH} at 10 s^{-1} and M_L from 12 min at 177 °C by MDR, giving a comparison between the nine rubber compounds investigated and the nine industrial production runs having long process stability without the relevant quality issue of final parts, including the DIA-AEM70-1-OK run. Therefore, a good correlation was established between the results of the laboratory test, M_L, and the technological parameter (η_{SH}) and characterized by a proportional trend with R^2 of 0.936 according to a power regression law.

Table 4 Average data of shear heating parameter (η_{SH}) at 10 s^{-1}

Rubber compound	Shear heating parameter (η_{SH})* Pa s	Log shear heating parameter Log(η_{SH})* Log Pa s
DIA-AEM60-1	1.50×10^6	6.18
DIA-AEM60-2	5.37×10^5	5.73
DIA-AEM70-1-OK	9.68×10^5	5.99
DIA-AEM70-1-KO	2.11×10^6	6.32
DIA-AEM60-3	3.64×10^5	5.56
PO-EPDM60	1.67×10^6	6.22
S-EPDM60	1.31×10^6	6.12
DIA-HNBR60-1	6.69×10^5	5.83
DIA-HNBR60-2	5.77×10^5	5.76
PO-FKM60	1.06×10^6	6.02

*At 10 s^{-1} and ΔT_{SH}

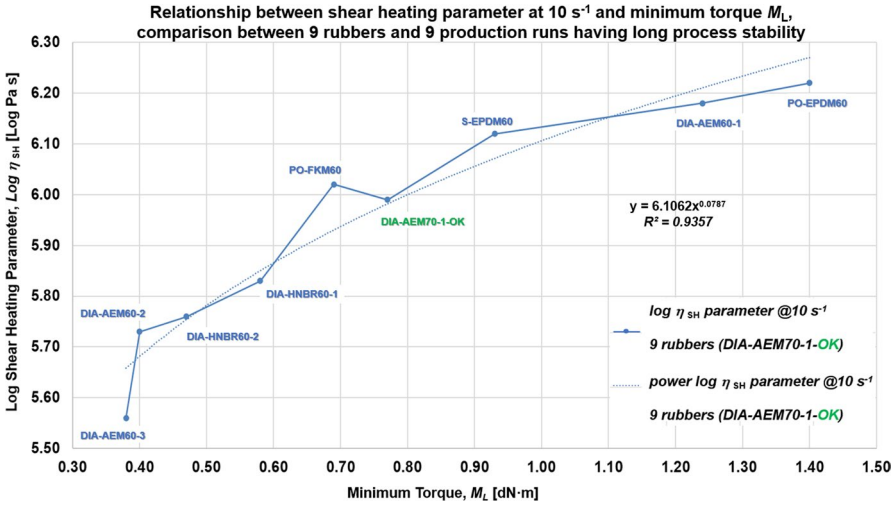

Fig. 6 Relationship between shear heating parameter η_{SH} at 10 s^{-1} and minimum torque M_L, comparison between 9 rubbers and 9 production runs having long process stability

A similar roadmap was previously shown by the authors [19] for the following eight rubber systems: DIA-AEM60-1, DIA-AEM60-2, DIA-AEM60-3, PO-EPDM60, S-EPDM60, DIA-HNBR60-1, DIA-HNBR60-2 and PO-FKM60.

In the present work, the previous investigation was extended to DIA-AEM70-1 rubber compound to obtain the correlation in Fig. 6. The existence of such a correlation is, therefore, confirmed and strengthened by the new data based on 70 Shore-A of hardness. It is interesting to remark that the newly introduced compound has a higher hardness compared to the others: This seems to indicate that the validity of such correlations is not strictly related to rubber of the same hardness degree.

The nine industrial production runs investigated in this work are characterized by different injection molding machines, different molded part geometries and by very stable production runs, with very little scrap after molded part stabilization, deburring and post-cure. Therefore, this roadmap was found to be useful for process control and allows to make predictions on different rubber compounds, with the purpose of supporting the process engineer and the plant operator, in the improvement of process control by thermal online measurements.

In this work, AEM rubber parts affected by scorch problems, mold fouling and thermal degradation due to plasticizer loss are investigated as follows. Figure 7a, b shows the cavities of movable plate during the DIA-AEM70-1 production runs, DIA-AEM70-1-OK (within the material shelf life) and DIA-AEM70-1-KO (out of the material shelf life), respectively. These production runs were chosen as a case study to show how the rubber compound shelf life, once exceeded, affects negatively on the rubber shear heating temperature, processing behavior and mold fouling.

Particularly, Fig. 7a shows the movable mold plate of DIA-AEM70-1-OK, where a not excessively fouling, even after a week of production run, was found. Instead Fig. 7b shows the movable mold plate of DIA-AEM70-1-KO, where a

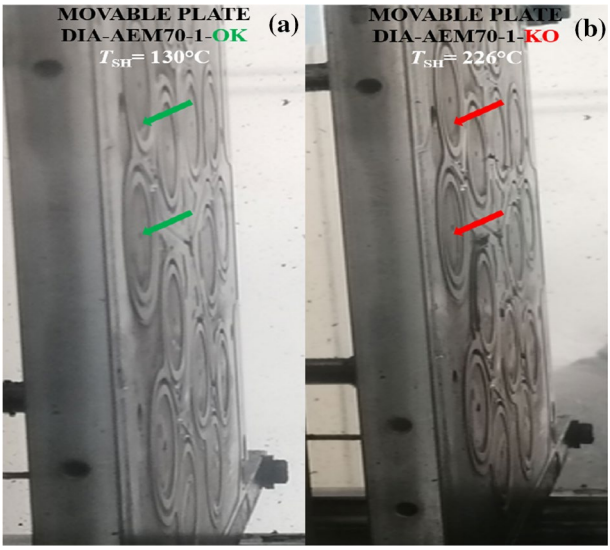

Fig. 7 **a** Cavities of movable plate during the DIA-AEM70-1-OK production run. **b** Cavities of movable plate during the DIA-AEM70-1-KO production run. Green arrows indicate clean cavities, and red arrows indicate some fouled cavities

significant fouling, even after 2 days of production run, was found, as pointed out by red arrows in the figure.

About the DIA-AEM70-1-OK production run, an average T_{SH} of 130 °C was measured during the daily process control and, after injection molding, stabilization, deburring, and post-cure of 4 h at 175 °C, no relevant quality issue of final parts was found, including IRHD M hardness value of 71.1 ± 0.1 points according to *ISO 48* (70.0 ± 5 required specification).

Whereas in the case of DIA-AEM70-1-KO production run, an average T_{SH} of 226 °C was measured during the daily process control and, after injection molding, stabilization, deburring and post-cure of 4 h at 175 °C, some surface hardened and cracked parts, 0.2–0.3% of the overall production (about 110,000 O-rings), were obtained. This amount of scraps, and especially this type of defect, is relevant because the automotive industry requires "zero defected" parts. A IRHD M hardness value of 82.4 ± 0.1 points was measured, thus out of the required specification.

The effect of exceeding rubber shelf life produced an increase of T_{SH} by 96 °C, which largely outcomes the effects produced by the variation of process setup parameters, at least within the range explored in this work. This suggests that the rubber properties have the significant effect on T_{SH}.

The significant increase of T_{SH} was the first indicator of DIA-AEM70-1 processability change due to its shelf life variation. Another relevant indicator was the quick mold fouling increase in the DIA-AEM70-1-KO production run (after only 2 days of production). The last condition obviously has negatively affected the productivity of DIA-AEM70-1-KO, thus subjected to extraordinary cleaning.

Furthermore, even modifying the process parameter setup such as injection pressure, injection speed and screw rotation speed, no reduction in this excessive shear heating was found.

Therefore, T_{SH} is already a useful parameter to guarantee a very fast online process control, that is, to collect information concerning the risk of scorching and thermal degradation, leading, for example, to the diffusion of compound ingredients (low volatile chemicals), stickiness, mold fouling and also color variation.

Moreover, monitoring also η_{SH} allows to get a more quantitative and precise indication of the quality of molded parts: By introducing η_{SH} of a new production run into the data of η_{SH} vs M_L correlation, the processability of the newly introduced production run can be inferred from the coefficient if determination R^2, as shown in the details in [19]. Moreover, η_{SH} and the use of the roadmap could provide information also about new compounds, whose T_{SH} limit for the obtainment of good quality parts is not known a priori, unless process trials are performed. Therefore, $\log\eta_{SH}$ was introduced to allow the comparison of process outputs between DIA-AEM70-1 and the other rubber compounds.

Figure 8 shows the relationship between $\log\eta_{SH}$ at 10 s^{-1} and M_L from 12 min at 177 °C by MDR for the eight rubber compounds with very stable industrial production runs, and the DIA-AEM70-1-KO run (R^2 of 0.797).

In more detail, new curve was created, starting from the roadmap reported in Fig. 6, by introducing the values of $\log\eta_{SH}$ at 10 s^{-1} and M_L of DIA-AEM70-1-KO, while keeping the values of the other eight productions runs constant.

By introducing the point of DIA-AEM70-1-KO, a relevant deviation from the previous proportional trend was observed, with decreased R^2 from 0.936 to 0.797, according to the power regression model.

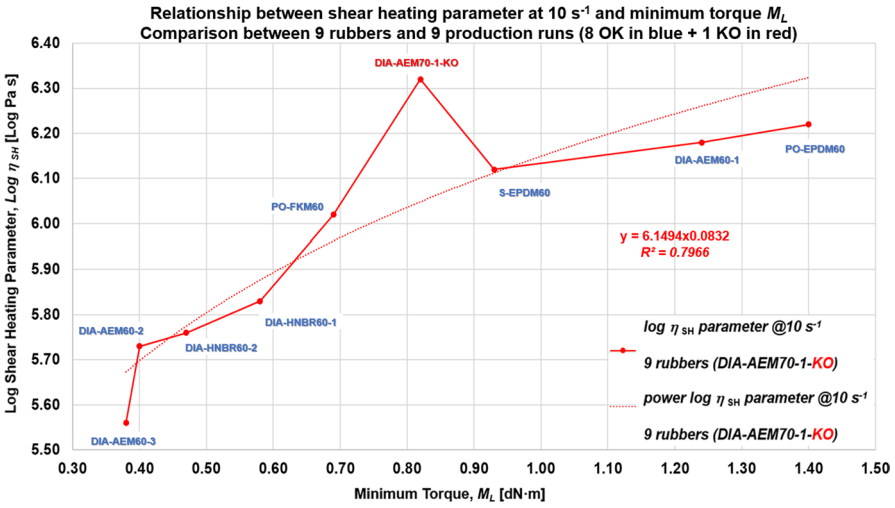

Fig. 8 Relationship between shear heating parameter η_{SH} at 10 s^{-1} and minimum torque M_L, comparison between 9 rubbers and 9 production runs: 8 OK runs and 1 KO run

Therefore, the coefficient of determination of $\log\eta_{SH}$ vs M_L curves provides a good indication of process stability of DIA-AEM70-1 runs.

Accordingly, the DIA-AEM70-1-KO run, out of the material shelf life, with M_L of 0.84 ± 0.07 dN·m, an average T_{SH} of 226 °C (+96 °C) and $\log\eta_{SH}$ at 10 s^{-1} of 6.32 ± 0.33 Pa·s, did not allow a stable production cycle, where hardened and cracked parts, 0.2–0.3% of final scraps, were produced.

Figure 8 clearly shows how $\log\eta_{SH}$ values of a production run, combined with M_L values, give indication of the "real output" of the injection molding process by comparison of this data with a well-established roadmap, obtained from stable production runs of different rubber compounds and process conditions. This monitoring has the advantage of being fast and provides information about the stability of the process, while it is running, well before completing the production run.

Conclusions

This work aimed to get new insights about the "process monitoring tool" proposed by authors for the online monitoring of the shear heating phenomenon to guarantee an optimal injection molding of technical rubber parts. The online monitoring is based on direct measurement of the surface rubber temperature (T_{SH}) by an infrared thermal camera at the nozzle outlet of the injection molding machine extruder. Therefore, a very fast process control is proposed and applied to an industrial case to investigate the processing behavior of AEM rubber compounds. The first investigation regards the rubber properties variation due to exceeding the shelf life (for the DIA-AEM70-1), and the second one regarding the process parameters setup (for the DIA-AEM60-2). Therefore, the relationships between T_{SH} vs injection pressure, vs injection speed, vs screw speed rotation and vs *L/D* ratio were investigated. The setup level of the four parameters is varied close to the limit of the operativity range, by ensuring the rubber compound processability without relevant cycle time variation.

About DIA-AEM60-2, T_{SH} is mainly influenced by the screw *L/D* ratio, followed by injection pressure and screw speed rotation (especially if set to higher levels), whereas the injection speed is the least effective parameter to reduce T_{SH}.

This measured T_{SH} led to the calculation of a technological parameter designated shear heating parameter, η_{SH}, which also takes into account physical material properties (density and specific heat capacity) and process conditions (*L/D* ratio). The authors compared this parameter with the previously found robust correlation between the shear heating parameter (η_{SH}) and the minimum torque measured in rheometric laboratory tests (M_L). The correlation is valid for different rubber compounds (based on AEM, EP(D)M, HNBR and FKM elastomers) and different injection molding machines (300 Ton Engel, 450 Ton IMG and 190 Ton MIR) and process parameters setup [6, 19].

About DIA-AEM70-1, the introduction of η_{SH} vs M_L values in the previously found robust correlation showed a significant deviation from the proportional trend, when the AEM rubber compound exceeded it shelf life. Therefore, the coefficient of

determination of $\log\eta_{SH}$ vs M_L curves provides a good indication of process stability of DIA-AEM70-1 runs.

The monitoring of T_{SH} has the advantage of being fast and provides information about the stability of the process, while it is running, well before completing the production run.

Moreover, the robust correlation between the shear heating parameter (η_{SH}) and the minimum torque measured in rheometric laboratory tests (M_L) can be used as a tool for process control and allows to predict the process parameter setup useful for molding of a new rubber compound.

Finally, the possibility to use T_{SH} and η_{SH} in the setup of computer-aided engineering simulations, useful for mold design and injection molding process optimization, will be investigated in future works.

Acknowledgements This paper is the result of a fruitful collaboration created by *Italian Gasket S.p.A.* and the Department of Mechanical and Industrial Engineering of the University of Brescia. The rubber compound characterization and the processing trials were performed in the *Italian Gasket* plant. The authors wish to thank Germana Bergomi, board member of *Italian Gasket*, for starting, in the 2019, the collaboration between *Italian Gasket S.p.A.* and the University of Brescia.

Funding Open access funding provided by Università degli Studi di Brescia within the CRUI-CARE Agreement.

References

1. Stanek M, Manas D, Manas M, Ovsik M, Senkerik V, Skrobak A (2014) Injection molding of rubber compound influenced by injection mold surface roughness. Adv Mater Res 1025–1026:283–287. https://doi.org/10.4028/www.scientific.net/AMR.1025-1026.283
2. Sommer J (2013) Troubleshooting Rubber Problems. Carl Hanser Verlag, Munich
3. Proske M, Bhogesra H (2016) Evaluating the root causes of rubber molding defects through virtual molding. Rubber World 255(3):20–26
4. Anderson A, Jones M (2011) Using low viscosity HNBR to increase productivity in high shear molding methods. Rubber World 245(3):25–32
5. Long H (1985) Basic Compounding and processing of rubber, Rubber Division of the ACS. University of Akron, Akron
6. Ramini M, Agnelli S (2020) Shear heating parameter of rubber compounds useful for process control in injection molding machine. Rubber Chem Technol 93(4):729–737. https://doi.org/10.5254/rct.20.79954
7. Nakashima K, Fukuta H, Mineki M (1973) Anisotropic shrinkage of injection-molded rubber. J Appl Polym Sci 17(3):769–778. https://doi.org/10.1002/app.1973.070170309
8. Nishizawa H (2016) Heat controls and rubber flow behaviour in screw of extruder and injection machine and the problems occurring in these processes. Int Polym Sci Technol. https://doi.org/10.1177/0307174X1604300409

9. Stritzke B (2009) Custom molding of thermoset elastomers a comprehensive approach to materials, mold design, and processing. Carl Hanser Verlag, Munich
10. Cox HW, Macosko CW (1974) Viscous dissipation in die flows. AIChE J 20:785–795. https://doi.org/10.1002/aic.690200421
11. Winter HH (1975) Temperature fields in extruder dies with circular, annular, or slit cross-section. Polym Eng Sci 15:84–89. https://doi.org/10.1002/pen.760150206
12. Tadmor Z, Gogos CG (2006) Principles of polymer engineering. Wiley, Hoboken
13. Ramini M, Viola GT, Paganin L, Battisti M (2019) Achieving savings in the post-curing process of fluoroelastomer compounds prepared by injection molding. Rubber World 261:46–51
14. Traintinger M, Kerschbaumer C, Lechner B, Friesenbichler W, Lucyshyn T (2021) Temperature profile in rubber injection molding: application of a recently developed testing method to improve the process simulation and calculation of curing kinetics. Polymers 13:380. https://doi.org/10.3390/polym13030380
15. Fasching M, Friesenbichler W, Berger GR (2015) Change of processing behavior of rubbers in injection molding caused by material storage. AIP Conf Proc 1779:070005-1-070005–5. https://doi.org/10.1063/1.4965537
16. Farahani S, Brown N, Loftis J, Krick C, Pichl F, Vaculik R, Pilla S (2019) Evaluation of in-mold sensors and machine data towards enhancing product quality and process monitoring via Industry 4.0. Int J Adv Manuf Technol 105:1371–1389. https://doi.org/10.1007/s00170-019-04323-8
17. Chen JY, Tseng CC, Huang MS (2019) Quality indexes design for online monitoring polymer injection molding. Adv Polym Technol. https://doi.org/10.1155/2019/3720127
18. Zhang N, Gilchrist MD (2012) Characterization of thermo-rheological behavior of polymer melts during the micro injection moulding process. Polym Test 31(6):748–758. https://doi.org/10.1155/2019/3720127
19. Ramini M, Agnelli S, Ramorino G (2022) Applications of shear heating parameter for injection molding process optimization of AEM rubber compounds. Express Polym Lett 16(4):354–367. https://doi.org/10.3144/expresspolymlett.2022.27
20. Vera-Sorroche J, Kelly AL, Brown EC, Coates PD (2015) Infrared melt temperature measurement of single screw extrusion. Polym Eng Sci 55(5):1059–1066. https://doi.org/10.1002/pen.23976
21. Straka K, Praher B, Hettrich-Keller M, Steinbichler G (2017) To the measurement and influences of process parameters variations on the axial melt temperature profile in the screw chamber of an injection molding machine. SPE ANTEC® Anaheim, California, pp 1645–1651
22. Ageyeva T, Horváth S, Kovacs JG (2019) In-Mold sensors for injection molding: on the way to industry 4.0. Sensors 19:3551. https://doi.org/10.3390/s19163551

MODULO DI EMBARGO DELLA TESI
(da compilare solo se si richiede un periodo di segretazione della tesi)

Il/La sottoscritto/a..RAMINI MATIA..... Nato/a il..06/03/1982.....
a (indicare anche l'eventuale paese estero)..FERRARA.....
provincia di (ovvero sigla del paese estero)..FERRARA.....
Dottorato di Ricerca in ..INGEGNERIA MECCANICA ED INDUSTRIALE.....
.....

DICHIARA

- che il contenuto della tesi **non può essere immediatamente consultabile per il seguente motivo**

SEGRETO INDUSTRIALE

La motivazione deve essere dettagliata e controfirmata obbligatoriamente dal Tutor e/o Relatore
(Brevetto, segreto industriale, motivi di priorità nella ricerca, motivi editoriali, altro)

- che il testo completo della tesi potrà essere reso consultabile dopo:

□ 6 mesi dalla data di conseguimento titolo
□ 12 mesi dalla data di conseguimento titolo
☒ 24 mesi dalla data di conseguimento titolo
□ altro periodo _____

- che sarà comunque consultabile immediatamente l'abstract della tesi, che viene caricato in Esse3, profilo studente.

Luogo e Data

PARATICO, 3/11/2022

Firma del Dichiarante

Ramini Matia

Controfirma del Tutor e/o Relatore del Dottorato
per la motivazione di embargo e il periodo.